



UNIVERSIDAD DE LOS ANDES  
FACULTAD DE INGENIERÍA Y  
CIENCIAS APLICADAS

STUDY OF ALTERNATIVE METABOLIC  
PATHWAYS FOR THE PRODUCTION OF  
(*R*)-3-HYDROXYBUTYRIC ACID IN  
POLYHYDROXYBUTYRATE  
PRODUCING BACTERIA

LUZ FRANCY YAÑEZ MENESES

THESIS PRESENTED IN PARTIAL  
FULFILLMENT OF THE REQUIREMENTS  
DOCTORADO EN CIENCIAS DE LA INGENIERÍA

ADVISOR: FELIPE SCOTT CONTADOR

SANTIAGO, 2022



*To Enrique Yañez, Ana Meneses,  
Rocky & Milo and my Higher-Self*

## ABSTRACT

Considerable rich literature has accumulated concerning biochemical, physiological, and genetic aspects of polyhydroxybutyrate (PHB) intracellular accumulation in bacteria. The costs of substrates and processing, including the extraction of the polymer accumulated in intracellular granules, still hampers a more widespread use of this family of polymers. The PHB monomeric unit, (*R*)-3-hydroxybutyric acid (R3HBA) has found uses at the biomedical, chemical and supplement industries. The literature shows that two main process engineering and metabolic engineering strategies have been identified aimed at the production of chiral R3HBA: (i) production from the accumulated polymer (polymerization and depolymerization system, PDS); (ii) by bypassing the accumulation of PHB using metabolically engineered bacteria. The later includes the use of thioesterases (thioesterase shortcut system, TSS) that removes CoA from R3HBA-CoA, resulting in the R3HBA release to extracellular medium.

This PhD thesis aims at broadening the understanding of the genetic and operational factors leading to PHB polymerization and R3HBA production in *Azohydromonas lata* DSM 1123, *Cupriavidus necator* H16 and *Methylocystis parvus* OBBP. Results showed that the growth associated PHB production observed in *A. lata* mimics an overflow metabolism, additionally, a successful PHB depolymerization in a two stage chemostat was obtained. The feasibility of producing R3HBA through *in-vivo* depolymerization of the intracellularly accumulated PHB in *M. parvus* was investigated. A PHB to R3HBA conversion of  $77.2 \pm 0.9\%$  (R3HBA titer of  $0.153 \pm 0.002 \text{ g L}^{-1}$ ) can be attained in a mineral medium containing  $1.0 \text{ g L}^{-1} \text{ KNO}_3$  at  $30 \text{ }^\circ\text{C}$  with shaking at 200 rpm and a constant pH of 11 for 72 hours. Nitrogen deprivation, oxygen limitation, the supplementation with exogenous R3HBA and neutral or acidic pHs strongly reduced the excreted R3HBA concentration and yield.

The implementation of the TSS system in *M. parvus* and *C. necator* by the construction of an expression vector containing *tesB* was hampered by inconsistencies in the constructed plasmids pLY01 and pLY02. Finally, the production of R3HBA by redirecting fluxes in the PHB metabolic pathway was investigated in *C. necator*; two mutant strains were constructed using the suicide vector pT18mobsacB: *C. necator*  $\Delta\textit{phaC}$  and *C. necator*  $\Delta\textit{phaC} \Delta\textit{hbd}$ , both unable to polymerize PHB and the last one incapable to transform R3HBA into acetoacetate. The mutant strains released pyruvate and R3HBA, suggesting that a native thioesterase of *C. necator* may play a role in the release of R3HBA by removing CoA from R3HBA-CoA. A protein homology on the genome of *C. necator* showed an enzyme encoded as WP\_037025319.1 with a percent identity of 44 % in comparison with Ycia that may trigger R3HBA release.

The results obtained in this work demonstrated the feasibility of R3HBA production by reducing or eliminating the fluxes of the reactions consuming R3HBA via operational manipulation as described in *M. parvus* and *A. lata* or via gene knock outs in *C. necator*.

## RESUMEN

Se ha acumulado una abundante literatura sobre los aspectos bioquímicos, fisiológicos y genéticos de la acumulación intracelular de polihidroxibutirato (PHB) en bacterias. Los costos de los sustratos y procesamiento, incluida la extracción del polímero acumulado en los gránulos intracelulares, dificultan un uso más generalizado de esta familia de polímeros. La unidad monomérica del PHB, ácido (*R*)-3-hidroxibutírico (R3HB), ha encontrado usos en la industria biomédica, química y de suplementos. La literatura muestra que se han identificado dos estrategias principales de ingeniería de procesos e ingeniería metabólica para la producción de R3HB: (i) producción a partir del polímero acumulado (sistema de polimerización y despolimerización, SPD); (ii) evitando la acumulación de PHB utilizando bacterias modificadas metabólicamente. Este último incluye el uso de tioesterasas (sistema acceso-directo con tioesterasas, SADT) que elimina el CoA de R3HB-CoA, lo que da como resultado la liberación extracelular de R3HB.

Esta tesis doctoral tiene como objetivo ampliar la comprensión de los factores genéticos y operativos que conducen a la polimerización de PHB y la producción de R3HB en *Azohydromonas lata* DSM 1123, *Cupriavidus necator* H16 y *Methylocystis parvus* OBBP. Los resultados mostraron que la producción de PHB está asociada con el crecimiento en *A. lata* e imita un metabolismo de desbordamiento; además, se obtuvo una despolimerización exitosa de PHB en un quimiostato de dos etapas. Se estudio la viabilidad de producir R3HB a través de la despolimerización *in-vivo* del PHB acumulado intracelularmente en *M. parvus*. La conversión de PHB a R3HB de  $77.2 \pm 0.9\%$  (concentración R3HB de  $0.153 \pm 0.002 \text{ g L}^{-1}$ ) se pudo lograr en un medio mineral que contiene  $1.0 \text{ g L}^{-1} \text{ KNO}_3$  a  $30 \text{ }^\circ\text{C}$  con agitación a 200 rpm y un pH constante de 11 por 72 horas. La privación de nitrógeno, limitación de oxígeno, suplementación con R3HB exógeno y los pHs neutros o ácidos redujeron fuertemente la concentración y el rendimiento de R3HB excretado.

La implementación del sistema SADT en *M. parvus* y *C. necator* mediante la construcción de un vector de expresión que contenía *tesB* se vio afectada por inconsistencias en los plásmidos construidos pLY01 y pLY02. Finalmente, se investigó la producción de R3HB mediante la redirección de flujos en la ruta metabólica de PHB en *C. necator*; se construyeron dos cepas mutantes utilizando el vector suicida pT18mobsacB: *C. necator*  $\Delta\text{phaC}$  y *C. necator*  $\Delta\text{phaC} \Delta\text{hbd}$ , ambas incapaces de polimerizar PHB y el último incapaz de transformar R3HB en acetoacetato. Las cepas mutantes liberaron piruvato y R3HB, lo que sugiere que una tioesterasa nativa de *C. necator* puede desempeñar un papel en la liberación de R3HB mediante la eliminación de CoA de R3HB-CoA. Una homologación proteica en el genoma de *C. necator* mostró una enzima codificada como WP\_037025319.1 con un porcentaje de identidad del 44 % con Ycia, la cual puede desencadenar la liberación de R3HB.

Los resultados obtenidos en este trabajo demostraron la viabilidad de producir R3HB al reducir o eliminar los flujos de las reacciones que consumen R3HB a través de manipulaciones operacionales como se describe en *M. parvus* y *A. lata* o mediante la delección de genes en *C. necator*.

## ACKNOWLEDGMENTS

First, I would like to express sincere gratitude to my supervisors Dr. Felipe Scott and Dr. Raul Muñoz for kindly guiding with research and for their continued support throughout my PhD journey. Thank you for providing me with all the great scientific opportunities, all the resources for my work and for making a stressful move to Chile and Spain easy. Specially, I feel very grateful with Dr. Felipe Scott for being a friend and for encouraging my way.

I wish to thank the Universidad de Los Andes for the provision of a *Fondo de Ayuda a la Investigación* (FAI) grant that facilitated these studies. Thanks to the Universidad de Valladolid for the opportunity of study through the double degree agreement between Universidad de los Andes (Chile) and Universidad de Valladolid (Spain). Additionally, the financial support to my work from the National Agency for Research and Development (ANID Chile), projects ANID/CONICYT Fondecyt Regular 1211434 and ANID/CONICYT Fondecyt Regular 1190521; *Apoyo a la Formación de Redes Internacionales entre Centros de Investigación* REDES190137 (CONICYT-PCI) and the regional government of Castile and Leon and the EU-FEDER program (CLU 2017-09, UIC 315) are also gratefully acknowledgment.

Thanks to all the current and previous members of the G-Tech group lab for being great lab mates and always keeping a friendly and collegial working atmosphere. Special thanks to the VOC and Microalgae group for the enthusiastic welcomed, all the deep scientific and philosophic discussions, Tapas night and for all your support and encouragement. Special thanks to Yadira Rodriguez, a great friend, working with her has been a rewarding experience.

To my family and friends who encouraged me all the way until here. Without them, this would have been much harder. To my parents who taught me about never giving up and always staying by my side. Finally, I want to thank Harvey Hernandez for standing beside me throughout this thesis and specially our journey. His faithful support, love, patience, and advice are greatly appreciated.

## CONTENTS

NOTATION AND ABBREVIATIONS.....	14
1. INTRODUCTION.....	16
1.1 Hypothesis .....	19
1.2 Objectives .....	21
1.3 Organization of this document.....	21
2. LITERATURE REVIEW .....	22
2.1. POTENTIAL USES OF PHAs AND THEIR MONOMERS .....	22
2.2. SUBSTRATES TO PRODUCE PHAs AND THEIR MONOMERS .....	25
2.3. ACCUMULATION AND MOBILIZATION OF PHAs.....	27
2.4. PRODUCTION OF R3HAs FROM PHAs.....	32
2.4.1. <i>In-vitro</i> strategies.....	32
2.4.2. <i>In-vivo</i> strategies.....	35
3. MATERIALS AND METHODS .....	43
3.1. MATERIALS.....	43
3.1.1. Chemicals .....	43
3.1.2. Bacterial strains .....	43
3.1.3. Growth media .....	44
3.1.4. Primers.....	45
3.1.5. <i>E. coli</i> strains and plasmids .....	46
3.2. METHODS .....	47

3.2.1.	Preliminary depolymerization and viability assay in PHB accumulated cells of <i>A. lata</i> DSM 1123 .....	47
3.2.2.	Bioreactor experiments with <i>A. lata</i> .....	47
3.2.3.	Optimization of PHB depolymerization in <i>M. parvus</i> .....	48
3.2.4.	Biomass quantification and culture supernatant collection and analysis .....	51
3.2.5.	Raman spectroscopy .....	51
3.2.6.	Analytical procedures .....	52
3.2.7.	Vector construction for <i>tesB</i> expression .....	52
3.2.8.	Gene knock-out via pT18mobsacB for <i>C. necator</i> H16 .....	53
3.2.9.	Standard polymerase chain reaction .....	54
3.2.10.	Colony PCR .....	54
3.2.11.	Agarose gel electrophoresis .....	55
3.2.12.	Preparation of electrocompetent <i>E. coli</i> cells .....	55
3.2.13.	Transformation of <i>E. coli</i> cells .....	56
3.2.14.	Characterization of <i>C. necator</i> H16 and mutant strains .....	56
3.2.15.	Calculations .....	57
4.	RESULTS AND DISCUSSIONS .....	60
4.1.	EFFECTS OF NUTRIENT LIMITATION AND DILUTION RATE ON PHB AND BIOMASS PRODUCTION IN <i>A. lata</i> .....	60
4.1.1.	Nitrogen limited-chemostat culture .....	60
4.1.2.	Oxygen limited-chemostat cultures .....	62
4.1.3.	Glucose-limited chemostat culture .....	63
4.1.4.	Preliminary <i>in-vivo</i> depolymerization and viability assay in PHB accumulated cells of <i>A. lata</i> DSM 1123 .....	64
4.1.5.	Sequential PHB depolymerization in a nitrogen-limited chemostat .....	65
4.2.	STUDY OF <i>in-vivo</i> PHB DEPOLYMERIZATION IN <i>M. parvus</i> .....	66
4.2.1.	Influence of the presence of nitrate, O <sub>2</sub> and pH on PHB depolymerization .....	66
4.2.2.	Optimization of pH during depolymerization .....	71

4.2.3.	Influence of temperature on the kinetic of PHB depolymerization.....	72
4.2.4.	Influence of the aeration rate and R3HBA exogenous on PHB depolymerization .....	74
4.3.	PLASMID CONSTRUCTION FOR <i>tesB</i> EXPRESSION IN <i>C. necator</i> H16 AND <i>M. parvus</i> .....	77
4.4.	GENERATION OF MUTANT STRAINS OF <i>C. necator</i> VIA SUICIDE VECTOR pT18mobsacB.....	80
4.4.1.	Biomass, PHB and R3HBA production in <i>C. necator</i> and knockout mutant strains .....	82
5.	CONCLUSIONS.....	88
5.1.	Future directions .....	89
	REFERENCES .....	91
	APPENDICES .....	118

## LIST OF APPENDICES

APPENDIX I. RAW DATA AND CALIBRATION CURVES .....	118
APPENDIX II. PRIMERS AND GENES FOR THE CONSTRUCTION OF <i>tesB</i> EXPRESSION VECTOR.....	119
APPENDIX III. PUBLICATIONS.....	121

## LIST OF TABLES

Table 1. Genotype and source of bacterial strains.....	43
Table 2. Growth media for the bacterial strains .....	44
Table 3. Primers and their sequences used for the construction of gene knock outs .....	45
Table 4. Vector backbones and their relevant genotype.....	46
Table 5. Equations defining specific uptakes and production rates .....	58
Table 6. Summary of the PHB conversion, R3HBA excreted and cell viability at pH 4, 5 and 7 in <i>A. lata</i> cells .....	65

## LIST OF FIGURES

Figure 1. Effects of the dilution rate and nutrient limitation in chemostat culture on PHB accumulation.....	61
Figure 2. CH <sub>4</sub> and O <sub>2</sub> consumption profile and R3HBA released at different depolymerization conditions in <i>M. parvus</i> .....	67
Figure 3. Schematic metabolic pathways involved in the polymerization and depolymerization of PHB in <i>M. parvus</i> .....	70
Figure 4. R3HBA released at pH 10, 11 and 12 in presence or absence of CH <sub>4</sub> in <i>M. parvus</i> .....	71
Figure 5. Time course of biomass and CH <sub>4</sub> , O <sub>2</sub> and CO <sub>2</sub> in viability assay of <i>M. parvus</i> .....	73
Figure 6. Influence of the oxygen mass transfer rate on the kinetics of R3HBA release in <i>M. parvus</i> .....	74
Figure 7. HPLC chromatograms of depolymerization assays at different filling ratios in E-flasks.....	75
Figure 8. Influence of R3HBA exogenous in the R3HBA excretion in <i>M. parvus</i> .....	76
Figure 9. PCR product amplification of plasmids constructed for the expression of <i>tesB</i> in <i>M. parvus</i> and <i>C. necator</i> H16.....	78
Figure 10. Maps of the plasmid designed for <i>tesB</i> expression in <i>M. parvus</i> .....	79

Figure 11. Maps of the plasmid designed for <i>tesB</i> expression in <i>C. necator</i> H16.....	80
Figure 12. PCR colony amplification of <i>phaC</i> and <i>hbd</i> genes in wild type and mutant <i>C. necator</i> strains.....	81
Figure 13. Cell growth and fructose consumption in <i>C. necator</i> H16.....	82
Figure 14. Cell growth, fructose consumption, R3HBA and pyruvate production and yield in <i>C. necator</i> 541.....	83
Figure 15. Cell growth, fructose consumption, R3HBA and pyruvate production and yield in <i>C. necator</i> $\Delta$ <i>phaC</i> .....	84
Figure 16. Cell growth, fructose consumption, R3HBA and pyruvate production and yield in <i>C. necator</i> $\Delta$ <i>phaC</i> $\Delta$ <i>hbd</i> .....	86
Figure 17. Influence of pHs conditions in PHB depolymerization and R3HBA release in <i>C. necator</i> H16.....	87

## NOTATION AND ABBREVIATIONS

$\mu$	Specific growth rate
D	Dilution rate
v/v	Volume per volume
w/v	Weight per volume
<i>Amp</i> <sup>R</sup>	<i>Ampicillin resistance gene</i>
ATP	Adenosine triphosphate
CDW	Cell dry weight
DO	Dissolved oxygen
E-flask	Erlenmeyer flask
GC	Gas chromatograph
GHG	Greenhouse gases
<i>hbd</i>	R3HBA dehydrogenase gene
HPLC	High performance liquid chromatography
LB	Luria Bertani
mcl	medium-chain-length
NAD <sup>+</sup>	Nicotinamide adenine dinucleotide
NADP	Nicotinamide adenine dinucleotide phosphate
NFMS	Nitrate free mineral salts medium

NMS	Nitrate mineral salts medium
OD <sub>600</sub>	Optical density at 600 nm
PCR	Polymerase chain reaction
PDS	Depolymerization system
PHA	Polyhydroxyalkanoate
<i>phaA</i>	$\beta$ -ketothiolase gene
<i>phaC</i>	PHB synthase gene
PHB	Polyhydroxybutyrate
PHBi	Initial PHB content
PHV	Polyhydroxyvalerate
R3HA	( <i>R</i> )-3-hydroxyalkanoic acid
R3HBA	( <i>R</i> )-3-hydroxybutyric acid or ( <i>R</i> )-3-hydroxybutyrate acid
R3HBA-CoA	( <i>R</i> )-3-hydroxybutyryl-Coenzyme A
R3HD	( <i>R</i> )-3-hydroxydecanoic acid
R3HDD	( <i>R</i> )-3-hydroxydodecanoic acid
R3HHx	( <i>R</i> )-3-hydroxyhexanoic acid
R3HO	( <i>R</i> )-3-hydroxyoctanoic acid
TCA cycle	Tricarboxylic acid cycle
TSS	Thioesterase shortcut system

## 1. INTRODUCTION

Climate change presents a series of unprecedented challenges to natural and human systems (Beaumont et al., 2011; Riahi et al., 2022). Despite the ongoing public debate on the causal role of anthropogenic Greenhouse Gases (GHG) (Carmichael & Brulle, 2017; Howe et al., 2015; van der Linden et al., 2017), the Intergovernmental Panel on Climate Change (IPCC) determined through a near-unanimous scientific consensus that forcing from anthropogenic emissions is the primary driver of climate change (Riahi et al., 2022). With continuous economic development, industrialization, and fossil fuel consumption, GHGs emissions have exceeded the buffering capacity of the atmosphere. A total of 73.2% of the global GHG emissions are emitted by the energy sector, out of which 32.9% is attributed to different stages of global oil production, including its extraction, distribution, and refining (Mohamad Noh, 2017). The sources of agricultural GHG emissions are from land-use change (carbon dioxide, CO<sub>2</sub>), enteric fermentation (methane, CH<sub>4</sub>), and manure management (nitrous oxide, N<sub>2</sub>O) (Vergé et al., 2007). Thus, anthropogenic GHG emission are increasingly threatening the sustainability of natural ecosystem and human societies, raising the earth's temperature and leading to one of the critical environmental issues nowadays, global warming.

Among the most prevailing GHGs is CH<sub>4</sub>, which accounts for almost one-quarter of the cumulative radiative forcing of CO<sub>2</sub> and NO<sub>2</sub> combined since 1750 (Etminan et al., 2016). Indeed, CH<sub>4</sub> exhibits a global warming potential 86 times stronger per unit of mass than CO<sub>2</sub> on a 20-year timescale and approximately 28 times more powerful on a 100-year time scale (Edenhofer, 2014). The global CH<sub>4</sub> emissions have been steadily increasing over the past few decades up to April 2020 with a global concentration of 1876.3 ppb (Dlugokencky, 2020), exerting a negative effect on the environment. Today, global CH<sub>4</sub> can be captured from anthropogenic sources (125 Mton per year), wastewater treatment (68 Mton per year), agriculture (145 Mton per year), biomass (16 Mton per year), and natural gas production (92 Mton per year) (IEA, 2020) but the main sources are natural gas and biogas (Ghasemi Ghodrati et al., 2018; Strong et al., 2015). Bioconversion of CH<sub>4</sub> offers a broad range of alternatives that can be valorized as an energy vector or as a feedstock for biotechnological processes for the production of ectoine, biopolymers such a polyhydroxyalkanoates (PHAs),

and single cells protein, among others (Jawaharraj et al., 2020) or for the catalytic production of methanol (Latimer et al., 2018).

Emissions of GHGs are also related to plastic's life cycle. Recent estimates have forecasted to cumulative emissions from plastics production and use reaching 56 Gton of carbon by 2050, being equivalent to 10–13% of the remaining carbon budget to stay below 2 °C (Hamilton et al., 2019). Synthetic polymers, such as polyolefins mainly produced from petroleum-based monomers, are non-biodegradable and non-renewable materials. As a result, plastics accumulate, rather than decompose, in the environment and close to 60% of all plastics produced from 1950 to 2015 can be found in landfills or the natural environment, amounting to approximately 4900 Mton (Geyer et al., 2017). PHAs are a family of thermoplastic polymers of renewable, bio-based and biodegradable polyesters that are expected to reduce the impacts of plastic production and use, including greenhouse gas emissions. One of the most promising biopolymers is polyhydroxybutyrate (PHB), a biogenic short chain PHA, produced by various bacteria as a storage compound under nutrient-deficient conditions when a carbon source is present in excess. PHB can be synthesized from a wide range of carbohydrates and lipids including sucrose (Yamane et al., 1996). The use of CH<sub>4</sub> or H<sub>2</sub>:CO<sub>2</sub>:O<sub>2</sub> (knallgas) (Brigham, 2019) mixtures could help to mitigate climate change by lowering the emissions of harmful gases and tackling the conversion of CO<sub>2</sub> into useful products.

The PHB monomeric unit, (*R*)-3-hydroxybutyric acid (R3HBA), has found uses as a chiral building block for the synthesis of fine chemicals such as antibiotics, vitamins, aromatics, and pheromones (Chiba & Nakai, 1985; Seebach et al., 2001; Steinbüchel & Valentin, 1995). R3HBA has also been known to exhibit antimicrobial, insecticidal, and antiviral activities (Chen & Wu, 2005; Peypoux et al., 1999; Shiraki et al., 2006). Studies have shown that R3HBA confers partial protection and stability to neurons during glucose deprivation (Holmes, 1985; Massieu et al., 2003). There is also evidence that R3HBA could offer neuroprotection in Parkinson's and Alzheimer's disease (Kashiwaya et al., 2000). Additionally, R3HBA may suppress the effects of hyperglycemia, lactic acidemia and hyperalaninemia in hemorrhagic stress (Katayama et al., 1994). Recently, R3HBA has been

commercialized as a supplement for athletes and people following keto diets, further expanding its uses (Martin, Thomas & Soni, 2021). This monomer can be produced either by *in-vivo* depolymerization of the accumulated PHB, by fermentation for the direct production of (*R*)-3-hydroxyalkanoates (R3HAs) into the culture media and by conversion of purified PHB, although the production of R3HAs from recovered PHAs requires more steps. The advantage of the first alternative lies in the fact that R3HBAs production does not require the extraction of the intracellular PHB.

An efficient method to produce R3HBA is through the tuning of pH values that switch the activity of intracellular PHA depolymerase and R3HBA dehydrogenase. *Azohydromonas lata* (formerly *Alcaligenes latus*) is a Gram-negative facultative autotroph, capable of using knallgas and organic molecules (including sucrose and glucose) for growth and PHB production, having the highest volumetric productivity of PHB accumulation reported up to date (Lee et al., 1997). Interestingly, PHB depolymerization and R3HBA release in *A. lata* has been achieved at pH 4 and 35 °C, with a PHB to R3HBA conversion of 96% in 30 min and a decrease to a yield of 31% at a pH 5 (Lee et al., 1999).

One potential candidate for study the R3HBA production, is the well characterized PHB producer, *Cupriavidus necator* H16 (formerly *Ralstonia eutropha*), which is a Gram-negative bacteria and obligate aerobe. *C. necator* growth and PHB accumulation can be achieved using knallgas, sugars, and organic acids as substrates. PHB accumulation in *C. necator* follows a non-growth associated pattern; *i.e.*, the specific PHB productivity decreases as the growth rate increases in chemostat culture. R3HBA production in *C. necator* has only been reported by (Lee et al., 1999) where cells that accumulated polyhydroxybutyrate co-valerate (PHB/V) were incubated in water at pH 7 and other low pH values at 30 °C. Under these conditions, a depolymerization mixture was obtained, consisting of R3HBA (5.8 g L<sup>-1</sup>) and (*R*)-3-hydroxyvalerate (0.6 g L<sup>-1</sup>) at pH 7. Other pH values did not improve PHB/V depolymerization, which suggest that the depolymerization mechanisms are not influenced by changes of pH values.

The production of R3HBA from PHB produced from sugar-based bacterial processes is expensive nowadays. The costs of supplying the required carbon and energy source for microbial growth and PHB production are estimated to be between 30 and 50% of the product cost if sugars are used (Choi et al., 1999; Levett et al., 2016). However, there is a group of Gram-negative bacteria, collectively termed methanotrophs, that can grow and synthesize value-added products such as biopolymers, from CH<sub>4</sub>. Bacteria in this group are classified according to the pathways used for the assimilation of the formaldehyde produced directly from CH<sub>4</sub> into type I and type II methanotrophs. Type I use the ribulose monophosphate pathway for formaldehyde assimilation, and type II methanotrophs use the serine pathway (Nguyen, et al., 2021). The ability to form biopolymer inclusions as PHB is under growth-essential nutrient deprivation (e.g. nitrogen or phosphorous) and methane availability (Asenjo & Suk, 1986; Hanson & Hanson, 1996). A representative type-II methanotrophs is *Methylocystis parvus* a bacteria that is also capable of nitrogen fixation (del Cerro et al., 2012; Vecherskaya et al., 2009). *M. parvus* shows a higher specific growth rate ( $\mu$ ) compared to other species of the *Methylocystis* genera (Bordel et al., 2019) and the ability to synthesize PHB under nitrogen-limited conditions (Rostkowski et al, 2013) leading to accumulations of more than 50% (Pieja et al., 2011; Wendlandt et al., 2001). Up to date, the operational conditions that control the enzyme activity that allows the release of R3HBA are unknown.

## 1.1 Hypothesis

From the analysis of literature, two systems can be identified for the production of R3HBA in PHB and non-PHB producing bacteria. In the first system, herein termed polymerization and Depolymerization System (PDS), PHB is accumulated and then depolymerized to R3HBA without -or with a reduced activity of- the R3HBA dehydrogenase enzyme that otherwise would transform R3HBA to acetoacetate. Production of R3HBA in *A. lata* by Lee et al (1999) is a prime example of the PDS system.

Nevertheless, the use of PDS system requires a two-stage fermentation: accumulation of the polymer followed by depolymerization. Thereby the required cultivation times are typically long. Hence, the interest in the last decades has focused on the direct microbial production

of extracellular R3HA monomers without going through these two stages and achieving a straightforward, less energy demanding and time-consuming process.

The alternative pathway is called Thioesterase Shortcut System (TSS), which is characterized by the creation of a bypass without PHB accumulation by the insertion of a thioesterase (TesB or Ycia) enzyme that removes the Coenzyme A (CoA) from (*R*)-3-hydroxybutyryl-Coenzyme A (R3HBA-CoA), thus resulting in a R3HBA monomer release to the extracellular medium (Guevara-Martínez et al., 2019; Liu et al., 2007) and the recycling of CoA. The study of TSS mechanism have been reported only in *E. coli* strain is due to that TesB and Ycia are native thioesterases and needs the insertion of *phaA* ( $\beta$ -ketothiolase) and *phaB* (acetoacetyl coenzyme A reductase) genes for evaluating the role of this thioesterases. High production of R3HBA with TesB by the TSS mechanism has been reported in recombinant *E. coli* harboring genes of *phaA* and *phaB* up to 12 g L<sup>-1</sup> in a 6 L fermenter (Liu et al., 2007). But interestingly, Guevara-Martinez and co-workers described that *tesB* deletion resulted in R3HBA yield reduction of 10%, whereas for *ycia* was 43%. This system shows the importance of evaluating thioesterases native or non-native within a specific pathway and how it involves the PHB-producing strains to achieve significant R3HBA titers.

At present, there is no evidence of the application of the TSS system in PHB-producing bacteria and the PDS system has not been broadly studied in other PHB-producing bacteria that use gaseous substrates (syngas, knallgas, and methane) that can be valorized. Based on the previous information, this work proposed the application of TSS (TesB) and PDS in *C. necator* H16, *A. lata* DSM 1123 and *M. parvus* for R3HBA production. The hypothesis driving this PhD Thesis is:

“R3HBA can be produced by reducing or eliminating the fluxes of the reactions consuming R3HBA, via operational manipulations or gene knock outs, and simultaneously enhancing the supply of R3HBA from PHB (via PHB depolymerase) or R3HBA-CoA hydrolysis using a heterologous *tesB* gene”.

## 1.2 Objectives

### General Objective

To broaden the understanding of the genetic and operational factors leading to PHB polymerization and R3HBA production in *A. lata*, *C. necator* H16 and *M. parvus*.

### Specifics Objectives

- i) To assess the PHB accumulation and depolymerization yield and productivity via operational manipulations in chemostat cultures of *A. lata* DSM 1123 as a benchmark of R3HBA production.
- ii) To study a set of operational conditions allowing the depolymerization of the accumulated PHB in *M. parvus*.
- iii) To obtain a characterization of PHB and R3HBA production capabilities of PHB synthase (*phaC*) and R3HBA dehydrogenase (*hbd*) knock out mutants of *C. necator* H16.
- iv) To quantify the R3HBA titer, yield and productivity of the parent strains obtained in iii) and of strains with the insertion of *tesB*.

## 1.3 Organization of this document

Chapter 2 presents a literature review summarizing the most important information supporting this thesis, including the developments leading to the current understanding of the mechanisms of PHB accumulation and depolymerization. Chapter 3 presents the materials and methods used to attain the proposed objectives while Chapter 4 summarizes the results obtained, comparing them with relevant information from the literature. Finally, Chapter 5 outlines the conclusion of this thesis and states future research directions and opportunities.

## 2. LITERATURE REVIEW

This chapter is organized as follows. Section 2.1 presents the main applications of PHAs and their monomers in several industrial fields and the recent uses as a biomedical target. Section 2.2 summarizes the carbon and energy substrates currently used to produce PHAs and the potential of moving to lignocellulosic substrates, agro-food wastes, sugars and abundant gaseous substrates such as syngas, knallgas, or CH<sub>4</sub>. Section 2.3 is a brief analysis concerning the regulation of PHB biosynthesis and the influence of the growth factors for its mobilization. Finally, section 2.4 provides insights about strategies based on operational changes or genetic modifications that have been devised for the production of chiral hydroxyalkanoic acids.

### 2.1. POTENTIAL USES OF PHAs AND THEIR MONOMERS

PHAs have been extensively investigated to identify possible applications. Homopolymers, random copolymers, and block copolymers can be produced depending on the structure of the polymer chain, which in turn is dictated by the species of bacteria and the substrate used for the accumulation of PHA (Braunegg, G., Bona, R; Koller, 2004). The diversity of applications is wide, including production of biodegradable plastics that are environmentally friendly for use in packaging (Khosravi-Darani & Bucci, 2015; Koller, 2014), fibers (Dietrich et., 2017), biodegradable and biocompatible implants (Misra et al., 2006), drugs and fine chemical (Rathbone et., 2010), and biofuels (Zhang et al., 2009).

As biomedical materials, PHAs have been used in suture materials and repair patches, meniscus restoration devices, cardiovascular patches, orthopedic pins, and cartilage regeneration aids, among others (Volova et al., 2003; Wang, Wu, Chen, &, 2005). Many of these uses are related to the customizable composition and properties of PHAs, which allow them to have favorable mechanical properties, biocompatibility, and to degrade in reasonable times under specific physiological conditions (Hazer et al., 2012; Misra et al., 2006). In particular, medium-chain-length-PHAs (mcl-PHAs), have potential applications in coatings and in medical temporary implants such as scaffoldings for the regeneration of arteries and

nerve axons (Witholt & Kessler, 1999). On the other hand, the use of these polymers has been studied for controlled drug delivery (Shah et al., 2010). The kinetics of drug release can be engineered by altering the degradation rate of the PHA matrix coating. In this regard, mcl-PHAs have been used as drug carriers since their low fusion point and low crystallinity makes them suitable for controlled drug release (Ueda & Tabata, 2003).

Finally, PHA-derived compounds can be used as biofuels after the esterification of PHB of mcl-PHAs with methanol for their conversion to hydroxyalkanoate methyl esters (Zhang. et al., 2009). These hydroxyalkanoate methyl esters can be mixed with gasoline or diesel in ratios of 10 to 30%. In particular, (*R*)-3-hydroxy-methyl-butyrate was reported to have similar or superior properties as a fuel additive (oxygen content, dynamic viscosity, flash point, and boiling point) compared to ethanol (Wang et al., 2010). Using PHA derivatives as biofuels can be viewed as a promising application since mixtures of PHA can be used without a costly separation step (Gao et al., 2011).

The most well-known R3HAs is R3HBA, which can be used as a building block in the synthesis of fine chemicals and pharmaceuticals such as antibiotics (Ren, Grubelnik, Hoerler, Ruth, Hartmann, et al., 2005), bulk chemicals for the polymer industry (such as hydrogenation to 1,3-butanediol), fragrances and insecticides (Matsuyama et al., 2001). R3HBA can be esterified with butanol or ethanol or converted to ethers by reaction with alcohols using the catalytic Williamson ether synthesis (Fuhrmann & Talbiersky, 2005) or dehydrated to crotonic acid, which upon hydrogenation yields butyric acid and *n*-butanol (Schweitzer et al., 2015).

Similarly, (*R*)-3-hydroxypropionic acid (R3HPA), a non-chiral compound, can yield upon chemical modifications to acrylic acid, acrylamide, and acrylonitrile, all with market sizes larger than one billion dollars, and other niche market compounds such as 1,3-propanediol, methyl acrylate and malonic acid (Jers et al., 2019).

More than three decades ago Seebach et al. (1986) reported the synthesis of the macrolide antibiotics pyrenophorin, colletodiol, garamycin A1 and elaiophylidene starting from

R3HBA and malate. R3HBA and its derivatives have also been used as potential drugs. Cao et al. (2014) showed that R3HBA and R3HBA methyl ester inhibit the development of osteoporosis in mice kept under simulated microgravity. Using *in-vivo* studies with mice suffering from Alzheimer's disease, Zhang et al. (2013) showed that intragastric administration of R3HBA methyl ester reduced amyloid- $\beta$  deposition in mouse brains and improved the performance of the treatment group in the Morris water maze (a standardized test in the study of spatial learning and memory) compared to the control group. In a related study in mice, Tieu et al. (2003) showed that the infusion of R3HBA led to improved mitochondrial respiration and ATP production in mice treated with the neurotoxin 1-methyl-4-phenyl-1,2,3,6-tetrahydropyridine causing a mitochondrial deficit reminiscent of Parkinson disease. Finally, Yamanashi et al. (2017) showed that R3HBA could act as a therapeutic candidate for the treatment of stress-related mood disorders (depression). The mechanism involves an anti-inflammatory effect mediated by a reduction in the levels of the inflammatory cytokines inter-leukine 1 $\beta$  and tumor necrosis factor  $\alpha$  in the hippocampus of mice. Recently, other positive effects after a R3HBA administration is the reduction of proliferation of colonic crypt cells and potential suppression of intestinal tumour growth (Dmitrieva-Posocco et al., 2022).

Other potential uses of R3HBA include its use as a chemical chaperone for amelioration of heat-mediated denaturation and oxidative damage by  $\text{Cu}^{2+}$  and  $\text{H}_2\text{O}_2$  produced on industrially relevant enzymes such as lipases and lysozymes (Obruca et al., 2016).

Finally, R3HAs can be used as building blocks that can be biologically produced, excreted from cells, and then polymerized or co-polymerized to yield PHAs with tunable mechanical and thermal properties (Wang et al., 2018). Advantages of the *ex-situ* polymerization starting from biomonomers over the conventional approach of biopolymer accumulation inside cells include (Adkins et al., 2012): (i) simplified downstream product recovery of the extracellular biomonomers compared to the intracellular polymers, (ii) the polymerization in controlled chemocatalytic environments allows for polymers with finely tuned properties and high purities, and (iii) higher diversity of plastics thanks to the ability to co-polymerize different monomers. Examples of *in-vitro* synthesis include the production of PHB from R3HBA by

a three-enzyme system that only consumes ATP and the monomer (Jossek et al., 1998). The yield of this system was recently improved by using a thermostable acetyl-CoA synthetase, CoA transferase and PHA synthase (Tajima et al., 2016). A polymer incorporating lactate and R3HBA residues was produced by Tajima et al. (2012), using an engineered PHA synthase capable of lactate polymerization. An excellent revision of the chemosynthesis of copolymers containing different R3HAs monomers and lactate was recently published (Hiroe et al., 2019). However, a general drawback of these systems so far is the consumption of ATP, specifically to drive the activation of acetate to acetyl-CoA, a molecule that needs to be present in the reaction mixture to act as the CoA donor to yield the hydroxyacyl-CoAs required for the polymerization reaction.

## 2.2. SUBSTRATES TO PRODUCE PHAs AND THEIR MONOMERS

Substrates commonly used for the industrial production of PHAs include corn starch, sucrose obtained from sugar cane and vegetable oils, all edible feedstock requiring arable lands, and agricultural practices that affect both their economy and sustainability (Levett et al., 2016). Commercial PHAs are produced using sucrose in *A. lata* (Biomer Germany, with trade name Biomer™) and *Bacillus* sp. (PHB Industrial S.A. Brazil, Biocycle™); glucose from corn in *C. necator* (Metabolix, Mirela™ and Tianan Biologic Material, Enmat™); or fatty acids using *Pseudomonas putida* (ETH, PHA™) or *C. necator* by Kaneka Corporation and marketed as Kaneka PHBH™ (Bugnicourt et al., 2014; Chen, 2009; Możejko-Ciesielska & Kiewisz, 2016).

Due to the high costs and sustainability concerns associated with the raw materials traditionally used in the production of PHAs, the use of agro-food waste, food industry waste, and other non-food industry residues, have been increasingly studied (Braunegg et al., 2004). For example, several solid residues have been examined such as rice bran (Oh et al., 2015), pea-shells (Kumar et al., 2016), chicory roots (Haas et al., 2015), potato peels, apple pomace, onion peels (Kumar et al., 2016), grape pomace (Follonier et al., 2015), animal farm waste, poultry litter (Bhati & Mallick, 2016) and palm oil (Loo et al., 2005). In the case of food wastes for PHAs production, literature report on the use of spent coffee grounds (Cruz et al.,

2014), food waste composite (Amulya et al., 2015), and used cooking oil (Borrero-de Acuña et al., 2019; Gómez Cardozo et al., 2016).

Finally, non agro-food residues are generated by biodiesel manufacturing: crude glycerol (de Paula et al., 2017); oil cake hydrolysate (Bera et al., 2015), and biodiesel fatty acid by-product from glycerol purification (Cruz et al., 2016). Glycerol can be used for the accumulation of mcl-PHAs and short-chain-length PHAs in *Pseudomonas putida* strains (Poblete-Castro et al., 2014), *C. necator* DSMZ 4058 (Mothes et al., 2007) and *Bacillus megaterium* (Naranjo et al., 2013), among others.

The availability and sustainability issues of conventional substrates have motivated the exploration of alternative feedstocks as sources of carbon and energy for microbial production of chemicals, such as lignocellulose which can be obtained from the “residues” left after the harvest of agricultural products or from dedicated high yield cultivars (poplar, *eucalyptus*, *miscanthus*) (Loow et al., 2016), thus reducing the environmental burden associated with their production. Reducing even further water and land usage, compounds containing one carbon atom, such as methanol and formate can be obtained from the reduction of CO<sub>2</sub> using electrons harnessed from solar energy (Agarwal et al., 2011; Pérez-Fortes et al., 2016; Yishai et al., 2016).

Among inexpensive substrates that are readily available for reducing the total cost of PHAs production, certain C1 carbon sources, e.g., methane, methanol, and CO<sub>2</sub> have received a great deal of attention due to their contribution to global warming (Khosravi-Darani et al., 2013). Production of PHB from waste methane may help reducing the impact of the greenhouse effect of this gas. Accumulation of PHB, but not other PHAs, has been reported in several *Methylocystis* species using methane and *Methylobacterium* from methanol (Strong et al. (2016). In this regard, Listewnik et al. (2007) estimated a price of 6.35 UK pounds per kg of PHB produced from natural gas in a two-stage plant producing 500 tons PHB per year. Similarly, Levett et al. (2016) estimated a production cost range of 4.1 to 6.8 USD per kg of PHB, with a reduction in the share of the carbon source in the total product cost from 30% when sugar feedstocks are used to 22% for methane. However, these

production costs are high when compared to the estimations made by Posada et al. (2011), who performed a techno-economic evaluation of PHB production from glycerol as energy and carbon source. They reported production costs between 1.9 and 2.5 USD per kg and a substrate share between 5 and 8%. The higher production cost when methane is used as a substrate is greatly influenced by the low overall mass transfer coefficient of methane into the medium. This leads to large reactors and, thereby high investment and operating costs.

Knallgas bacteria, such as *C. necator* H16 and *A. lata*, can use mixtures of hydrogen, carbon dioxide and oxygen for the accumulation of PHB (Reinecke & Steinbüchel, 2009), biofuels (Brigham, 2019) or acetoin (Windhorst & Gescher, 2019). Albeit the production of PHB has been studied thoroughly with cultures of *R. eutropha* or *Ideonella* sp. O-1, accumulating over 60 g L<sup>-1</sup> of PHB (Tanaka et al., 1995; 2011), no reports of PHAs accumulation aside PHB are available.

### 2.3. ACCUMULATION AND MOBILIZATION OF PHAs

The model organism for PHB production is *C. necator* a gram-negative, obligate aerobe, capable of autotrophic growth in the presence of hydrogen, CO<sub>2</sub> and oxygen, and heterotrophic growth and PHB production from a wide variety of carbon sources including sugars (chiefly fructose in the wild type organism *C. necator* H16 ATCC 17699) and organic acids (Lu et al., 2016). For example, using glucose in a fed-batch culture of *R. eutropha* NCIMB 11599, a mutant of *R. eutropha* H16 capable of using glucose, a concentration of biomass of 164 g L<sup>-1</sup> was obtained, with a PHB content of 74% (Kim et al., 1994).

In *C. necator*, synthesis of PHB occurs when excess carbon in the form of acetyl-CoA is condensed via a  $\beta$ -ketothiolase (EC 2.3.1.16) to generate acetoacetyl-CoA, which is then reduced to R3HBA-CoA by a NADPH-dependent acetoacetyl-CoA reductase (EC 1.1.1.36). Finally, the enzyme PHB synthase (EC 3.1.1.75) catalyzes the polymerization of (*R*)-3-hydroxybutyryl-CoA monomers. This pathway is the most widespread route in bacteria for providing R3HBA-CoA monomers (Steinbüchel & Hein, 2001). Production of mcl-PHAs, such as the polymers accumulated in *Pseudomonas* spp., requires precursors derived from

the dissociated fatty acid biosynthesis pathway unless these precursors are supplied through related carbon sources (such as octanoic acid for the synthesis of poly(3-hydroxyoctanoate). For details regarding this pathway, the reviews by Lu et al. (2009) and Suriyamongkol et al. (2007) are highly recommended.

The regulation of PHB biosynthesis is tightly connected to the cellular levels of reduced nicotinamide nucleotides. Lee et al. (1995) found that when *R. eutropha* was cultivated in nitrogen-limited media, the NADPH/NADP and NADH/NAD<sup>+</sup> ratios and the intracellular concentrations of NADH and NADP were higher than those found under nitrogen-sufficient conditions. Moreover, the rate of PHB accumulation was found to increase with both NADH/NAD<sup>+</sup> and NADPH/NADP ratios. This effect was explained through the analysis of citrate synthase activity. Citrate synthase was inhibited by NADPH and NADH, thus funneling the carbon to PHB instead of being directed to the tricarboxylic acid cycle. Similar conclusions were reported by Henderson & Jones (1997).

Although PHB accumulation occurs under unfavorable conditions for growth induced by nutrient limitation of oxygen, nitrogen or phosphorous, with excess carbon (Steinbüchel & Hein, 2001), these conditions impact the productivity of the PHB accumulation phase. Grousseau et al. (2013) showed that sustaining a controlled residual growth rate, by feeding a controlled amount of phosphate along with the carbon source (butyric acid), allows for an improved specific productivity and high yield of PHB. Interestingly, using Metabolic Flux Balances they showed that the maximal specific PHB production rate is defined by the maximum specific rate of NADPH produced. When a low growth rate is allowed in the fed-batch fermentation (for example, feeding a nitrogen source), the NADPH is produced in the Entner-Doudoroff pathway, whereas without biomass production regeneration of NADPH is only possible via isocitrate dehydrogenase.

Another possibility to increase PHB volumetric productivities is to rely on microorganisms where growth and PHB production occur simultaneously. In this regard, *A. lata* consumes glucose, sucrose and acetic acid (Chen et al., 1991), but it does not consume xylose, accumulating PHB during its growth (Yamane et al., 1996). In a fed-batch culture using

sucrose as the carbon source and continuous feeding of ammonia, controlled by the decrease in pH as the culture consumes the source of nitrogen (pH-stat), 143 g L<sup>-1</sup> of cells with 50% PHB were attained with a PHB productivity of 3.97 g L<sup>-1</sup>h<sup>-1</sup>, one of the highest ever reported (Yamane et al., 1996). One year later, Wang and Lee (1997) reported even higher productivity (4.94 g L<sup>-1</sup>h<sup>-1</sup>) and PHB intracellular content in *A. lata* (88%) applying nitrogen limitation in a two-stage fed-batch culture (nitrogen sufficient followed by nitrogen-limited culture).

Assuming that PHAs act as a reserve compound of carbon and energy, without a source of carbon and energy, but in the presence of other growth factors (such as nitrogen or oxygen), PHAs should be depolymerized into their monomers and incorporated into the metabolism, using the degradation products for growth and survival, a process termed PHA mobilization. This behavior has been shown at least in *C. necator* H16 (Juengert et al., 2017; Uchino et., 2007), *A. lata* (Lee et al., 1999), *Legionella pneumophila* (James et al., 1999), *Hydrogenophaga pseudoflava* (Choi et al., 1999) and *Halomonas* sp. KM-1 (Kawata et al., 2015).

Compared to PHB accumulation, depolymerization of PHB to R3HBA, and its transformation to acetyl-CoA, has been less studied as confirmed by fewer reports in the literature. However, evidence exists indicating that the granules of PHB and other PHAs are supramolecular complexes (called carbonosomes), constituted by a polymer core and a surface layer of at least a dozen proteins (Sznajder et al., 2015), but without a phospholipids membrane (Bresan et al., 2016). The proteins in the carbonosomes include the PHA synthase (PhaC) and PHB depolymerases (PhaZs), which are thought to be constitutively expressed (Brigham et al., 2012; Lawrence et al., 2005).

It has been reported that PHB synthesis and its degradation can happen simultaneously in the model PHB accumulating organism *C. necator* (Doi et al., 1990; Taidi et al., 1995). Doi and co-workers concluded this after cultivating *C. necator* in butyrate as the carbon source under nitrogen-free conditions, thus inducing the accumulation of PHB, and changing the carbon source to pentanoic acid. After the shift in the substrate, the accumulated PHB was gradually

replaced by poly(3-hydroxyvalerate-co-3-hydroxybutyrate) without a net increase of total polymer content in the cells. This indicates that PHB was degraded and replaced by polyhydroxyvalerate (PHV) even in the absence of a nitrogen source. Similarly, Taidi et al. (1995) showed a turnover of PHB after the accumulation of the polymer ceased in a nitrogen-limited batch culture with glucose as the sole carbon and energy source. The turnover was evidenced by the incorporation of radioactivity into the accumulated polymer after feeding labeled glucose (D-[U-<sup>14</sup>C] glucose). Interestingly, the high-molecular-weight polymer accumulated during the unlabeled glucose phase was replaced by a low-molecular-weight polymer during the labeled glucose experiment. These observations are in agreement with the evidence showing the constitutive expression of PHB synthase and PHB depolymerase in *R. eutropha* (Lawrence et al., 2005; Sznajder et al., 2015). Confirmation of constitutive expression of PHB synthase and depolymerase in other organisms is scarce, except for the study of Kim et al. (1996) who found simultaneous activities of both enzymes during the batch culture of *A. lata* under nitrogen-limited conditions.

Thereby, this leads to the intriguing question of how the synthesis and mobilization of PHAs are regulated and particularly, how a cycle of simultaneous synthesis and degradation is avoided. Considering that the simultaneous polymerization and depolymerization of PHB and its conversion to acetyl-CoA through R3HBA, acetoacetate and acetoacetyl-CoA requires one NADPH molecule and one ATP molecule and produces only one NADH molecule, the cycle would consume energy for the formation of thioester bonds, thus creating a futile cycle.

To tackle this unsolved issue, Uchino et al. (2007) isolated native PHB granules produced in *R. eutropha* by glycerol gradient centrifugation to preserve the proteins bound to the granule and discovered that in the presence of CoA, these granules produced R3HBA-CoA and small amounts of acetyl-CoA. If NAD<sup>+</sup>, but not NADH, is added to the initial reaction mixture, R3HBA-CoA remains undetectable, but the concentration of acetyl-CoA increases five-fold. The authors assumed that in the presence of NAD<sup>+</sup>, the intermediately formed R3HBA-CoA is rapidly transformed to acetyl-CoA in NAD<sup>+</sup> dependent reactions. The authors also found, as expected, that the native granules release R3HBA in pH-stat experiments using methods previously described (Gebauer & Jendrossek, 2006). Therefore, it remains unclear which

depolymerization mechanism, hydrolysis or thiolysis, is used *in-vivo* for the mobilization of PHB.

In order to identify the enzymes responsible for the thiolytic cleavage, Uchino et al. (2007) incorporated the PHB synthesis genes *phaCAB* in *E. coli* S17-1 along with the phasin gene *phaP1*, the depolymerase gene *phaZa1* or *phaP1 + phaZa1*. Interestingly, the recombinant strain only produced R3HBA-CoA in the presence of CoA when both *phaP1* and *phaZa1* were present in a *phaCAB* background. Moreover, no significant amounts of acetyl-CoA were detected in this experiment, an indication that downstream enzymes for the use of R3HBA-CoA were absent in *E. coli*.

The study of Uchino et al. (2007), suggests that *in-vivo* intracellular depolymerization of PHB does not represent a futile cycle and an energy waste in the form of thioester bonds. If the main product of PHB polymerization, at least in *R. eutropha*, is R3HBA-CoA instead of R3HBA, then there is no loss of energy for the formation of acetoacetyl-CoA from acetoacetate.

Regarding the regulation of PHB synthesis and degradation, Juengert et al. (2017), found that the degradation of the accumulated PHB in *C. necator* was fast and efficient in the absence of the alarmone (p)ppGpp, and when present, (p)ppGpp directly or indirectly inhibits PHB mobilization. (p)ppGpp is a key signaling molecule, which, when present at high concentrations, induces the stringent response in *E. coli* and other bacterial species. This alarmone accumulates in amino acids starved cells and inhibit the synthesis of ribosomal and transfer RNAs (Srivatsan & Wang, 2008). The results suggest that PHB accumulation under nitrogen-limited conditions is favored by the inhibition of PhaZ1 by (p)ppGpp as shown by the observed PHB accumulation in a triple knockout mutant ( $\Delta spoT1 + \Delta spoT2 + \Delta phaZa1$ ), which was unable to produce (p)ppGpp. In contrast, the double knockout mutant  $\Delta spoT1 + \Delta spoT2$  accumulated negligible amounts of PHB. In subsequent work, Juengert et al. (2018) identified that PhaC1 was phosphorylated in multiple phosphosites during the stationary growth phase in nutrient broth medium with gluconate as carbon source, but it was not modified during the exponential and PHB accumulation phases or when grown in a

fructose-mineral medium. On the other hand, PhaZa1 was phosphorylated in Ser35 both during the exponential and stationary growth phases. Mutagenesis of the identified residues showed that PHB accumulation was unaffected for most mutants of PhaC1, except for a mutant with changes to four aminoacid residues. On the other hand, exchanging the phosphorylated residues in PhaZa1 to aspartate (a phosphomimetic<sup>1</sup> residue) produced mutants with a strongly reduced ability to mobilize the accumulated PHB.

Little experimental evidence exists concerning the role of the stringent response on the accumulation of PHA in other organisms. In this regard, Mozejko-Ciesielska et al. (2017) obtained a *relA/spot* mutant of *P. putida* KT2440. This mutant, unable to induce the stringent response, was used to assess the accumulation of PHA under nitrogen deprived and optimal nitrogen conditions. Results show that this mutant was able to accumulate mcl-PHAs under both conditions.

## 2.4. PRODUCTION OF R3HAs FROM PHAs

Two categories of strategies to produce chiral hydroxyalkanoic acids have been identified in native PHB producers bacteria, *ex-vivo* strategies and *in-vivo* strategies using non-genetically modified organisms.

### 2.4.1. *In-vitro* strategies

Under this approach, the accumulated PHAs are extracted from cells and then subjected to a chemical or enzymatic depolymerization process. The PHA recovery process starts when cells are separated by centrifugation to increase product concentration and to remove the components of the culture media. The concentration step is followed by drying or

---

<sup>1</sup> Phosphomimetic are amino acid substitutions that mimic a phosphorylated protein, thereby activating (or deactivating) the protein.

lyophilization of the concentrated biomass. The extraction of PHAs from the dried biomass can be performed by solvent extraction, by dissolving the biomass using oxidizing agents or by disrupting cells to liberate the PHAs granules (Kosseva & Rusbandi, 2018). Mechanical cell disruption techniques, such as bead milling and high-pressure homogenization, have been widely used to release intracellular protein and have been adapted for PHAs recovery (Kunasundari & Sudesh, 2011; Tamer, 1998). Tamer and colleagues compared bead milling and high-pressure homogenization for the recovery of PHB accumulated in *A. lata*. They recommended bead milling over high-pressure homogenization as the preferred method for recovering PHB from heat-shocked cells of *A. lata*. Interestingly, since PHB is recovered without solubilizing it, the native amorphous morphology of the polymer was conserved.

The common method for PHAs extraction is the use of solvents due to its speed and simplicity. Solvents alter cell membrane and then dissolve the polymers. PHAs are recovered by solvent evaporation or precipitation with an anti-solvent (Hänggi, 1990; Liddell, 1999). In the solvents category, the chlorinated hydrocarbons chloroform, 1,2-dichloroethane and methylene chloride are used (Ramsay et al., 1994). Non-chlorinated solvents have been proposed such as ethylene carbonate and 1,2-propylene (Lafferty & Heinzle, 1977) or solvent mixtures of acetone/ethanol/propylene carbonate (Fei et al., 2016). On the other hand, the precipitation of PHAs is generally induced by non-solvent agents such as water, ethanol, and methanol (Ramsay et al., 1994; Mikkili et al., 2014). In summary, solvent extraction is characterized by numerous advantages such as the elimination of endotoxins and low polymer degradation (Liddell, 1999). However, there are limitations in the use of solvents, including their high cost (Poirier et al., 1995), high energy consumption for the separation of miscible solvents and anti-solvents, and risks both for the operator and for the environment that needs to be considered during the process design stage (Gorenflo et al., 2001).

On the other hand, digestion with sodium hypochlorite decomposes the cells allowing high levels of PHA purity to be reached (Hahn et al., 1994; Kim et al., 2003). However, sodium hypochlorite degrades PHB, resulting in a polymer with low molecular weight (Mikkili et al., 2014; Ramsay et al., 1990).

#### 2.4.1.1. Chemical and enzymatic hydrolysis of recovered PHAs

After recovery and purification, the extracted PHAs can be chemically or enzymatically converted into high-purity 3-hydroxyalkanoic acids. Chemical methods for modifying PHB have been reported for the production of (*R*)-methyl 3-hydroxybutanoate and (*R*)-3-hydroxybutanoic acid, these methods involve the use of methanol and sulfuric acid and methanol and *p*-toluenesulfonic acid monohydrate, respectively (Seebach et al., 2003). Another approach, reported by Lee et al. (2000), considers the acidic alcoholysis of PHB, yielding methyl, ethyl and *n*-propyl esters of R3HBA, using 1,2-dichloroethane as solvent with either sulfuric acid or hydrochloric acid as catalyst. De Roo et al. (2002) extended this method to produce *mcl*-(*R*)-3-hydroxyalkanoic acids (*mcl*-R3HAs) from the *mcl*-PHAs accumulated in *P. putida*. After a step of acid methanolysis, the obtained R3HA methyl esters were distilled into fractions and saponified to yield the corresponding (*R*)-3-hydroxycarboxylic acids.

The multistep chemical processes outlined in the previous paragraph can be efficiently catalyzed by PHA depolymerases in a single step. This subject has been recently reviewed (Roohi et al., 2018). Thus, only some selected works will be covered. Several extracellular depolymerases have been identified and characterized (an excellent tool for its classification was presented by Knoll et al., 2009). Extracellular PHA depolymerases degrade denatured PHA granules whose structure has been altered during the extraction process and are not covered by the native layer of proteins surrounding the granule. One exception is the PHB depolymerase from *Pseudomonas lemoignei*, which is active against native PHB granules (Handrick et al., 2001).

PHB degradation studies by extracellular depolymerases are typically performed using PHB films as substrate, producing R3HBA as the hydrolysis product (Polyák et al., 2018), thus limiting the access of enzymes to its substrate. In order to achieve high R3HBA titers, a high initial concentration of PHB should be used. However, due to its water-insoluble nature, only low PHB concentrations can be suspended in water. For example, 24 g L<sup>-1</sup> of 3RHBA were produced from 25 g L<sup>-1</sup> of suspended PHB powder using an extracellular PHB depolymerase

from *Pseudomonas* sp. DS1001a (Li et al., 2016). Similarly to with chemical hydrolysis methods, enzymatic hydrolysis requires the separation and partial purification of the PHA accumulated in cells and this contributes to increase the overall costs of R3HAs production. These disadvantages could be eliminated in processes where R3HAs are produced directly from the PHAs accumulated by the cells using their own intracellular enzymes for the depolymerization process.

#### 2.4.2. *In-vivo* strategies

##### 2.4.2.1. Hydroxy-acids production by *in-vivo* depolymerization of PHAs: the polymerization-depolymerization system

*In-vivo* depolymerization of accumulated PHAs to R3HAs has been reported to occur with high yields in *A. lata* (Lee et al., 1999) and *Pseudomonas putida* GPO1 (Ren, Grubelnik, Hoerler, Ruth, Hartmann, et al., 2005). The depolymerization process has been shown to be highly dependent on pH. Lee et al. (1999), in a pioneering work, achieved the depolymerization of PHB to R3HBA in *A. lata* cells grown in a mineral medium with sucrose as the carbon and energy source. The depolymerization process was carried out at different initial pHs in water, after washing the cells, at 37 °C and without shaking to minimize oxygen transfer. Exceedingly high R3HBA yields and productivities, as high as 96% in 30 minutes were found at pH 4, but not at higher pH values. This result was explained in terms of the effects of pH on PHB depolymerase and Hbd activities. The highest activity of PHB depolymerase was achieved at pHs 3 and 4, at which the monomer production rate was also the highest. Interestingly, no activity of Hbd was detected at pH 4 in *A. lata*, therefore it was argued that no R3HBA was degraded to acetoacetate. At pH 5, the attained depolymerization yield was 31% and decreased towards neutral pHs. From the work of Lee et al. (1999), it is not possible to ascertain whether these lower yields are due to the consumption of the released R3HBA or a decrease in the amount of PHB depolymerized. Presumably the latter is true since the depolymerization assays were performed without shaking, thus restricting the ability of cells to regenerate NADH into NAD<sup>+</sup>, a cofactor of Hbd.

Following the high depolymerization yields obtained at low pHs, the authors assayed the *in-vivo* depolymerization in *Ralstonia eutropha* NCIMB 11599, *Pseudomonas oleovorans* ATCC 29347 and *Pseudomonas aeruginosa* PAO1 (DSM 1707) at pH values below 7. The depolymerization yields and productivities were close to 20% for *C. necator* and below 10% for *Pseudomonas* species.

Ren et al. (2005) showed that for *P. putida* GPo1, the PHB depolymerization rate was higher at pH 11 in citrate buffer, which helps to control the pH drop caused by the accumulation of R3HAs. The released monomers corresponded to (*R*)-3-hydroxyoctanoic (R3HO) acid and (*R*)-3-hydroxyhexanoic acid (R3HHx), in a proportion closely matching the ratio of monomers in the copolymer accumulated under continuous cultivation with octanoic acid as carbon and energy source. The depolymerization was performed for 6 hours, thus decreasing the volumetric productivity compared to the work of Lee et al. (1999). A second factor decreasing the volumetric productivity was the low initial PHA concentration used. However, this work showed that R3HAs different than R3HBA could be obtained with high yields by using the correct pH during the depolymerization process. This work was further extended by Ruth et al. (2007) showing that applying the same depolymerization process at pH 10 to PHAs accumulated in *P. putida* GPo1, grown under continuous cultivation with either octanoic, undecanoic or 10-undecenoic acid, led to the production of R3HO, R3HHx, (*R*)-3-hydroxy-10-undecenoic acid, (*R*)-3-hydroxy-8-nonenic acid, (*R*)-3-hydroxy-6-heptenoic acid, (*R*)-3-hydroxyundecanoic acid, (*R*)-3-hydroxynonanoic acid and (*R*)-3-hydroxyheptanoic acid.

Recently, Anis et al. (2018) studied the *in-vivo* depolymerization of PHAs accumulated in *P. putida* Bet001 after 48 hours of batch culture with lauric acid as the carbon source and under nitrogen-limited conditions. The depolymerization was performed for 48 hours in 0.2 M Tris-HCl buffer, pH 9 and 30 °C. Unlike the report of Lee et al. (1999) using *Pseudomonas aeruginosa* PAO1 (DSM 1707), *P. putida* Bet001 produced R3HO, R3HHx, (*R*)-3-hydroxydecanoic acid (R3HD) and (*R*)-3-hydroxydodecanoic acid (R3HDD) with very different yields, the highest depolymerization yield being achieved for R3HD. It is not clear if this difference in yields was due to a channeling of R3HO, R3HHx and R3HDD toward

cell metabolism or if they have yet to be hydrolyzed from the granules and thus, reflects an affinity of the PHA depolymerases.

The experiments performed by Lee et al. (1999), Ren et al. (2005) and Ruth et al. (2007) used either water or phosphate buffer as depolymerization media at a pH initially set at a given value. However, the release of R3HAs resulted in a decrease in the initial pH, potentially affecting process efficiency. This factor was recognized by Wang et al. (2007), leading to the design and application of a pH-stat process. In this system, the pH is controlled at a setpoint by the automatic addition of an alkaline solution (NaOH). Interestingly, the amount of NaOH added in time (the flow of the alkaline solution), if recorded, allows the estimation of the release rate of acids (hydroxy acids and protons). Using a pH-stat apparatus coupled to a dissolved oxygen meter, Wang et al. (2007) investigated the behavior of the wild type *P. putida* GPO1 strain and a PHA depolymerase negative mutant. Results showed that the rate of acid production (not necessarily hydroxy acids) of the mutant strain was only 27 % of the rate obtained with the wild type. Analysis of the supernatants revealed that the acids released by the wild type were R3HO and R3HHx. On the other hand, no detectable amounts of these compounds were found in the supernatants of the depolymerase mutant. Moreover, oxygen consumption measurements indicated a low respiratory activity for the wild type and a high respiration rate for the mutant. Finally, they also found that the acid production rate of the mutant, but not of the wild type, could be enhanced by aeration. These results support the hypothesis that the high depolymerase activity allowed the wild type strain to compensate for the high external pH. On the other hand, in the PHA depolymerase deficient mutant this could only be performed by the production of protons in aerobic conditions.

Although the results obtained by Wang et al. (2007) supported this hypothesis for the depolymerization of PHAs to R3HAs at high pHs, the compensatory mechanism of pH involved in it does not explain the behavior recorded in *A. lata* at low pH values. Thus, the only conclusion applicable for both species is that the depolymerization process in *A. lata* and *P. putida* GPO1 the depolymerization process is enhanced at a certain pH and simultaneously the consumption of the released monomers is impaired.

Process engineering strategies for R3HAs production are nearly nonexistent with except for the work of Ren et al. (2007), who coupled a chemostat culture of *P. putida* GPO1 (nitrogen-limited,  $D=0.1 \text{ h}^{-1}$ , octanoic acid as the sole carbon source) to a second continuous depolymerization stirred tank reactor. The depolymerization tank was operated as a pH-stat at a pH of 10 and its discharge was sent to a plug-flow reactor with a residence time of 6 hours. This continuous system does not require the separation of cells or the exchange of the culture media to water or buffer. Only a simple pH shift was enough to achieve a depolymerization yield of 90%, however, the volumetric productivity was not different from previously reported works using batch depolymerization (Ren, Grubelnik, Hoerler, Ruth, Hartmann, et al., 2005). Clearly, the volumetric productivity could be improved by increasing the concentration of PHA produced in the chemostat.

A different strategy for the *in-vivo* production of R3HBA has been reported using several strains of *Halomonas*. Using *Halomonas* sp. KM-1,  $15.2 \text{ g L}^{-1}$  of R3HBA could be obtained under microaerobic conditions from  $16.4 \text{ g L}^{-1}$  of PHB that was accumulated under aerobic conditions using glycerol as the sole carbon and energy source. The initial concentration of the nitrogen source was  $12.5 \text{ g L}^{-1}$  (sodium nitrate), hence the limiting nutrient was presumably different from nitrogen, although this was not clarified (Kawata et al., 2012). These conditions, when applied to cultures grown in glucose (Kawata et al., 2014), did not result in any R3HBA secretion. The glucose concentration decreased from 20% to 6% during the first 36 hours of culture and then remained constant. Thus, in this experiment, a nitrogen shortage was suspected.

When extra nitrate was pulse fed at 24, 36 and 48 h to a culture of *Halomonas* sp. KM-1 with 20% (w/v) glucose, then  $40.3 \text{ g L}^{-1}$  R3HBA were secreted with a productivity of  $0.48 \text{ g L}^{-1}\text{h}^{-1}$  after a shift from aerobic cultivation for 60 h to microaerobic cultivation for 24 hours. No R3HBA was secreted when no extra nitrate was supplemented (Kawata et al., 2014) indicating that a regulatory mechanism was controlling the activity of the PHB depolymerase, presumably related to the stringent response. Glucose concentration during the depolymerization phase under microaerobic conditions was zero and a decrease in total cell concentration was observed. This behavior is consistent with the depolymerization of the

accumulated PHB with only partial use of the released R3HBA for growth (the calculations show that 79% of the depolymerized PHB was recovered as R3HBA, equivalent to 55 % of the maximum recovery if all the accumulated PHB is transformed to R3HBA). This can be ascribed to the microaerobic conditions applied which limited the use of acetyl-CoA for growth and the regeneration of NAD<sup>+</sup> from NADH. Since NAD<sup>+</sup> is the cofactor used by Hbd, this could explain the high titers of R3HBA. Unfortunately, no nitrate concentrations during the growth or depolymerization phase were reported to ascertain whether it is consumed or not during the microaerobic cultivation. Moreover, PHB was not completely mobilized. Since no information regarding the pH of the culture (or its control) was presented, presumably the lack of complete depolymerization was caused by a decrease in pH.

A new species of *Halomonas*, *Halomonas* sp. OITC1261 was isolated by Yokaryo et al. (2017). Unlike *Halomonas* sp. KM-1, *Halomonas* sp. OITC1261 produces R3HBA under aerobic conditions and, apparently, without the need to supplement with extra nitrogen source once the carbon source is exhausted to promote PHB depolymerization. In fact, the data presented by Yokaryo et al. (2017) showed that R3HBA is produced concomitantly with PHB after approximately 10 hours of cell growth. Presumably, PHB and R3HBA started to accumulate after the exhaustion of the nitrogen source, which could also explain the increase in the dissolved oxygen concentration. It is not clear whether the production of R3HBA occurs through PHB *in-vivo* depolymerization or proceeds directly from (*R*)-3-hydroxybutyryl-CoA or acetoacetate.

#### 2.4.2.2. Production of R3HAs in genetically modified microorganisms

- Mutants of native PHA producers

The exploration of alternative pathways for the production of R3HAs emerges from the recognition of two characteristics found in native PHA producers: (i) depolymerization products can be metabolized [for example, R3HBA is converted to acetoacetate by the Hbd enzyme (Tokiwa & Ugwu, 2007)] and (ii) producing R3HA is a two-stage process where PHA is accumulated and then depolymerized in a subsequent step often requires a change in

media or process conditions. A process for the isolation of *hbd* null mutants was described more than 40 years ago (Lafferty & Heinzle, 1977), including UV mutagenesis, followed by the destruction using antibiotics of the bacteria capable of R3HBA assimilation and the selection of *hbd* null mutants by spread plating of the individuals surviving the treatment with bactericidal.

Ugwu et al. (2008) reported the production of R3HBA in *C. necator* through the acetoacetate pathway induced by random mutation using UV radiation. The mutants achieved a titer of 0.150 g L<sup>-1</sup> of R3HBA in a 5 L fermenter after 48 hours of cultivation using either glucose or sucrose as carbon source. The concentration of R3HBA was increased by feeding lithium acetoacetate to resting cells of the mutant strain, reaching 0.84 g L<sup>-1</sup> of R3HBA. The results were interpreted as indicative of a disruption in the *phbB* gene (coding for acetoacetyl-CoA reductase), making this strain unable of PHB accumulation. Ugwu et al. (2008) reasoned that the excess of acetoacetyl-CoA produced under conditions allowing for PHB accumulation was channeled towards R3HBA via acetoacetate.

Using UV mutagenesis, Ugwu et al. (2011) obtained an R3HBA-producing mutant of *A. lata*. When cells of this mutant were resuspended in phosphate buffer containing glucose (1 % v/w), ethylacetoacetate (2% v/v) or (*R,S*)-1,3-butanediol (3 % v/v), the resting cells produced R3HBA at concentrations of 6.5, 7.3 and 8.7 g L<sup>-1</sup>, respectively.

- Recombinant *E. coli* strain: An approximation of thioesterase shortcut system

An alternative process to produce R3HBA is the use of recombinant methods to express PHA related genes in well-characterized non-PHA producing and fast-growing microorganisms such as *E. coli* (Chen et al., 2013). Lee and co-workers modified *E. coli* strains by inserting two plasmid systems containing the *phaA<sub>Re</sub>*, *phbB<sub>Re</sub>*, and *phbC<sub>Re</sub>* genes and the *phaZI<sub>Re</sub>* depolymerase from *Ralstonia eutropha* (Lee & Lee, 2003). This design achieved an R3HBA concentration of 9.6 g L<sup>-1</sup> in 51 hours of fermentation using glucose as a carbon source. Similarly, Shiraki et al. (2006) engineered *E. coli* and *R. eutropha* to express the same enzymes leading to the production of PHB but different depolymerases. The strains compared

were an *R. eutropha* null mutant for *hbd* and a recombinant *E. coli* strain harboring the synthetic PHB operon of *R. eutropha* and an extracellular depolymerase of *Paucimonas lemoignei*. The production of R3HBA by the *hbd* null mutant of *R. eutropha* was found to be dependent on the supply of oxygen, achieving a R3HBA concentration of 3.13 g L<sup>-1</sup> under anaerobic conditions and concentrations in the range of 0.41–1.04 g L<sup>-1</sup> under aerobic culture conditions. Presumably, the accumulated PHB was depolymerized under aerobic conditions to a molecule different than R3HBA, such as R3HBA-CoA, or the produced R3HBA was metabolized using pathways not using Hbd. In fact, Shiraki et al. (2006) verified that no *hbd* was expressed and no Hbd was found in the supernatant fraction of cells grown under PHB accumulation conditions. However, it was not verified whether the mutant could grow in R3HBA. On the other hand, the recombinant *E. coli* harboring the PHB operon and the *P. lemoignei* depolymerase reached a concentration of approximately 7.3 g L<sup>-1</sup> of R3HBA after 100 hours. Since *E. coli* is not a native PHB producer, presumably there were no alternative pathways for R3HBA production or consumption different from the inserted genes (Shiraki et al., 2006).

Alternatively, there are pathways that can be constructed without accumulation and depolymerization of PHB. For example, R3HBA-CoA can be directly hydrolyzed into R3HBA using TesB, a class II thioesterase enzyme that catalyzes the hydrolysis of the CoA moiety from acyl-CoAs (Naggert et al., 1991). Liu et al. (2007) used *E. coli* BW25113 as host for the expression of *phbA* and *phbB* genes from *R. eutropha* and *tesB* from *E. coli*. This strain produced 3.98 g L<sup>-1</sup> R3HBA in a shake flask culture using 11.4 g L<sup>-1</sup> of glucose. When using a fed-batch strategy, 12.2 g L<sup>-1</sup> R3HBA were accumulated in 24 hours. The productivity achieved in this system (0.51 g L<sup>-1</sup> h<sup>-1</sup>) is among the highest reported so far for the direct production of R3HBA. Previous to this work, it was well established that TesB was capable of releasing CoA from acyl CoA of C<sub>6</sub>-C<sub>18</sub> carbon length, as well as 3-hydroxyacyl-CoA esters, to their corresponding free fatty acids (Naggert et al., 1991), but not from short-chain length hydroxyacyl-CoA. In this regard, Zheng et al. (2004) reported the production of R3HD from fructose by a recombinant *E. coli*. The recombinant strain contains the *phaG* gene from *P. putida* encoding for (*R*)-3-hydroxydecanoyl-acyl carrier protein-coenzyme A transacylase. PhaG links fatty acid de novo biosynthesis and PHA production by catalyzing

the conversion between (*R*)-3-hydroxydecanoyl-acyl carrier protein and (*R*)-3-hydroxydecanoyl-CoA (Rehm et al., 1998). When the *E. coli* strain containing only PhaG was cultured in shake flasks with 20 g L<sup>-1</sup> fructose, 0.64 g L<sup>-1</sup> of R3HD, and 2.11 g L<sup>-1</sup> of biomass were obtained. The R3HD titer was increased to 1.02 g L<sup>-1</sup> when a plasmid expressing *tesB* was also inserted into the strain along with *phaG*, suggesting that the activity of TesB in the strain containing only *phaG* was insufficient for efficient hydrolysis of the produced (*R*)-3- hydroxydecanoyl-CoA.

Other authors have studied the production of R3HBA using the native *E. coli* acyl-CoA thioesterases (*fadM*, *tesA*, *tesB*, *ybgC*, *ydiI*, and *yciA*) that also are active with acetyl-CoA as substrate. Interestingly, Guevara-Martínez et al. (2019) working with the recombinant strain *E. coli* AF1000 carrying  $\beta$ -ketothiolase (*t3*) and acetoacetyl-CoA reductase (*rx*) from *Halomonas boliviensis* and overexpressing the glucose-6-phosphate dehydrogenase gene (*zwf*) showed that the deletion of *tesA* or *fadM* resulted in minor decreases in R3HBA production, while deletion of *tesB* and *yciA* decreased the R3HBA titer by 11 and 33 %, respectively. These results suggest that YciA, and not TesB, is the acyl-CoA thioesterase largely responsible for R3HBA production from R3HBA-CoA in *E. coli*.

In the same way, the implementation of the thioesterase shortcut system (TSS) has been shown in other microorganisms. A mutant of *Saccharomyces cerevisiae* strain was modified by the insertion of acetyl-CoA C-acetyltransferase (Erg10p from *S. cerevisiae* BY4741), acetoacetyl-CoA reductase (Acr from *C. acetobutylicum* ATCC 824) and TesB (*E. coli* K-12 MG1655). The *S. cerevisiae* mutant was studied in fed-batch cultures using ethanol as a substrate and 12 g L<sup>-1</sup> of (*S*)-3-hydroxybutyric acid (S3HBA) was obtained in 200 hours (Yun et al., 2015). In addition, the use of photosynthetic organisms for R3HAs also has been explored. A mutant of *Synechocystis* sp. with the insertion of *phaA*, *phaB1* and *tesB* genes produced a R3HBA titer of 1.84 g L<sup>-1</sup> in 10 days in photoautotrophic culture (Wang et al., 2018).

### 3. MATERIALS AND METHODS

#### 3.1. MATERIALS

##### 3.1.1. Chemicals

All chemicals used in this work were of laboratory or reagent grade purity and were from established suppliers, such as Sigma-Aldrich (St. Louis, MO, USA), Thermo Scientific (Waltham, MA, USA) and PanReac AppliChem (Spain).

##### 3.1.2. Bacterial strains

Overview of the bacterial strains used in the course of this work, their genotype and source are described in the Table 1.

Table 1. Genotype and source of bacterial strains

Name	Genotype	Source
<i>Azohydromonas lata</i> DSM 1123 (strain H-1)	Wild type strain isolate	DSMZ (Germany)
<i>Methylocystis parvus</i> OBBP	Wild type strain isolate	Biopolis S.L. (Valencia, Spain)
<i>Cupriavidus necator</i> H16 DSM 428	Wild type strain isolate	DSMZ (Germany)
<i>C. necator</i> H16 PHB-4 DSM 541	<i>C. necator</i> H16 mutant with PhaC truncated protein	DSMZ (Germany)
<i>C. necator</i> $\Delta phaC$	<i>C. necator</i> H16 knock out for <i>phaC</i> gene	This work
<i>C. necator</i> $\Delta phaC \Delta hbd$	<i>C. necator</i> H16 knock out for <i>phaC-hbd</i> gene	This work

### 3.1.3. Growth media

Table 2 shows the composition of the growth media used for the mutant and wild type strains.

Table 2. Growth media for the bacterial strains

Name	Components in gram per liter	Bacteria	Reference
AL1	1.5 KH <sub>2</sub> PO <sub>4</sub> , 9 Na <sub>2</sub> HPO <sub>4</sub> ×12 H <sub>2</sub> O, 0.2 MgSO <sub>4</sub> ×7 H <sub>2</sub> O, 0.01 CaCl <sub>2</sub> ×2 H <sub>2</sub> O, 0.1 citric acid and 1 mL of trace element solution: 20 FeSO <sub>4</sub> ×7 H <sub>2</sub> O, 0.3 H <sub>3</sub> BO <sub>4</sub> , 0.2 CoCl <sub>2</sub> ×6 H <sub>2</sub> O, 0.03 ZnSO <sub>4</sub> ×7 H <sub>2</sub> O, 0.03 MnCl <sub>2</sub> ×4 H <sub>2</sub> O, 0.03 (NH <sub>4</sub> ) <sub>6</sub> Mo <sub>7</sub> O <sub>24</sub> ×4 H <sub>2</sub> O, 0.03 NiSO <sub>4</sub> ×7 H <sub>2</sub> O and 0.01 CuSO <sub>4</sub> ×5 H <sub>2</sub> O	<i>A. lata</i> DSM 1123	Wang & Lee, 1997
NMS	1 KNO <sub>3</sub> , 1.1 MgSO <sub>4</sub> ×7 H <sub>2</sub> O, 0.8 Na <sub>2</sub> HPO <sub>4</sub> ×12 H <sub>2</sub> O, 0.26 KH <sub>2</sub> PO <sub>4</sub> and 0.2 CaCl <sub>2</sub> ×2 H <sub>2</sub> O and 1 mL of trace element solution: 0.3 Na <sub>2</sub> MoO <sub>4</sub> ×2 H <sub>2</sub> O, 0.3 Na <sub>2</sub> EDTA×2 H <sub>2</sub> O, 1 CuSO <sub>4</sub> ×5H <sub>2</sub> O, 0.5 FeSO <sub>4</sub> ×7 H <sub>2</sub> O, 0.4 ZnSO <sub>4</sub> ×7 H <sub>2</sub> O, 0.03 CoCl <sub>2</sub> , 0.02 MnCl <sub>2</sub> ×4 H <sub>2</sub> O, 0.015 H <sub>3</sub> BO <sub>3</sub> , 0.01 NiCl <sub>2</sub> ×6 H <sub>2</sub> O and 0.38 Fe-EDTA	<i>M. parvus</i> OBBP	Rodríguez et al., 2022
NFMS	Identical to NMS medium except without KNO <sub>3</sub>	<i>M. parvus</i> OBBP	Rodríguez et al., 2022
RE1	20 fructose, 1 (NH <sub>4</sub> ) <sub>2</sub> SO <sub>4</sub> , 1.5 KH <sub>2</sub> PO <sub>4</sub> , 6.7 Na <sub>2</sub> HPO <sub>4</sub> ×7 H <sub>2</sub> O, 0.2 MgSO <sub>4</sub> ×7 H <sub>2</sub> O, 1 mL of trace element solution: 10 FeSO <sub>4</sub> ×7 H <sub>2</sub> O, 2.25 ZnSO <sub>4</sub> ×7 H <sub>2</sub> O, 1 CuSO <sub>4</sub> ×5 H <sub>2</sub> O, 0.58 MnCl <sub>2</sub> ×4H <sub>2</sub> O, 2 CaCl <sub>2</sub> ×2H <sub>2</sub> O, 0.14 Na <sub>2</sub> B <sub>4</sub> O <sub>7</sub> ×10 H <sub>2</sub> O, 0.16 H <sub>3</sub> BO <sub>3</sub> and 35% HCl 10 mL	<i>C. necator</i> H16 DSM 428, <i>C. necator</i> 541, <i>C. necator</i> <i>ΔphaC</i> , <i>C.</i> <i>necator ΔphaC</i> <i>Δhbd</i>	Adapted from Kim et al., 1994
SOC/ SOB	20 Tryptone, 5 yeast extract, 0.5 NaCl, 10 mL of 250 mM solution of KCl and 2 M MgCl <sub>2</sub> . For SOC is identical to SOB medium except with 1 M glucose solution	<i>E. coli</i> DH5α and <i>E. coli</i> S17-1	Hanahan, 1983
Luria Bertani (LB)	10 Tryptone, 5 yeast extract, 10 NaCl	<i>E. coli</i> and <i>C.</i> <i>necator</i> strains	Bertani, 1951

### 3.1.4. Primers

All primers used in this work (Table 3 and Table II-1, APPENDIX II) were designed in SnapGene® and ordered to IDT (USA) via Fermelo, Chile. Primers were received as lyophilized pellets and the stock solutions were prepared at 100 µM in Mili-Q water, DNAase free water and were stored at –20 °C. Then, primer working stocks were prepared as 10 µM concentrated solutions with double-distilled water and stored at –20 °C.

Table 3. Primers and their sequences used for the construction of gene knock outs

<b>Primers</b>	<b>Sequence 5'-3'</b>
pT18mobsacB-MCS_deleted_fwd_phac	cgc atggg c gatgcc aagctca agcttgg cactgg ccgctc
pT18mobsacB-MCS_deleted_rev_phac	gcgctgatgatggcgatcacgtaatcatgtcatagctgtttcctgtgtg
phaC1_upstream_fwd	aacagctatgacatgattacgtgatcgccatcatcagegc
phaC1_upstream_rev	cgccggcactcatgcaagcggatttgattgtctctctgccgctc
phaC1_downstream_fwd	ggcagagagacaatcaaaccgcttgcatgagtgccggcg
phaC1_downstream_rev	gacggccagtgcc aagcttgagcttggcatcgcccatcg
pT18mobSac_MCS_deleted_fwd_hbd	gctgattg cgcggctcaacgcaagcttggcactggccgctc
pT18mobSac_MCS_deleted_rev_hbd	gcaggcaggctgacctgcgggtaatcatgtcatagctgtttcctgtgtg
hbdH1_downstream_fwd	aacagctatgacatgattaccgcaggtcagcctgcctgc
hbdH1_downstream_rev	ttctctgacggaggcttacggagcaaacgatgcaacgacgca
hbdH1_upstream_fwd	gtcgttgcatcgtttgctccgtaagcctccgctcgagagaaagga
hbdH1_upstream_rev	gacggccagtgcc aagcttgcgttgagccgcgcaatcage

### 3.1.5. *E. coli* strains and plasmids

Three vector backbones, acquired from Addgene, were used for the genetic modifications. pBBR1MCS-2, a low copy vector was used for the expression of *tesB* (*E. coli* K12) in *C. necator* H16. pAWP89 vector was used for the expression of *tesB* in *M. parvus* OBBP. The pT18mobsacB suicide vector was used for the construction and knock-out of *phaC1*, *hbd* by mating with *E. coli* S17-1 in *C. necator* H16. The *E. coli* strains DH5 $\alpha$  or S17-1 were used for the bacterial transformation with the plasmids constructed. Table 4 gives an overview of the most important features of the plasmids, *E. coli* and mutant strains used or constructed in the course of this work.

Table 4. Vector backbones and their relevant genotype

Strains and plasmids	Relevant genotype	Source
<i>E. coli</i> DH5 $\alpha$	F <sup>-</sup> , <i>endA1</i> , <i>hsdR17</i> , ( <i>rk</i> <sup>-</sup> , <i>mk</i> <sup>+</sup> ), <i>supE44</i> , <i>thi-1</i> , $\lambda$ <sup>-</sup> , <i>recA1</i> , <i>gyrA96</i> , $\Delta$ <i>lacU169</i> ( $\Phi$ 80 <i>lacZ</i> $\Delta$ M15)	NEB
<i>E. coli</i> S17-1 DSM 9079	<i>thi pro hsdR hsdM</i> <sup>+</sup> <i>recA RP4-2-Tc::Mu::Tn7</i> $\lambda$ <i>pir</i>	DSMZ (Germany)
pBBR1MCS-2	<i>lacPOZ</i> , <i>mobRP4</i> , Kanamycin resistance ( <i>km</i> <sup>R</sup> )	Addgene
pAWP89	<i>IncP</i> , <i>dTomato</i> by the tac promoter, <i>km</i> <sup>R</sup>	Addgene
pBAD24- sfGFPx2	super folder (sf) <i>GFP</i> , Ampicilin resistance ( <i>Amp</i> <sup>R</sup> )	Addgene
pT18mobsacB	pMB1 <i>mob sacB</i> ; Suc <sup>S</sup> , Tetraciclina (Tc <sup>R</sup> )	Addgene
pL51	pT18mobsacB- $\Delta$ <i>phaC</i> plasmid with <i>phaC</i> upstream and downstream	This work
pL52	from pL51 with <i>hbd</i> upstream and downstream, pT18mobsacB- $\Delta$ <i>phaC</i> - $\Delta$ <i>hbd</i>	This work

## 3.2. METHODS

### 3.2.1. Preliminary depolymerization and viability assay in PHB accumulated cells of *A. lata* DSM 1123

Flask cultures of *A. lata* DSM 1123 were carried out for PHB accumulation in a shaking incubator with 1.0 L Erlenmeyer Flask (E-flask) containing 200 mL of AL1 medium with 10 g L<sup>-1</sup> glucose and 0.5 g L<sup>-1</sup> of (NH<sub>4</sub>) SO<sub>4</sub> at 30°C and 200 rpm for 20 hours. Then, the cells were washed with phosphate buffer and were resuspended in phosphate buffer 50 mM to test the depolymerization at three pHs, 4, 5 and 7. A hot plate stirrer was adapted with a thermoregulated bath at 30°C that containing inside a beaker of 100 mL with 20 mL of PHB accumulated cell suspension at pH of 4, 5 or 7 (two biological replicates) for depolymerization. The pH was controlled by addition of NaOH solution (4 M) to provide a pH constant condition. PHB and R3HBA were measured at the end of the experiment.

To test the viability of the cells at the end of the depolymerization phase, 100 ul of cells suspension were spread on Petri dishes with AL1 agar (AL1 media with 12 g L<sup>-1</sup>) and incubated at 30 °C for 3 days. The growth was measured by colony counting.

### 3.2.2. Bioreactor experiments with *A. lata*

#### 3.2.2.1. Chemostat cultivation

Chemostats experiments were performed in a 3.6 L (total volume, 2.3 L working volume) fermenter (Labfors 5, Infors-HT, Basel, Switzerland) equipped with pH, dissolved oxygen (DO) and temperature controllers. Temperature was maintained at 30 °C and water evaporated from the broth was condensed using a water-cooled condenser. DO was controlled above 40% of oxygen saturation in air (except for the oxygen-limited cultures where 1 vvm air and 250 rpm were used) by varying the stirring speed between 300 and 600 rpm and the gas mixture between air and pure oxygen in a cascade control at 2 vvm. Gas

flows were controlled by mass flow controllers and refer to normal conditions. The pH was maintained at 6.8 by the addition of a 2 M NaOH solution. The culture medium was the mineral salt medium AL2 (Wang & Lee, 1997) with 10 g L<sup>-1</sup> glucose as the carbon and energy source.

Nitrogen-limited, oxygen-limited and glucose-limited chemostats were performed by altering the inlet medium composition or the oxygen transfer rate. The nitrogen-limited feeding medium contained 0.5 g L<sup>-1</sup> ammonium sulfate while 3 g L<sup>-1</sup> was used for the glucose and oxygen-limited conditions. Dilution rates ranging from 0.05 to 0.4 h<sup>-1</sup> were applied under each nutrient limitation condition. Changes between dilution rates were randomized. Cultures were sampled after achieving steady-state (at least after 4 residence times) and checking for signs of contamination using optical microscopy and Raman spectroscopy.

#### 3.2.2.2. Two-stage chemostat for *in-vivo* depolymerization and R3HBA production

A bioreactor was built using a 200 mL Schott flask equipped with a temperature control system, a pH control system, a U-tube for level control and agitation provided by a magnetic stirrer. This bioreactor was connected to the discharge of a nitrogen-limited chemostat culture operated at a D=0.2 h<sup>-1</sup> and pH 6.8. The depolymerization reactor was operated at pH 4 with a 30 min residence time for 300 min.

#### 3.2.3. Optimization of PHB depolymerization in *M. parvus*

The experiments were performed batch wise using PHB containing *M. parvus* biomass in 125 mL serum bottles (working volume of 45 mL) crimp sealed (three biological replicates). The bottles were incubated at 30 °C (except Test 3) and 230 rpm in an orbital shaker.

### Test 1: Influence of the presence of nitrate and O<sub>2</sub> and pH

The assays were performed with NMS and NFMS media at both pH 4 and pH 11 in triplicate for 48 hours. All cultures were inoculated with 10 mL of concentrated *M. parvus* culture previously grown in NFMS for 10 days (1.3 gTSS L<sup>-1</sup> with 51.4% of PHB) and were incubated for two days under an O<sub>2</sub>:CH<sub>4</sub> headspace (66.7:33.3%) and a He:CH<sub>4</sub> atmosphere (66.7:33.3%). A control test at pH 7 under a O<sub>2</sub>: CH<sub>4</sub> headspace (66.7:33.3%) and NMS medium was also carried out. Culture samples were collected periodically for the quantification of the R3HBA concentration. Cell dry weights (CDW), total nitrogen, PHAs and pH were determined at the beginning and end of the experiment.

### Test 2: Optimization of pH during PHB depolymerization

PHB depolymerization under an O<sub>2</sub>:CH<sub>4</sub> atmosphere (66.7:33.3 %) was assessed in triplicate at pH 10, pH 11 and pH 12 with NMS medium as above described for 48 hours. The pH of the cultures was monitored three times per day and manually adjusted using 5 M NaOH, while the concentration of extracellular R3HBA was quantified once per day. The biomass concentration (estimated as CDW) and PHB cells content were determined at the beginning and the end of the experiment.

### Test 3: Influence of temperature on the kinetic of PHB depolymerization

PHB depolymerization at pH 11 on NMS medium was assessed in triplicate at 25 and 35 °C for 3 hours using fresh *M. parvus* with a concentration and PHB cell content of 4.17 gCDW L<sup>-1</sup> and 44.7 %. The determination of extracellular R3HBA concentration was conducted at 15, 30, 60, 120 and 180 min. At the end of the experiment, cell viability was evaluated using the pellets obtained after centrifugation of the biomass from depolymerized cells. Cell viability tests were performed at 25 °C in 2.2 L serum bottles with a working volume of 0.4 L of both NMS and NFMS medium. The bottles were capped with aluminum caps and chlorobutyl rubber stoppers under and O<sub>2</sub>:CH<sub>4</sub> atmosphere (66.7:33.3 %) and

incubated as above described until complete CH<sub>4</sub> depletion. CDW, CH<sub>4</sub>, O<sub>2</sub> and CO<sub>2</sub> concentrations were periodically measured.

#### Test 4: Influence of the initial R3HBA concentration and aeration rate

The influence of the oxygen mass transfer rate on PHB depolymerization and R3HBA yield was investigated in E-flasks incubated at 200 rpm and 30 °C in an orbital shaker for 72 hours. The lowest oxygen mass transfer rate was achieved in 100 mL E-flasks containing 100 mL of medium, while the highest oxygen transfer rate was reached in 250 mL E-flasks containing 50 mL of cultivation broth. An intermediate condition was tested in 100 mL E-flasks containing 50 mL of cultivation broth. The initial biomass concentration and PHB content of the cell suspension was  $0.51 \pm 0.005$  gCDW L<sup>-1</sup> and  $31.9 \pm 1.9\%$  PHB, respectively. The experiments were conducted in duplicate.

The potential inhibitory effect of extracellular R3HBA over PHB depolymerization was investigated using R3HBA produced in-house following the procedure described by Lee et al. (1999). Then, *M. parvus* cells containing PHB were washed and resuspended in NMS medium at pH 11 supplemented with R3HBA at concentrations of 0, 120, 330 and 650 mg L<sup>-1</sup>. Cell incubation was performed in 100 mL E-flasks containing 50 mL of cell suspension with the corresponding R3HBA concentration at 30 °C and 200 rpm in an orbital shaker. Culture samples were collected at 0, 3, 6, 48 and 72 hours for R3HBA and crotonic acid quantification. The biomass and PHB cell content were monitored at the beginning and the end of experiments.

- R3HBA production by *A. lata* DSM 1123

*A. lata* DSM 1123 was cultivated from a frozen stock culture in a nutrient agar plate. A single colony was picked and used to inoculate a 500 mL E-flask with 100 mL of AL1 medium. This culture served as the inoculum for a batch bioreactor cultivation of this bacterium in a Labfors 5 bioreactor (Infors HT, Switzerland). The bioreactor was operated with 1 L of AL2

(Wang & Lee, 1997) medium containing an initial glucose concentration of 30 g L<sup>-1</sup> and an initial ammonium sulfate concentration of 2 g L<sup>-1</sup>. Dissolved oxygen was maintained above 40 % saturation by varying the stirring speed up to 700 rpm at 1 vvm air. When necessary, pure oxygen was automatically mixed with the inlet air flow under a cascade control. After 24 hours of cultivation, approximately 12.0 gCDWL<sup>-1</sup> of biomass were retrieved containing a PHB cell content of 75%. Cells were collected by centrifugation, washed twice with distilled water and resuspended in water at a concentration of approximately 120 gCDW L<sup>-1</sup>. PHB depolymerization was started by adjusting the pH to 4 with HCl and lasted for one hour. The pH was controlled at 4 using 2 M NaOH. Following the purification procedure outlined in Lee et al. (1999), a solution containing 34.2 g L<sup>-1</sup> of sodium (*R*)-3-hydroxybutyrate was obtained for the study of inhibitory effect of extracellular R3HBA.

#### 3.2.4. Biomass quantification and culture supernatant collection and analysis

For the estimation of biomass concentration, aliquots of culture were centrifuged (2470 RCF, 10 min) to separate a cell-free supernatant and a biomass pellet. The pellet was washed twice with Type II water, dried and used to determine the cell dry weight concentration. Culture supernatants were obtained by centrifuging broth samples in Eppendorf tubes at 17000 RCF for 1 min at 4 °C and used immediately or stored at -20 °C. Glucose concentration was determined in culture supernatants and feed media using an enzymatic assay (D-glucose assay kit GOPOD, Megazyme, Ireland) according to the manufacturer's instructions or High-Performance Liquid Chromatography (HPLC) analysis (see analytical methods). The concentration of NH<sub>4</sub><sup>+</sup> was determined using an ammonium-ion electrode (EW-27504-00, Cole-Parmer, USA).

#### 3.2.5. Raman spectroscopy

Raman analyses of dry biomass harvested from the cultures, washed twice with Type II water and dried at 70 °C on a Raman grade CaF<sub>2</sub> supports (Crystan, UK) were performed using a Horiba XploRA™ PLUS Raman microscope with a ×50 objective lens. A diode laser of 532 nm was used, and the collected Raman radiation was dispersed with a 1200 lines

(750 nm) grating. All spectra were obtained in the spectral window of 600-1800  $\text{cm}^{-1}$  using 60 seconds of acquisition time and 2 accumulations. The Raman spectra were baseline corrected and normalized using the LabSpec 6 suite. The analysis of the characteristic frequencies and intensities was performed using previously reported Raman spectra (Samek et al., 2016) and the spectra of pure PHB (sc-255438, Santa Cruz Biotechnology).

### 3.2.6. Analytical procedures

$\text{CH}_4$ ,  $\text{CO}_2$  and  $\text{O}_2$  gas concentrations were measured in a gas chromatograph (GC) coupled with a Thermal Conductivity Detector (Bruker 430 GC-TCD, Bruker Corporation, USA) following the method described by Estrada et al. (2014). The optical density of the cultures samples was measured by spectrophotometry at 600 nm (UV-2550, Shimadzu, Japan). CDW and pH were analyzed according to Rodríguez et al. (2020). PHB was quantified via Gas Chromatography-Mass Spectrometry (GC-MS) (Rodríguez et al., 2020) or GC-FID (Scott et al., 2021). The concentration of R3HBA was determined using a commercial R3HBA Assay Kit (Megazyme, Ireland) according to manufacturer's protocol or using HPLC with a UV-Vis detector at 210 nm and a refractive index detector (Prominence, Shimadzu) according to Scott et al. (2021). Citrate, succinate, pyruvate, acetate, glucose, malate and crotonic acids (Sigma-Aldrich catalog number, 113018) were quantified using the HPLC-UV-IR method described by Scott et al. (2021). The organic acids standard was purchased from Biorad (catalog number, 125-0586).

### 3.2.7. Vector construction for *tesB* expression

For the construction of the expression vector for *C. necator* H16, *tesB* was amplified from the synthesized pUC57 plasmid with *tesB* gene fragment (*E. coli* K12) no codon optimized. The RBS and linker sequences used were tested and described by (Lu et al., 2012). The terminator fragment was amplified from the pBAD24-sfGFPx2 plasmid (450 pb) following the plasmid construction strategy described by (Crépin et al, 2016). The fragments were assembled in pBBR1MCS2 plasmid using Gibson Assembly.

The construction of the expression vector for *M. parvus* was assembled in pAWP89 plasmid by the insertion of a promoter and terminator fragments (Section 0, APPENDIX II) from the PHB synthesis of *M. parvus* and *tesB* gene (*E. coli* K12). These were taken from the synthesized pUC57-kan plasmid containing these fragments. All plasmid assemblies were achieved by one-step isothermal DNA assembly protocol (Gibson et al., 2009).

Briefly, the assembly reaction was carried out by mixing the insert(s) and vector backbone with 5  $\mu$ L Gibson Assembly® Master Mix (New England Biolabs, Ipswich, MA, USA) and Mili-Q and DNase free water to a total reaction volume of 10  $\mu$ L. The amount of each insert to be used was calculated following the next equation, where the units of vector and insert amount are in nanograms, vector and insert length in kb.

$$\left( \frac{\text{Insert}}{\text{amount}} \right) = \left( \frac{\text{Vector amount}}{\text{Vector length}} \right) \left( \frac{\text{Insert}}{\text{length}} \right) \left( \frac{\text{Molar ratio}}{\text{insert : vector}} \right)$$

Around 50-100 ng of vector backbone were used and a molar insert-vector ratio of 3:1 was used for the assembly of up to three or four fragments (including the vector). The Gibson assembly reaction was incubated for 1 hour at 50 °C. Then, the reactions were stored at 20 °C for subsequent transformations.

### 3.2.8. Gene knock-out via pT18mobsacB for *C. necator* H16

Two homologous templates which were about 500 bp upstream and downstream of *phaC* or *hbd* were amplified from *C. necator* H16 by colony PCR. The fragments were cloned in the pT18mobsacB plasmid backbone (pL51 and pL52) via Gibson assembly (Gibson et al., 2009) and transformed into *E. coli* S17-1 by electroporation, then identified and transferred to *C. necator* H16 via conjugation. Single colonies were cultured in LB without NaCl but with 15 mg L<sup>-1</sup> gentamicin and 20 mg L<sup>-1</sup> tetracycline at 30 °C. A pair of primers with one bound to the genome and another to the plasmid was used for colony PCR to identify strains with the knockout plasmid integrated. Then confirmed colonies were incubated for the second recombination in LB without NaCl and tetracycline, but with 50 g L<sup>-1</sup> sucrose and 15 mg L<sup>-1</sup>

gentamicin at 30 °C for 72 hours or until visible colonies appear. Then, colony PCR was used for the screening of the *C. necator* colony knock out for *phaC* or *hbd* using the primers listed in Table 3.

### 3.2.9. Standard polymerase chain reaction

The mixture used for the standard PCR reaction in this work was the GoTaq Green mastermix polymerase from Promega®. The thermostable Phusion™ High-Fidelity DNA polymerase from Thermo Fisher scientific was used for Gibson PCR applications. Once prepared, the reaction mixture was placed in a PCR thermocycler and a PCR program was run on the machine following the technical specification of the PCR master mix manufacturer. Time and temperature required for each step of the program were carefully adapted to allow for the successful amplification of the desired target fragment. For Phusion High-Fidelity DNA polymerase the denaturation temperature was set to 98 °C and the initial denaturation was carried out for 30 seconds for all plasmid-based templates. The elongation time was calculated based on the desired fragment length. After completion of the PCR, the amplified sequences were recovered using agarose gel electrophoresis and subsequent gel extraction and purification with GeneJET extraction kit (Thermo Fisher scientific).

### 3.2.10. Colony PCR

Colony PCR was used to amplify the desired target sequence from a bacterial colony without previous purification of the DNA from the bacterial cells. Here, colony PCRs were mostly carried out to assess the transformation status of positive colony indicator after transformation.

A bacterial colony was picked from an agar plate using the tip of a sterile white 10 µL pipette tip, before resuspending it in 10 µL double distilled water. Next, 1 µL of the suspension were transferred into a PCR tube and were incubated at 95 °C for 5 min at 90 °C. After incubation, 1 µL of the suspension was added to PCR mastermix.

### 3.2.11. Agarose gel electrophoresis

Agarose gel electrophoresis was carried out to separate DNA fragments and vectors according to their respective sizes in an electric field using 1% agarose gels (w/v). All gels were supplemented with GelRed<sup>®</sup> Nucleic Acid Gel Stain and prepared with TAE 1X. Samples were mixed with Gel loading purple dye (New England Biolabs, Ipswich, MA, USA) and 1-3  $\mu$ L were loaded into the pockets. In addition, 0.5  $\mu$ L of 1 kb DNA ladder (Bionner, Korea) were loaded into one well on the gel to estimate the size and quantity of individual fragments and plasmids. A voltage of 90 V was applied for the electrophoreses. After 40 min, the electrophoresis was stopped, and the agarose gel was recovered to visualize DNA fragments under ultraviolet light in Firereader V6 transilluminator.

### 3.2.12. Preparation of electrocompetent *E. coli* cells

To create electrocompetent *E. coli* cells, the S17-1 strain was streaked out on LB agar plate. One picked colony was inoculated in a 50 mL sterile E-flask (working volume 20 mL of LB-medium) at 37 °C and 200 rpm overnight. After growth for 14 hours, a calculated enough volume for 1:50 dilution of pre-culture was used for inoculating a 500 mL sterile E-flask (working volume of 100 mL) at 37 °C and 200 rpm until reach ingan optical density (OD<sub>600</sub>) of 0.35-0.40 after about 3-4 hours of growth time. Next, the main culture was chilled into two 50 mL centrifuge tubes which had been pre-cooled on ice for 5 min. After 10 min on ice, the cells were harvested by 5 min centrifugation at 4000g and room temperature. The supernatant was decanted and the pellets were resuspended in 50 mL chilled double distilled water (4 °C). The tubes were centrifuged at the same condition mentioned above. The same procedure was repeated once more with 20 mL and the pellet was resuspended a final volume of 1 mL of ice-cold 10% glycerol. The suspension OD<sub>600</sub> was measured and aliquoted in fraction of 50  $\mu$ L in chilled tubes to be frozen at -80°C.

### 3.2.13. Transformation of *E. coli* cells

For the transformation of electrocompetent *E. coli* cells with newly constructed plasmids, a 50  $\mu\text{L}$  aliquot of electrocompetent cells was thawed on ice. Once completely thawed, 1-2  $\mu\text{L}$  of Gibson assembly reaction mixture containing the constructed plasmid, were added to the cells. A 0.2 mm pre-cooled electroporation cuvette with cells mixture was placed in an electroporator from Bio-rad and a pulse of 2-5 kV was sent through the cuvette. Immediately after electroporation, 900  $\mu\text{L}$  of SOC medium were added and carefully resuspending by pipetting was undertaken. The cells solution was recovered and transferred into a sterile 1.5 mL microcentrifuge tube and then incubated for 1 hour at 37 °C and 200 rpm.

After incubation, 100 and 900  $\mu\text{L}$  fractions were taken from the transformed cells solution and were placed on individual LB-agar plates supplemented with the respective antibiotic, lactose (1 g L<sup>-1</sup>) and X- gal (20  $\mu\text{g}$  L<sup>-1</sup>) for blue-white screening of bacterial colonies. The plates were incubated at 37 °C for 24-48 hours. White colonies were checked using colony PCR. The transformation of chemocompetent *E. coli* DH5 $\alpha$  cells was followed by the technical specifications of NEB BioLabs and cultured by the instructions above mentioned.

### 3.2.14. Characterization of *C. necator* H16 and mutant strains

Glycerol stocks of *C. necator* H16, *C. necator*  $\Delta\text{phaC}$ , *C. necator*  $\Delta\text{phaC}$   $\Delta\text{hbd}$  and *C. necator* 541 were streaked on a LB agar petri dish without NaCl and incubated at 30 °C. After 24-48 hours one colony was used to inoculate a pre-seed 100 mL E-flask with 20 mL of RE1 mineral medium and incubated for 15-20 hours at 30°C and 250 rpm. This seed culture was used to inoculate a 500 mL E-flask with 100 mL RE1 and incubated for 48 hours. Culture samples were collected periodically for the quantification of biomass, fructose, R3HBA, pyruvate and PHB. Three biological replicates were performed for each strain.

For *C. necator* H16 a depolymerization test was assayed in order to see the R3HBA production at different pHs conditions as described by Lee et al. (1999). At the end of the

48 hours of culture, accumulated PHB cell of *C. necator* H16 were washed two times with mineral RE1 medium (without fructose) and resuspended in E-flasks of 100 mL with a working volume of 20 mL with mineral medium (without fructose) at 3, 4, 7 and 10 pHs. The depolymerization cultures were incubated at 30°C and 250 rpm for 24 hours. CDW, PHB, R3HBA and pH were determined at the beginning and end of the experiment.

### 3.2.15. Calculations

#### i). Chemostat cultures

Each chemostat culture is presented as a single data point corresponding to the mean of two or three analytical determinations, along with its standard deviation. Therefore, each data point at a given dilution rate is a biological replicate. Percentages are mass-based and CDW refer to residual (active or PHB free) biomass.

The analysis of the chemostat cultures was carried out using the standard definitions of specific uptake rates and specific productivities following equations reported in Table 5, where  $D$  is the dilution rate ( $\text{h}^{-1}$ ),  $F$  the PHB fraction ( $\text{gPHB g total CDW}^{-1}$ ),  $X_T$  is the total CDW biomass concentration ( $\text{g L}^{-1}$ ),  $S_o$  and  $S$  the inlet and outlet glucose concentration,  $C_{AS}$  the ammonium sulfate concentration ( $\text{g L}^{-1}$ ) and  $V$  the reactor volume. Error propagation was performed using standard formulas based on standard deviations and its respective defining equation, where  $\|\mathbf{v}\|$  is the Euclidean norm of vector  $\mathbf{v}$ . The following formulas allow the calculation of an error that is latter plotted as an error bar.

Table 5. Equations defining specific uptakes and production rates

Description	Equation and experimental error propagated
Glucose uptake rate [g gCDW <sup>-1</sup> h <sup>-1</sup> ]	$\frac{1000}{180} D \frac{S_o - S}{(1 - F)X_T}$ Error = $\frac{50}{9} D \left\  \left\  \frac{\Delta S_o}{(1 - F)X_T}, \frac{\Delta S}{(1 - F)X_T}, \frac{(S_o - S)\Delta F}{(1 - F)^2 X_T}, \frac{(S_o - S)\Delta X_T}{(F - 1)X_T^2} \right\  \right\ $
Ammonium uptake rate [mmol gCDW <sup>-1</sup> h <sup>-1</sup> ]	$\frac{1000 \cdot 2}{132.14} D \frac{3 - C_{AS}}{(1 - F)X_T}$ Error = $6.40738 D \left\  \left\  \frac{(C_{AS} - 3)\Delta X_T}{(F - 1)X_T^2}, \frac{(C_{AS} - 3)\Delta F}{(1 - F)^2 X_T}, \frac{\Delta C_{AS}}{(F - 1)X_T} \right\  \right\ $
PHB production rate [g gCDW <sup>-1</sup> h <sup>-1</sup> ]	$\frac{1000}{104} D \frac{F}{1 - F}$ Error = $\frac{125}{13} \left\  \left\  \frac{D \Delta F}{(1 - F)^2} \right\  \right\ $
PHB free or residual biomass [g L <sup>-1</sup> ]	$(1 - F)X_T$ Error = $\ (1 - F)\Delta X_T, X_T \Delta F\ $

ii). PHB depolymerization and R3HBA yields calculation used in *M. parvus* experiments

The R3HBA molar yield ( $Y_{R3HBA}$ ) was calculated as the ratio of the moles of R3HBA excreted and the moles of PHB consumed, considering that PHB hydrolysis consumes one mol of water per mol of R3HBA produced. Then PHB depolymerization percentage conversion ( $C_{PHB}$ ) and  $Y_{R3HBA}$  were calculated the following Eq. 1 and 2.

$$C_{PHB} = \frac{X_{PHB}^i - X_{PHB}^f}{X_{PHB}^i} \times 100 \quad \text{Eq. 1}$$

$$Y_{R3HBA} = \left( \frac{104.1 - 18.01}{104.1} \right) \frac{X_{R3HBA}^f - X_{R3HBA}^i}{X_{PHB}^i - X_{PHB}^f} \times 100 \quad \text{Eq. 2}$$

Where  $X_{PHB}^i$  and  $X_{PHB}^f$  correspond to the initial and final PHB concentrations ( $\text{g L}^{-1}$ ) respectively, and  $X_{R3HBA}^i$  and  $X_{R3HBA}^f$  represent the initial and final concentrations of R3HBA ( $\text{g L}^{-1}$ ) respectively. A similar calculation was used for the crotonic acid yield ( $Y_{croton}$ ). The conversion of PHB to R3HBA can be calculated by Eq.3.

$$C_{PHB, R3HBA} = 0.01 Y_{R3HBA} \cdot C_{PHB} \quad \text{Eq. 3}$$

Finally, the specific R3HBA release rate per gram of initial intracellular PHB ( $q_{R3HBA}$ ) was calculated as follows:

$$q_{R3HBA} = \frac{m}{X_{PHB}^i} \quad \text{Eq. 4}$$

Where  $m$  is the slope of the line whose independent and dependent variables are the depolymerization time and R3HBA concentration ( $\text{mg L}^{-1}$ ) respectively.

## 4. RESULTS AND DISCUSSIONS

### 4.1. EFFECTS OF NUTRIENT LIMITATION AND DILUTION RATE ON PHB AND BIOMASS PRODUCTION IN *A. lata*

Part of the results presented in this section, were published in the following paper “Two internal bottlenecks cause the overflow metabolism leading to poly(3-hydroxybutyrate) production in *Azohydromonas lata* DSM1123” with DOI:

<https://10.1016/j.jece.2021.105665>

*A. lata* DSM 1123 was grown in chemostat culture at dilution rates ranging from 0.05 to 0.4 h<sup>-1</sup> with mineral medium and glucose as the sole carbon and energy source. Panels A-F in Figure 1 show culture parameters and their relationship with the dilution rate under nitrogen, oxygen or glucose limiting conditions.

#### 4.1.1. Nitrogen limited-chemostat culture

The PHB content under nitrogen limitation slightly decreases from an average of 75 % at a  $D=0.05 \text{ h}^{-1}$  to 65% at the maximum  $D=0.4 \text{ h}^{-1}$  (Figure 1, panel A), a slight decrease in sharp contrast to nitrogen-limited chemostats of *C. necator*, where a linear decrease from a PHB content of 80% to less than 10% was reported as the dilution rate increases from 0.025 to 0.4 h<sup>-1</sup> (Henderson & Jones, 1997). The glucose and ammonium sulfate concentration in the chemostat runs (Figure 1, panels C and D) is consistent with an ammonium limited condition: glucose was present at every dilution rate and the titer of ammonium sulfate was negligible at  $D < 0.2 \text{ h}^{-1}$ . As the growth rate increases, the overall PHB yield on glucose decreases from  $0.41 \pm 0.02$  ( $D=0.05 \text{ h}^{-1}$ ) to  $0.30 \pm 0.03 \text{ gPHB g glucose}^{-1}$  ( $D=0.4 \text{ h}^{-1}$ ).

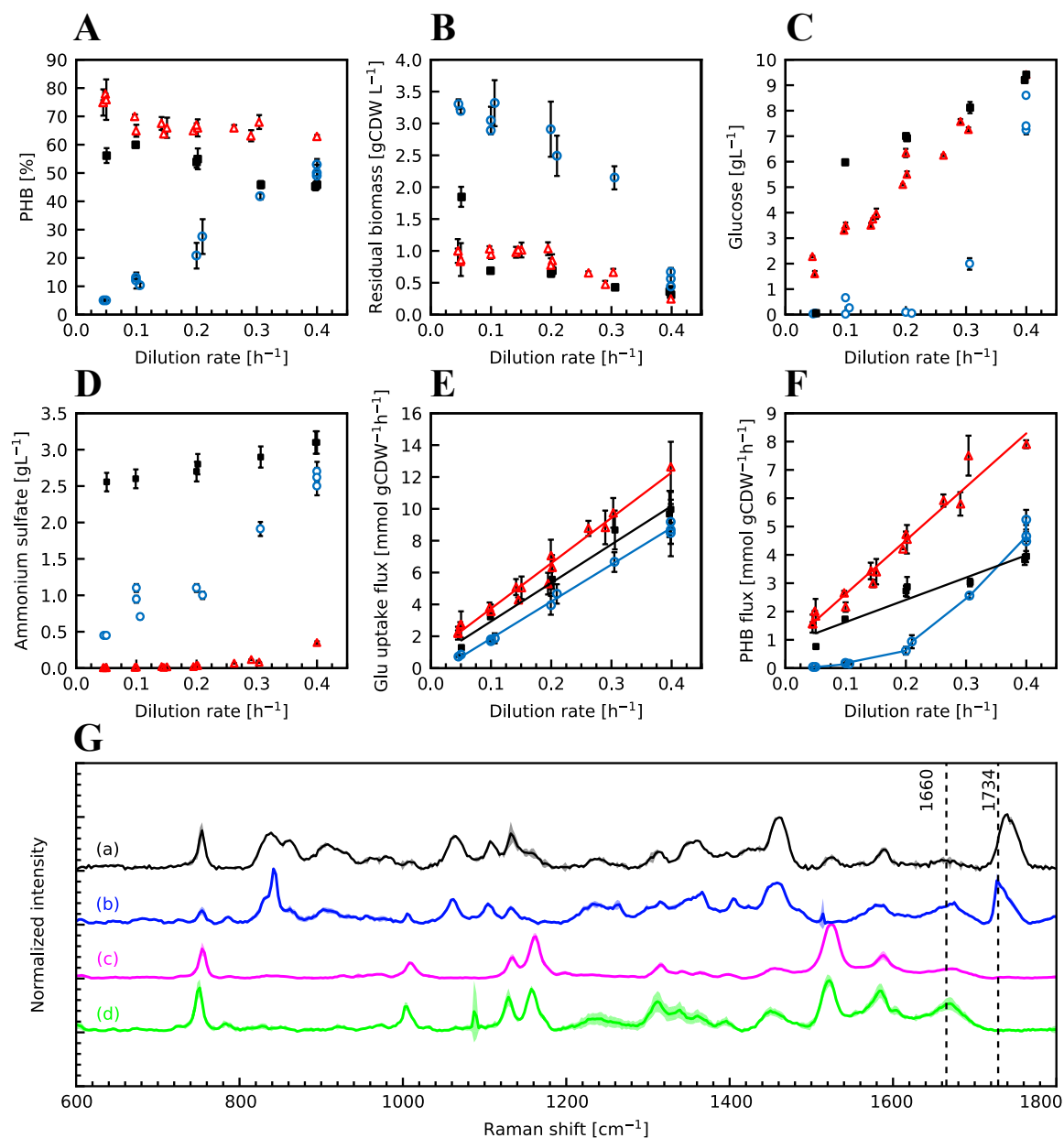


**Figure 1. Effects of the dilution rate and nutrient limitation in chemostat culture on PHB accumulation.** (A), residual (PHB free) biomass (B), glucose (C) and ammonium sulfate (D) concentration, specific glucose uptake rate per gram of residual biomass (E) and specific PHB accumulation rate per gram of residual biomass (F). Red triangles correspond to nitrogen-limited chemostats, black squares to oxygen-limited chemostats and blue circles to glucose-limited chemostats. Raman spectra of washed and dried biomass samples withdrawn from (G): (a) nitrogen-limited chemostat at  $D=0.05 \text{ h}^{-1}$ , (b), (c) and (d) oxygen-limited chemostat at dilution rates of 0.3, 0.05 and  $0.1 \text{ h}^{-1}$ , respectively. The shaded area represents the standard deviation.

The maximum specific PHB accumulation rate (Figure 1, panel F) was found under nitrogen limitation at a  $D$  of  $0.4 \text{ h}^{-1}$  corresponding to  $7.9 \pm 0.14 \text{ mmol gCDW}^{-1} \text{ h}^{-1}$  (equivalent to  $0.69 \text{ gPHB gCDW}^{-1} \text{ h}^{-1}$ ). This value agrees with the instantaneous specific PHB synthesis rate reported by Wang and Lee (1997), with a maximum of  $0.87 \text{ gPHB gCDW}^{-1} \text{ h}^{-1}$  after the onset of nitrogen limitation in a batch culture of *A. lata* DSM1123 using sucrose as carbon and energy source. The difference can be explained by the increased specific sucrose uptake rate compared to the glucose uptake rate reported for this microorganism (Wang & Lee, 1997).

Comparatively, the PHB flux values found in this work are much higher, especially for the nitrogen-limited cultures, than for those found in nitrogen-limited chemostats with glucose as the carbon source for *C. necator* [ $0.15 \text{ gPHB gCDW}^{-1} \text{ h}^{-1}$  (Atlić et al., 2011) or  $0.23 \text{ gPHB gCDW}^{-1} \text{ h}^{-1}$  (Henderson & Jones, 1997)]. A maximum of  $10.6 \text{ mM}$  of succinic acid was measured at a  $D=0.1 \text{ h}^{-1}$  and  $2 \text{ mM}$  of malic acid at a  $D=0.2 \text{ h}^{-1}$  (the complete set of organic acid measurements is presented in Table I-1, APPENDIX I).

#### 4.1.2. Oxygen limited-chemostat cultures

PHB accumulation in chemostats under oxygen limitation showed a decrease of the PHB fraction at low dilution rates compared with the results obtained under ammonia-limited conditions (Figure 1, panel A).

Glucose and ammonium sulfate titers are consistent with an oxygen limited chemostat. PHB yield on glucose was  $0.27 \pm 0.03 \text{ g PHB g glucose}^{-1}$ , irrespectively of the dilution rate. PHB content reached a maximum of  $60\%$  at a  $D=0.1 \text{ h}^{-1}$  decreasing to  $46\%$  at a  $D=0.4 \text{ h}^{-1}$ . Using a kinetic model for PHB production and cell growth in *A. lata* DSM 1123, Papapostolou et al. (2019) reported an intracellular PHB content of  $43.3\%$  at the end of a 43 hours fed-batch culture, where the dissolved oxygen concentration was maintained at  $6\%$  of its saturation value. A maximum of  $7.9 \text{ mM}$  succinic acid at a  $D=0.2 \text{ h}^{-1}$  and  $1.6 \text{ mM}$  of malic acid at a  $D=0.1 \text{ h}^{-1}$  were measured (see Table I-1, APPENDIX I).

#### 4.1.3. Glucose-limited chemostat culture

The trends of PHB accumulation under oxygen and nitrogen are in agreement with the general behavior of PHB accumulation in other organisms: PHB accumulation triggers when a nutrient, different from the carbon source, is limiting (Steinbüchel & Hein, 2001). On the other hand, PHB accumulation in glucose limiting chemostats showed a completely different trend (Figure 1, panel A). At a  $D=0.05\text{ h}^{-1}$  the PHB percentage was as low as  $4.85 \pm 0.35\%$ , increasing linearly to  $50.7 \pm 2.1\%$  at a  $D=0.4\text{ h}^{-1}$ . The PHB accumulation obtained at dilution rates of 0.3 and  $0.4\text{ h}^{-1}$  were in good agreement with the PHB content of exponentially growing batch cultures (and of the exponential growth zone of fed-batch cultures) where the carbon source is the limiting nutrient, with reported values close to 50% PHB (Wang & Lee, 1997; Yamane et al., 1996) and 53% (Ramsay et al., 1990). This is the first report where a low PHB content is described in a culture of *A. lata* under glucose-limiting conditions. To confirm this result, samples of biomass were analyzed using Raman spectroscopy (Figure 1, panel G). The Raman spectrum revealed characteristic emission lines attributable to proteins (amide I at  $1660\text{-}1662\text{ cm}^{-1}$ ) and PHB ( $1734\text{-}1736\text{ cm}^{-1}$ ) (Samek et al., 2016). A PHB standard (data not shown) shows several Raman peaks where the most intense peaks corresponded to  $837$  and  $1734\text{-}1736\text{ cm}^{-1}$ . Samples from a nitrogen-limited chemostat at a  $D=0.05\text{ h}^{-1}$  (Figure 1, panel G, spectrum a) and glucose-limited chemostat at a  $D=0.3\text{ h}^{-1}$  showed clear PHB peak at  $1734\text{ cm}^{-1}$ , with PHB to amide I peak heights ratios of 5.5 and 2.2, respectively. These results agree with the PHB content of the samples, 42% ( $D=0.3\text{ h}^{-1}$ , glucose-limited) and 75% ( $D=0.05\text{ h}^{-1}$ , nitrogen-limited) assuming that a positive linear correlation exists between the PHB/Amide I ratio and PHB content (Samek et al., 2016). The analysis of the glucose-limited chemostats at dilution rates of 0.05 and  $0.1\text{ h}^{-1}$  (Figure 1, panel E, spectrums c and d) shows a nearly absent PHB peak at  $1734\text{ cm}^{-1}$ , confirming the results of the GC analysis. The accumulation of PHA under unrestricted growth conditions at high dilution rates was also observed in cultures of *P. oleovorans*, although the maximum content was 10% (Durner et al., 2000).

Figure 1, panel E shows the calculated glucose uptake rates in  $\text{mmol gCDW}^{-1}\text{ h}^{-1}$ . Glucose uptake rates under oxygen and nitrogen limitation were found to be higher than those

obtained under glucose limiting conditions at every dilution rate. The specific glucose uptake rates in chemostats of *C. necator* operated at  $D=0.1 \text{ h}^{-1}$  were found to be similar and to decrease in the same order as the one found in our work: ammonia limited ( $4.2 \text{ mmol gCDW}^{-1} \text{ h}^{-1}$ ) followed by oxygen-limited ( $3.1 \text{ mmol gCDW}^{-1} \text{ h}^{-1}$ ) and glucose-limited ( $2.0 \text{ mmol gCDW}^{-1} \text{ h}^{-1}$ ) conditions (Henderson & Jones, 1997). The production of organic acids was negligible.

The PHB flux, (specific PHB productivity based on the residual biomass) is shown in Figure 1, panel F. A linear trend was found between PHB flux and the dilution rate for the ammonia limited and oxygen-limited chemostat. For the glucose-limited cultures, the relationship between PHB flux and dilution rate is best described considering two linear zones, with an almost negligible PHB accumulation rate at dilution rates below  $0.1 \text{ h}^{-1}$ . Interestingly, *Azohydromonas australica* DSM1124, a species closely related to *A. lata* DSM1123, showed no PHB accumulation during the growth phase in batch culture (before ammonium exhaustion) using glycerol as the sole carbon and energy source (Haage et al., 2001). The authors attributed this change in the behavior of a strain known for PHB accumulation during exponential growth to the use of a carbon source other than glucose (Haage et al., 2001). However, since the cells grew at a  $\mu = 0.075 \text{ h}^{-1}$ , our results indicate that the reduced PHB accumulation it is not related to the nature of the substrate, but to the failure of glycerol to produce an uptake rate of carbon compatible with a  $\mu$  sufficiently high to promote the accumulation of PHB.

#### 4.1.4. Preliminary *in-vivo* depolymerization and viability assay in PHB accumulated cells of *A. lata* DSM 1123

By providing the environmental condition in which cells have high activity of intracellular PhaZ and low activity of Hbd, R3HBA could be produced with a yield of 96 % in only 30 min by *in-vivo* depolymerization of PHB in *A. lata* (Lee et al., 1999). In order to replicate the experiment of Lee et al. (1999), PHB accumulated cells of *A. lata* were incubated for 5 hours in phosphate buffer to assess PHB depolymerization at different pHs. At pH 4, the PHB conversion was 38.6 % higher than those obtained at pHs of 5 (29.4 %) and 7 (8.05 %) (Table

6). This pattern was consistent with the R3HBA titer and R3HBA yield of 2.42 g L<sup>-1</sup> and 93.6 % at 4 pH and decreasing toward neutral pHs. The results are similar to the pioneering work of Lee et al. (1999) where the R3HBA yield reached up to 96 % in 30 min at pH 4, but not at higher pH values. The *in-vivo* depolymerization of *A. lata* is highly influenced by the effect of pH on PhaZ and Hbd activities. Lee et al. (1999) observed that the highest PhaZ activity is attained between pHs 3 and 4; whereas no activity was recorded at pH 4 for Hbd. Then R3HBA could not be converted to acetoacetate and was excreted to the extracellular medium.

Table 6. Summary of the PHB conversion, R3HBA excreted and cell viability at pH 4, 5 and 7 in *A. lata* cells

<b>pH</b>	<b>Initial biomass</b> [g L <sup>-1</sup> ]	<b>Initial</b> <b>PHB</b>	<b>Final</b> <b>PHB</b>	<b>R3HBA</b> [g L <sup>-1</sup> ]	<b>Yield</b> <b>R3HBA/PHB</b>	<b>Viable</b> <b>colonies</b>
4	3.50	63.9 %	25.3 %	2.42	93.6 %	2.72 %
5	3.14	59.4 %	30.0 %	0.196	9.32 %	10.8 %
7	3.60	66.0 %	58.0 %	0.019	1.76 %	32.2 %

After 5 hours of *in vivo* depolymerization, cells were plated on AL1 agar and the viability was quantified by colony counting. A viability of 50 % was considered positive. Table 6 indicated that the number of viable colonies increased with the pH toward neutral values, but no condition achieved 50 % of viability. A possible explanation is that *in-vivo* depolymerization and incubation with buffer phosphate can trigger cellular stress, thus causing death cell.

#### 4.1.5. Sequential PHB depolymerization in a nitrogen-limited chemostat

A depolymerization bioreactor was coupled to the discharge of a nitrogen-limited chemostat operated at  $D=0.2 \text{ h}^{-1}$  and was maintained at pH 4 with a 30 min of residence time. After ten residence times, a sample withdrawn from the depolymerization reactor showed a depolymerization yield of  $92.3 \pm 2.0\%$  mol R3HBA per mol PHB calculated after measuring R3HBA using an enzymatic assay specific for R3HBA and PHB quantification by GC after

propanolysis. Considering the short residence time in the second bioreactor and the lack of metabolic activity of *A. lata* DSM1123 at pH 4, this result suggests that the PhaZ and Hbd are active under nitrogen-limited conditions. An HPLC measurement of the culture supernatant of the first reactor indicates the presence of R3HBA at a concentration of 18 mg L<sup>-1</sup>. These results confirm the low activity of phaZ in neutral pHs as described by Lee et al.,(1999), where 40 mg L<sup>-1</sup> of R3HBA titer was obtained at pH 7, the difference of amount obtained in this work with Lee and co-workers may be related by an active Hbd at this pH. Lee et al., (1999) showed Hbd activity of 15.12 U mg<sup>-1</sup> protein at pH of 7 instead of 0 U mg<sup>-1</sup> at 4 pH.

#### 4.2. STUDY OF *in-vivo* PHB DEPOLYMERIZATION IN *M. parvus*

The results presented in this section, were published in the following paper “Production of (*R*)-3-hydroxybutyric acid from methane by *in vivo* depolymerization of polyhydroxybutyrate in *Methylocystis parvus* OBBP” with DOI:

<https://doi.org/10.1016/j.biortech.2022.127141>

##### 4.2.1. Influence of the presence of nitrate, O<sub>2</sub> and pH on PHB depolymerization

Figure 2 shows the CH<sub>4</sub> and O<sub>2</sub> consumption for the 48 hours depolymerization experiments performed with NMS (panels A and B) and NFMS (panels C and D) at pH 4, 7 and 11. Consumption of methane and oxygen was faster in the control experiment with NMS at pH 7 compared to that in NFMS medium, an expected result considering that NMS allows for balanced growth. In the absence of oxygen at pH 7, methane consumption was negligible in NFMS medium and close to 10% in the NMS cultures. In this regard, Bordel et al. (2019) showed that *M. parvus* can use stored PHB as an energy source under anoxic conditions only when nitrate is available in the cultivation broth. The annotated genome of *M. parvus* contains the genes involved in nitrate reduction and revealed that denitrification is the only mechanism supporting the use of methane or PHB as an energy source in the absence of oxygen (Bordel et al., 2019).

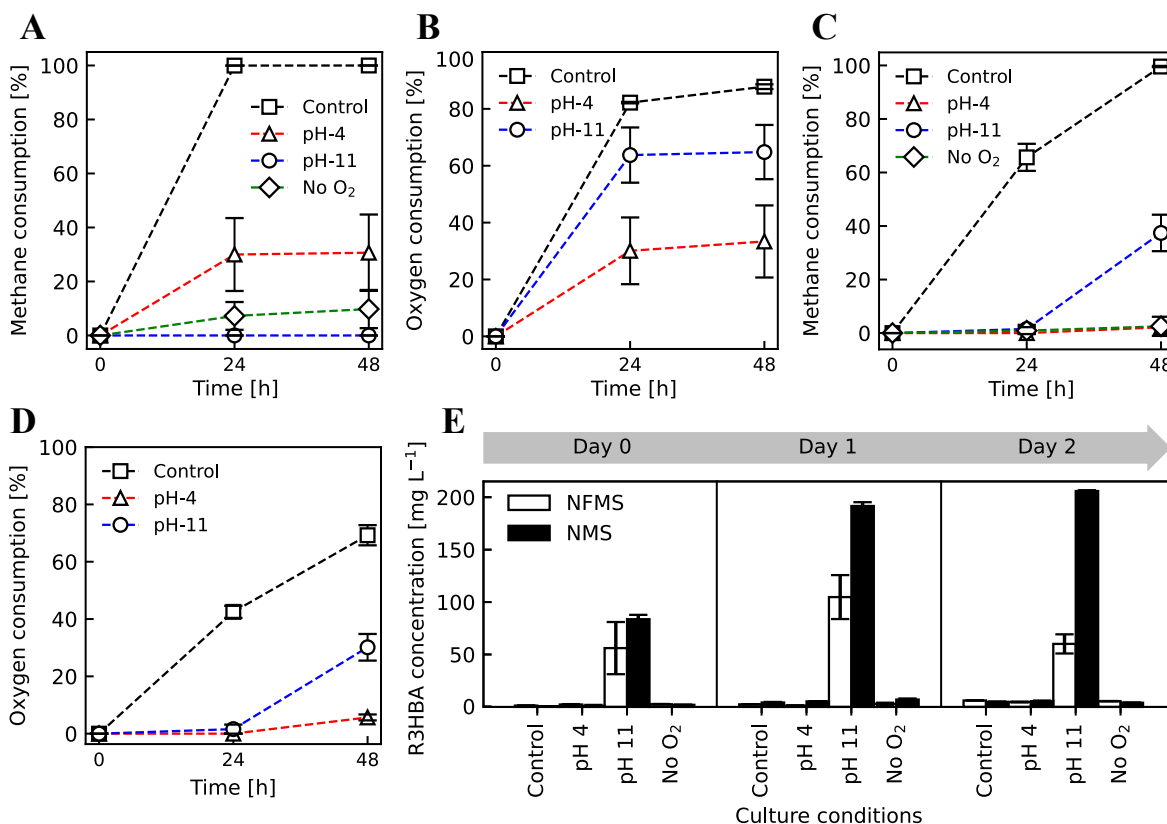


**Figure 2. CH<sub>4</sub> and O<sub>2</sub> consumption profile and R3HBA released at different depolymerization conditions in *M. parvus*.** CH<sub>4</sub> and O<sub>2</sub> consumption during PHB depolymerization in *M. parvus* cultivated in NMS (A, B) and NFMS (C, D) medium at pH 4 (triangles), pH 11 (circles), pH 7 (squares) and w/o oxygen at pH 7 (diamonds). (E) R3HBA released at pHs 4, 11, 7 (w/ and w/o oxygen) in NMS (black bars) and NFMS (white bars) medium.

On the other hand, neither methane nor oxygen consumption was recorded at pH 4 in NFMS medium. Similarly, at pH 11 the final consumption of CH<sub>4</sub> ( $37.41 \pm 6.81$  %) and the O<sub>2</sub> uptake ( $30.14 \pm 4.65$  %) were reduced compared to the control. In NMS, nitrate was consumed only in the control assays at pH 7 from the initial  $130.1 \text{ mgN L}^{-1}$  (measured as total nitrogen) to  $47.8 \pm 11.5 \text{ mgN L}^{-1}$  at the end of the 48 hours incubation period. Nitrate consumption at pHs 4 and 11 was lower than  $2.6 \text{ mgN L}^{-1}$  during the same period and only  $0.3 \text{ mgN L}^{-1}$  was consumed in the assay at pH 7 in the absence of oxygen. Therefore, no significant cell growth occurred except in the control (neutral pH).

Interestingly, extracellular R3HBA was only detected at pH 11 in both NMS and NFMS medium (Figure 2, panel E). At pH 11 in NMS,  $80.6 \pm 0.8$  % of PHB was depolymerized and R3HBA secretion reached  $205.8 \pm 1.2$  mg L<sup>-1</sup>, a higher concentration compared with the assay in NFMS, where  $25.7 \pm 7.9$  % of PHB was depolymerized and a R3HBA titer of  $60.1 \pm 12.9$  mg L<sup>-1</sup> was measured after 48 h. The mechanisms by which nitrogen influences the depolymerization extent and rate seem to be related in other bacteria species to the alleviation of the stringent response. In the amino acid starved cells, the alarmone ppGpp accumulates and destabilizes the RNA polymerase  $\sigma 70$ , resulting in an induction of genes under the control of alternative sigma  $\sigma$  factors, such as  $\sigma 54$  (Brigham et al., 2012). ppGpp has also been implicated in the inhibition of translation (Irving et al., 2021). In *C. necator* H16, PHB mobilization occurs in the absence of the alarmone ppGpp, which in turn requires the presence of a source of nitrogen (Juengert et al., 2017). As further evidence of this mechanism, the genome of *M. parvus* OBBP contains the necessary bifunctional (p)ppGpp synthetase/hydrolase (WP\_016921527.1) required for the synthesis and degradation of ppGpp.

PHB depolymerization at pH 4 and pH 7 (with or without O<sub>2</sub>) in NMS produced extracellular R3HBA titers of  $5.42 \pm 0.67$  mg L<sup>-1</sup>,  $4.83 \pm 0.37$  mg L<sup>-1</sup> and  $4.01 \pm 0.15$  mg L<sup>-1</sup>, respectively. Similarly, extracellular R3HBA concentrations of  $4.68 \pm 0.37$  mg L<sup>-1</sup>,  $6.17 \pm 0.22$  mg L<sup>-1</sup> and  $5.50 \pm 0.15$  mg L<sup>-1</sup> were measured after 48 hours in NFMS at pH 4 and pH 7 with or without oxygen, respectively. The final pH of the culture broth in the assays initially adjusted to pH 11 in NMS and NFMS media decreased to 8.28 and 6.23, respectively, confirming the secretion of the acidic R3HBA. No significant changes in pH were measured in the rest of the experiments, which agreed with the limited R3HBA release. The estimated  $Y_{R3HBA}$  are  $31.5 \pm 0.08$  % and  $28.9 \pm 0.91$  %, which equates to a PHB to R3HBA conversion of  $25.4 \pm 0.03$  % and  $7.4 \pm 2.1$  %, for the experiments at initial pH of 11 in NMS and NFMS respectively.

The *in-vivo* depolymerization of the intracellularly accumulated PHAs to hydroxy acids has been reported in several bacterial strains. For instance, the depolymerization process in *A. lata* was carried out in water without shaking to minimize oxygen transfer, at 37 °C and

pH 4 and achieved a depolymerization efficiency of 96% of the initial PHB to R3HBA in only 30 min (Lee et al., 1999). These authors also evaluated PHB depolymerization in *Pseudomonas aeruginosa* PAO1 (DSM 1707), *Pseudomonas oleovorans* (ATCC 29347) and *Cupriavidus necator* (NCIMB 11599) at pH values below 7 (Lee et al., 1999). The PHA to hydroxy acids conversion was 20 % for *C. necator* and less than 10 % for *Pseudomonas* species (Lee et al., 1999).

The conversion of PHA to hydroxy acids in *Pseudomonas putida* GPo1 was improved by changing the depolymerization conditions to an alkaline medium. This strain excreted R3HO and R3HHx at pH 11 in citrate buffer for 6 hours with a PHA degradation efficiency and monomer production yields above 90 % (w/w) (Ren et al., 2005). Ruth et al. (2007) engineered a depolymerization strategy at pH 10 in *P. putida* GPo1 under continuous mode with a production of R3HO, R3HHx, (*R*)-3-hydroxy-10-undecenoic acid, (*R*)-3-hydroxy-8-nonenic acid, (*R*)-3-hydroxy-6-heptenoic acid, (*R*)-3-hydroxyundecanoic acid, (*R*)-3-hydroxynonanoic acid and (*R*)-3-hydroxyheptanoic acid. The study herein presented confirmed the key role of high pH on PHA depolymerization, which is a common feature in *Pseudomonas* species. Hence, *P. putida* GPo1 released 3-hydroxyoctanoic acid and 3-hydroxyhexanoic acid from intracellular PHA at pH 11 with conversions of 76 % (0.356 g L<sup>-1</sup>) and 21% (0.015 g L<sup>-1</sup>) in 6 hours, respectively (Ren et al., 2005). Similarly, *P. putida* Bet001 can depolymerize PHAs up to 98 % in 0.2 Tris-HCl buffer at pH 9.1 within 48 hours (Anis et al., 2018). In Type II methanotrophs, the production of hydroxy acids has only been described in a genetically engineered *Methylosinus trichosporum* OB3b strain able to synthesize (*R*)-4-hydroxybutyrate acid (R4HBA) from CH<sub>4</sub> via the tricarboxylic acid cycle (TCA cycle) and the overexpression phosphoenolpyruvate carboxylase (Ppc), isocitrate dehydrogenase (Icd) and 2-oxoglutarate dehydrogenase (SucAB). The highest 4-hydroxybutyrate titer obtained was 10.5 mg L<sup>-1</sup> after 6 culture days (Nguyen et al., 2021).

PHB synthesis and degradation in methanotrophic bacteria seem to be similar to the metabolic processes carried out by most heterotrophic PHB producers (Vecherskaya et al., 2001). However, there is a limited understanding of the mechanisms that control the intracellular PHB depolymerization and the formation of its monomer acids such as R3HBA

and crotonic acid in Type II methanotrophs. Vecherskaya et al. (2001) demonstrated how products from the anaerobic fermentation of PHB in methanotrophs can be bioconverted in R3HBA, butyrate, acetate, succinate, and other reduced compounds. Figure 3 shows the pathways of PHB depolymerization and formation of different metabolites in *M. parvus* OBBP based on a genome-scale metabolic model (Bordel et al., 2019) that has been recently reported. This model shows the fluxes of the PHB degradation from crotonyl-CoA to methylmalyl-CoA, which is dissociated into glyoxylate and propionyl-CoA. The glyoxylate originated from methylmalyl-CoA is incorporated into the serine cycle and the propionyl-CoA is carboxylated into succinyl-CoA by the ethylmalonyl-CoA cycle (EMC) and then incorporated into the TCA cycle (Bordel et al., 2019). Another parallel pathway involves the enzymatic conversion of crotonyl-CoA to butyryl-CoA and finally to butyrate (Vecherskaya et al., 2001).

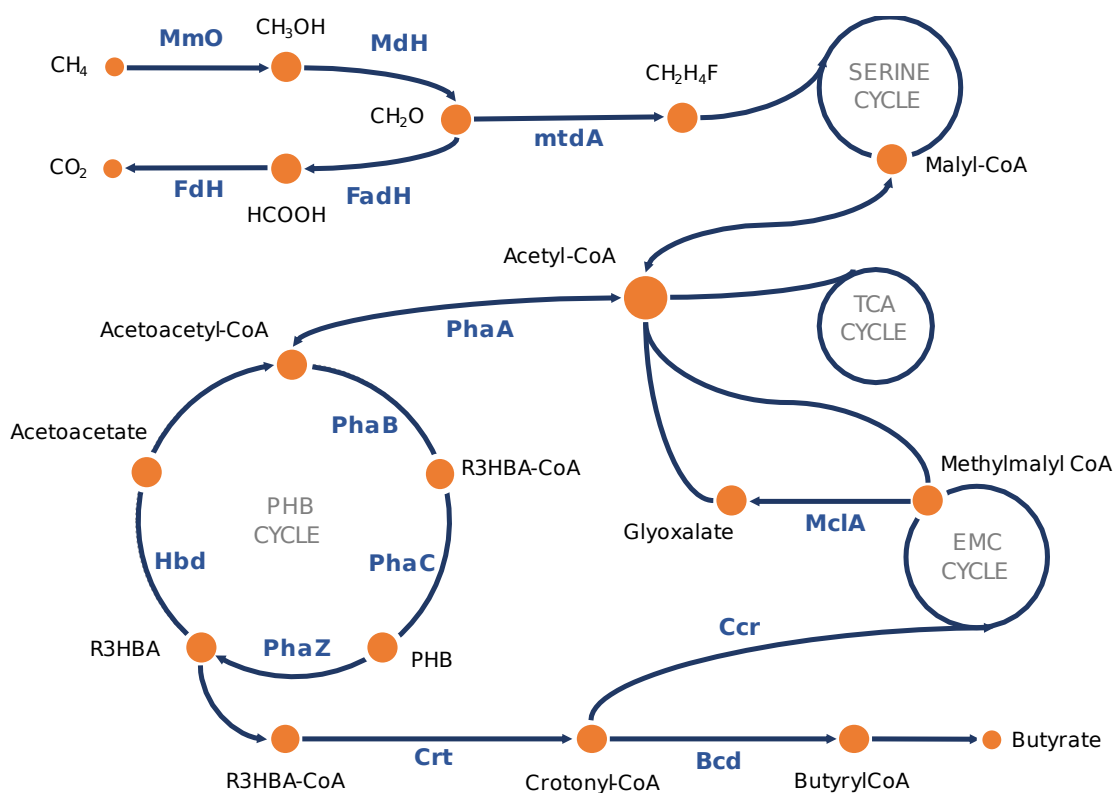


Figure 3. **Schematic metabolic pathways involved in the polymerization and depolymerization of PHB in *M. parvus*.** MmO, methane monooxygenase; MdH, methanol dehydrogenase; FadH, formaldehyde dehydrogenase; FdH, formate dehydrogenase; MtdA, methylene tetrahydromethanopterin dehydrogenase; PhaB, acetoacetyl-CoA reductase; Crt, 3-hydroxybutyryl-CoA dehydratase; Ccr, crotonyl-CoA carboxylase/reductase; MclA, malyl-CoA lyase; Bcd, butyryl-CoA dehydrogenase.

#### 4.2.2. Optimization of pH during depolymerization

The results showed in Figure 4 indicate that PHB depolymerization at pH 11 in NMS was superior to the result obtained at low pHs in NFMS. However, these results do not clarify if pHs closer to 11 could result in higher R3HBA titers, if pH control could improve R3HBA yields or if methane plays a role in the depolymerization of PHB. In this context, *M. parvus* cells containing 18.1 % of PHB were resuspended in NMS medium at  $1.32 \pm 0.02 \text{ gTSS L}^{-1}$  and depolymerization was assessed at pHs of 10, 11 and 12 as above described. Unlike previous experiments, the pH of the cultivation broth was periodically monitored and controlled with NaOH during the course of the depolymerization.

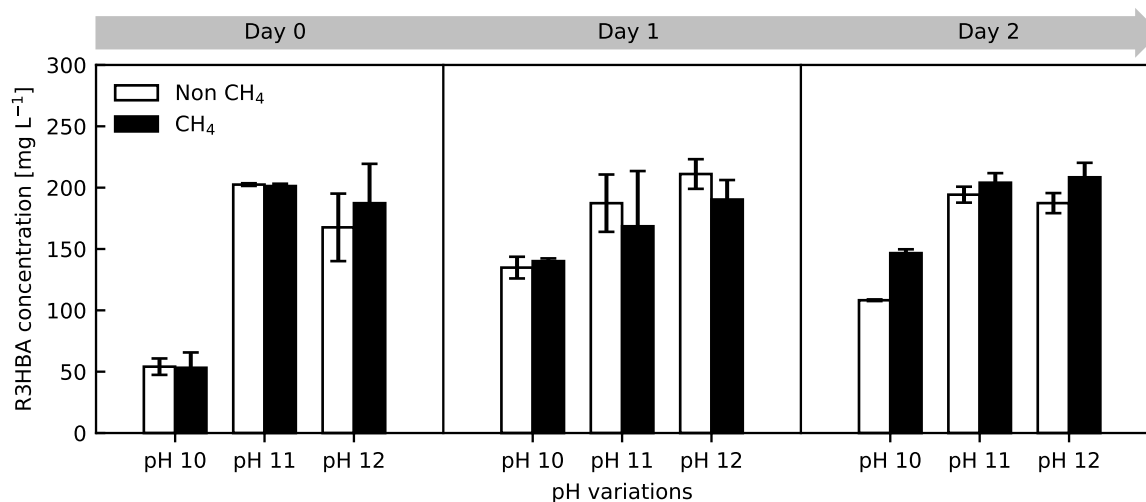


Figure 4. **R3HBA released at pH 10, 11 and 12 in presence or absence of CH<sub>4</sub> in *M. parvus*.** PHB accumulated cells cultured in NMS medium with (black bars) or without (white bars) CH<sub>4</sub> for 48 h at 37°C.

*M. parvus* cells rapidly released R3HBA in the pH range of 10-12 following pH adjustment. Thus, the final extracellular monomer concentration reached  $146.6 \pm 3.11 \text{ mg L}^{-1}$  and  $108.2 \pm 0.66 \text{ mg L}^{-1}$  with or without methane at pH 10 (Figure 4). On the other hand, the influence of methane was negligible at pH 11 and pH 12, reaching a PHB depolymerization efficiency of  $96.6 \pm 2.22\%$  and  $92.9 \pm 1.5\%$ , respectively (corresponding to  $204 \pm 7.8 \text{ mg L}^{-1}$  and  $208.4 \pm 11.8 \text{ mg L}^{-1}$  of R3HBA) in the presence of CH<sub>4</sub>. Similar PHB depolymerization

efficiencies of  $98.2 \pm 1.10\%$  and  $93.6 \pm 1.33\%$ , respectively (corresponding to  $194.3 \pm 6.5 \text{ mg L}^{-1}$  and  $187.4 \pm 8.2 \text{ mg L}^{-1}$  of R3HBA) were recorded in the absence of  $\text{CH}_4$  at the end of the experiment at pH 11 and 12, respectively. These data suggested that methane did not play a significant role on PHB depolymerization and that pHs beyond 11 exerted little influence on R3HBA release. Based on these results, pH 11 in NMS and in the absence of  $\text{CH}_4$  was selected for further experiments. Under this condition, a PHB to R3HBA conversion of  $68.0 \pm 3.2 \%$  was estimated.

The fine-tuning of pH played a key role in R3HBA release and PHB depolymerization in other bacteria species. For instance, Ren et al. (2005) demonstrated that PHA depolymerization in *Pseudomonas Gpo1* produced the highest titer of monomers ( $360 \text{ mg L}^{-1}$  of (*R*)-3-hydroxyoctanoic acid at an initial pH of 11, while a significantly smaller concentration of monomers ( $50 \text{ mg L}^{-1}$ ) was measured at pH 12. Similarly, depolymerization and R3HBA release in *A. lata* peaked at a pH of 4 with a PHB to R3HBA conversion of 96 % in 30 min and decreased to 31 % at a pH 5 (Lee et al., 1999). The production of R3HBA *in vivo* requires a concomitant high PHB depolymerization activity and a low enzymatic activity of Hbd (Jendrossek and Handrick, 2002). While intracellular depolymerases have an optimum pH range of 8-10 (Jendrossek; Handrick, 2002), Hbd activity is reported to be pH-dependent, with an activity range of 5-10 and an optimal pH range of 7.5-8.5, decreasing abruptly above pH 10 (Mountassif et al., 2010; Takanashi & Saito, 2006). In this context, this study suggests that the PhaZ enzyme, responsible of the depolymerization of PHB towards R3HBA, of *M. parvus* exhibits a high activity at pH 11.

#### 4.2.3. Influence of temperature on the kinetic of PHB depolymerization

Since the optimal temperature for both growth and PHB accumulation in *M. parvus* is  $30 \text{ }^\circ\text{C}$  and no growth occurs at temperatures greater than  $40 \text{ }^\circ\text{C}$  (Soni et al., 1998), the kinetics of PHB depolymerization and R3HBA released were investigated at  $25$  and  $35 \text{ }^\circ\text{C}$ , and pH 11 (manually adjusted to compensate for the R3HBA release). The R3HBA titers quantified at  $25$  and  $35 \text{ }^\circ\text{C}$  were  $240 \pm 3.81 \text{ mg L}^{-1}$  and  $282 \pm 20.04 \text{ mg L}^{-1}$ , respectively, after 3 hours of depolymerization in a cell suspension with an initial PHB concentration of  $1.86 \pm 0.006 \text{ g L}^{-1}$ .

The R3HBA production rates of initial PHB were  $48.6 \pm 6.0$  mg R3HBA mg PHBi<sup>-1</sup> h<sup>-1</sup> at 25 °C and  $52.7 \pm 2.3$  mg R3HBA mgPHBi<sup>-1</sup> h<sup>-1</sup> at 35 °C, while PHB depolymerization reached 16.5% ( $Y_{R3HBA}=64.5\%$ ) and 24.8% ( $Y_{R3HBA}=50.5\%$ ) at 25 and 35 °C, respectively. These results were similar to those obtained by Lee et al. (1999) during the depolymerization of PHB accumulated in *A. lata* at 30, 37 and 45 °C. A moderate increase in R3HBA production rate was found when the temperature increased from 30 to 37 °C, while PHB depolymerization suddenly stopped at 45 °C likely due to enzymatic denaturation. Since R3HBA production rate slightly increased with temperature, but R3HBA yields severely decreased, the following experiments were performed at 30 °C.

After 3 hours at 25 °C and pH 10.8, cells were harvested and cultured in NMS (to assess cell growth) and NFMS (to assess PHB accumulation) media in the presence of CH<sub>4</sub> to analyze the viability of the cells post-depolymerization.

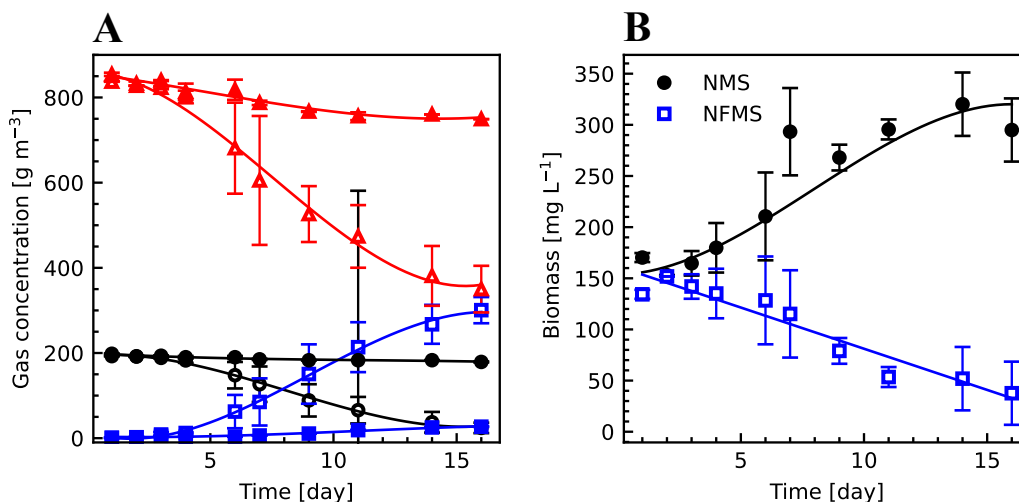


Figure 5. **Time course of biomass and CH<sub>4</sub>, O<sub>2</sub> and CO<sub>2</sub> in viability assay of *M. parvus*.** Concentrations of biomass (A) and CH<sub>4</sub> (circles), O<sub>2</sub> (triangles) and CO<sub>2</sub> (square) (B) during the viability assays of *M. parvus* cells previously subjected to a 3 h depolymerization phase at pH 11. Filled and empty symbols correspond to the experiments carried out in NMS and NFMS media, respectively.

Cells incubated in NMS medium started to consume methane and oxygen by day 4, these gases fully being depleted after 16 days (Figure 5, panel A). Biomass concentration increased

from  $170 \text{ mg L}^{-1}$  to  $295 \text{ mg L}^{-1}$  (Figure 5, panel B). However, the  $\mu$  of post-depolymerization cells was  $0.058 \text{ h}^{-1}$ , which has lower than the  $\mu = 0.107 \text{ h}^{-1}$  reported for fresh *M. parvus* cultures (Bordel et al., 2019). On the other hand, the culture incubated in NFMS medium experienced cell death during the cell viability experiment, presumably due to nitrogen limitation.

#### 4.2.4. Influence of the aeration rate and R3HBA exogenous on PHB depolymerization

To assess the effect of oxygen availability on PHB depolymerization in *M. parvus*, three tests with different liquid to air surface ratios in E-flasks were carried out at a constant pH of 11. Figure 6 panel A, shows the kinetics of R3HBA release for the 72 hours experiment and the depolymerization, crotonic acid and R3HBA yields in Figure 6 panel B.

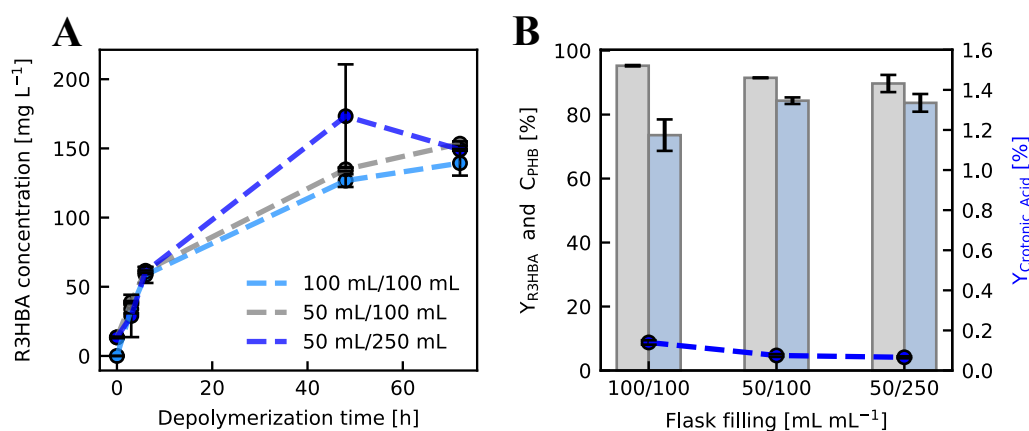


Figure 6. **Influence of the oxygen mass transfer rate on the kinetics of R3HBA release in *M. parvus*.** Timeline of the R3HBA release at different aeration conditions (A), depolymerization (grey bars) and R3HBA yields (blue bars) (B).

The final R3HBA concentration was similar regardless of the  $\text{O}_2$  supply, while the largest differences were obtained for the R3HBA yield. Indeed, the lowest R3HBA yield ( $73.6 \pm 4.9 \%$ ) occurred under the condition restricting  $\text{O}_2$  mass transfer (100 mL of broth in a 100 mL E-flask) while under less restrictive  $\text{O}_2$  supply rates, R3HBA yields reached  $84.3 \pm 1.0 \%$  and  $83.7 \pm 2.8 \%$  at 50 mL/100 mL and 50 mL/250 mL filling ratios, respectively. In terms of PHB to R3HBA conversion, these values correspond to  $91.5 \pm 0.1 \%$

and  $89.7 \pm 2.7\%$ , respectively. Literature suggests that the oxygen content during the depolymerization process could influence the fate of the monomers produced in rather unpredictable manners. In this regard, the PHB accumulated with glycerol as substrate can be depolymerized to R3HBA in *Halomonas* sp. KM-1 under microaerobic conditions (25 mL of broth in 200 mL E-flasks agitated at 50 rpm) in the presence of a nitrogen source. Indeed,  $15.2 \text{ g L}^{-1}$  of R3HBA were produced in 66 hours with a 76.6% PHB to R3HBA conversion under these conditions (Kawata et al., 2012). On the other hand, *Halomonas* sp. OITC1261 behaves differently despite its taxonomic closeness with *Halomonas* sp. KM-1, synthesizing R3HBA concomitantly with PHB under aerobic conditions without extra nitrogen supplementation (Yokaryo et al., 2017).

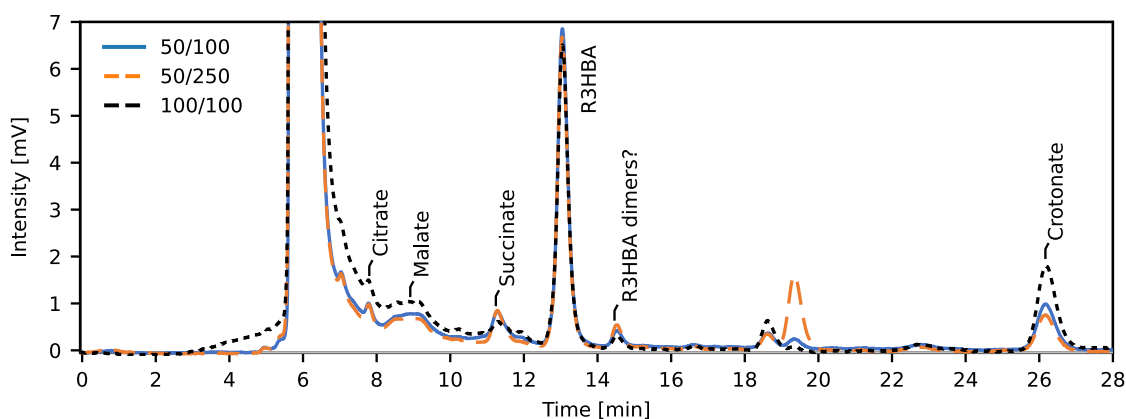


Figure 7. **HPLC chromatograms of depolymerization assays at different filling ratios in E-flasks.** Supernant of samples culture taken after 72 h of depolymerization at pH 11 in NMS medium.

HPLC analysis (Figure 7) of the depolymerization broth at 72 hours showed that citric acid (ranging between 1 and 3  $\text{mg L}^{-1}$  depending on the  $\text{O}_2$  supply rate), malate (20-45  $\text{mg L}^{-1}$ ), succinate (5-20  $\text{mg L}^{-1}$ ) and crotonate (less than 0.2  $\text{mg L}^{-1}$ ) were present along with R3HBA and two unidentified compounds at 18.5 and 19.5 min in the incubation broth drawn after 72 hours of depolymerization assay. In addition, a peak at 14.6 min was resolved, presumably corresponding to R3HBA dimers based on previous reports (Lu et al., 2014).

The oxygen consumption during the PHB depolymerization process at pH 11 (Figure 2, panel B) and the fact that the yield of R3HBA decreased as the supply of oxygen decreased

below a certain threshold, suggests that part of the electrons released from the conversion of the depolymerized PHB towards acetyl-CoA are aerobically oxidized for the provision of maintenance energy. This follows from the subsequent findings: (i) the production of acetoacetate from R3HBA produces a molecule of NADH that could be used for ATP production if O<sub>2</sub> is available, (ii) a negligible nitrate consumption was measured at pH 11 during the depolymerization experiment, thus growth can be disregarded, (iii) a limited supply of O<sub>2</sub>, achieved by carrying out the depolymerization process in an almost filled E-flask, decreased the R3HBA yield, suggesting that R3HBA was routed towards other metabolites to provide energy for maintenance. The latter finding can be considered as a less extreme version of the experiments by Vecherskaya et al. (2001) under anaerobic conditions, where products characteristics of a fermentative metabolism for energy production were obtained.

On the other hand, R3HBA might act as an inhibitor of the enzymatic depolymerization activity. To test this hypothesis in *M. parvus*, depolymerization assays were carried out adding exogenous R3HBA before the onset of the depolymerization at concentrations ranging from 0 to 650 mg L<sup>-1</sup>. The higher limit was higher than the R3HBA titers achieved in previous experiments, where values slightly above 200 mg L<sup>-1</sup> were found after 48 hours of depolymerization at pH 11 with or without methane.

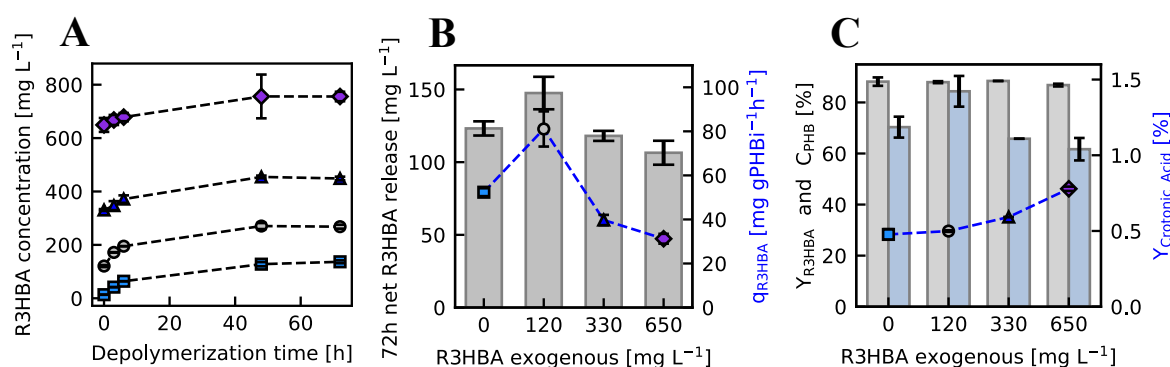


Figure 8. **Influence of R3HBA exogenous in the R3HBA excretion in *M. parvus*.** Time course of R3HBA concentration at 0 (square), 120 (circle), 330 (triangle) and 650 (diamond) mg L<sup>-1</sup> of initial R3HBA (A), net release (bars) and initial production rate of R3HBA (scatter plot) (B) and R3HBA yield (blue bars), depolymerization yield (gray bars) and crotonic acid yields (scatter plot) (C) at pH 11 and NMS medium in *M. parvus* after 72 h.

Figure 8 panel A shows the total R3HBA concentration during the 72 hours depolymerization experiment, while the net R3HBA released at the end of the experiment (72 h) is shown in Figure 8 panel B. No significant differences were found between R3HBA concentration released after 72 hours with no added R3HBA and any of the experiments with addition of exogenous R3HBA. Figure 8 panel B, also shows the specific initial rate of R3HBA release calculated during the first 6 hours. This parameter increased from  $52.4 \pm 1.8$  mg of R3HBA per gram of initial PHB (PHBi) per hour in the absence of exogenous R3HBA to  $81.1 \pm 8.0$  mg g PHBi<sup>-1</sup>h<sup>-1</sup> in the presence of 120 mg R3HBA L<sup>-1</sup>. This increase could be related to impurities in the *in-house* produced R3HBA, although this was not further investigated. Additional increases in the initial R3HBA concentration led to a decrease in the specific initial rate of R3HBA release. Finally, Figure 8 panel C shows no differences on the depolymerization yield regardless of the initial R3HBA concentration. Interestingly, the  $Y_{R3HBA}$  was reduced at 330 and 650 mg L<sup>-1</sup> ( $65.8 \pm 0$  and  $61.7 \pm 4.40$  %) compared to non R3HBA addition or to 120 mg R3HBA L<sup>-1</sup> added, while an increment of the crotonic acid yield to  $0.78 \pm 0.014$  % was evidenced at the highest initial R3HBA concentration.

Surprisingly, literature is scarce regarding the effect of R3HBA on the depolymerization kinetics, although R3HBA is the main reaction product. Scherer et al, (1999) found that an extracellular PHB depolymerase from *Aspergillus fumigatus* was reversibly inhibited by trimers of R3HBA, but no data was presented concerning inhibition by R3HBA.

#### 4.3. PLASMID CONSTRUCTION FOR *tesB* EXPRESSION IN *C. necator* H16 AND *M. parvus*

The implementation of the TSS system in *M. parvus* was explored by the construction of an expression vector containing *tesB*. A synthetic operon including promoter, *tesB* and terminator cassette was amplified from a pUC57 plasmid and assembled in the pAWP89 backbone resulting in pLY01 plasmid. Figure 9C1-C3 showed the bands of approximately 1300 bp corresponding to the promoter, *tesB* and terminator cassette assembled in pLY01 plasmid. Then, this was sequenced in order to confirm the correct construction of the plasmid. Figure 10 indicates the comparison between the main features in the designed pAWP89-*tesB*

(Figure 10A) and the constructed and sequenced plasmid pLY01 (Figure 10B). Although *tesB* is present, the construction of the plasmid yield and unexpected result. The features displayed in pLY01 such as *Amp<sup>R</sup>* and *lac* promoter did not correspond to the features of the backbone pAWP89 plasmid, suggesting that incorrect fragments of the pUC57 plasmid were assembled in pLY01 instead of the corresponding *tesB* cassette. The reasons of the inconsistent construction are unknown, consequently the application of TSS system in *M. parvus* was not possible.

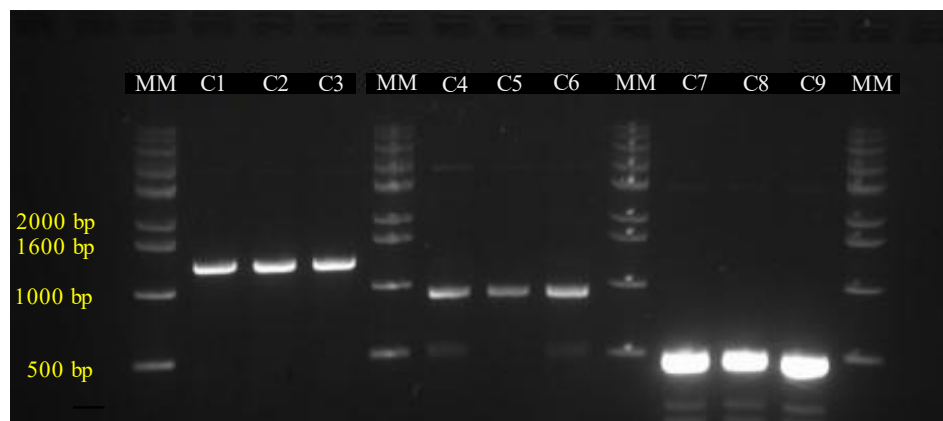


**Figure 9. PCR product amplification of plasmids constructed for the expression of *tesB* in *M. parvus* and *C. necator* H16.** Samples from constructed plasmids in *E. coli* DH5 $\alpha$  for visualization through agarose gel by electrophoresis at 90 V for 45 min and using a molecular size marker (MM) of 1 kb DNA AccuLadder from Bionner. The bands, C1-C3 are the cassette containing promoter, *tesB* and terminator gene amplified from pLY01 plasmid; the following lanes correspond to amplified products from pLY02 plasmid, C4-C6: *tesB* gene, C7-C9: terminator fragment.

For the construction of vector carrying *tesB* gene for its expression in *C. necator* H16, the fragments *tesB* and terminator were amplified from pUC57 and pBAD24-sfGFPx2 plasmid and assembled through Gibson using the backbone plasmid pBBR1MCS2 (details in methods section), resulting in pLY02 plasmid. Then, the assembled plasmid was transferred to the chemocompetent *E. coli* DH5 $\alpha$  and the confirmation of the insertion of *tesB* and terminators fragment is presented in Figure 9C4-C9.

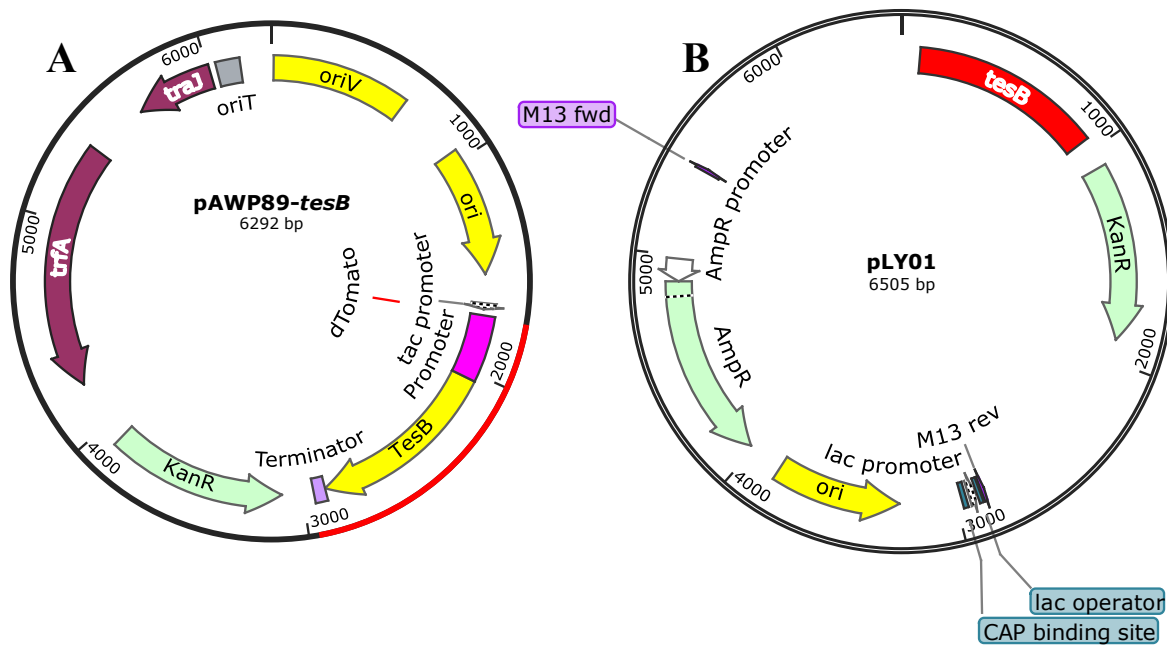


Figure 10. **Maps of the plasmid designed for *tesB* expression in *M. parvus*.** Main features contained in the plasmids (A) pAWP89-*tesB* (6292 bp) and (B) pLY01 plasmid from Gibson assembly (6505 bp). Created by SnapGene® 6.1.1.

According to Figure 9, the lanes C4-C9 shows the amplified bands corresponding to *tesB* (Figure 9 C4-C6) and terminator (Figure 9 C7-C9) fragments with 900 bp and 450 bp, respectively. Thus, plasmid was sequenced in order to confirm the correct insertion of the fragments. Figure 11 revealed the main features obtained in the sequenced pLY02 plasmid (Figure 11B) in comparison to the designed pBBR1MCS2-*tesB* (Figure 11A). pLY02 had a total length of 6522 bp and contains the *tesB* and *Amp<sup>R</sup>* gene, the last one not corresponding with the antibiotic resistance gene of pBBR1MCS2-*tesB*. The *Amp<sup>R</sup>* gene is contained in pBAD24-sfGFPx2 and pUC57 plasmids, suggesting that the terminator fragment wasn't assembled in the Gibson cocktail and remnants of pBAD24-sfGFPx2 or pUC57 plasmids were linked to the product plasmid, pLY02. Moreover, the origin replication site and protein replication fragment from pBBR1MCS2-*tesB* backbone plasmid does not appear pLY01-*tesB*. Due these negative results, the application of TSS system in *C. necator* was not possible.

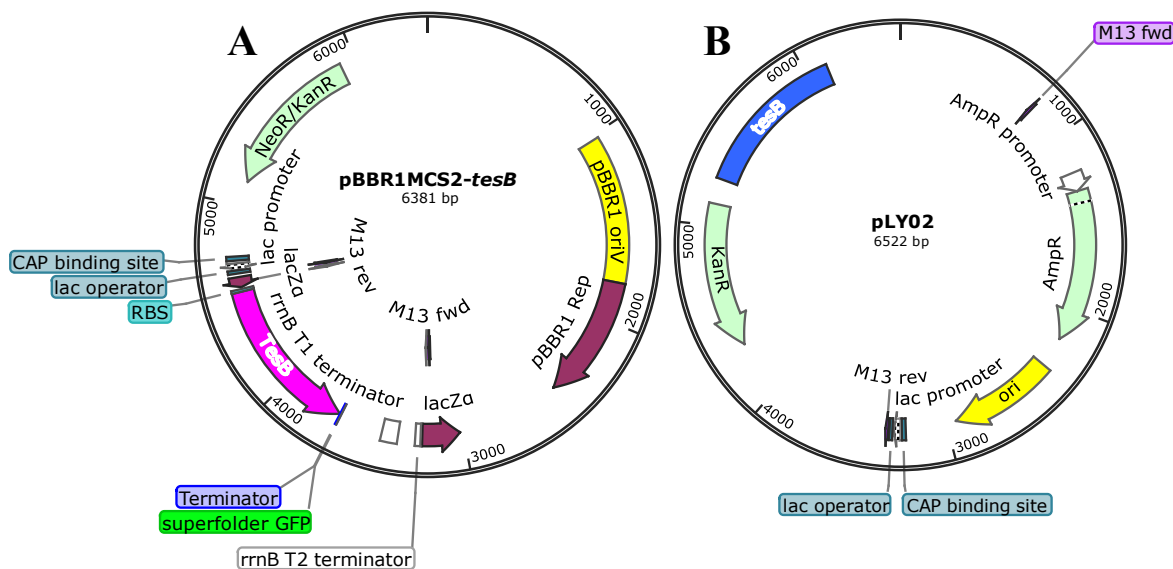


Figure 11. **Maps of the plasmid designed for *tesB* expression in *C. necator* H16.** Main features contained in the plasmids (A) pBBR1MCS2-*tesB* (6381 bp) and (B) pLY02 from Gibson assembly (6522 bp). Created by SnapGene® 6.1.1.

#### 4.4. GENERATION OF MUTANT STRAINS OF *C. necator* VIA SUICIDE VECTOR pT18mobsacB

Another way of studying the production of R3HBA can be through redirecting fluxes in the PHB metabolic pathway that allows the release of R3HBA without being converted into acetoacetate. Two mutant strains were constructed via suicide vector pT18mobsacB. The first strain was *C. necator*  $\Delta$ *phaC* which is a mutant strain with a *phaC* knock out, the gene encoding for the only active PHA synthase in *C. necator*. This strain is unable to polymerize PHB. The second strain is *C. necator*  $\Delta$ *phaC*  $\Delta$ *hbd*, which is the same *C. necator*  $\Delta$ *phaC* with the deletion of *hbd* gene encoding for the hydroxybutyrate dehydrogenase, unable to polymerize PHB and to transform R3HBA into acetoacetate.

The Figure 12 shows the amplification of *phaC* and *hbd* genes in the *C. necator* strains studied. The total length of *phaC* in *C. necator* H16 corresponds to 1770 pb (Figure 12A *phaC* lane 1), which have the same length with *C. necator* 541 because is a chemically induced mutant with G320A point mutation in *phaC* gene that cause a stop codon producing a truncated and non-functional PHA synthase (Raberg et al., 2014). Lanes 3 and 4 (Figure

12A *phaC*) correspond to *C. necator*  $\Delta$ *phaC* and *C. necator*  $\Delta$ *phaC*  $\Delta$ *hbd* which showed a length of 1000 bp with a *phaC* null fragment (Figure 12B). This confirms the deletion of the *phaC* gene in these mutant strains.

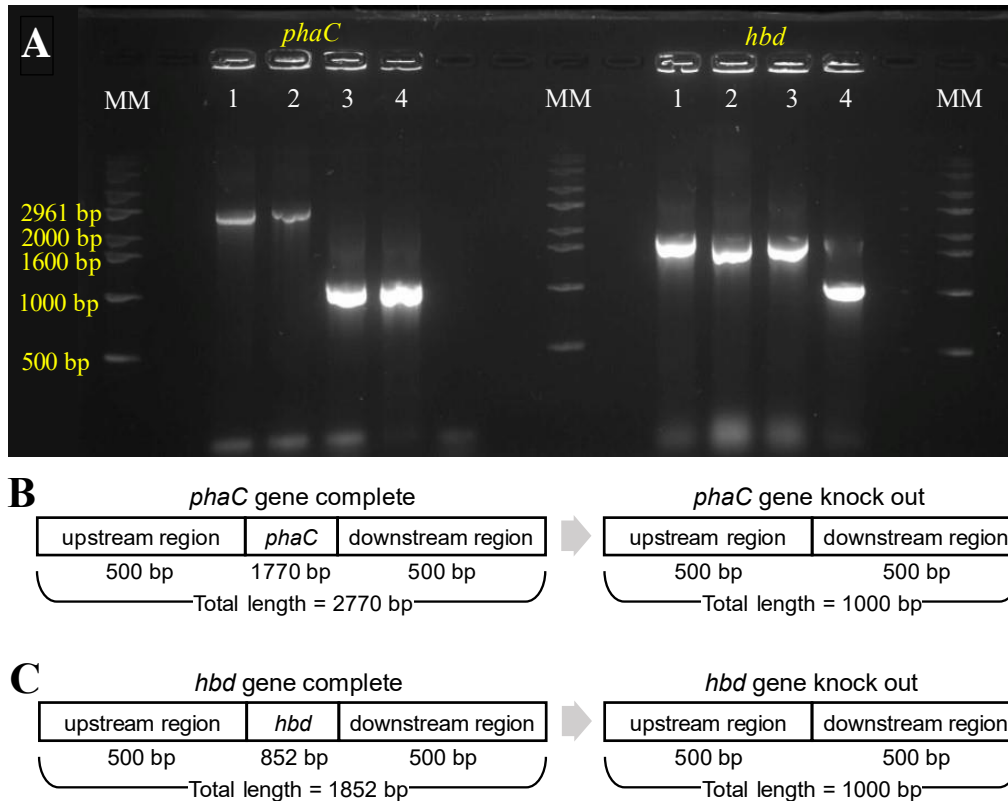


Figure 12. **PCR colony amplification of *phaC* and *hbd* genes in wild type and mutant *C. necator* strains.** The lanes positions (1) *C. necator* H16; (2) *C. necator* 541; (3) *C. necator*  $\Delta$ *phaC* and (4) *C. necator*  $\Delta$ *phaC*  $\Delta$ *hbd*. The molecular size marker (MM) used is 1 kb DNA AccuLadder from Bionner. The left and right positions indicated the *phaC* or *hbd* gene amplified with the primers listed in materials section. Samples were analyzed by electrophoresis through a 1 % agarose gel and visualized by GelRed staining. (A). Schematic representation of the lengths of *phaC* (B) and *hbd* (C) fragments.

A null *hbd* mutant was successfully obtained. Figure 12 shows a band length of 1000 bp confirming the successful deletion of *hbd* in *C. necator*  $\Delta$ *phaC*  $\Delta$ *hbd* (Figure 12 *hbd* lane 4) in comparison with the band obtained for the wild type strain with 1852 pb (Figure 12 *hbd* lane 1). *C. necator* 541 and *C. necator*  $\Delta$ *phaC* had a total band length of 1852 bp, which confirmed the conservation of the expression of *hbd* gene.

#### 4.4.1. Biomass, PHB and R3HBA production in *C. necator* and knockout mutant strains

In order to elucidate the growth, fructose consumption and R3HBA production patterns, all strains were cultured at 30 °C for 48 hours in RE1 mineral medium with approximately 20 g L<sup>-1</sup> fructose and 1.0 g L<sup>-1</sup> of ammonium sulphate. During the first 10 h, *C. necator* H16 reached a total biomass concentration of 0.237 ± 0.024 g L<sup>-1</sup> and  $\mu=0.21$  h<sup>-1</sup> (Figure 13). The mutant, *C. necator* 541 grew faster than the wild type with a  $\mu=0.25$  h<sup>-1</sup>, and reached lower cell concentration of 0.49 ± 0.014 g L<sup>-1</sup> (Figure 14, panel A). Similarly, the mutant strains *C. necator*  $\Delta phaC$  and *C. necator*  $\Delta phaC \Delta hbd$  attained biomass concentration at 10 hours of culture equal to 0.252 ± 0.019 g L<sup>-1</sup> and 0.213 ± 0.003 g L<sup>-1</sup> with a specific growth rate of 0.21 h<sup>-1</sup> and 0.20 h<sup>-1</sup>, respectively (Figures 15-16, panel A). These results show that the maximum specific growth rate was not affected by the deletion of *phaC* and *hbd*. After 48 hours of growth and PHB accumulation, important differences were found between the wild type and mutant strains PHB accumulation in cells occurred only *C. necator* H16 (80%), whereas in the mutant PHB was null, confirming the successful gene knock out of *phaC* in these strains.

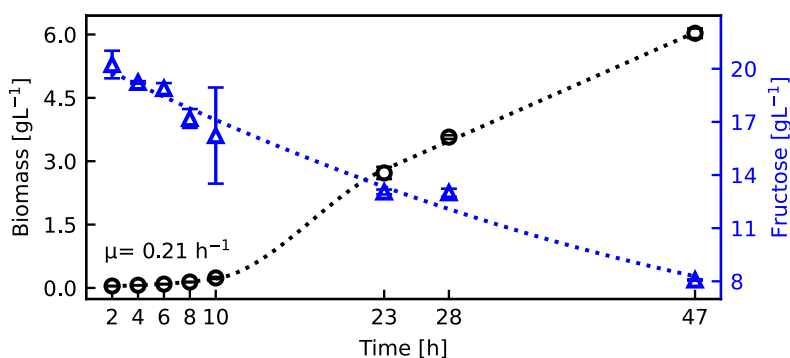


Figure 13. **Cell growth and fructose consumption in *C. necator* H16.** The cultures were carried out in RE1 medium with 20 g L<sup>-1</sup> of fructose and 1.0 g L<sup>-1</sup> of ammonium sulphate at pH 7 and incubated at 30 °C for 48 h.

Figures 13-16 panel A, describes the continuous consumption of fructose. The highest final fructose consumption occurred for *C. necator* H16 (12.4 ± 0.040 g L<sup>-1</sup>) followed by *C. necator*  $\Delta phaC$  (9.00 ± 0.25 g L<sup>-1</sup>), *C. necator* 541 (7.16 ± 0.39 g L<sup>-1</sup>) and

*C. necator*  $\Delta phaC \Delta hbd$  ( $6.32 \pm 0.19 \text{ g L}^{-1}$ ). These results suggest that fructose was not the limiting nutrient and that the nitrogen source was totally consumed. The maximum biomass concentration free of PHB attained for all cultures in *C. necator* H16 ( $1.21 \pm 0.02 \text{ g L}^{-1}$ ) is consistent with a complete consumption of the nitrogen source.

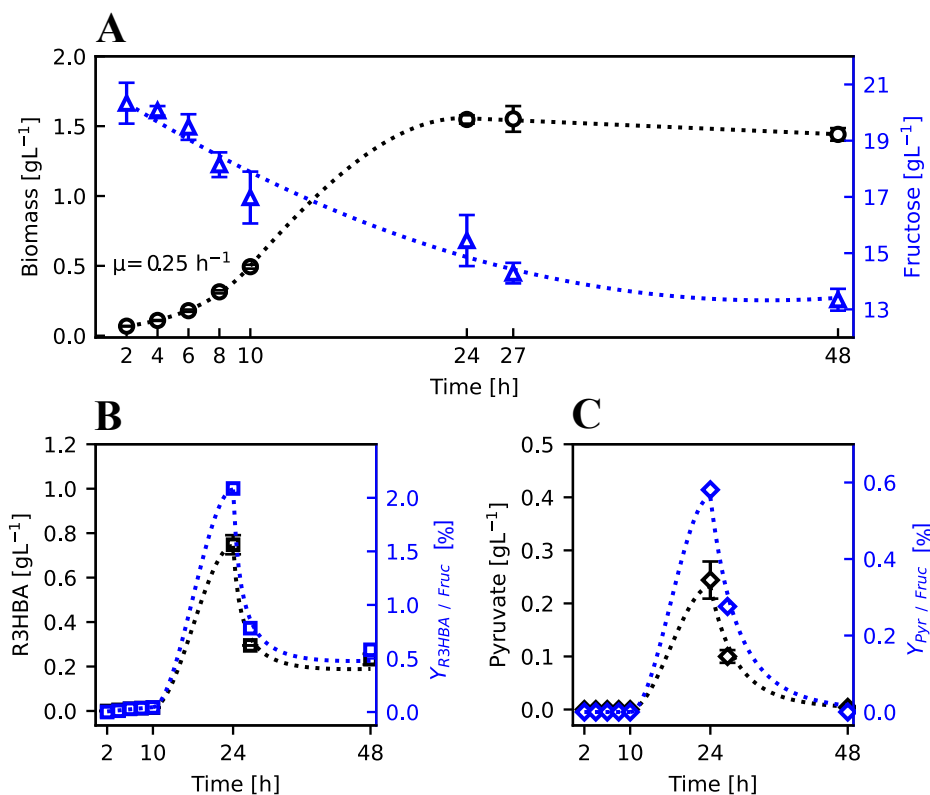


Figure 14. **Cell growth, fructose consumption, R3HBA and pyruvate production and yield in *C. necator* 541.** The cultures were carried out in RE1 medium with  $20 \text{ g L}^{-1}$  of fructose and  $1.0 \text{ g L}^{-1}$  of ammonium sulphate at pH 7 and incubated at  $30 \text{ }^\circ\text{C}$  for 48 h.

All mutant strains presented the first R3HBA peak production at 23 hours with  $0.748 \pm 0.043 \text{ g L}^{-1}$ ,  $0.492 \pm 0.027 \text{ g L}^{-1}$ ,  $0.115 \pm 0.025 \text{ g L}^{-1}$  for *C. necator* 541, *C. necator*  $\Delta phaC \Delta hbd$  and *C. necator*  $\Delta phaC$ , respectively (Figures 14-16, panel B). Interestingly, at the end of the culture, the R3HBA production of *C. necator*  $\Delta phaC \Delta hbd$  increased to  $0.677 \pm 0.050 \text{ g L}^{-1}$  with a carbon mole of R3HBA per carbon mole of fructose yield of  $Y_{R3HBA/Fruc} = 12.5 \%$ , whereas in *C. necator* 541 decreased to  $0.233 \pm 0.024 \text{ g L}^{-1}$  ( $Y_{R3HBA/Fruc} = 0.58 \%$ ) and in *C. necator*  $\Delta phaC$  of  $0.068 \pm 0.013 \text{ g L}^{-1}$

( $Y_{R3HBA/Fruc}=1.13\%$ ). No significant peaks were obtained for *C. necator* H16. The second confirmation of the successful *hbd* gene knock out for *C. necator*  $\Delta phaC \Delta hbd$  was evidenced by the reduced mobilization of R3HBA.

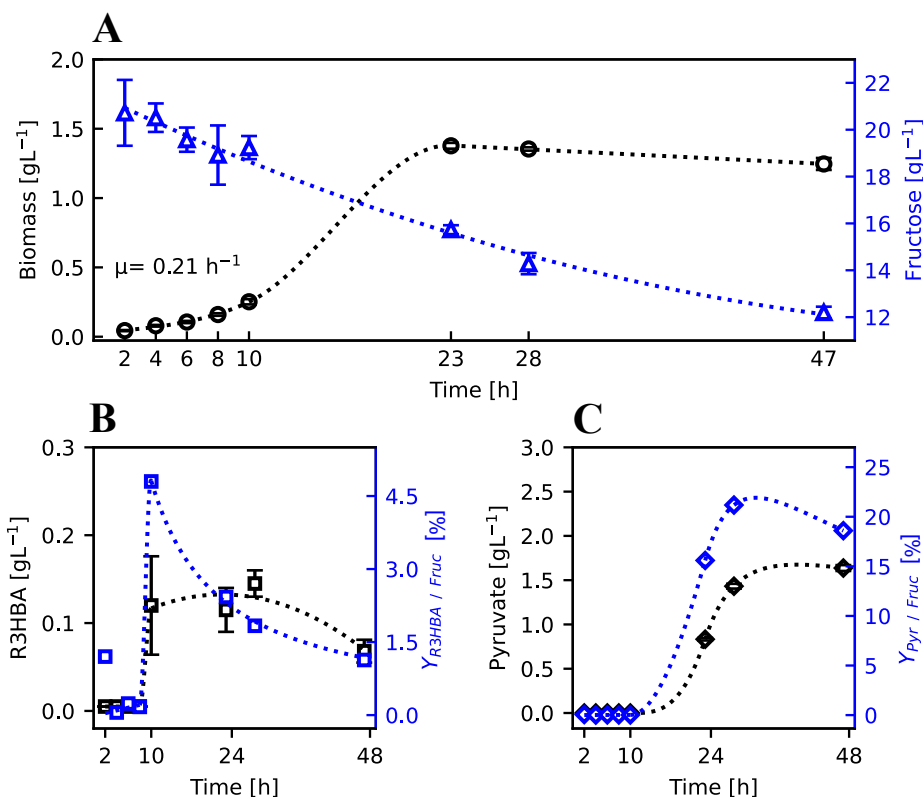


Figure 15. **Cell growth, fructose consumption, R3HBA and pyruvate production and yield in *C. necator*  $\Delta phaC$ .** The cultures were carried out in RE1 medium with 20 g L<sup>-1</sup> of fructose and 1.0 g L<sup>-1</sup> of ammonium sulphate at pH 7 and incubated at 30 °C for 48 h.

Shiraki et al. (2006) constructed a *C. necator* strain (H16\_ *bhd1*) capable of accumulating PHB but without Hbd activity by the deletion of *hbd* gene using suicide vector. After 60 hours of culture, both the wild type *C. necator* and the  $\Delta hbd$  accumulated nearly 50% PHB from 2% w/v of fructose. In this point, the culture was spiked with ammonium sulphate to yield 5 g L<sup>-1</sup>. Under aerobic conditions, a spike of R3HBA was produced with a maximum of 10 mM (1 g L<sup>-1</sup>) after 24 hours of depolymerization. The released R3HBA rapidly decreased by an unidentified mechanism. On the other hand, under anaerobic conditions in presence of ammonium sulphate, the R3HBA released by H16\_ *bhd1* increased to 3.1 g L<sup>-1</sup>, higher than

the titer achieved using the wild-type strain, which released  $0.520 \text{ g L}^{-1}$ . Unfortunately, these titers required a depolymerization time of 100 hours under anaerobic conditions.

The strategy presented by Shiraki et al., (2006) relied on the depolymerization of the accumulated PHB. On the other hand, the *C. necator*  $\Delta phaC$  and *C. necator*  $\Delta phaC \Delta hbd$  strains are unable to accumulate PHB but still release R3HBA, suggesting the presence of a native thioesterase enzyme that removes the CoA of R3HBA. A search in MetaCyc of thioesterase enzymes of *C. necator* resulted in 24 enzymes that were compared by protein BLAST analysis with *E. coli*'s Ycia enzyme sequence. The analysis showed that one enzyme in *C. necator*, WP\_037025319.1 shows a percent identity of 44 % with Ycia. Probably this homologous thioesterase is related to the R3HBA release by removing a CoA when the PhaC are absent, but its mechanism and activation conditions are currently unknown.

The extracellular concentration of pyruvate was measured during the cultivation. After 23 hours of cultivation and when nitrogen was the limiting nutrient, pyruvate excretion of *C. necator*  $\Delta phaC$  strain was  $0.833 \pm 0.014 \text{ g L}^{-1}$  (Figure 15, panel C) and 24 hours after this concentration increased by 2-fold up to  $1.64 \pm 0.033 \text{ g L}^{-1}$  ( $Y_{PYR/Fruc}=18.6 \%$ ). It was hypothesized that pyruvate during unbalanced conditions started to accumulate inside the cell by the blockage of PHB synthesis and then was excreted into extracellular medium. The effect of a truncated PHB pathway produce an accumulation of acetyl-CoA, acetoacetyl-CoA and R3HBA-CoA, where the release of pyruvate is a response of the inhibitory effect of acetyl-CoA on the activity of pyruvate dehydrogenase (Jung & Lee, 1997). This behavior is a general characteristic of PHB-negative mutant strains and it has been previously described that the pyruvate excretion pattern of the PHB-negative mutant strains is according to the PHB accumulation pattern in the wild type strain (Jung & Lee, 1997). However, when a nitrogen source is added, pyruvate is consumed (Cook & Schlegel, 1978). The maximum value at 23 h time for *C. necator* 541 and *C. necator*  $\Delta phaC \Delta hbd$  of  $0.244 \pm 0.035 \text{ g L}^{-1}$  (Figure 14, panel C),  $0.576 \pm 0.009 \text{ g L}^{-1}$  (Figure 16, panel C) and then decreased almost to zero both according to the yield pattern of the pyruvate. Probably, the pyruvate consumed directs to synthesis of several amino acids (Raberg et al., 2014).

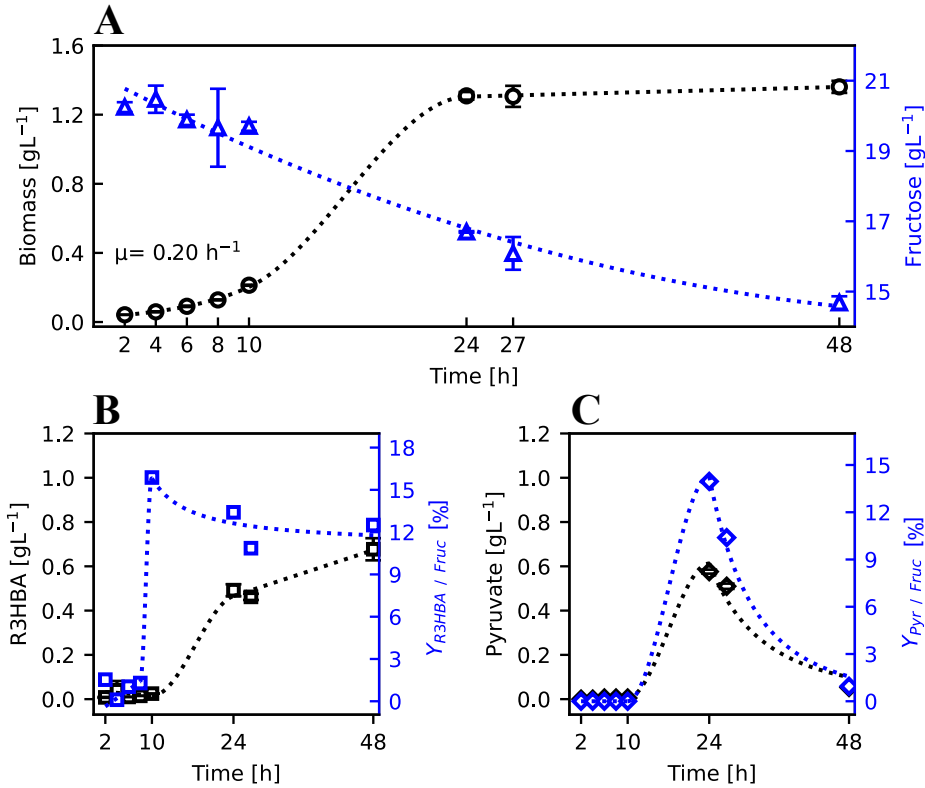


Figure 16. **Cell growth, fructose consumption, R3HBA and pyruvate production and yield in *C. necator*  $\Delta phaC \Delta hbd$ .** The cultures were carried out in RE1 medium with 20 g L<sup>-1</sup> of fructose and 1.0 g L<sup>-1</sup> of ammonium sulfate at pH 7 and incubated at 30 °C for 48 h.

Finally, an experiment for confirming the influence of nitrogen and different pHs on the PHB depolymerization and R3HBA release in *C. necator* H16 was assayed. Figure 17 shows an assay for the R3HBA production in presence of a nitrogen source. *C. necator* H16 cells containing 80 % ( $8.92 \pm 0.19 \text{ g L}^{-1}$ ) of PHB were washed and cultured in RE1 medium without fructose at 30 °C and, 250 rpm for 24 hours and subjected to pHs of 4, 7 and 10. The PHB concentration decreased under all pHs conditions. While at pH 4 and 7, similar PHB titer was found ( $4.69 \pm 0.40 \text{ g L}^{-1}$ ,  $3.99 \pm 0.39 \text{ g L}^{-1}$ ), at pH 10 the PHB titer was reduced to  $2.64 \pm 0.44 \text{ g L}^{-1}$  with a R3HBA concentration of title of  $10 \text{ mg L}^{-1}$  and a final pH of 8. At the initial pHs of 4 and 7, no R3HBA could be detected, suggesting that PHB was mobilized and used for growth and maintenance due to the presence of a nitrogen source and the constant aeration by the agitation. (Handrick et al, 2000).

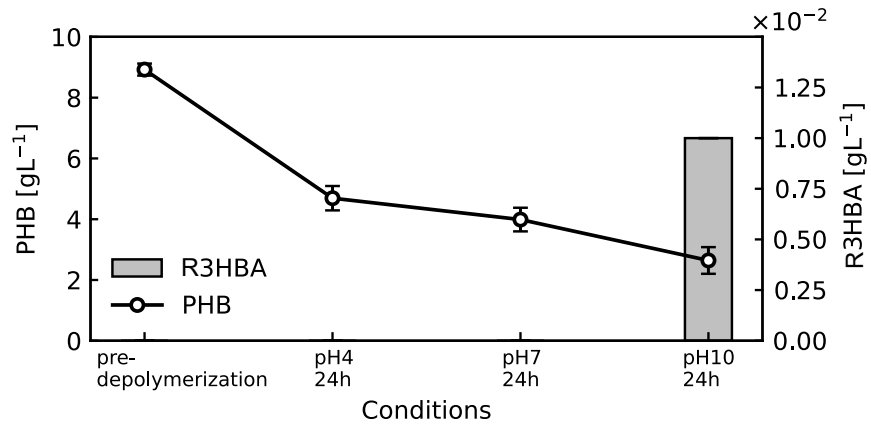


Figure 17. **Influence of pHs conditions in PHB depolymerization and R3HBA release in *C. necator* H16.** PHB accumulated cells of *C. necator* H16 were resuspended in RE1 medium w/o fructose at 4, 7, 10 pHs and incubated at 30 °C, 250 rpm for 24 h.

## 5. CONCLUSIONS

The results obtained in this work demonstrated the feasibility of R3HBA production by reducing or eliminating the fluxes of the reactions consuming R3HBA via operational manipulation as described in *M. parvus* and *A. lata* or via gene knock outs in *C. necator*.

*A. lata* DSM 1123 is a gram-negative facultative autotroph, with a growth associated PHB production. A complete characterization of this strain under chemostat cultures was undertaken in this thesis. Results showed that a significant PHB accumulation occurred under nitrogen, oxygen and especially in glucose-limited conditions. Dilution rates higher than  $0.2 \text{ h}^{-1}$  under glucose-limited chemostat resulted in an overflow of PHB. This suggests a counterintuitive PHB accumulation under glucose-limited conditions when only biomass production should be affected as seen in other bacteria (Ackermann & Babel, 1997; Page & Knosp, 1989). On other hand, *in vivo* PHB depolymerization was possible with a R3HBA yield of 93.4% at pH 4, but cell recycling was not feasible after incubation at acidic pH. The successful depolymerization in a two stage chemostat (a polymerization reactor followed by depolymerization tank) suggests that the genes *PhaZ* and *Hbd* are active under nitrogen-limited conditions.

R3HBA can be obtained in the supernatant from PHB accumulated cells of *M. parvus* using  $\text{CH}_4$  as the sole carbon and energy source. The process, which involves the *in-vivo* depolymerization of PHB (PDS system) mediated by intracellular enzymes of *M. parvus*, attained a PHB to R3HBA conversion of  $77.2 \pm 0.9\%$  after 72 hours of depolymerization at pH 11 in a mineral medium containing nitrate under aerobic conditions. The reduction of  $\text{O}_2$  supply affected negatively the R3HBA yield, reducing it to 73% under microaerobic conditions. Similarly, increasing concentrations of exogenous R3HBA added to the broth at the beginning of the depolymerization process hindered the initial R3HBA release rate and the R3HBA yield, but not the PHB depolymerization yield. Finally, cells exposed to a reduced depolymerization time of 3 hours at pH 11 were able to grow in the presence of nitrogen and  $\text{CH}_4$ . However, the long times required at pH 11 for full PHB depolymerization (up to 72 h) limit the applicability of cell recycling.

The implementation of PDS system in *C. necator* was studied through the construction of two mutants: *C. necator*  $\Delta phaC$  and *C. necator*  $\Delta phaC \Delta hbd$ . No accumulation of PHB was recorded. A maximum R3HBA titer of  $0.145 \pm 0.015 \text{ g L}^{-1}$  was reached out in *C. necator*  $\Delta phaC$  at 28 hours whereas for *C. necator*  $\Delta phaC \Delta hbd$  a R3HBA titer of  $0.677 \pm 0.05 \text{ g L}^{-1}$  at 48 hours was observed, as expected by the *hbd* deletion. Interestingly, the truncated pathway of PHB synthesis provided an insight into the cell's metabolic situation: cells released R3HBA, exposed to a significant titer of pyruvate (as high as  $1.63 \pm 0.03 \text{ g L}^{-1}$  in the strain *C. necator*  $\Delta phaC$ ), which was likely caused by the inhibitory effect of acetyl-CoA on the activity of pyruvate dehydrogenase (Jung & Lee, 1997).

*C. necator*  $\Delta phaC$ , *C. necator*  $\Delta phaC \Delta hbd$  and *C. necator* 541 attained a peak R3HBA titer at 24 hours of culture, which was then completely consumed except in *C. necator*  $\Delta phaC \Delta hbd$  that R3HBA was not converted into acetoacetate. These results suggest that a native thioesterase of *C. necator* may play a role in the release of R3HBA by removing CoA from R3HBA-CoA. A protein homology on the genome of *C. necator* showed an enzyme encoded as WP\_037025319.1 with a percent identity of 44 % in comparison with Ycia that may trigger R3HBA release.

The implementation of TSS system through of *tesB* via expression vector was not possible by inconsistencies in the assembly of the fragments in the constructed plasmids pLY01 and pLY02. These plasmids contained the *tesB* gene but showed other features as antibiotic resistance, an incomplete promoter fragment, and the origin replication site that were not suitable for the transformation in *C. necator* and *M. parvus*.

## 5.1. Future directions

*A. lata* showed an overflow metabolism that led to PHB accumulation under glucose conditions but it is necessary to identify the possible internal bottlenecks in fluxes of the central metabolism.

To further understand the effects of high R3HBA concentrations on the depolymerization kinetics in *M. parvus*, future work will include depolymerization experiments carried out at high initial PHB concentrations. Indeed, PHB concentrations between 1-100 g L<sup>-1</sup> could be attained through biomass concentration using centrifugation to test the possibility of achieving high R3HBA titers without sacrificing yield or increasing the depolymerization time.

A first approach for the implementation of TSS in *M. parvus* will consider the elimination of fluxes involved in the reactions that consume R3HBA using genetic strategies via gene knock outs and could be complemented by the expression of *tesB* and *ycia* genes.

This work showed the R3HBA release in *C. necator* mutants with truncated PHB pathway synthesis, which suggests the existence of a native thioesterase that may act by removing the CoA of R3HBA-CoA. A natural next step should be addressing the knockout and the overexpression of this enzyme in *C. necator*  $\Delta$ *phaC* and *C. necator*  $\Delta$ *phaC*  $\Delta$ *hbd* to investigate its physiological role and its biotechnological potential.

## REFERENCES

- Ackermann, J. U & Babel, W. (1997). Growth-associated synthesis of poly(hydroxybutyric acid) in *Methylobacterium rhodesianum* as an expression of an internal bottleneck. *Applied Microbiology and Biotechnology*, 47(2), 144–149. <https://doi.org/10.1007/s002530050903>
- Adkins, J., Pugh, S., McKenna, R., & Nielsen, D. R. (2012). Engineering microbial chemical factories to produce renewable “biomonomers.” *Frontiers in Microbiology*, 3(Aug), 1–12. <https://doi.org/10.3389/fmicb.2012.00313>
- Agarwal, A. S., Zhai, Y., Hill, D., & Sridhar, N. (2011). The electrochemical reduction of carbon dioxide to formate/formic acid: Engineering and economic feasibility. *ChemSusChem*, 4(9), 1301–1310. <https://doi.org/10.1002/cssc.201100220>
- Amulya, K., Jukuri, S., & Venkata Mohan, S. (2015). Sustainable multistage process for enhanced productivity of bioplastics from waste remediation through aerobic dynamic feeding strategy: Process integration for up-scaling. *Bioresource Technology*, 188, 231–239. <https://doi.org/10.1016/j.biortech.2015.01.070>
- Anis, S. N. S., Annuar, M. S. M., & Simarani, K. (2018). Microbial biosynthesis and *in vivo* depolymerization of intracellular medium-chain-length poly-3-hydroxyalkanoates as potential route to platform chemicals. *Biotechnology and Applied Biochemistry*, 65(6), 784–796. <https://doi.org/10.1002/bab.1666>
- Asenjo, J. A., & Suk, J. S. (1986). Microbial Conversion of Methane into poly- $\beta$ -hydroxybutyrate (PHB): Growth and intracellular product accumulation in a type II methanotroph. *Journal of Fermentation Technology*, 64(4), 271–278. [https://doi.org/10.1016/0385-6380\(86\)90118-4](https://doi.org/10.1016/0385-6380(86)90118-4)
- Atlić, A., Koller, M., Scherzer, D., Kutschera, C., Grillo-Fernandes, E., Horvat, P., Chiellini, E., & Braunegg, G. (2011). Continuous production of poly([R]-3-hydroxybutyrate) by *Cupriavidus necator* in a multistage bioreactor cascade. *Applied Microbiology and Biotechnology*, 91(2), 295–304. <https://doi.org/10.1007/s00253-011-3260-0>

- Beaumont, L. J., Pitman, A., Perkins, S., Zimmermann, N. E., Yoccoz, N. G., & Thuiller, W. (2011). Impacts of climate change on the world's most exceptional ecoregions. *Proceedings of the National Academy of Sciences of the United States of America*, 108(6), 2306–2311. <https://doi.org/10.1073/pnas.1007217108>
- Bera, A., Dubey, S., Bhayani, K., Mondal, D., Mishra, S., & Ghosh, P. K. (2015). Microbial synthesis of polyhydroxyalkanoate using seaweed-derived crude levulinic acid as co-nutrient. *International Journal of Biological Macromolecules*, 72, 487–494. <https://doi.org/10.1016/j.ijbiomac.2014.08.037>
- Bertani, G. (1951). Studies on lysogenesis. I. The mode of phage liberation by lysogenic *Escherichia coli*. *Journal of Bacteriology*, 62(3), 293–300.
- Bhati, R., & Mallick, N. (2016). Carbon dioxide and poultry waste utilization for production of polyhydroxyalkanoate biopolymers by *Nostoc muscorum* Agardh: a sustainable approach. *Journal of Applied Phycology*, 28(1), 161–168. <https://doi.org/10.1007/s10811-015-0573-x>
- Bordel, S., Rojas, A., & Muñoz, R. (2019). Reconstruction of a Genome Scale Metabolic Model of the polyhydroxybutyrate producing methanotroph *Methylocystis parvus* OBBP. *Microbial Cell Factories*, 18(1), 1–11. <https://doi.org/10.1186/s12934-019-1154-5>
- Borrero-de Acuña, J. M., Aravena-Carrasco, C., Gutierrez-Urrutia, I., Duchens, D., & Poblete-Castro, I. (2019). Enhanced synthesis of medium-chain-length poly(3-hydroxyalkanoates) by inactivating the tricarboxylate transport system of *Pseudomonas putida* KT2440 and process development using waste vegetable oil. *Process Biochemistry*, 77, 23–30. <https://doi.org/10.1016/j.procbio.2018.10.012>
- Braunegg, G., Bona, R; Koller, M. (2004). Sustainable polymer production. *Polymer-Plastics Technology and Engineering*, 43, 1779–1793. <https://doi.org/doi:10.1081/PPT-200040130>
- Bresan, S., Sznajder, A., Hauf, W., Forchhammer, K., Pfeiffer, D., & Jendrossek, D. (2016). Polyhydroxyalkanoate (PHA) granules have no phospholipids. *Scientific Reports*, 6(March), 1–13. <https://doi.org/10.1038/srep26612>

- Brigham, C. (2019). Perspectives for the biotechnological production of biofuels from CO<sub>2</sub> and H<sub>2</sub> using *Ralstonia eutropha* and other ‘Knallgas’ bacteria. *Applied Microbiology and Biotechnology*, 103(5), 2113–2120. <https://doi.org/10.1007/s00253-019-09636-y>
- Brigham, C. J., Speth, D. R., Rha, C. K., & Sinskey, A. J. (2012). Whole-genome microarray and gene deletion studies reveal regulation of the polyhydroxyalkanoate production cycle by the stringent response in *Ralstonia eutropha* H16. *Applied and Environmental Microbiology*, 78(22), 8033–8044. <https://doi.org/10.1128/AEM.01693-12>
- Bugnicourt, E., Cinelli, P., Lazzeri, A., & Alvarez, V. (2014). Polyhydroxyalkanoate (PHA): Review of synthesis, characteristics, processing and potential applications in packaging. *Express Polymer Letters*, 8(11), 791–808. <https://doi.org/10.3144/expresspolymlett.2014.82>
- Cao, Q., Zhang, J., Liu, H., Wu, Q., Chen, J., & Chen, G. Q. (2014). The mechanism of anti-osteoporosis effects of 3-hydroxybutyrate and derivatives under simulated microgravity. *Biomaterials*, 35(28), 8273–8283. <https://doi.org/10.1016/j.biomaterials.2014.06.020>
- Carmichael, J. T., & Brulle, R. J. (2017). Elite cues, media coverage, and public concern: an integrated path analysis of public opinion on climate change, 2001–2013. *Environmental Politics*, 26(2), 232–252. <https://doi.org/10.1080/09644016.2016.1263433>
- Chen, G. Q. (2009). A microbial polyhydroxyalkanoates (PHA) based bio- and materials industry. *Chemical Society Reviews*, 38(8), 2434–2446. <https://doi.org/10.1039/b812677c>
- Chen, G. Q., König, K. H., & Lafferty, R. M. (1991). Production of poly-D(-)-3-hydroxybutyrate and poly-D(-)-3-hydroxyvalerate by strains of *Alcaligenes latus*. *Antonie van Leeuwenhoek*, 60(1), 61–66. <https://doi.org/10.1007/BF00580443>
- Chen, G. Q., & Wu, Q. (2005). Microbial production and applications of chiral hydroxyalkanoates. *Applied Microbiology and Biotechnology*, 67(5), 592–599. <https://doi.org/10.1007/s00253-005-1917-2>

- Chen, X., Zhou, L., Tian, K., Kumar, A., Singh, S., Prior, B. A., & Wang, Z. (2013). Metabolic engineering of *Escherichia coli*: A sustainable industrial platform for bio-based chemical production. *Biotechnology Advances*, 31(8), 1200–1223. <https://doi.org/10.1016/j.biotechadv.2013.02.009>
- Chiba, T., & Nakai, T. (1985). A Synthetic Approach To (+)-Thienamycin From Methyl (R)-3-Hydroxybutanoate. A New Entry To (3 R , 4 R )-3-[(R)-1-Hydroxyethyl]-4-Acetoxy-2-Azetidinone. *Chemistry Letters*, 14(5), 651–654. <https://doi.org/10.1246/cl.1985.651>
- Choi, M. H., Yoon, S. C., & Lenz, R. W. (1999). Production of poly(3-hydroxybutyric acid-Co-4-hydroxybutyric acid) and poly(4-hydroxybutyric acid) without subsequent degradation by *Hydrogenophaga pseudoflava*. *Applied and Environmental Microbiology*, 65(4), 1570–1577. <https://doi.org/10.1128/aem.65.4.1570-1577.1999>
- Cook, A. M., & Schlegel, H. G. (1978). Metabolite concentrations in *Alcaligenes eutrophus* H 16 and a mutant defective in poly- $\beta$ -hydroxybutyrate synthesis. *Archives of Microbiology*, 119(3), 231–235. <https://doi.org/10.1007/BF00405400>
- Crépin, L., Lombard, E., & Guillouet, S. E. (2016). Metabolic engineering of *Cupriavidus necator* for heterotrophic and autotrophic alka(e)ne production. *Metabolic Engineering*, 37, 92–101. <https://doi.org/10.1016/j.ymben.2016.05.002>
- Cruz, M. V., Freitas, F., Paiva, A., Mano, F., Dionísio, M., Ramos, A. M., & Reis, M. A. M. (2016). Valorization of fatty acids-containing wastes and byproducts into short- and medium-chain length polyhydroxyalkanoates. *New Biotechnology*, 33(1), 206–215. <https://doi.org/10.1016/j.nbt.2015.05.005>
- Cruz, M. V., Paiva, A., Lisboa, P., Freitas, F., Alves, V. D., Simões, P., Barreiros, S., & Reis, M. A. M. (2014). Production of polyhydroxyalkanoates from spent coffee grounds oil obtained by supercritical fluid extraction technology. *Bioresource Technology*, 157, 360–363. <https://doi.org/10.1016/j.biortech.2014.02.013>

- de Paula, F. C., Kakazu, S., de Paula, C. B. C., Gomez, J. G. C., & Contiero, J. (2017). Polyhydroxyalkanoate production from crude glycerol by newly isolated *Pandoraea* sp. Polyhydroxyalkanoate production from crude glycerol. *Journal of King Saud University - Science*, 29(2), 166–173. <https://doi.org/10.1016/j.jksus.2016.07.002>
- de Roo, G., Kellerhals, M. B., Ren, Q., Witholt, B., & Kessler, B. (2002). Production of Chiral R -3-Hydroxyalkanoic Acids and R -3-Hydroxyalkanoic Acid Methylesters via Hydrolytic Degradation of Polyhydroxyalkanoate Synthesized by *Pseudomonas* sp. 3–8. <https://doi.org/10.1002/bit.10134>
- del Cerro, C., García, J. M., Rojas, A., Tortajada, M., Ramón, D., Galán, B., Prieto, M. A., & García, J. L. (2012). Genome sequence of the methanotrophic poly- $\beta$ -hydroxybutyrate producer *Methylocystis parvus* OBBP. *Journal of Bacteriology*, 194(20), 5709–5710. <https://doi.org/10.1128/JB.01346-12>
- Dietrich, K., Dumont, M. J., Del Rio, L. F., & Orsat, V. (2017). Producing PHAs in the bioeconomy—Towards a sustainable bioplastic. *Sustainable Production and Consumption*, 9, 58–70. <https://doi.org/10.1016/j.spc.2016.09.001>
- Dlugokencky, E. (2020). *Trends in Atmospheric Methane*. [https://gml.noaa.gov/ccgg/trends\\_ch4/](https://gml.noaa.gov/ccgg/trends_ch4/)
- Dmitrieva-Posocco, O., Wong, A. C., Lundgren, P., Golos, A. M., Descamps, H. C., Dohnalová, L., Cramer, Z., Tian, Y., Yueh, B., Eskiocak, O., Egervari, G., Lan, Y., Liu, J., Fan, J., Kim, J., Madhu, B., Schneider, K. M., Khoziainova, S., Andreeva, N., et al. (2022).  $\beta$ -Hydroxybutyrate suppresses colorectal cancer. *Nature*, 605(7908), 160–165. <https://doi.org/10.1038/s41586-022-04649-6>
- Doi, Y., Segawa, A., Kawaguchi, Y., & Kunioka, M. (1990). Cyclic nature of poly(3-hydroxyalkanoate) metabolism in *Alcaligenes eutrophus*. *FEMS Microbiology Letters*, 67(1–2), 165–169. <https://doi.org/10.1111/j.1574-6968.1990.tb13856.x>

- Durner, R., Witholt, B., & Egli, T. (2000). Accumulation of poly[(R)-3-hydroxyalkanoates] in *Pseudomonas oleovorans* during growth with octanoate in continuous culture at different dilution rates. *Applied and Environmental Microbiology*, 66(8), 3408–3414. <https://doi.org/10.1128/AEM.66.8.3408-3414.2000>
- Edenhofer, O. (2014). IPCC 2014 Mitigation of Climate Change. Contribution of Working Group III to the Fifth Assessment Report of the Intergovernmental Panel on Climate Change. In *Cambridge: Cambridge University Press*.
- Estrada, J. M., Lebrero, R., Quijano, G., Pérez, R., Figueroa-González, I., García-Encina, P. A., & Muñoz, R. (2014). Methane abatement in a gas-recycling biotrickling filter: Evaluating innovative operational strategies to overcome mass transfer limitations. *Chemical Engineering Journal*, 253, 385–393. <https://doi.org/10.1016/j.cej.2014.05.053>
- Etminan, M., Myhre, G., Highwood, E. J., & Shine, K. P. (2016). Radiative forcing of carbon dioxide, methane, and nitrous oxide: A significant revision of the methane radiative forcing. *Geophysical Research Letters*, 43(24), 614–623. <https://doi.org/10.1002/2016GL071930>
- Fei, T., Cazeneuve, S., Wen, Z., Wu, L., & Wang, T. (2016). Effective Recovery of Poly- $\beta$ -Hydroxybutyrate (PHB) Biopolymer from *Cupriavidus necator* Using a Novel and Environmentally Friendly Solvent System. *Biotechnology progress*. 32(3), 678–685 <https://doi.org/10.1002/btpr.2247>
- Follonier, S., Riesen, R., & Zinn, M. (2015). Pilot-scale production of functionalized mcl-PHA from grape pomace supplemented with fatty acids. *Chemical and Biochemical Engineering Quarterly*, 29(2), 113–121. <https://doi.org/10.15255/CABEQ.2014.2251>
- Fuhrmann, E., & Talbiersky, J. (2005). Synthesis of alkyl aryl ethers by catalytic Williamson ether synthesis with weak alkylation agents. *Organic Process Research and Development*, 9(2), 206–211. <https://doi.org/10.1021/op050001h>
- Gao, X., Chen, J. C., Wu, Q., & Chen, G. Q. (2011). Polyhydroxyalkanoates as a source of chemicals, polymers, and biofuels. *Current Opinion in Biotechnology*, 22(6), 768–774. <https://doi.org/10.1016/j.copbio.2011.06.005>

- Gebauer, B., & Jendrossek, D. (2006). Assay of poly(3-hydroxybutyrate) depolymerase activity and product determination. *Applied and Environmental Microbiology*, 72(9), 6094–6100. <https://doi.org/10.1128/AEM.01184-06>
- Geyer, R., Jambeck, J. R., & Law, K. L. (2017). Production, use, and fate of all plastics ever made. *Science Advances*, 3(7), 3–8. <https://doi.org/10.1126/sciadv.1700782>
- Ghasemi Ghodrat, A., Tabatabaei, M., Aghbashlo, M., & Mussatto, S. I. (2018). Waste Management Strategies; the State of the Art. In M. Tabatabaei & H. Ghanavati (Eds.), *Biogas: Fundamentals, Process, and Operation* (pp. 1–33). Springer International Publishing. [https://doi.org/10.1007/978-3-319-77335-3\\_1](https://doi.org/10.1007/978-3-319-77335-3_1)
- Gibson, D. G., Young, L., Chuang, R. Y., Venter, J. C., Hutchison, C. A., & Smith, H. O. (2009). Enzymatic assembly of DNA molecules up to several hundred kilobases. *Nature Methods*, 6(5), 343–345. <https://doi.org/10.1038/nmeth.1318>
- Gómez Cardozo, J. R., Mora Martínez, A. L., Yepes Pérez, M., & Correa Londoño, G. A. (2016). Production and Characterization of Polyhydroxyalkanoates and Native Microorganisms Synthesized from Fatty Waste. *International Journal of Polymer Science*, 2016, 6541718. <https://doi.org/10.1155/2016/6541718>
- Gorenflo, V., Schmack, G., Vogel, R., & Steinbu, A. (2001). Development of a Process for the Biotechnological Large-Scale Production of 4-Hydroxyvalerate-Containing Polyesters and Characterization of Their Physical and Mechanical Properties. 45–57. *Biomacromolecules*. 20012 (1),45-57. doi: 10.1021/bm0000992
- Grousseau, E., Blanchet, E., Déléris, S., Albuquerque, M. G. E., Paul, E., & Uribelarrea, J. L. (2013). Impact of sustaining a controlled residual growth on polyhydroxybutyrate yield and production kinetics in *Cupriavidus necator*. *Bioresource Technology*, 148, 30–38. <https://doi.org/10.1016/j.biortech.2013.08.120>

- Guevara-Martínez, M., Perez-Zabaleta, M., Gustavsson, M., Quillaguamán, J., Larsson, G., & van Maris, A. J. A. (2019). The role of the acyl-CoA thioesterase “YciA” in the production of (R)-3-hydroxybutyrate by recombinant *Escherichia coli*. *Applied Microbiology and Biotechnology*, 103(9), 3693–3704. <https://doi.org/10.1007/s00253-019-09707-0>
- Haage, G., Wallner, E., Bona, R., Schellauf, F., & Braunegg, G. (2001). Production of Poly-3-hydroxybutyrate-co-3-hydroxy-valerate with *Alcaligenes latus* DSM 1124 on Various Carbon Sources. *Biorelated Polymers*, 147–155. [https://doi.org/10.1007/978-1-4757-3374-7\\_13](https://doi.org/10.1007/978-1-4757-3374-7_13)
- Haas, C., Steinwandter, V., De Apodaca, E. D., Madurga, B. M., Smerilli, M., Dietrich, T., & Neureiter, M. (2015). Production of PHB from chicory roots-Comparison of three *Cupriavidus necator* strains. *Chemical and Biochemical Engineering Quarterly*, 29(2), 99–112. <https://doi.org/10.15255/CABEQ.2014.2250>
- Hahn, S. K., Chang, Y. K., Kim, B. S., & Chang, H. N. (1994). Optimization of microbial poly(3-hydroxybutyrate) recover using dispersions of sodium hypochlorite solution and chloroform. *Biotechnology and Bioengineering*, 44(2), 256–261. <https://doi.org/10.1002/bit.260440215>
- Hamilton, Li. A., Feit, S., Muffet, C., Kelso, M., Rubright, S., & Bernhardt, Co. (2019). *Executive Summary. Plastic Proliferation Threatens the Climate on a Global Scale*. <https://www.ciel.org/wp-content/uploads/2019/05/Plastic-and-Climate-FINAL-2019.pdf>
- Hanahan, D. (1983). Studies on transformation of *Escherichia coli* with plasmids. *Journal of Molecular Biology*, 166(4), 557–580. [https://doi.org/10.1016/S0022-2836\(83\)80284-8](https://doi.org/10.1016/S0022-2836(83)80284-8)
- Handrick, R., Reinhardt, S., Focarete, M. L., Scandola, M., Adamus, G., Kowalczyk, M., & Jendrossek, D. (2001). A New Type of Thermoalkalophilic Hydrolase of *Paucimonas lemoignei* with High Specificity for Amorphous Polyesters of Short Chain-length Hydroxyalkanoic Acids. *Journal of Biological Chemistry*, 276(39), 36215–36224. <https://doi.org/10.1074/jbc.M101106200>

- Handrick, R., Reinhardt, S., & Jendrossek, D. (2000). Mobilization of poly(3-hydroxybutyrate) in *Ralstonia eutropha*. *Journal of Bacteriology*, 182(20), 5916–5918. <https://doi.org/10.1128/JB.182.20.5916-5918.2000>
- Hänggi, U. J. (1990). Pilot scale production of PHB with *Alcaligenes latus*. *Novel Biodegradable Microbial Polymers*, 65–70. [https://doi.org/10.1007/978-94-009-2129-0\\_6](https://doi.org/10.1007/978-94-009-2129-0_6)
- Hanson, R. S., & Hanson, T. E. (1996). Methanotrophic bacteria. *Microbiological Reviews*, 60(2), 439–471. <https://doi.org/10.1128/mr.60.2.439-471.1996>
- Hazer, D. B., Kiliçay, E., & Hazer, B. (2012). Poly(3-hydroxyalkanoate)s: Diversification and biomedical applications: A state of the art review. *Materials Science and Engineering C*, 32(4), 637–647. <https://doi.org/10.1016/j.msec.2012.01.021>
- Henderson, R. A., & Jones, C. W. (1997). Physiology of poly-3-hydroxybutyrate (PHB) production by *Alcaligenes eutrophus* growing in continuous culture. *Microbiology*, 143(7), 2361–2371. <https://doi.org/10.1099/00221287-143-7-2361>
- Hiroe, A., Chek, M. F., Hakoshima, T., Sudesh, K., & Taguchi, S. (2019). Synthesis of Polyesters III: Acyltransferase as Catalyst. In: *Enzymatic Polymerization towards Green Polymer Chemistry. Green Chemistry and Sustainable Technology*. Springer [https://doi.org/10.1007/978-981-13-3813-7\\_7](https://doi.org/10.1007/978-981-13-3813-7_7)
- Holmes, P. A. (1985). Applications of PHB - A microbially produced biodegradable thermoplastic. *Physics in Technology*, 16(1), 32–36. <https://doi.org/10.1088/0305-4624/16/1/305>
- Howe, P. D., Mildenerger, M., Marlon, J. R., & Leiserowitz, A. (2015). Geographic variation in opinions on climate change at state and local scales in the USA. *Nature Climate Change*, 5(6), 596–603. <https://doi.org/10.1038/nclimate2583>
- IEA. (2020). *Methane Tracker 2020*. <https://www.iea.org/reports/methane-tracker-2020>

- Irving, S. E., Choudhury, N. R., & Corrigan, R. M. (2021). The stringent response and physiological roles of (pp)pGpp in bacteria. *Nature Reviews Microbiology*, 19(4), 256–271. <https://doi.org/10.1038/s41579-020-00470-y>
- J. A. Ramsay, E. Berger, R. Voyer, C. Chavarie, B. A. R. (1994). Extraction of poly-3-hydroxybutyrate using chlorinated solvents. 8(8), 589–594.
- James, B. W., Mauchline, W. S., Dennis, P. J., Keevil, C. W., & Wait, R. (1999). Poly-3-hydroxybutyrate in *Legionella pneumophila*, an energy source for survival in low-nutrient environments. *Applied and Environmental Microbiology*, 65(2), 822–827. <https://doi.org/10.1128/aem.65.2.822-827.1999>
- Jawaharraj, K., Shrestha, N., Chilkoor, G., Dhiman, S. S., Islam, J., & Gadhamshetty, V. (2020). Valorization of methane from environmental engineering applications: A critical review. *Water Research*, 187, 116400. <https://doi.org/10.1016/j.watres.2020.116400>
- Jendrossek, D; Handrick, R. (2002). Microbial degradation of polyhydroxyalkanoates. *Annual Review of Microbiology*, 56(1), 403–432. <https://doi.org/10.1146/annurev.micro.56.012302.160838>
- Jers, C., Kalantari, A., Garg, A., & Mijakovic, I. (2019). Production of 3-Hydroxypropanoic Acid From Glycerol by Metabolically Engineered Bacteria. *Frontiers in Bioengineering and Biotechnology*, 7(May), 1–15. <https://doi.org/10.3389/fbioe.2019.00124>
- Jossek, R., Reichelt, R., & Steinbüchel, A. (1998). *In vitro* biosynthesis of poly(3-hydroxybutyric acid) by using purified poly(hydroxyalkanoic acid) synthase of *Chromatium vinosum*. *Applied Microbiology and Biotechnology*, 49(3), 258–266. <https://doi.org/10.1007/s002530051166>
- Juengert, J. R., Borisova, M., Mayer, C., Wolz, C., Brigham, C. J., & Sinskey, A. J. (2017). Absence of ppGpp Leads to Increased Mobilization of Intermediately Accumulated Poly(3-Hydroxybutyrate) in *Ralstonia eutropha* H16. *Applied and Environmental Microbiology*, 83(13), 1–16. <https://doi.org/https://doi.org/10.1128/AEM.00755-17>

- Juengert, J. R., Cameron, P., Dieter, J., & Maia, K. (2018). Poly(3-Hydroxybutyrate) (PHB) Polymerase PhaC1 and PHB Depolymerase PhaZa1 of *Ralstonia eutropha* Are Phosphorylated *In Vivo*. *Applied and Environmental Microbiology*, 84(13), e00604-18. <https://doi.org/10.1128/AEM.00604-18>
- Jung, Young-Mi; Lee, Y.-H. (1997). Investigation of Regulatory Mechanism of Flux of Acetyl-CoA in *Alcaligenes eutrophus* Using PHB-negative Mutant and Transformants Harboring Cloned *phbCAB* Genes. *Journal of Microbiology and Biotechnology*, 7(4), 215–222.
- Kashiwaya, Y., Takeshima, T., Mori, N., Nakashima, K., Clarke, K., & Veech, R. L. (2000). D- $\beta$ -hydroxybutyrate protects neurons in models of Alzheimer's and Parkinson's disease. *Proceedings of the National Academy of Sciences of the United States of America*, 97(10), 5440–5444. <https://doi.org/10.1073/pnas.97.10.5440>
- Katayama, M., Hiraide, A., Sugimoto, H., Yoshioka, T., & Sugimoto, T. (1994). Effect of Ketone Bodies on Hyperglycemia and Lactic Acidemia in Hemorrhagic Stress. *Journal of Parenteral and Enteral Nutrition*, 18(5), 442–446. <https://doi.org/10.1177/0148607194018005442>
- Kawata, Y., Ando, H., Matsushita, I., & Tsubota, J. (2014). Efficient secretion of (R)-3-hydroxybutyric acid from *Halomonas* sp. KM-1 by nitrate fed-batch cultivation with glucose under microaerobic conditions. *Bioresource Technology*, 156, 400–403. <https://doi.org/10.1016/j.biortech.2014.01.073>
- Kawata, Y., Kawasaki, K., & Shigeri, Y. (2012). Efficient secreted production of (R)-3-hydroxybutyric acid from living *Halomonas* sp. KM-1 under successive aerobic and microaerobic conditions. *Applied Microbiology and Biotechnology*, 96(4), 913–920. <https://doi.org/10.1007/s00253-012-4218-6>
- Kawata, Y., Nojiri, M., Matsushita, I., & Tsubota, J. (2015). Improvement of (R)-3-hydroxybutyric acid secretion during *Halomonas* sp. KM-1 cultivation with saccharified Japanese cedar by the addition of urea. *Letters in Applied Microbiology*, 61(4), 397–402. <https://doi.org/10.1111/lam.12473>

- Khosravi-Darani, K., & Bucci, D. Z. (2015). Application of poly(hydroxyalkanoate) in food packaging: Improvements by nanotechnology. In *Chemical and Biochemical Engineering Quarterly* (Vol. 29, Issue 2, pp. 275–285). <https://doi.org/10.15255/CABEQ.2014.2260>
- Khosravi-Darani, K., Mokhtari, Z. B., Amai, T., & Tanaka, K. (2013). Microbial production of poly(hydroxybutyrate) from C1 carbon sources. *Applied Microbiology and Biotechnology*, 97(4), 1407–1424. <https://doi.org/10.1007/s00253-012-4649-0>
- Kim, B. S., Lee, S. C., Lee, S. Y., Chang, H. N., Chang, Y. K., & Woo, S. I. (1994). Production of poly(3-hydroxybutyric acid) by fed-batch culture of *Alcaligenes eutrophus* with glucose concentration control. *Biotechnology and Bioengineering*, 43, 892–898. doi: 10.1002/bit.260430908
- Kim, M., Cho, K., Ryu, H. W., Lee, E. G., & Chang, Y. K. (2003). Recovery of poly (3-hydroxybutyrate) from high cell density culture of *Ralstonia eutropha* by direct addition of sodium dodecyl sulfate. *Biotechnology Letters*, 25(1), 55–59. doi: 10.1023/a:1021734216612
- Kim, T.W., Park, J.S., & Lee, Y.H. (1996). Enzymatic Characteristics of Biosynthesis and Degradation of Poly- $\beta$ -hydroxybutyrate of *Alcaligenes latus*. *Journal of Microbiology and Biotechnology*, 6, 425-431.
- Knoll, M., Hamm, T. M., Wagner, F., Martinez, V., & Pleiss, J. (2009). The PHA Depolymerase Engineering Database : A systematic analysis tool for the diverse family of polyhydroxyalkanoate (PHA) depolymerases. *BMC Bioinformatics*, 10, 1–8. <https://doi.org/10.1186/1471-2105-10-89>
- Koller, M. (2014). Poly(hydroxyalkanoates) for Food Packaging: Application and Attempts towards Implementation. *Applied Food Biotechnology*, 1, 3–15. <https://doi.org/doi.org/10.22037/afb.v1i1.7127>
- Kosseva, M. R., & Rusbandi, E. (2018). International Journal of Biological Macromolecules Trends in the biomanufacture of polyhydroxyalkanoates with focus on downstream processing. *International Journal of Biological Macromolecules*, 107, 762–778. <https://doi.org/10.1016/j.ijbiomac.2017.09.054>

- Kumar, P., Ray, S., & Kalia, V. C. (2016). Production of co-polymers of polyhydroxyalkanoates by regulating the hydrolysis of biowastes. *Bioresource Technology*, 200, 413–419. <https://doi.org/10.1016/j.biortech.2015.10.045>
- Kunasundari, B., & Sudesh, K. (2011). Isolation and recovery of microbial polyhydroxyalkanoates. *Polymer letters*, 5(7), 620–634. <https://doi.org/10.3144/expresspolymlett.2011.60>
- Lafferty, R. M., & Heinzle, E. (1977). Cyclic carbonic acid esters as solvents for poly-( $\beta$ )-hydroxybutyric acid. In *U.S. Patent*. <https://patents.google.com/patent/US4101533>
- Latimer, A. A., Kakekhani, A., Kulkarni, A. R., & Nørskov, J. K. (2018). Direct Methane to Methanol: The Selectivity-Conversion Limit and Design Strategies. *ACS Catalysis*, 8(8), 6894–6907. <https://doi.org/10.1021/acscatal.8b00220>
- Lawrence, A. G., Schoenheit, J., He, A., Tian, J., Liu, P., Stubbe, J., & Sinskey, A. J. (2005). Transcriptional analysis of *Ralstonia eutropha* genes related to poly-(R)-3-hydroxybutyrate homeostasis during batch fermentation. *Applied Microbiology and Biotechnology*, 68(5), 663–672. <https://doi.org/10.1007/s00253-005-1969-3>
- Lee, I. Y., Kim, M. K., Chang, H. N., & Park, Y. H. (1995). Regulation of poly- $\beta$ -hydroxybutyrate biosynthesis by nicotinamide nucleotide in *Alcaligenes eutrophus*. In *FEMS Microbiology Letters*, 131(1), 35–39. [https://doi.org/10.1016/0378-1097\(95\)00231-S](https://doi.org/10.1016/0378-1097(95)00231-S)
- Lee, S. Y., & Lee, Y. (2003). Metabolic Engineering of *Escherichia coli* for Production of Enantiomerically Pure (R)-(-)-Hydroxycarboxylic Acids. *Applied and Environmental Microbiology*, 69(6), 3421–3426. <https://doi.org/10.1128/AEM.69.6.3421-3426.2003>
- Lee, S. Y., Lee, Y., & Wang, F. (1999). Chiral compounds from bacterial polyesters: Sugars to plastics to fine chemicals. *Biotechnology and Bioengineering*, 65(3), 363–368. [https://doi.org/10.1002/\(SICI\)1097-0290\(19991105\)65:3<363::AID-BIT15>3.0.CO;2-1](https://doi.org/10.1002/(SICI)1097-0290(19991105)65:3<363::AID-BIT15>3.0.CO;2-1)

- Lee, Y., Hyun, S., Taek, I., Han, K., & Yup, S. (2000). Preparation of alkyl (R)-(-)-3-hydroxybutyrate by acidic alcoholysis of poly-(R)-(-)-3-hydroxybutyrate. *Enzyme and Microbial Technology*, 27, 33–36. [https://doi.org/10.1016/s0141-0229\(00\)00146-0](https://doi.org/10.1016/s0141-0229(00)00146-0)
- Levett, I., Birkett, G., Davies, N., Bell, A., Langford, A., Laycock, B., Lant, P., & Pratt, S. (2016). Techno-economic assessment of poly-3-hydroxybutyrate (PHB) production from methane - The case for thermophilic bioprocessing. *Journal of Environmental Chemical Engineering*, 4(4), 3724–3733. <https://doi.org/10.1016/j.jece.2016.07.033>
- Li, F., Zhang, C., Liu, Y., Liu, D., Xia, H., & Chen, S. (2016). Efficient production of (R)-3-hydroxybutyric acid by *Pseudomonas* sp. DS1001a and its extracellular poly(3-hydroxybutyrate) depolymerase. *Process Biochemistry*, 51(3), 369–373. <https://doi.org/10.1016/j.procbio.2015.12.016>
- Liddell, J. M. (1999). Process for the recovery of Polyhydroxyalkanoic acid. In *U.S. Patent*.
- Listewnik, H. F., Wendlandt, K. D., Jechorek, M., & Mirschel, G. (2007). Process design for the microbial synthesis of Poly- $\beta$ -hydroxybutyrate (PHB) from natural gas. *Engineering in Life Sciences*, 7(3), 278–282. <https://doi.org/10.1002/elsc.200620193>
- Liu, Q., Ouyang, S. P., Chung, A., Wu, Q., & Chen, G. Q. (2007). Microbial production of R-3-hydroxybutyric acid by recombinant *E. coli* harboring genes of *phbA*, *phbB*, and *tesB*. *Applied Microbiology and Biotechnology*, 76(4), 811–818. <https://doi.org/10.1007/s00253-007-1063-0>
- Loo, C. Y., Lee, W. H., Tsuge, T., Doi, Y., & Sudesh, K. (2005). Biosynthesis and characterization of poly(3-hydroxybutyrate-co-3-hydroxyhexanoate) from palm oil products in a *Wautersia eutropha* mutant. *Biotechnology Letters*, 27(18), 1405–1410. <https://doi.org/10.1007/s10529-005-0690-8>
- Loow, Y. L., Wu, T. Y., Jahim, J. M., Mohammad, A. W., & Teoh, W. H. (2016). Typical conversion of lignocellulosic biomass into reducing sugars using dilute acid hydrolysis and alkaline pretreatment. *Cellulose*, 23(3), 1491–1520. <https://doi.org/10.1007/s10570-016-0936-8>

- Lu, J., Brigham, C. J., Gai, C. S., & Sinskey, A. J. (2012). Studies on the production of branched-chain alcohols in engineered *Ralstonia eutropha*. *Applied Microbiology and Biotechnology*, 96(1), 283–297. <https://doi.org/10.1007/s00253-012-4320-9>
- Lu, J., Brigham, C. J., Li, S., & Sinskey, A. J. (2016). *Ralstonia eutropha* H16 as a Platform for the Production of Biofuels, Biodegradable Plastics, and Fine Chemicals from Diverse Carbon Resources. In *Biotechnology for Biofuel Production and Optimization*. Elsevier B.V. <https://doi.org/10.1016/B978-0-444-63475-7.00012-1>
- Lu, J., Takahashi, A., & Ueda, S. (2014). 3-Hydroxybutyrate oligomer hydrolase and 3-hydroxybutyrate dehydrogenase participate in intracellular polyhydroxybutyrate and polyhydroxyvalerate degradation in *Paracoccus denitrificans*. *Applied and Environmental Microbiology*, 80(3), 986–993. <https://doi.org/10.1128/AEM.03396-13>
- Lu, J., Tappel, R. C., & Nomura, C. T. (2009). Mini-review: Biosynthesis of poly(hydroxyalkanoates). *Polymer Reviews*, 49(3), 226–248. <https://doi.org/10.1080/15583720903048243>
- Martin, Robert; Thomas, Jhon; Soni, M. (2021). Evaluation of the generally recognized as safe (GRAS) status of D-6-hydroxybutyrate (D-BHB) as a food ingredient. <https://www.fda.gov/media/157969/download>
- Massieu, L., Haces, M. L., Montiel, T., & Hernández-Fonseca, K. (2003). Acetoacetate protects hippocampal neurons against glutamate-mediated neuronal damage during glycolysis inhibition. *Neuroscience*, 120(2), 365–378. [https://doi.org/10.1016/S0306-4522\(03\)00266-5](https://doi.org/10.1016/S0306-4522(03)00266-5)
- Matsuyama, A., Yamamoto, H., Kawada, N., & Kobayashi, Y. (2001). Industrial production of (R)-1,3-butanediol by new biocatalysts. *Journal of Molecular Catalysis B: Enzymatic*, 11(4–6), 513–521. [https://doi.org/10.1016/S1381-1177\(00\)00032-1](https://doi.org/10.1016/S1381-1177(00)00032-1)
- Mikkili, I., Karlapudi, A.P., JohnBabu, D., Nath, S., & Kodali, V.P. (2014). Isolation, Screening and Extraction of Polyhydroxybutyrate (PHB) producing bacteria from Sewage sample. *International Journal of PharmTech Research*, 6(2), 850-857

- Misra, S. K., Valappil, S. P., Roy, I., & Boccaccini, A. R. (2006). Polyhydroxyalkanoate (PHA)/inorganic phase composites for tissue engineering applications. *Biomacromolecules*, 7(8), 2249–2258. <https://doi.org/10.1021/bm060317c>
- Mohamad Noh, N. (2017). Catalytic Route for the Synthesis of Cyclic Organic Carbonates from Renewable Polyols [Doctoral dissertation]. <https://livrepository.liverpool.ac.uk/id/eprint/3012167>
- Mothes, G., Schnorpfeil, C., & Ackermann, J. U. (2007). Production of PHB from crude glycerol. *Engineering in Life Sciences*, 7(5), 475–479. <https://doi.org/10.1002/elsc.200620210>
- Mountassif, D., Andreoletti, P., Cherkaoui-Malki, M., Latruffe, N., & Kebbaj, M. S. El. (2010). Structural and catalytic properties of the D-3-hydroxybutyrate dehydrogenase from *Pseudomonas aeruginosa*. *Current Microbiology*, 61(1), 7–12. <https://doi.org/10.1007/s00284-009-9568-7>
- Mozejko-Ciesielska, J., Dabrowska, D., Szalewska-Palasz, A., & Ciesielski, S. (2017). Medium-chain-length polyhydroxyalkanoates synthesis by *Pseudomonas putida* KT2440 relA/spoT mutant: bioprocess characterization and transcriptome analysis. *AMB Express*, 7(1). <https://doi.org/10.1186/s13568-017-0396-z>
- Mozejko-Ciesielska, J., & Kiewisz, R. (2016). Bacterial polyhydroxyalkanoates: Still fabulous? *Microbiological Research*, 192(2016), 271–282. <https://doi.org/10.1016/j.micres.2016.07.010>
- Naggert, J., Narasimhan, M. L., DeVeaux, L., Cho, H., Randhawa, Z. I., Cronan, J. E., Green, B. N., & Smith, S. (1991). Cloning, sequencing, and characterization of *Escherichia coli* thioesterase II. *Journal of Biological Chemistry*, 266(17), 11044–11050. [https://doi.org/10.1016/s0021-9258\(18\)99125-8](https://doi.org/10.1016/s0021-9258(18)99125-8)
- Naranjo, J. M., Posada, J. A., Higuera, J. C., & Cardona, C. A. (2013). Valorization of glycerol through the production of biopolymers: The PHB case using *Bacillus megaterium*. *Bioresource Technology*, 133, 38–44. <https://doi.org/10.1016/j.biortech.2013.01.129>

- Nguyen, D. T. N., Lee, O. K., Nguyen, T. T., & Lee, E. Y. (2021). Type II methanotrophs: A promising microbial cell-factory platform for bioconversion of methane to chemicals. *Biotechnology Advances*, 47(January), 107700. <https://doi.org/10.1016/j.biotechadv.2021.107700>
- Obruca, S., Sedlacek, P., Mravec, F., Samek, O., & Marova, I. (2016). Evaluation of 3-hydroxybutyrate as an enzyme-protective agent against heating and oxidative damage and its potential role in stress response of poly(3-hydroxybutyrate) accumulating cells. *Applied Microbiology and Biotechnology*, 100(3), 1365–1376. <https://doi.org/10.1007/s00253-015-7162-4>
- Oh, Y. H., Lee, S. H., Jang, Y. A., Choi, J. W., Hong, K. S., Yu, J. H., Shin, J., Song, B. K., Mastan, S. G., David, Y., Baylon, M. G., Lee, S. Y., & Park, S. J. (2015). Development of rice bran treatment process and its use for the synthesis of polyhydroxyalkanoates from rice bran hydrolysate solution. *Bioresource Technology*, 181, 283–290. <https://doi.org/10.1016/j.biortech.2015.01.075>
- Page, W. J., & Knosp, O. (1989). Hyperproduction of poly- $\beta$ -hydroxybutyrate during exponential growth of *Azotobacter vinelandii* UWD. *Applied and Environmental Microbiology*, 55(6), 1334–1339. <https://doi.org/10.1128/aem.55.6.1334-1339.1989>
- Papapostolou, A., Karasavvas, E., & Chatzidoukas, C. (2019). Oxygen mass transfer limitations set the performance boundaries of microbial PHA production processes – A model-based problem investigation supporting scale-up studies. *Biochemical Engineering Journal*, 148(March), 224–238. <https://doi.org/10.1016/j.bej.2019.04.024>
- Pérez-Fortes, M., Schöneberger, J. C., Boulamanti, A., & Tzimas, E. (2016). Methanol synthesis using captured CO<sub>2</sub> as raw material: Techno-economic and environmental assessment. *Applied Energy*, 161, 718–732. <https://doi.org/10.1016/j.apenergy.2015.07.067>
- Peypoux, F., Bonmatin, J. M., & Wallach, J. (1999). Recent trends in the biochemistry of surfactin. *Applied Microbiology and Biotechnology*, 51(5), 553–563. <https://doi.org/10.1007/s002530051432>

- Pieja, A. J., Sundstrom, E. R., & Criddle, C. S. (2011). Poly-3-hydroxybutyrate metabolism in the type II Methanotroph *Methylocystis parvus* OBBP. *Applied and Environmental Microbiology*, 77(17), 6012–6019. <https://doi.org/10.1128/AEM.00509-11>
- Poblete-Castro, I., Binger, D., Oehlert, R., & Rohde, M. (2014). Comparison of mcl-poly(3-hydroxyalkanoates) synthesis by different *Pseudomonas putida* strains from crude glycerol: Citrate accumulates at high titer under PHA-producing conditions. *BMC Biotechnology*, 14(1), 1–11. <https://doi.org/10.1186/s12896-014-0110-z>
- Poirier, Y., Nawrath, C., & Somerville, C. (1995). Production of Polyhydroxyalkanoates, a Family of Biodegradable Plastics and Elastomers, in Bacteria and Plants. *Bio/Technology*, 13(2), 142–150. <https://doi.org/10.1038/nbt0295-142>
- Polyák, P., Dohovits, E., Nagy, G. N., Vértessy, B. G., Vörös, G., & Pukánszky, B. (2018). Enzymatic degradation of poly-[(R)-3-hydroxybutyrate]: Mechanism, kinetics, consequences. *International Journal of Biological Macromolecules*, 112, 156–162. <https://doi.org/10.1016/j.ijbiomac.2018.01.104>
- Posada, J. A., Naranjo, J. M., López, J. A., Higueta, J. C., & Cardona, C. A. (2011). Design and analysis of poly-3-hydroxybutyrate production processes from crude glycerol. *Process Biochemistry*, 46(1), 310–317. <https://doi.org/10.1016/j.procbio.2010.09.003>
- Raberg, M., Voigt, B., Hecker, M., & Steinbüchel, A. (2014). A closer look on the polyhydroxybutyrate- (PHB-) negative phenotype of *Ralstonia eutropha* PHB<sup>-</sup>4. *PLOS ONE*, 9(5), 1–11. <https://doi.org/10.1371/journal.pone.0095907>
- Ramsay, B. A., Lomaliza, K., Chavarie, C., Dube, B., Bataille, P., & Ramsay, J. A. (1990). Production of poly-(beta-hydroxybutyric-co-beta-hydroxyvaleric) acids. *Applied and Environmental Microbiology*, 56(7), 2093–2098. <https://doi.org/https://doi.org/10.1128/aem.56.7.2093-2098.1990>
- Ramsay, J. A., Berger, E., Ramsay, B. A., & Chavarie, C. (1990). Recovery of Poly-3-hydroxyalkanoic acid granules by a surfactant-hypochlorite treatment. *Biotechnology Techniques*, 4(4), 221–226.

- Rathbone, S., Furrer, P., Lübben, J., Zinn, M., & Cartmell, S. (2010). Biocompatibility of polyhydroxyalkanoate as a potential material for ligament and tendon scaffold material. *Journal of Biomedical Materials Research - Part A*, 93(4), 1391–1403. <https://doi.org/10.1002/jbm.a.32641>
- Rehm, B. H. A., Krüger, N., & Steinbüchel, A. (1998). A new metabolic link between fatty acid de novo synthesis and polyhydroxyalkanoic acid synthesis. The *phaG* gene from *Pseudomonas putida* KT2440 encodes a 3-hydroxyacyl-acyl carrier protein-coenzyme a transferase. *Journal of Biological Chemistry*, 273(37), 24044–24051. <https://doi.org/10.1074/jbc.273.37.24044>
- Reinecke, F., & Steinbüchel, A. (2009). *Ralstonia eutropha* Strain H16 as Model Organism for PHA Metabolism and for Biotechnological Production of Technically Interesting Biopolymers. *Microbial Physiology*, 16(1–2), 91–108. <https://doi.org/10.1159/000142897>
- Ren, Q., Grubelnik, A., Hoerler, M., Ruth, K., Hartmann, R., Felber, H., & Zinn, M. (2005). Bacterial poly(hydroxyalkanoates) as a source of chiral hydroxyalkanoic acids. *Biomacromolecules*, 6(4), 2290–2298. <https://doi.org/10.1021/bm050187s>
- Ren, Q., Ruth, K., Thöny-Meyer, L., & Zinn, M. (2007). Process engineering for production of chiral hydroxycarboxylic acids from bacterial polyhydroxyalkanoates. *Macromolecular Rapid Communications*, 28(22), 2131–2136. <https://doi.org/10.1002/marc.200700389>
- Riahi, K; R. Schaeffer, J; Arango, K. et al. (2022). *IPCC, 2022: Climate Change 2022: Mitigation of Climate Change. Chapter 3: Mitigation pathways compatible with long-term goals.*
- Rodríguez, Y., Firmino, P. I. M., Arnáiz, E., Lebrero, R., & Muñoz, R. (2020). Elucidating the influence of environmental factors on biogas-based polyhydroxybutyrate production by *Methylocystis hirsuta* CSC1. *Science of the Total Environment*, 706. <https://doi.org/10.1016/j.scitotenv.2019.135136>

- Rodríguez, Y., García, S., Pérez, R., Lebrero, R., & Muñoz, R. (2022). Optimization of nitrogen feeding strategies for improving polyhydroxybutyrate production from biogas by *Methylocystis parvus* str. OBBP in a stirred tank reactor. *Chemosphere*, 299. <https://doi.org/10.1016/j.chemosphere.2022.134443>
- Roohi, Zaheer, M. R., & Kuddus, M. (2018). PHB (poly- $\beta$ -hydroxybutyrate) and its enzymatic degradation. In *Polymers for Advanced Technologies*, 29(1), 30–40. <https://doi.org/10.1002/pat.4126>
- Rostkowski, K. H., Pfluger, A. R., & Criddle, C. S. (2013). Stoichiometry and kinetics of the PHB-producing Type II methanotrophs *Methylosinus trichosporium* OB3b and *Methylocystis parvus* OBBP. *Bioresource Technology*, 132, 71–77. <https://doi.org/10.1016/j.biortech.2012.12.129>
- Ruth, K., Grubelnik, A., Hartmann, R., Egli, T., Zinn, M., & Ren, Q. (2007). Efficient production of (R)-3-hydroxycarboxylic acids by biotechnological conversion of polyhydroxyalkanoates and their purification. *Biomacromolecules*, 8(1), 279–286. <https://doi.org/10.1021/bm060585a>
- Samek O, Obruča S, Šiler M, Sedláček P, Benešová P, Kučera D, Márova I, Ježek J, Bernatová S, Zemánek P. (2016). Quantitative Raman Spectroscopy Analysis of Polyhydroxyalkanoates Produced by *Cupriavidus necator* H16. *Sensors*, 16(11), 1808. <https://doi.org/10.3390/s16111808>
- Scherer, T. M., Fuller, R. C., Lenz, R. W., & Goodwin, S. (1999). Production, purification and activity of an extracellular depolymerase from *Aspergillus fumigatus*. *Journal of Environmental Polymer Degradation*, 7(3), 117–125. <https://doi.org/10.1023/A:1022881204565>
- Schweitzer, D., Mullen, C. A., Boateng, A., & Snell, K. D. (2015). Biobased n-Butanol Prepared from Poly-3-hydroxybutyrate: Optimization of the Reduction of n-Butyl Crotonate to n-Butanol. *Organic Process Research and Development*, 19(7), 710–714. <https://doi.org/10.1021/op500156b>

- Scott, F., Yañez, L., Conejeros, R., Araya, B., & Vergara-Fernández, A. (2021). Two internal bottlenecks cause the overflow metabolism leading to poly(3-hydroxybutyrate) production in *Azohydromonas lata* DSM1123. *Journal of Environmental Chemical Engineering*, 9(4). <https://doi.org/10.1016/j.jece.2021.105665>
- Seebach, D., Albert, M., Arvidsson, P. I., Rueping, M., & Schreiber, J. V. (2001). From the Biopolymer PHB to Biological Investigations of Unnatural  $\beta$ - and  $\gamma$ -Peptides. *CHIMIA*, 55(4), 345. <https://doi.org/10.2533/chimia.2001.345>
- Seebach, D., Beck, A. K., Breitschuh, R., & Job, K. (2003). Direct Degradation of the Biopolymer Poly[(R)-3-Hydroxybutyric Acid] to (R)-3-Hydroxybutanoic Acid and its Methyl Ester. In *Organic Syntheses*, 71, 39. <https://doi.org/https://doi.org/10.1002/0471264180.os071.05>
- Seebach, D., Chow, H. -F, Jackson, R. F. W., Sutter, M. A., Thaisrivongs, S., & Zimmermann, J. (1986). (+)-11,11'-Di-O-methylelaiohylidene – preparation from elaiophylin and total synthesis from (R)-3-hydroxybutyrate and (S)-malate. *Liebigs Annalen Der Chemie*, 1986(7), 1281–1308. <https://doi.org/10.1002/jlac.198619860714>
- Shah, M., Naseer, M. I., Choi, M. H., Kim, M. O., & Yoon, S. C. (2010). Amphiphilic PHA-mPEG copolymeric nanocontainers for drug delivery: Preparation, characterization and in vitro evaluation. *International Journal of Pharmaceutics*, 400(1–2), 165–175. <https://doi.org/10.1016/j.ijpharm.2010.08.008>
- Shiraki, M., Endo, T., & Saito, T. (2006). Fermentative production of (R)-(-)-3-hydroxybutyrate using 3-hydroxybutyrate dehydrogenase null mutant of *Ralstonia eutropha* and recombinant *Escherichia coli*. *Journal of Bioscience and Bioengineering*, 102(6), 529–534. <https://doi.org/10.1263/jbb.102.529>
- Soni, B. K., Conrad, J., Kelley, R. L., & Srivastava, V. J. (1998). Effect of temperature and pressure on growth and methane utilization by several methanotrophic cultures. *Applied Biochemistry and Biotechnology*, 70–72, 729–738. <https://doi.org/10.1007/BF02920184>

- Srivatsan, A., & Wang, J. D. (2008). Control of bacterial transcription, translation and replication by (p)ppGpp. *Current Opinion in Microbiology*, *11*(2), 100–105. <https://doi.org/10.1016/j.mib.2008.02.001>
- Steinbüchel, A., & Hein, S. (2001). Biochemical and molecular basis of microbial synthesis of polyhydroxyalkanoates in microorganisms. *Advances in Biochemical Engineering/Biotechnology*, *71*, 81–123. [https://doi.org/10.1007/3-540-40021-4\\_3](https://doi.org/10.1007/3-540-40021-4_3)
- Steinbüchel, A., & Valentin, H. E. (1995). Diversity of bacterial polyhydroxyalkanoic acids. *FEMS Microbiology Letters*, *128*(3), 219–228. [https://doi.org/10.1016/0378-1097\(95\)00125-O](https://doi.org/10.1016/0378-1097(95)00125-O)
- Strong, P. J., Xie, S., & Clarke, W. P. (2015). Methane as a resource: Can the methanotrophs add value? *Environmental Science and Technology*, *49*(7), 4001–4018. <https://doi.org/10.1021/es504242n>
- Strong, P., Laycock, B., Mahamud, S., Jensen, P., Lant, P., Tyson, G., & Pratt, S. (2016). The Opportunity for High-Performance Biomaterials from Methane. *Microorganisms*, *4*(1), 11. <https://doi.org/10.3390/microorganisms4010011>
- Suriyamongkol, P., Weselake, R., Narine, S., Moloney, M., & Shah, S. (2007). Biotechnological approaches for the production of polyhydroxyalkanoates in microorganisms and plants - A review. *Biotechnology Advances*, *25*(2), 148–175. <https://doi.org/10.1016/j.biotechadv.2006.11.007>
- Sznajder, A., Pfeiffer, D., & Jendrossek, D. (2015). Comparative proteome analysis reveals four novel polyhydroxybutyrate (PHB) granule-associated proteins in *Ralstonia eutropha* H16. *Applied and Environmental Microbiology*, *81*(5), 1847–1858. <https://doi.org/10.1128/AEM.03791-14>
- Taidi, B., Mansfield, D. A., & Anderson, A. J. (1995). Turnover of poly(3-hydroxybutyrate) (PHB) and its influence on the molecular mass of the polymer accumulated by *Alcaligenes eutrophus* during batch culture. *FEMS Microbiology Letters*, *129*(2–3), 201–205. [https://doi.org/10.1016/0378-1097\(95\)00158-2](https://doi.org/10.1016/0378-1097(95)00158-2)

- Tajima, K., Han, X., Hashimoto, Y., Satoh, Y., Satoh, T., & Taguchi, S. (2016). *In vitro* synthesis of polyhydroxyalkanoates using thermostable acetyl-CoA synthetase, CoA transferase, and PHA synthase from thermotolerant bacteria. *Journal of Bioscience and Bioengineering*, 122(6), 660–665. <https://doi.org/10.1016/j.jbiosc.2016.06.001>
- Tajima, K., Han, X., Satoh, Y., Ishii, A., Araki, Y., Munekata, M., & Taguchi, S. (2012). *In vitro* synthesis of polyhydroxyalkanoate (PHA) incorporating lactate (LA) with a block sequence by using a newly engineered thermostable PHA synthase from *Pseudomonas* sp. SG4502 with acquired LA-polymerizing activity. *Applied Microbiology and Biotechnology*, 94(2), 365–376. <https://doi.org/10.1007/s00253-011-3840-z>
- Takanashi, M., & Saito, T. (2006). Characterization of two 3-hydroxybutyrate dehydrogenases in poly(3-hydroxybutyrate)-degradable bacterium, *Ralstonia pickettii* T1. *Journal of Bioscience and Bioengineering*, 101(6), 501–507. <https://doi.org/10.1263/jbb.101.501>
- Tamer, I. M., Moo-young, M., & Chisti, Y. (1998). Disruption of *Alcaligenes latus* for Recovery of Poly ( $\beta$ -hydroxybutyric acid ): Comparison of High-Pressure Homogenization , Bead Milling , and Chemically Induced Lysis. *Industrial and Engineering Chemistry Research*, 5885(97), 1807–1814.
- Tanaka, K., Ishizaki, A., Kanamaru, T., & Kawano, T. (1995). Production of poly (D-3-hydroxybutyrate) from CO<sub>2</sub>, H<sub>2</sub>, and O<sub>2</sub> by high cell density autotrophic cultivation of *Alcaligenes eutrophus*. *Biotechnology and Bioengineering*, 45(3), 268–275. <http://onlinelibrary.wiley.com/doi/10.1002/bit.260450312/abstract>
- Tanaka, K., Miyawaki, K., Yamaguchi, A., Khosravi-Darani, K., & Matsusaki, H. (2011). Cell growth and P(3HB) accumulation from CO<sub>2</sub> of a carbon monoxide-tolerant hydrogen-oxidizing bacterium, *Ideonella* sp. O-1. *Applied Microbiology and Biotechnology*, 92(6), 1161–1169. <https://doi.org/10.1007/s00253-011-3420-2>
- Tieu, K., Perier, C., Caspersen, C., Teismann, P., Wu, D. C., Yan, S. Du, Naini, A., Vila, M., Jackson-Lewis, V., Ramasamy, R., & Przedborski, S. (2003). D- $\beta$ -Hydroxybutyrate rescues mitochondrial respiration and mitigates features of Parkinson disease. *Journal of Clinical Investigation*, 112(6), 892–901. <https://doi.org/10.1172/JCI200318797>

- Tokiwa, Y., & Ugwu, C. U. (2007). Biotechnological production of (R)-3-hydroxybutyric acid monomer. *Journal of Biotechnology*, 132(3), 264–272. <https://doi.org/10.1016/j.jbiotec.2007.03.015>
- Uchino, K., Saito, T., Gebauer, B., & Jendrossek, D. (2007). Isolated poly(3-hydroxybutyrate) (PHB) granules are complex bacterial organelles catalyzing formation of PHB from acetyl coenzyme A (CoA) and degradation of PHB to acetyl-CoA. *Journal of Bacteriology*, 189(22), 8250–8256. <https://doi.org/10.1128/JB.00752-07>
- Ueda, H., & Tabata, Y. (2003). Polyhydroxyalkanoate derivatives in current clinical applications and trials. *Advanced Drug Delivery Reviews*, 55(4), 501–518. [https://doi.org/10.1016/S0169-409X\(03\)00037-1](https://doi.org/10.1016/S0169-409X(03)00037-1)
- Ugwu, C. U., Tokiwa, Y., Aoyagi, H., Uchiyama, H., & Tanaka, H. (2008). UV mutagenesis of *Cupriavidus necator* for extracellular production of (R)-3-hydroxybutyric acid. *Journal of Applied Microbiology*, 105(1), 236–242. <https://doi.org/10.1111/j.1365-2672.2008.03774.x>
- Ugwu, C. U., Tokiwa, Y., & Ichiba, T. (2011). Production of (R)-3-hydroxybutyric acid by fermentation and bioconversion processes with *Azohydromonas lata*. *Bioresource Technology*, 102(12), 6766–6768. <https://doi.org/10.1016/j.biortech.2011.03.073>
- van der Linden, S., Leiserowitz, A., Rosenthal, S., Maibach, E., Howe, P. D., Mildemberger, M., Marlon, J. R., & Leiserowitz, A. (2017). Inoculating the Public against Misinformation about Climate Change. *Global Challenges*, 1(2), 596–603. <https://doi.org/10.1002/gch2.201600008>
- Vecherskaya, M., Dijkema, C., Saad, H. R., & Stams, A. J. M. (2009). Microaerobic and anaerobic metabolism of a *Methylocystis parvus* strain isolated from a denitrifying bioreactor. *Environmental Microbiology Reports*, 1(5), 442–449. <https://doi.org/10.1111/j.1758-2229.2009.00069.x>
- Vecherskaya, M., Dijkema, C., & Stams, A. J. M. (2001). Intracellular PHB conversion in a Type II methanotroph studied by <sup>13</sup>C NMR. *Journal of Industrial Microbiology and Biotechnology*, 26(1–2), 15–21. <https://doi.org/10.1038/sj.jim.7000086>

- Vergé, X. P. C., De Kimpe, C., & Desjardins, R. L. (2007). Agricultural production, greenhouse gas emissions and mitigation potential. *Agricultural and Forest Meteorology*, *142*(2–4), 255–269. <https://doi.org/10.1016/j.agrformet.2006.06.011>
- Volova, T; Shishatskaya, E; Sevastianov, V; Efremov, S; and Mogilnaya, O. (2003). Results of biomedical investigations of PHB and PHB/PHV fibers. *Biochemical Engineering Journal*, *16*, 125–133.
- Wang, B., Xiong, W., Yu, J., Maness, P. C., & Meldrum, D. R. (2018). Unlocking the photobiological conversion of CO<sub>2</sub> to (R)-3-hydroxybutyrate in cyanobacteria. *Green Chemistry*, *20*(16), 3772–3782. <https://doi.org/10.1039/c8gc01208c>
- Wang, F., & Lee, S. Y. (1997). Poly(3-hydroxybutyrate) production with high productivity and high polymer content by a fed-batch culture of *Alcaligenes latus* under nitrogen limitation. *Applied and Environmental Microbiology*, *63*(9), 3703–3706. <https://doi.org/10.1128/aem.63.9.3703-3706.1997>
- Wang, L., Armbruster, W., & Jendrossek, D. (2007). Production of medium-chain-length hydroxyalkanoic acids from *Pseudomonas putida* in pH stat. *Applied Microbiology and Biotechnology*, *75*(5), 1047–1053. <https://doi.org/10.1007/s00253-007-0920-1>
- Wang, S. Y., Wang, Z., Liu, M. M., Xu, Y., Zhang, X. J., & Chen, G. Q. (2010). Properties of a new gasoline oxygenate blend component: 3-Hydroxybutyrate methyl ester produced from bacterial poly-3-hydroxybutyrate. *Biomass and Bioenergy*, *34*(8), 1216–1222. <https://doi.org/10.1016/j.biombioe.2010.03.020>
- Wang, Y. W., Wu, Q., Chen, J., & Chen, G. Q. (2005). Evaluation of three-dimensional scaffolds made of blends of hydroxyapatite and poly(3-hydroxybutyrate-co-3-hydroxyhexanoate) for bone reconstruction. *Biomaterials*, *26*(8), 899–904. <https://doi.org/10.1016/j.biomaterials.2004.03.035>
- Wendlandt, K. D., Jechorek, M., Helm, J., & Stottmeister, U. (2001). Producing poly-3-hydroxybutyrate with a high molecular mass from methane. *Journal of Biotechnology*, *86*(2), 127–133. [https://doi.org/10.1016/S0168-1656\(00\)00408-9](https://doi.org/10.1016/S0168-1656(00)00408-9)

- Windhorst, C., & Gescher, J. (2019). Efficient biochemical production of acetoin from carbon dioxide using *Cupriavidus necator* H16. *Biotechnology for Biofuels*, *12*(1), 1–11. <https://doi.org/10.1186/s13068-019-1512-x>
- Witholt, B., & Kessler, B. (1999). Perspectives of medium chain length poly(hydroxyalkanoates), a versatile set of bacterial bioplastics. *Current Opinion in Biotechnology*, *10*(3), 279–285. [https://doi.org/10.1016/S0958-1669\(99\)80049-4](https://doi.org/10.1016/S0958-1669(99)80049-4)
- Yamanashi, T., Iwata, M., Kamiya, N., Tsunetomi, K., Kajitani, N., Wada, N., Iitsuka, T., Yamauchi, T., Miura, A., Pu, S., Shirayama, Y., Watanabe, K., Duman, R. S., & Kaneko, K. (2017). Beta-hydroxybutyrate, an endogenous NLRP3 inflammasome inhibitor, attenuates stress-induced behavioral and inflammatory responses. *Scientific Reports*, *7*(1), 7677. <https://doi.org/10.1038/s41598-017-08055-1>
- Yamane, T., Fukunaga, M., & Lee, Y. W. (1996). Increased PHB productivity by high-cell-density fed-batch culture of *Alcaligenes latus*, a growth-associated PHB producer. *Biotechnology and Bioengineering*, *50*(2), 197–202. [https://doi.org/10.1002/\(sici\)1097-0290\(19960420\)50:2<197::aid-bit8>3.3.co;2-6](https://doi.org/10.1002/(sici)1097-0290(19960420)50:2<197::aid-bit8>3.3.co;2-6)
- Yishai, O., Lindner, S. N., Gonzalez de la Cruz, J., Tenenboim, H., & Bar-Even, A. (2016). The formate bio-economy. *Current Opinion in Chemical Biology*, *35*, 1–9. <https://doi.org/10.1016/j.cbpa.2016.07.005>
- Yokaryo, Hiroto; Teruya, Morimi ; Hanashiro, Ryuji ; Goda, Masahiro; Tokiwa, Y. (2017). Direct Production of (R)-3-Hydroxybutyric Acid of High Optical Purity by *Halomonas* sp. OITC1261 Under Aerobic conditions. *Biotechnology Journal*, *13*(2), 1–23. <https://doi.org/10.1002/biot.201700343>
- Yun, E. J., Kwak, S., Kim, S. R., Park, Y. C., Jin, Y. S., & Kim, K. H. (2015). Production of (S)-3-hydroxybutyrate by metabolically engineered *Saccharomyces cerevisiae*. *Journal of Biotechnology*, *209*, 23–30. <https://doi.org/10.1016/j.jbiotec.2015.05.017>

Zhang, X., Luo, R., Wang, Z., Deng, Y., and Chen, G.-Q. (2009). Application of (R)-3-Hydroxyalkanoate Methyl Esters Derived from Microbial Polyhydroxyalkanoates as Novel Biofuels. *Biomacromolecules*, 10, 707–711. <https://doi.org/10.1021/bm801424e>

Zhang, J., Cao, Q., Li, S., Lu, X., Zhao, Y., Guan, J. S., Chen, J. C., Wu, Q., & Chen, G. Q. (2013). 3-Hydroxybutyrate methyl ester as a potential drug against Alzheimer's disease via mitochondria protection mechanism. *Biomaterials*, 34(30), 7552–7562. <https://doi.org/10.1016/j.biomaterials.2013.06.043>

Zheng, Zhong; Gong, Qiang; Chen, G. (2004). A Novel Method for Production of 3-Hydroxydecanoic Acid by Recombinant *Escherichia coli* and *Pseudomonas putida*. *Chinese Journal of Chemical Engineering*, 12(4), 550–555.

## APPENDICES

### APPENDIX I. RAW DATA AND CALIBRATION CURVES

Table I-1. Acids concentration in nutrient limitation chemostats in *A. lata* by HPLC

<b>Nutrient limited</b>	<b>D</b> [h <sup>-1</sup> ]	<b>Citric</b> [mM in broth]	<b>Malic</b> [mM in broth]	<b>Succinic</b> [mM in broth]	<b>Pyruvic</b> [mM in broth]	<b>R3HBA</b> [mM in broth]
O <sub>2</sub>	0.05	0.18	0.32	0.57	0.01	0.01
	0.05	0.15	0.28	1.83	0.02	0.88
	0.10	0.38	1.61	4.75	0.01	0.01
	0.20	0.73	0.98	7.86	0.01	0.01
Gluc	0.05	0.08	0.58	1.24	0.00	0.33
	0.05	0.03	0.25	0.60	0.03	0.00
	0.10	0.03	0.24	0.53	0.01	0.01
	0.20	0.00	0.00	0.00	0.01	0.00
	0.40	0.00	0.00	0.00	0.22	0.01
N	0.05	0.10	0.00	0.17	0.00	0.22
	0.10	0.34	1.56	10.65	0.01	0.01
	0.20	0.51	2.02	3.43	0.00	0.01
	0.20	0.00	1.14	5.26	0.01	0.22

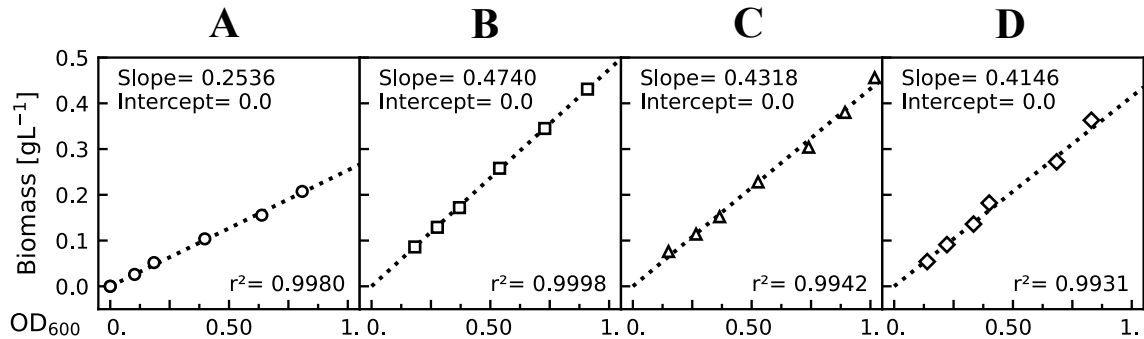


Figure I-1. **Calibration curves of absorbance and *C. necator* derived mutants concentration.** Correlation of the specific absorbance (600 nm) and cell concentration in RE1 medium at different dilution factors. (A) *C. necator* H16; (B) *C. necator* 541; (C) *C. necator*  $\Delta$ *phaC* and (D) *C. necator*  $\Delta$ *phaC*  $\Delta$ *hbd*.

APPENDIX II. PRIMERS AND GENES FOR THE CONSTRUCTION OF *tesB* EXPRESSION VECTOR

Table II-1. Primers used for the expression of *tesB* in *M. parvus* and *C. necator* H16

Primers	Sequence 5' - 3'	Plasmid
tesb_parvus_F	GAAACAGCTataaacgacgattggcgtatTTTTgatg	pAWP89_tesb
tesb_parvus_F	CCCGACAACtAttatcttgtgcaatgccatggttattg	pAWP89_tesb
vector_p89_F	cacaagataaTAGTTGTCGGGAAGATGCGTGATCTGA	pAWP89_tesb
vector_p89_R	cgtcgtttatAGCTGTTTCCTGTGTGAATACCTCC	pAWP89_tesb
tesb_pbbr1_FOR	ACAAAAGCTGATGAGTCAGAAAGGAGGACAACCATGAGTCAGGCGCTAAAAAATTTACTGAC	pBBR1MCS2_tesb
tesb_pbbr1_REV	TCTAGACCTTCCTTCCTTAATTGTGATTACGCATCACC	pBBR1MCS2_tesb
T1T2_FOR	ATTAAGGAAGGAAGGTCTAGAGTCGACCTGCAG	pBBR1MCS2_tesb
T1T2_REV	GCGAATTGCGCAAAAAAAAAAAGGCCATCCGTCAGGATGG	pBBR1MCS2_tesb
vector.for	CTGACTCATCAGCTTTTGTCCCTTTAGTGAGGG	pBBR1MCS2_tesb
vector.rev	TTTTTGCGCAATTCGCCCTATAGTGAGTCGTAT	pBBR1MCS2_tesb

II-1. Sequences synthesized ordered for the expression of *tesB* in *M. parvus* or *C. necator* H16

*tesB* gene from *E. coli* K12 (without codon optimization)

5'–ATGAGTCAGGCGCTAAAAAATTTACTGACATTGTAAATCTGGAAAAAATTGAGGAAGGACTCTTTCGCGGCCAGAGTGAAGATTTAGGTTTACGCCAGGTGTTGGCGGCCAGGTCGTGGGTCAGGCCTTGTATGCTGCAAAAGAGACCGTCCCTGAAGAGCGGCTGGTACATTCGTTTCACAGCTACTTTCTTCGCCCTGGCGATAGTAAGAAGCCGATTATTTATGATGTCGAAACGCTGCGTGACGGTAACAGCTTCAGCGCCCGCCGGGTTGCTGCTATTCAAACGGCAAACCGATTTTTTATATGACTGCC

TCTTTCCAGGCACCAGAAGCGGGTTTCGAACATCAAAAAACAATGCCGTCCGC  
GCCAGCGCCTGATGGCCTCCCTTCGGAAACGCAAATCGCCCAATCGCTGGCGC  
ACCTGCTGCCGCCAGTGCTGAAAGATAAATTCATCTGCGATCGTCCGCTGGAA  
GTCCGTCCGGTGGAGTTTCATAACCCACTGAAAGGTCACGTCGCAGAACCACA  
TCGTCAGGTGTGGATCCGCGCAAATGGTAGCGTGCCGGATGACCTGCGCGTTC  
ATCAGTATCTGCTCGGTTACGCTTCTGATCTTAACTTCCTGCCGGTAGCTCTACA  
GCCGCACGGCATCGGTTTTCTCGAACCGGGGATTCAGATTGCCACCATTGACCA  
TTCCATGTGGTTCCATCGCCCGTTTAATTTGAATGAATGGCTGCTGTATAGCGT  
GGAGAGCACCTCGGCGTCCAGCGCACGTGGCTTTGTGCGCGGTGAGTTTTATAC  
CCAAGACGGCGTACTGGTTGCCTCGACCGTTCAGGAAGGGGTGATGCGTAATC  
ACAATTAA-3'

Promoter gene extracted from GenBank accession number AJTV00000000

5'-ATAAACGACGATTGGCGTATTTTTTGATGGTTGTCGGTTTCTTCTCGGTCCGC  
ATACGCCTGACAGTGCTCCCCTCGCCGCTCGGGCAGCCTAAAAAAGGTCAAG  
CCCAGCCGATTGACGATAGACGCATTTTGGCGCCTGCGGCAATATTTTCTTGG  
CGAAGCCTTTCGCTCCCCCAATTCCGTGCAAACGGGCCGCGGCTTGACGA  
ACGCAAGCGCGAAATGCTCAACCACATCCGCCCCGGCCGGGCGCTGAGGGCCT  
CGAGAGCTCGACCATCTTTAAAAGGGAGACAGAT-3'

Terminator gene extracted from GenBank accession number AJTV00000000

5'-GGAAGGCGCGGGCATCGCTTTTTCTATAAATCATCCGGCCATTTTTGAGCAA  
TAAA-3'

### APPENDIX III. PUBLICATIONS



# Beyond Intracellular Accumulation of Polyhydroxyalkanoates: Chiral Hydroxyalkanoic Acids and Polymer Secretion

Luz Yañez<sup>1</sup>, Raúl Conejeros<sup>2</sup>, Alberto Vergara-Fernández<sup>1</sup> and Felipe Scott<sup>1\*</sup>

<sup>1</sup> Green Technology Research Group, Facultad de Ingeniería y Ciencias Aplicadas, Universidad de los Andes, Santiago, Chile,

<sup>2</sup> Escuela de Ingeniería Bioquímica, Pontificia Universidad Católica de Valparaíso, Valparaíso, Chile

## OPEN ACCESS

### Edited by:

Ignacio Poblete-Castro,  
Andres Bello University, Chile

### Reviewed by:

Prasun Kumar,  
Chungbuk National University,  
South Korea  
Jose Manuel Borrero De Acuña,  
Technische Universität  
Braunschweig, Germany

### \*Correspondence:

Felipe Scott  
fscott@miuandes.cl

### Specialty section:

This article was submitted to  
Industrial Biotechnology,  
a section of the journal  
Frontiers in Bioengineering and  
Biotechnology

**Received:** 06 December 2019

**Accepted:** 10 March 2020

**Published:** 03 April 2020

### Citation:

Yañez L, Conejeros R,  
Vergara-Fernández A and Scott F  
(2020) Beyond Intracellular  
Accumulation of  
Polyhydroxyalkanoates: Chiral  
Hydroxyalkanoic Acids and Polymer  
Secretion.  
*Front. Bioeng. Biotechnol.* 8:248.  
doi: 10.3389/fbioe.2020.00248

Polyhydroxyalkanoates (PHAs) are ubiquitous prokaryotic storage compounds of carbon and energy, acting as sinks for reducing power during periods of surplus of carbon source relative to other nutrients. With close to 150 different hydroxyalkanoate monomers identified, the structure and properties of these polyesters can be adjusted to serve applications ranging from food packaging to biomedical uses. Despite its versatility and the intensive research in the area over the last three decades, the market share of PHAs is still low. While considerable rich literature has accumulated concerning biochemical, physiological, and genetic aspects of PHAs intracellular accumulation, the costs of substrates and processing costs, including the extraction of the polymer accumulated in intracellular granules, still hampers a more widespread use of this family of polymers. This review presents a comprehensive survey and critical analysis of the process engineering and metabolic engineering strategies reported in literature aimed at the production of chiral (*R*)-hydroxycarboxylic acids (RHAs), either from the accumulated polymer or by bypassing the accumulation of PHAs using metabolically engineered bacteria, and the strategies developed to recover the accumulated polymer without using conventional downstream separations processes. Each of these topics, that have received less attention compared to PHAs accumulation, could potentially improve the economy of PHAs production and use. (*R*)-hydroxycarboxylic acids can be used as chiral precursors, thanks to its easily modifiable functional groups, and can be either produced *de-novo* or be obtained from recycled PHA products. On the other hand, efficient mechanisms of PHAs release from bacterial cells, including controlled cell lysis and PHA excretion, could reduce downstream costs and simplify the polymer recovery process.

**Keywords:** 3-hydroxyalkanoic acids, polyhydroxyalkanoates, chiral compounds, biosynthesis, metabolic engineering

## INTRODUCTION

Synthetic plastics produced from petroleum-derived monomers, such as ethylene, propylene, styrene, and polyethylene terephthalate, are non-biodegradable polymers that undergo slow fragmentation to micron-size particles (Kubowicz and Booth, 2017). Nearly 60% of all plastics produced between 1950 and 2015, equivalent to 4,900 metric tons, can be found in landfills or

in the natural environment. Another 800 metric tons were incinerated and 600 MT recycled. Only 10% of the recycled plastics have been recycled more than once (Geyer et al., 2017).

The environmental burden imposed by the production of petroleum-derived polymers can be ascribed to its persistence in the environment and its impact on climate change. On the former, evidence suggests a complex toxicology of microplastics on marine life and in the food chain (Worm et al., 2017). Regarding the latter, each stage in the current plastic lifecycle generates greenhouse gases (GHGs): fossil fuel extraction and transport, monomer production, plastic refining and manufacturing, and plastic waste management. Estimations indicate that if plastic production grows at the current rate, by 2050 the cumulative emissions from plastic use could account for over 56 gigatons of carbon. This is equivalent to 10–13% of the remaining carbon budget (Hamilton et al., 2019).

The search for biodegradable polymers with a reduced emission of GHGs has led to the development of microbial-based processes using natural or genetically engineered microorganisms capable of producing polymers (e.g., polylactic acid and polyhydroxyalkanoates) or monomers (lactic acid, succinic acid, caproic acid, and hydroxyalkanoic acids) with the potential of replacing the current petroleum-based methods (Tsuge et al., 2016).

Renewable bio-based and biodegradable polymers are expected to play a key role in curbing the impacts of plastic production and use in the near future (Zheng and Suh, 2019). One of the most studied biopolymers is poly(*R*-3-hydroxybutyrate), PHB, an intracellular polyester accumulated in many bacteria. PHB is a member of a large family of renewable and biodegradable bio-polyesters collectively known as polyhydroxyalkanoates (PHAs). They are built by (*R*)-3-hydroxy fatty acid monomers varying from 3 to 5 carbon atoms (short-chain-length PHAs, scl-PHA) and from 6 to 14 carbons (medium-chain-length PHAs, mcl-PHA). Although as many as 150 different congeners of PHA are known with different monomers (Steinbüchel and Valentin, 1995), PHB is the most extensively studied and excellent reviews have been published regarding strategies to improve its production (Peña et al., 2014) and its process technology (Alves et al., 2017).

PHB has been studied for decades as a source of a renewable polymer for the substitution of fossil-derived plastics (Chen and Patel, 2012). However, its use as a substitute for thermoplastics has been hampered by high production costs, dominated by the cost of substrates for the fermentation stage and the costs of downstream extraction and purification. The costs of supplying the required carbon and energy source for microbial growth and PHB production are estimated to be between 30 and 50% of the product cost if sugars are used (Choi and Lee, 1999; Levett et al., 2016). On the other hand, the downstream processes rely on hypochlorite (Heinrich et al., 2012) and solvents (Jiang et al., 2018) for the extraction and precipitation of the polymers. Solvent recovery further adds to processing costs and energy use.

Finally, the large variety of monomers that can be incorporated into PHAs makes PHB only one member of a large family of polymers with different physical properties. Costs are further increased by the precursors required for the production of customized thermoplastics, such as

poly(3-hydroxybutyrate-*co*-3-hydroxyvalerate) were valerate is used to change the polymer composition (Choi and Lee, 1999).

This review focuses on a simple but powerful concept, multiple carbon substrates can be funneled to poly(hydroxyalkanoates) and its enantiomerically pure monomers, 3-hydroxyalkanoic acids (3HAs). These monomers are a family of related compounds having at least two functional groups (a hydroxy group and a carboxyl group) that are amenable for chemical modification, they can play a role as building blocks for the synthesis of a large number of products, including diols, polyesters, and fine chemicals. These monomers can be produced either by *in-vivo* depolymerization of the accumulated PHAs, by fermentation for the direct production of 3HAs into the culture media and by conversion of purified PHAs. The advantage of the first two alternatives is that production does not require the extraction of the intracellular PHAs.

Here, we first introduce the potential uses of polyhydroxyalkanoates and its monomers (section Potential Uses of Polyhydroxyalkanoates and Its Monomers) followed by the substrates used for its production (section Substrates for the Production of Polyhydroxyalkanoates and Its Monomers). Section Accumulation and Mobilization of PHAs deals with the pathways and mechanisms of PHAs accumulation and mobilization in bacteria, with an emphasis on PHB. In section Production of *R*-3-Hydroxyalkanoic Acids From PHAs and Alternative Substrates and Microorganisms for 3HA Production, different strategies for the production of 3HAs are discussed, including *in-vivo* hydrolysis of PHAs and genetic modifications aimed at the direct production of these acids without a polymer accumulation step. Finally, section Secretion of PHAs discusses the research on alternative methods for PHAs liberation and recovery from bacteria to supply substrates for 3-hydroxy acids production.

## POTENTIAL USES OF POLYHYDROXYALKANOATES AND ITS MONOMERS

Polyhydroxyalkanoates (PHAs) have been extensively investigated to identify possible applications. Homopolymers, random copolymers, and block copolymers can be produced depending on the structure of the polymer chain, this is dictated by the species of bacteria and the substrate used for the accumulation of PHA (Braunegg et al., 2004). The diversity of applications is wide, including production of biodegradable plastics that are environmentally friendly for use in packaging (Koller, 2014; Khosravi-Darani, 2015), fibers (Dietrich et al., 2016), biodegradable and biocompatible implants (Misra et al., 2006), drugs and fine chemical (Rathbone et al., 2010), and biofuels (Zhang et al., 2009).

PHAs have been traditionally used in the packaging of a series of products as shampoo bottles, shopping bags, containers and paper coatings, utensils, carpets, compostable bags, and thermoformed articles (Bugnicourt et al., 2014).

As biomedical materials, PHAs have been used in suture materials and repair patches, meniscus restoration devices, cardiovascular patches, orthopedic pins, and cartilage

regeneration aids, among others (Volova et al., 2003; Wang et al., 2005). Many of these uses are related to the customizable composition and properties of PHAs, which allow them to have favorable mechanical properties, biocompatibility, and to degrade in reasonable times under specific physiological conditions (Misra et al., 2006; Hazer et al., 2012). In particular, mcl-PHAs have potential applications in coatings and in medical temporary implants such as scaffolds for the regeneration of arteries and nerve axons (Witholt and Kessler, 1999). On the other hand, the use of these polymers has been studied in controlled drug delivery (Shah et al., 2010). The kinetics of drug release can be engineered by altering the degradation rate of the PHA matrix coating. In this regard, mcl-PHA have been used as drug carriers since its low fusion point and low crystallinity makes them suitable for controlled drug release (Ueda and Tabata, 2003).

Finally, PHA derived compounds can be used as biofuels after the esterification of PHB and mcl-PHAs with methanol for its conversion to hydroxyalkanoate methyl esters (Zhang et al., 2009). These hydroxyalkanoate methyl esters can be mixed with gasoline and diesel in ratios of 10 to 30%. In particular, (*R*)-3-hydroxy-methyl-butyrate was reported to have similar or improved properties as a fuel additive (oxygen content, dynamic viscosity, flash point, and boiling point) compared to ethanol (Wang et al., 2010). Using PHA derivatives as biofuels can be viewed as a promising application since mixtures of PHA can be used without a costly separation step (Gao et al., 2011).

The most well-known (*R*)-3-hydroxyalkanoic acid, (*R*)-3-hydroxybutyric acid (R3HBA) can be used as a building block in the synthesis of fine chemicals and pharmaceuticals such as antibiotics (Ren et al., 2005), bulk chemicals for the polymer industry (such as hydrogenation to 1,3 butanediol), fragrances and insecticides (Matsuyama et al., 2001) (see **Figure 1**). 1,3 butanediol can be dehydrated to yield unsaturated alcohols which can be further dehydrated to form 1,3 butadiene (Nozawa et al., 2009), a building block for the production of styrene-butadiene rubber. The world consumption of butadiene reached 10 million metric tons in 2012 (Biddy et al., 2016). R3HBA can be esterified with butanol or ethanol or converted to ethers by reaction with alcohols using the catalytic Williamson ether synthesis (Fuhrmann and Talbiersky, 2005) or dehydrated to crotonic acid, which upon hydrogenation yields butyric acid and *n*-butanol (Schweitzer et al., 2015).

Similarly, 3-hydroxypropionic acid (3HPA), a non-chiral compound, can yield upon chemical modification access to acrylic acid, acrylamide and acrylonitrile, all with market sizes larger than 1 billion dollars, and other niche market compounds such as 1,3 propanediol, methyl acrylate, and malonic acid (Jers et al., 2019).

More than three decades ago Seebach et al. (1986), reported the synthesis of the macrolide antibiotics pyrenophorin, colletodiol, garamycin A1, and elaiophylidene starting from (*R*)-3-hydroxybutyrate and malate. R3HBA and its derivatives have also been used as potential drugs. Cao et al. (2014) showed that R3HBA and its derivative 3-hydroxybutyrate methyl ester inhibit the development of osteoporosis in mice kept under simulated microgravity. Using *in-vivo* studies with mice suffering

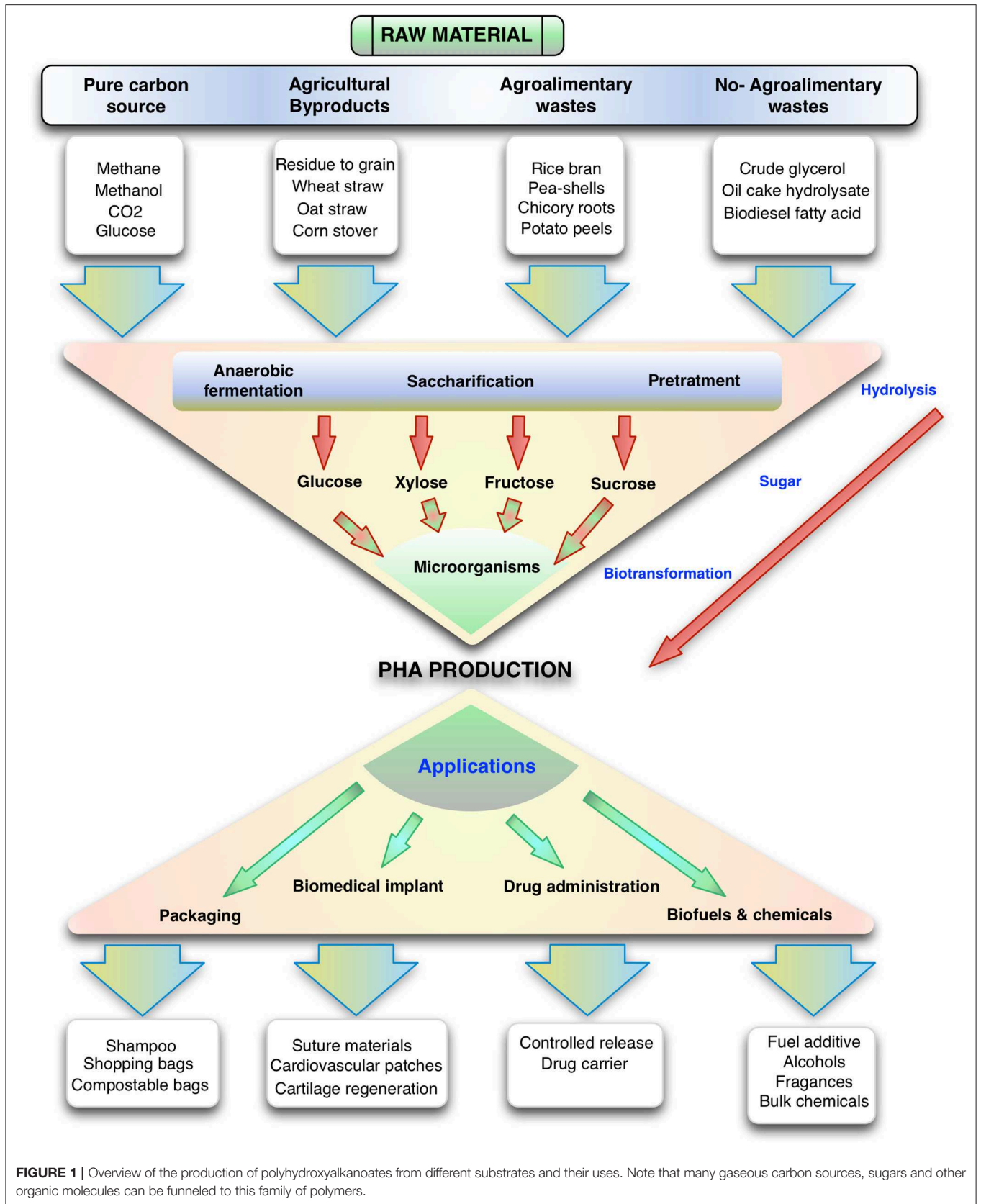
from Alzheimer's disease, Zhang et al. (2013) showed that intragastric administration of 3-hydroxybutyrate methyl ester reduced amyloid- $\beta$  deposition in mouse brains and improved the performance of the treatment group in the Morris water maze (a standardized test in the study of spatial learning and memory) compared to the control group. In a related study in mice, Tieu et al. (2003) showed that the infusion of R3HBA led to improved mitochondrial respiration and ATP production in mice treated with the neurotoxin 1-methyl-4-phenyl-1,2,3,6-tetrahydropyridine causing a mitochondrial deficit reminiscent of Parkinson disease. Finally, Yamanashi et al. (2017) showed that R3HBA could act as a therapeutic candidate for the treatment of stress-related mood disorders (depression). The mechanism involves an anti-inflammatory effect mediated by a reduction in the levels of the inflammatory cytokines inter-leukin 1 $\beta$  and tumor necrosis factor  $\alpha$  in the hippocampus of mice.

Other potential uses of R3HBA include its use as a chemical chaperone for heat-mediated denaturation and oxidative damage by  $\text{Cu}^{2+}$  and  $\text{H}_2\text{O}_2$  produced on industrially relevant enzymes such as lipases and lysozymes (Obruca et al., 2016).

Finally, (*R*)-3-hydroxyalkanoic acids can be used as building blocks that can be biologically produced, excreted from cells and then polymerized or co-polymerized to yield PHAs with the desirable mechanical and thermal properties (Wang et al., 2018). Advantages of the *ex-situ* polymerization starting from biomonomers over the conventional approach of biopolymer accumulation inside cells include (Adkins et al., 2012): (i) simplified downstream product recovery of the extracellular biomonomers compared to the intracellular polymers, (ii) polymerization in controlled chemocatalytic environments allows for polymers with finely tuned properties and high purities, and (iii) higher diversity of plastics thanks to the ability to co-polymerize different monomers. Examples of *in-vitro* synthesis include the production of PHB from R3HBA by a three-enzyme system that only consumes ATP and the monomer (Jossek and Steinbüchel, 1998). The yield of this system was recently improved by using a thermostable acetyl-CoA synthetase, CoA transferase, and PHA synthase (Tajima et al., 2016). A polymer incorporating lactate and R3HBA residues was produced by Tajima et al. (2012) by using an engineered PHA synthase capable of lactate polymerization. An excellent revision of the chemosynthesis of copolymers containing different 3HAs monomers and lactate was recently published (Hiroe et al., 2019). However, a general drawback of these systems so far is the consumption of ATP, specifically to drive the activation of acetate to acetyl-CoA, a molecule that needs to be present on the reaction mixture to act as the CoA donor to yield the hydroxyacyl-CoAs required for the polymerization reaction.

## SUBSTRATES FOR THE PRODUCTION OF POLYHYDROXYALKANOATES AND ITS MONOMERS

This section summarizes the carbon and energy substrates currently used for the production of PHA and the potential of moving to lignocellulosic substrates, agro-food wastes, and



abundant gaseous substrates such as syngas, knallgas, or methane. For a comprehensive review regarding the many substrates for PHA production, the reader is referred to Jiang et al. (2016). The production of 3-hydroxyalkanoic acids from these unconventional sources is presented in section Alternative Substrates and Microorganisms for 3HA Production.

Substrates commonly used for industrial production of PHAs are represented by corn starch, sucrose obtained from sugar cane and vegetable oils, all edible feedstock requiring arable lands and agricultural practices that affect both its economy and sustainability (Levett et al., 2016). Commercial PHAs are produced using sucrose in *Azohydromonas lata* (Biomer Germany, with trade name Biomer<sup>TM</sup>) and *Bacillus* sp. (PHB Industrial S.A. Brazil, Biocycle<sup>TM</sup>); glucose from corn in *C. necator* (Metabolix, Mirela<sup>TM</sup> and Tianan Biologic Material, Enmat<sup>TM</sup>); or fatty acids using *Pseudomonas putida* (ETH, PHA<sup>TM</sup>) or *C. necator* by Kaneka Corporation and marketed as Kaneka PHBH<sup>TM</sup> (Chen, 2009; Bugnicourt et al., 2014; Mozejko-Ciesielska and Kiewisz, 2016).

Due to the high costs and sustainability concerns associated with raw materials traditionally used in the production of PHA, the use of agro-food waste, food industry waste, and other non-food industry residues, have been increasingly studied (Braunegg et al., 2004). For example, several solid residues have been examined such as rice bran (Oh et al., 2015), pea-shells (Kumar et al., 2016), chicory roots (Haas, 2015), potato peels, apple pomace, onion peels (Kumar et al., 2016), grape pomace (Follonier, 2015), animal farm waste, poultry litter (Bhati and Mallick, 2016), and palm oil (Loo et al., 2005). In the case of food wastes for PHAs production, literature report on the use of spent coffee grounds (Cruz et al., 2014), food waste composite (Amulya et al., 2015), and used cooking oil (Gómez Cardozo et al., 2016; Borrero-de Acuña et al., 2019).

Finally, non agro-alimentary residues are generated by biodiesel manufacturing: crude glycerol (de Paula et al., 2017), oil cake hydrolysate (Bera et al., 2015), and biodiesel fatty acid by-product from glycerol purification (Cruz et al., 2016). Glycerol can be used for the accumulation of mcl-PHAs and scl-PHAs in *Pseudomonas putida* strains (Poblete-Castro et al., 2014), *C. necator* (Mothes et al., 2007), and *Bacillus megaterium* (Naranjo et al., 2013), among others.

The availability and sustainability issues of conventional substrates have motivated the exploration of alternative feedstock as sources of carbon and energy for microbial production of chemicals, such as lignocellulose which can be obtained from the “residues” left after the harvest of agricultural products or from dedicated high yield cultivars (poplar, eucalyptus, miscanthus) (Loow et al., 2016), thus reducing the environmental burden associated with its production. Reducing even further the water and land usage, compounds containing one carbon atom, such as methanol and formate can be obtained from the reduction of CO<sub>2</sub> using electrons harnessed from solar energy (Agarwal et al., 2011; Pérez-Fortes et al., 2016; Yishai et al., 2016).

Regarding the use of monomeric sugars obtained from lignocellulose, these are always accompanied by non-sugar compounds like acetic acid, furfural, and other organic acids and aromatic compounds that are produced during pretreatment

(Hodge et al., 2008). Biomass is pretreated to improve the action of carbohydrate hydrolases that break down cellulose and hemicellulose during saccharification. In dilute sulfuric acid hydrolysis of corn stover, a leading pretreatment technology, lignocellulosic biomass is deconstructed into pretreated corn stover: a solid fraction (or pulp), enriched in cellulose and lignin, and a liquid fraction (pretreatment liquor), containing oligomers and monomers of hemicellulose and acetic acid (Chen et al., 2012). To further break down cellulose and hemicellulose remaining in the pulp into fermentable sugars, an enzymatic hydrolysis step is necessary.

Regarding PHB production from sugars and acids present in lignocellulosic hydrolysates, albeit *A. lata* or *C. necator* are unable to use xylose, they are tolerant to acetic acid, furfural, and hydroxy-methyl-furfural (among other compounds found in lignocellulosic hydrolysates) (Dietrich et al., 2013). On the other hand, *Burkholderia sacchari* (Brämer et al., 2001) and *Burkholderia cepacia* can use xylose for growth and PHB production. In a fed-batch culture experiment using glucose and xylose to promote PHB accumulation in *B. cepacia*, 60 g L<sup>-1</sup> of biomass were attained in 70 h with 58% PHB content. The yield of PHB was 0.46 g PHB per gram of substrate (Silva et al., 2004). *B. cepacia* was able to incorporate vanillin to PHB (Pan et al., 2012; Dietrich et al., 2013), while levulinic acid was incorporated as hydroxyvalerate (Keenan et al., 2006). Both vanillin and levulinic acid are compounds present in lignocellulosic hydrolysates. Moreover, the minimum inhibitory concentrations of acetic acid, hydroxy-methyl-furfural and furfural reported for *B. cepacia* growth are 4.00, 6.00, and 6.00 g L<sup>-1</sup> respectively (Dietrich et al., 2013). Raposo et al. (2017) recently showed that in fed-batch cultures of *B. sacchari* DSM 17165, the catabolite repression of glucose on xylose consumption can be avoided by maintaining glucose concentration below 10 g L<sup>-1</sup>. Notably, they showed that when xylose concentration increases in the fermenter, xylitol appears as a second product (xylose concentration above 30–40 g L<sup>-1</sup>).

Among inexpensive substrates that are readily available for reducing the total cost of PHA production, certain C1 carbon sources, e.g., methane, methanol, and CO<sub>2</sub> have received a great deal of attention due to their contribution to global warming (Khosravi-Darani et al., 2013). Production of PHB from waste methane may help reduce the impact on the greenhouse effect of this gas. Accumulation of PHB, but not other PHAs, has been studied in several *Methylocystis* species using methane and *Methylobacterium* from methanol [cf. Strong et al. (2016)]. In this regard, Listewnik et al. (2007) estimated a price of 6.35 UK pound/kg for produced PHB from natural gas in a two-stage plant producing 500 t PHB per year. Similarly, Levett et al. (2016) estimated a production cost range of 4.1 to 6.8 USD per kg of PHB, with a reduction in the share of the carbon source in the total product cost from 30% when sugar feedstocks are used to 22% for methane. However, these production costs are high when compared to the estimations made by Posada et al. (2011), who performed a techno-economic evaluation of PHB production from glycerol as energy and carbon source. They reported production costs between 1.9 and 2.5 USD per kg and a substrate share between 5 and 8%. The higher production cost

when methane is used as substrate is greatly influenced by the slow mass transfer of methane into the media. This leads to large reactors and, thereby high investment costs.

Knallgas bacteria, such as *C. necator* and *A. lata* can use mixtures of hydrogen, carbon dioxide and oxygen for the accumulation of PHB (Reinecke and Steinbüchel, 2008), biofuels (Brigham, 2019), or acetoin (Windhorst and Gescher, 2019). Albeit the production of PHB has been studied thoroughly, with cultures of *C. necator* or *Ideonella* sp. O-1 accumulating over 60 g L<sup>-1</sup> of PHB (Tanaka et al., 1995, 2011), no reports of PHAs accumulation aside PHB are available (for a review on PHB production from C1 sources see Khosravi-Darani et al., 2013).

## ACCUMULATION AND MOBILIZATION OF PHAs

The model organism for PHB production is *Cupriavidus necator* (formerly *Ralstonia eutropha* and *Alcaligenes eutrophus*), a gram-negative, obligate aerobe, capable of autotrophic growth in the presence of hydrogen, CO<sub>2</sub> and oxygen, and heterotrophic growth and PHB production from a wide variety of carbon sources including sugars (chiefly fructose in the wild type organism *C. necator* H16 ATCC 17699) and organic acids (Lu et al., 2016). For example, using glucose in a fed-batch culture of *C. necator* NCIMB 11599, a mutant of *C. necator* H16 capable of using glucose, a concentration of biomass of 164 g L<sup>-1</sup> was obtained, with a PHB content of 74% (Kim et al., 1994).

In *C. necator*, synthesis of PHB occurs when excess carbon in the form of acetyl-CoA is condensed via a  $\beta$ -ketothiolase (EC 2.3.1.16) to generate acetoacetyl-CoA, which is then reduced to (R)-3-hydroxybutyryl-Coenzyme A by a NADPH-dependent acetoacetyl-CoA reductase (EC 1.1.1.36). Finally, the enzyme PHB synthase (EC 3.1.1.75) catalyzes the polymerization of (R)-3-hydroxybutyryl-CoA monomers. This pathway is the most widespread route in bacteria for providing 3-hydroxybutyryl-CoA monomers (Steinbüchel and Hein, 2001). Production of mcl-PHAs, such as the polymers accumulated in *Pseudomonas* spp., requires precursors derived from the dissociated fatty acid biosynthesis pathway unless these precursors are supplied through related carbon sources (such as octanoic acid for the synthesis of poly(3-hydroxyoctanoate). For details regarding this pathway, we point to the excellent reviews by Lu et al. (2009) and Suriyamongkol et al. (2007).

The regulation of PHB biosynthesis is tightly connected to the cellular levels of reduced nicotinamide nucleotides. Lee (1995) found that when *C. necator* was cultivated in nitrogen-limited media, the NADPH/NADP and NADH/NAD ratios and the intracellular concentrations of NADH and NADP were higher than those found under nitrogen sufficient conditions. Moreover, the rate of PHB accumulation was found to increase with both NADH/NAD and NADPH/NADP ratios. This effect was explained through the analysis of citrate synthase activity. Citrate synthase was inhibited by NADPH and NADH, thus funneling the carbon to PHB instead of being directed to the tricarboxylic acid cycle. Similar conclusions were reported by Henderson and Jones (1997).

Although PHB accumulation occurs under unfavorable conditions for growth induced by nutrient limitation of oxygen, nitrogen, or phosphorous, with excess carbon (Steinbüchel and Hein, 2001), these conditions impact the productivity of the PHB accumulation phase. Grousseau et al. (2013) showed that sustaining a controlled residual growth rate, by feeding a controlled amount of phosphate along with the carbon source (butyric acid), allows for an improved PHB specific productivity and high yield. Interestingly, using Metabolic Flux Balances they showed that the maximal specific PHB production rate is defined by the maximum specific rate of NADPH produced. When a low growth rate is allowed in the fed-batch fermentation (for example, feeding a nitrogen source), the NADPH is produced in the Entner-Doudoroff pathway; whereas without biomass production regeneration of NADPH is only possible via isocitrate dehydrogenase.

Another possibility to increase PHB volumetric productivities is to rely on microorganisms where growth and PHB production occur simultaneously. In this regard, *Azohydromonas lata* consumes glucose, sucrose and acetic acid (Chen et al., 1991), but it does not consume xylose, accumulating PHB during its growth (Yamane et al., 1996). In a fed-batch culture using sucrose as the carbon source and a continuous feeding of ammonia, controlled by the decrease in pH as the culture consumes the source of nitrogen (pH-stat), 143 g L<sup>-1</sup> of cells with 50% PHB were attained with a PHB productivity of 3.97 g L<sup>-1</sup> h<sup>-1</sup>, one of the highest ever reported (Yamane et al., 1996). One year later, Wang and Lee (1997) reported even higher productivity (4.94 g L<sup>-1</sup> h<sup>-1</sup>) and PHB intracellular content in *A. lata* (88%) applying nitrogen limitation in a two-stage fed-batch culture (nitrogen sufficient followed by nitrogen-limited culture).

Assuming that PHAs act as a reserve compound of carbon and energy, without a source of carbon and energy, but in the presence of other growth factors (such as nitrogen or oxygen), PHAs should be depolymerized to its monomers and incorporated into the metabolism, using the degradation products for growth and survival, a process termed PHA mobilization. This behavior has been shown at least in *C. necator* H16 (Uchino et al., 2007; Juengert et al., 2017), *A. lata* (Lee et al., 1999), *Legionella pneumophila* (James et al., 1999), *Hydrogenophaga pseudoflava* (Choi et al., 1999), and *Halomonas* sp. KM-1 (Kawata et al., 2015).

Compared to PHB accumulation, depolymerization of PHB to R3HBA, and its transformation to acetyl-CoA, has been less studied as confirmed by fewer reports in the literature. However, evidence exists pointing that the granules of PHB and other PHAs are supramolecular complexes (called carbonosomes), constituted by a polymer core and a surface layer of at least a dozen proteins (Sznajder et al., 2015), but without a phospholipids membrane (Bresan et al., 2016). The proteins in the carbonosomes include the PHA synthase (PhaC) and PHB depolymerases (PhaZs), which are thought to be constitutively expressed (Lawrence et al., 2005; Brigham et al., 2012).

It has been reported that PHB synthesis and its degradation can happen simultaneously in the model PHB accumulating organism *C. necator* (Doi, 1990; Taidi et al., 1995). Doi concluded this after cultivating *C. necator* in butyrate as

carbon source under nitrogen-free conditions, thus inducing the accumulation of PHB, and changing the carbon source to pentanoic acid. After the shift in the substrate, the accumulated PHB was gradually replaced by poly(3-hydroxyvalerate-co-3-hydroxybutyrate) without a net increase of total polymer content in the cells. This indicates that PHB was degraded and replaced by PHV even in the absence of a nitrogen source. Similarly, Taidi et al. (1995) showed a turnover of PHB after the accumulation of the polymer ceased in a nitrogen-limited batch culture with glucose as the sole carbon and energy source. The turnover was evidenced by the incorporation of radioactivity into the accumulated polymer after feeding labeled glucose (D-[U-<sup>14</sup>C] glucose). Interestingly, the high-molecular-weight polymer accumulated during the unlabeled glucose phase was replaced by a low-molecular-weight polymer during the labeled glucose experiment. These observations are in agreement with the evidence showing the constitutive expression of PHB synthase and PHB depolymerase in *C. necator* (Lawrence et al., 2005; Sznajder et al., 2015). Corroboration of constitutive expression of PHB synthase and depolymerase in other organisms is scarce, with the exception of the study of Kim et al. (1996) who found simultaneous activities of both enzymes during the batch culture of *Azohydromonas lata* under nitrogen-limited conditions.

Thereby, this leads to the intriguing question of how the synthesis and mobilization of PHAs are regulated, and particularly, how a cycle of simultaneous synthesis and degradation is avoided. Considering that the simultaneous polymerization and depolymerization of PHB and its conversion to acetyl-CoA through 3-hydroxybutyrate, acetoacetate, and acetoacetyl-CoA requires one NADPH molecule and one ATP molecule and produces only one NADH molecule, the cycle would consume energy for the formation of thioester bonds, thus creating a futile cycle.

To tackle this unsolved issue, Uchino et al. (2007) isolated native PHB granules produced in *C. necator* by glycerol gradient centrifugation to preserve the proteins bounded to the granule, and discovered that in the presence of CoA, these granules produced 3HB-CoA and small amounts of acetyl-CoA. If NAD<sup>+</sup>, but not NADH, is added to the initial reaction mixture, 3HB-CoA remains undetectable, but the concentration of acetyl-CoA increases 5-fold. The authors assumed that in the presence of NAD<sup>+</sup>, the intermediately formed 3HB-CoA is rapidly transformed to acetyl-CoA in NAD<sup>+</sup> dependent reactions. The authors also found, as expected, that the native granules release R3HBA in pH-stat experiments using methods previously described (Gebauer and Jendrossek, 2006). Therefore, it remains unclear which depolymerization mechanism, hydrolysis or thiolysis, is used *in-vivo* for the mobilization of PHB.

In order to identify the enzymes responsible for the thiolytic cleavage, Uchino et al. (2007) incorporated the PHB synthesis genes *phaCAB* in *E. coli* S17-1 along with the phasin gene *phaP1*, the depolymerase gene *phaZa1* or *phaP1* + *phaZa1*. Interestingly, the recombinant strain only produced 3HB-CoA in the presence of CoA when both *phaP1* and *phaZa1* were present in a *phaCAB* background. Moreover, no significant amounts of acetyl-CoA were detected in this experiment, an indication that downstream enzymes for the use of 3HB-CoA were absent in *E. coli*.

The study of Uchino et al. (2007), suggests that *in-vivo* intracellular depolymerization of PHB does not represent a futile cycle and an energy waste in the form of thioester bonds. If the main product of PHB polymerization, at least in *C. necator*, is 3HB-CoA instead of 3HB, then there is no loss of energy for the formation of acetoacetyl-CoA from acetoacetate (see **Figure 2**).

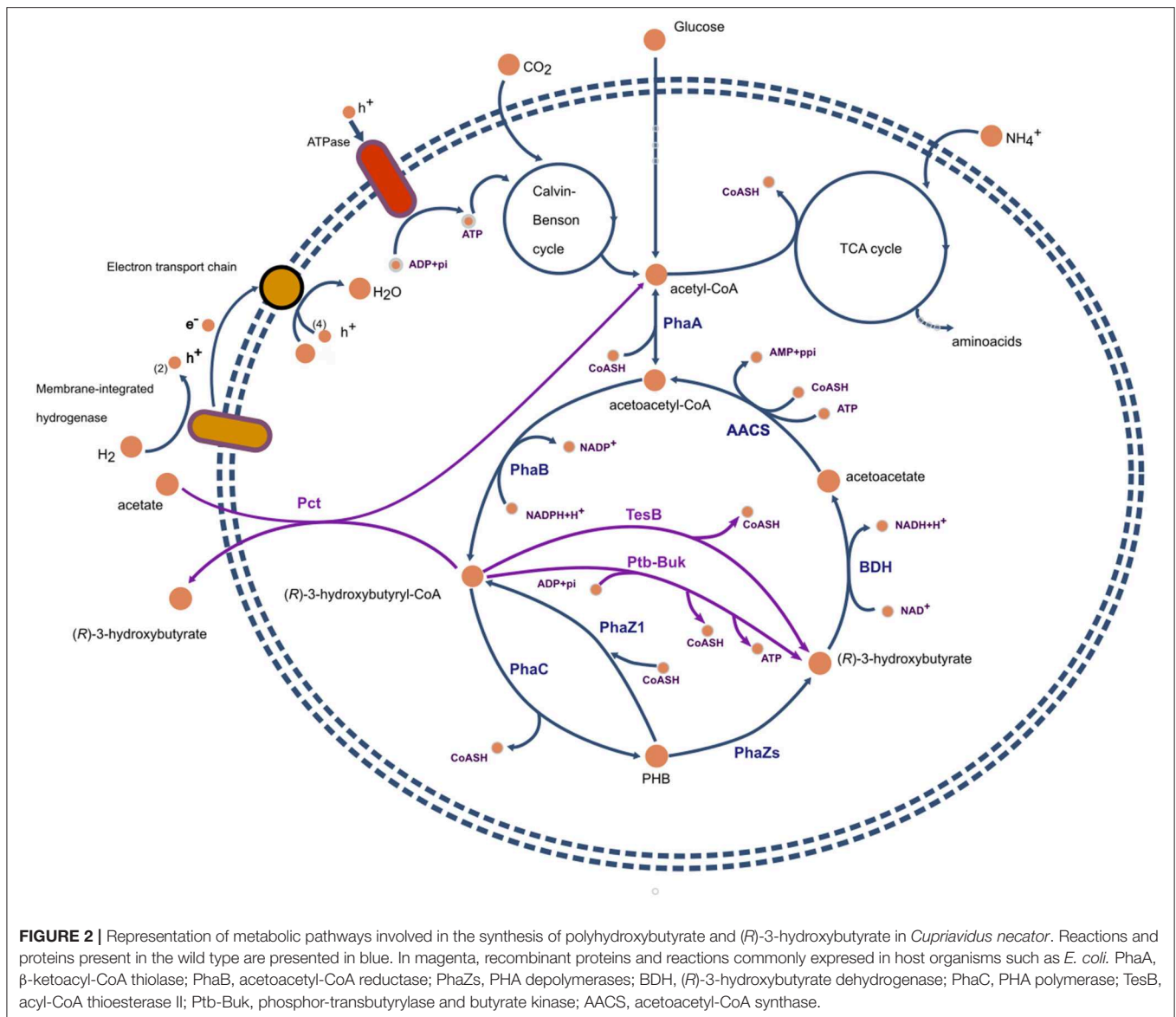
Regarding the regulation of PHB synthesis and degradation, Juengert et al. (2017), found that the degradation of the accumulated PHB in *Ralstonia eutropha* was fast and efficient in the absence of the alarmone (p)ppGpp, and that when present, (p)ppGpp directly or indirectly inhibits PHB mobilization. (p)ppGpp is a key signaling molecule, which, when present at high concentrations induces the stringent response in *E. coli* and other bacterial species. This alarmone accumulates in amino acids starved cells, and inhibit the synthesis of ribosomal and transfer RNAs (Srivatsan and Wang, 2008). The results suggest that PHB accumulation under nitrogen-limited conditions is favored by the inhibition of PhaZ1 by (p)ppGpp as shown by the observed PHB accumulation in a triple knockout mutant ( $\Delta spoT1 + \Delta spoT2 + \Delta phaZa1$ ) that was unable to produce (p)ppGpp. In contrast, the double knockout mutant  $\Delta spoT1 + \Delta spoT2$  accumulated negligible amounts of PHB. In a subsequent work, Juengert et al. (2018) identified that PhaC1 was phosphorylated in multiple phosphosites during the stationary growth phase in nutrient broth medium with gluconate as carbon source, but it was not modified during the exponential and PHB accumulation phases or when grown in a fructose-mineral medium. On the other hand, PhaZa1 was phosphorylated in Ser35 both during the exponential and stationary growth phases. Mutagenesis of the identified residues showed that PHB accumulation was unaffected for most mutants of PhaC1, except for a mutant with changes to four aminoacid residues. On the other hand, exchanging the phosphorylated residues in PhaZa1 to aspartate (a phosphomimetic residue) produced mutants with a strongly reduced ability to mobilize the accumulated PHB.

Little experimental evidence exists concerning the role of the stringent response in the accumulation of PHA in other organisms. In this regard, Mozejko-Ciesielska et al. (2017) obtained a *relA/spot* mutant of *P. putida* KT2440. This mutant, unable to induce the stringent response, was used to assess the accumulation of PHA under nitrogen deprived and optimal nitrogen conditions. Results show that this mutant is able to accumulate mcl-PHAs under both conditions.

Taken together, the works of Mozejko-Ciesielska et al. (2017) and Juengert et al. (2017; 2018) provide insights into the molecular basis of the regulation of PHB accumulation and mobilization. As it will be covered in section *in-vivo* Strategies these regulatory mechanisms play a key role in the production of R3HBA *in-vivo* from cells that accumulated PHB.

## PRODUCTION OF R-3-HYDROXYALKANOIC ACIDS FROM PHAs

Several strategies based on operational changes or genetic modifications have been devised for the production of chiral



hydroxyalkanoic acids. This section organizes such strategies in three categories, *ex-vivo* strategies, *in-vivo* strategies using non-genetically modified organisms and, finally, the construction of recombinant organisms. This material updates and complements the excellent review of Ren et al. (2010), that extensively covers the potential applications of hydroxyalkanoic acids and also focused on the chemical synthesis of these compounds and the review by Gao et al. (2011), dealing with a broader view, the synthesis of PHAs and its monomers.

### In-vitro Strategies

Under this approach, the accumulated PHAs are extracted from cells and then subjected to a chemical or enzymatic depolymerization process. The PHA recovery process starts when cells are separated by centrifugation to increase product concentration and to remove the components of the culture media. The concentration step is followed

by drying or lyophilization of the concentrated biomass. The extraction of PHAs from the dried biomass can be performed by solvent extraction, by dissolving the biomass using oxidizing agents or by disrupting cells to liberate the PHAs granules (Kosseva and Rusbandi, 2018). Mechanical cell disruption techniques, such as bead milling and high-pressure homogenization have been widely used to release intracellular protein, and have been adapted for PHAs recovery (Melih Tamer et al., 1998; Kunasundari and Sudesh, 2011). Melih Tamer et al. (1998) compared bead milling and high-pressure homogenization for the recovery of PHB accumulated in *Azohydromonas lata*. They recommended bead milling over high-pressure homogenization as the preferred method for recovering PHB from heat-shocked cells of *A. lata*. Interestingly, since PHB is recovered without solubilizing it, the native amorphous morphology of the polymer was conserved.

The common method for PHAs extraction is the use of solvents for its speed and simplicity. Solvents alter the cell membrane and then dissolve the polymers. PHAs are recovered by solvent evaporation or precipitation with an anti-solvent (Liddell, 1999; Hänggi, 2012). In the solvents category, the chlorinated hydrocarbons chloroform, 1,2-dichloroethane, and methylene chloride are used (Ramsay et al., 1994). Non-chlorinated solvents have been proposed such as ethylene carbonate and 1, 2-propylene (Lafferty and Heinzle, 1977) or solvent mixtures of acetone/ethanol/propylene carbonate (Fei et al., 2016). On the other hand, the precipitation of PHAs is generally induced by non-solvent agents such as water, ethanol, and methanol (Ramsay et al., 1994; Mikkili et al., 2014). In summary, solvent extraction is characterized by numerous advantages such as the elimination of endotoxins and low polymer degradation (Liddell, 1999). However, there are hurdles in the use of solvents, including their high cost (Poirier et al., 1995), high energy consumption for the separation of miscible solvents and anti-solvents, and risks both for the operator and for the environment that need to be considered during the process design stage (Gorenflo et al., 2001).

On the other hand, digestion with sodium hypochlorite decomposes the cells allowing high levels of PHA purity to be reached (Hahn et al., 1994; Kim et al., 2003), however, sodium hypochlorite degrades PHB, resulting in a polymer with low molecular weight (Ramsay et al., 1990; Mikkili et al., 2014).

### Chemical and Enzymatic Hydrolysis of Recovered PHAs

After recovery, and possible purification, the extracted PHAs can be chemically or enzymatically converted into high-purity 3-hydroxyalkanoic acids. Chemical methods for modifying PHB have been reported for the production of (*R*)-methyl 3-hydroxybutanoate and (*R*)-3-hydroxybutanoic acid, these methods involve the use of methanol and sulfuric acid and methanol and *p*-toluenesulfonic acid monohydrate respectively (Seebach et al., 2003). Another approach, reported by Lee et al. (2000), considers the acidic alcoholysis of PHB, yielding methyl, ethyl, and *n*-propyl esters of (*R*)-3-hydroxybutyrate, using 1,2 dichloroethane as solvent with either sulfuric acid or hydrochloric acid as catalyst. de Roo et al. (2002) extended this method for the production of mcl-3HAs from the mcl-PHAs accumulated in *P. putida*. After a step of acid methanolysis, the obtained (*R*)-3HA methyl esters were distilled into fractions and saponified to yield the corresponding (*R*)-3-hydroxycarboxylic acids.

The multistep chemical processes outlined in the previous paragraph can be efficiently catalyzed by PHA depolymerases in a single step. This subject has been recently reviewed (Roohi and Kuddus, 2018). Thus, only some selected works will be covered. Several extracellular depolymerases have been identified and characterized (an excellent tool for its classification was presented by Knoll et al., 2009). Extracellular PHA depolymerases degrade denatured PHA granules whose structure has been altered during the extraction process and are not covered by the native layer of proteins surrounding the granule. One exception

is the PHB depolymerase from *Pseudomonas lemoignei* which is active against native PHB granules (Handrick et al., 2001).

PHB degradation studies by extracellular depolymerases are typically performed using PHB films as substrate, producing R3HBA as the hydrolysis product (Polyák et al., 2018), thus limiting the access of enzymes to its substrate. In order to achieve high R3HBA titers, a high initial concentration of PHB should be used. However, due to its water-insoluble nature, only low PHB concentrations can be suspended in water. For example, 24 g L<sup>-1</sup> of 3RHBA were produced from 25 g L<sup>-1</sup> of suspended PHB powder using an extracellular PHB depolymerase from *Pseudomonas* sp. DS1001a (Li et al., 2016). As with chemical hydrolysis methods, enzymatic hydrolysis requires the separation and partial purification of the PHA accumulated in cells and this contributes to the overall costs of 3HAs. These disadvantages could be eliminated in processes where 3HAs are produced directly from the PHAs accumulated by the cells using their own intracellular enzymes for the depolymerization process.

### In-vivo Strategies

#### Hydroxy-Acids Production by *in-vivo* Depolymerization of PHAs

This section reviews the production of 3HAs obtained through the depolymerization of PHAs accumulated using sugars and fatty acids as carbon and energy sources. The analysis of 3HAs obtained from other carbon sources is deferred to section Alternative Substrates and Microorganisms for 3HA Production.

*In-vivo* depolymerization of accumulated PHAs to R3HAs has been reported to occur with high yields in *Azohydromonas lata* (Lee et al., 1999) and *Pseudomonas putida* GPo1 (Ren et al., 2005). The depolymerization process has been shown to be highly dependent on pH. Lee et al. (1999), in a pioneering work, achieved the depolymerization of PHB to R3HBA in *A. lata* cells grown in mineral medium with sucrose as the carbon and energy source. The depolymerization process was carried out at different initial pHs in water, after washing the cells, at 37°C and without shaking to minimize oxygen transfer. Exceedingly high R3HBA yields and productivities, as high as 96% in 30 min were found at pH 4.0, but not at higher pH values. This result was explained in terms of the effects of pH on PHB depolymerase and 3-hydroxybutyrate dehydrogenase activities. The highest activity of PHB depolymerase was achieved at pHs 3 and 4, at which the monomer production rate was also the highest. Interestingly, in *A. lata* no activity of (*R*)-3-hydroxybutyric acid dehydrogenase was detected at pH 4, therefore it was argued that no 3HBA was degraded to acetoacetate (see **Figure 2** for the degradation pathway).

At pH 5, the attained depolymerization yield was 31% and decreased toward neutral pHs. From the work of Lee et al. (1999), it is not possible to ascertain whether these lower yields are due to the consumption of the released R3HBA or a decrease in the amount of PHB depolymerized. Presumably the latter is true since the depolymerization assays were performed without shaking, thus restricting the ability of cells to regenerate NADH into NAD<sup>+</sup>, a cofactor of 3-hydroxybutyrate dehydrogenase.

Following the high depolymerization yields obtained at low pHs, the authors assayed the *in-vivo* depolymerization in

*Cupriavidus necator* NCIMB 11599, *Pseudomonas oleovorans* ATCC 29347, and *Pseudomonas aeruginosa* PAO1 (DSM 1707) at pH values below 7.0. The depolymerization yields and productivities were close to 20% for *C. necator* and below 10% for *Pseudomonas* species (see **Table 1**).

Ren et al. (2005) showed that for *Pseudomonas putida* GPO1, the PHB depolymerization rate was higher at pH 11 in citrate buffer, which helps to control the pH drop caused by the accumulation of R3HAs. The released monomers corresponded to (*R*)-3-hydroxyoctanoic (R3HO) acid and (*R*)-3-hydroxyhexanoic acid (R3HHx), in a proportion closely matching the ratio of monomers in the copolymer accumulated in continuous culture with octanoic acid as carbon and energy source. The depolymerization was performed for 6 h, thus decreasing the volumetric productivity compared to the work of Lee et al. (1999) (see **Table 1**). A second factor decreasing the volumetric productivity was the low initial PHA concentration used. However, this work showed that R3HAs different than R3HBA could be obtained with high yields by using the correct pH during the depolymerization process. This work was further extended by Ruth et al. (2007) showing that applying the same depolymerization process at pH 10 to PHAs accumulated in *P. putida* GPO1, grown in continuous culture with either octanoic, undecanoic or 10-undecenoic acid, led to the production of (*R*)-3-hydroxyoctanoic acid (R3HO), (*R*)-3-hydroxyhexanoic acid (R3HHx), (*R*)-3-hydroxy-10-undecenoic acid (R3C11-1), (*R*)-3-hydroxy-8-nonenic acid (R3C9-1), (*R*)-3-hydroxy-6-heptenoic acid (R3-C7-1), (*R*)-3-hydroxyundecanoic acid (R3-C11-0), (*R*)-3-hydroxynonanoic acid (R3-C9-0), and (*R*)-3-hydroxyheptanoic acid (R3-C7-1).

Recently, Anis et al. (2018) studied the *in-vivo* depolymerization of PHAs accumulated in *P. putida* Bet001 after 48 h of batch culture with lauric acid as the carbon source and under nitrogen-limited conditions. The depolymerization was performed for 48 h in 0.2M Tris-HCl buffer, pH 9, and 30 °C. Unlike the report of Lee et al. (1999) using *Pseudomonas aeruginosa* PAO1 (DSM 1707), *P. putida* Bet001 produced R3HO, R3HHx, (*R*)-3-hydroxydecanoic acid (R3HD), and (*R*)-3-hydroxydodecanoic acid (R3HDD) with very different yields (see **Table 1**), being the highest depolymerization yield achieved for R3HD. It is not clear if this difference in yields is due to a channeling of R3HO, R3HHx, and R3HDD toward cell metabolism or if they have yet to be hydrolyzed from the granules and thus, reflects an affinity of the PHA depolymerases.

The experiments performed by Lee et al. (1999), Ren et al. (2005), and Ruth et al. (2007) used either water or phosphate buffer as depolymerization media at a pH initially set at a given value. However, the release of 3HAs leads to a decrease in the initial pH, potentially affecting process efficiency. This factor was recognized by Wang et al. (2007), leading to the design and application of a pH-stat process. In this system, the pH is controlled at a setpoint by the automatic addition of an alkaline solution (NaOH). Interestingly, the amount of NaOH added in time (the flow of the alkaline solution), if recorded, allows the estimation of the release rate of acids (hydroxy acids and protons). Using a pH-stat apparatus coupled to a dissolved oxygen meter, Wang et al. (2007) investigated the behavior of

the wild type *P. putida* GPO1 strain and a PHA depolymerase negative mutant. Results showed that the rate of acid production (not necessarily hydroxy acids) of the mutant strain was only 27% of the rate obtained with the wild type. Analysis of the supernatants revealed that the acids released by the wild type were R3HO and R3HHx. On the other hand, no detectable amounts of these compounds were found in the supernatants of the depolymerase mutant. Moreover, oxygen consumption measurements indicated a low respiratory activity for the wild type and a high respiration rate for the mutant. Finally, they also found that the acid production rate of the mutant, but not of the wild type, could be enhanced by aeration. These results support the hypothesis that the high depolymerase activity allowed the wild type strain to compensate for the high external pH. On the other hand, in the PHA depolymerase deficient mutant this could only be performed by the production of protons in aerobic conditions.

Although the results obtained by Wang et al. (2007) support this hypothesis for the depolymerization of PHAs to 3HAs at high pHs, the compensatory mechanism of pH involved in it does not explain the behavior found for *A. lata* at low pH values. Thus, the only conclusion applicable for both species is that in *A. lata* and *P. putida* GPO1 the depolymerization process is enhanced at a certain pH and simultaneously the consumption of the released monomers is impaired.

Process engineering strategies for 3HAs production are nearly non-existent with the exception of the work of Ren et al. (2007) who coupled a chemostat culture of *P. putida* GPO1 (nitrogen-limited, dilution rate of 0.1 h<sup>-1</sup>, octanoic acid as the sole carbon source) to a second continuous depolymerization stirred tank reactor. The depolymerization tank was operated as a pH-stat at a pH of 10.0 and its discharge was sent to a plug-flow reactor with a residence time of 6 h. This continuous system does not require the separation of cells or the exchange of the culture media to water or buffer. Only a simple pH shift was enough to achieve a depolymerization yield of 90%, however, the volumetric productivity was not different from previously reported works using batch depolymerization (Ren et al., 2005). Clearly, the volumetric productivity could be improved by increasing the concentration of PHA leaving the chemostat.

A different strategy for the *in-vivo* production of R3HBA has been reported using several strains of *Halomonas*. Using *Halomonas* sp. KM-1, 15.2 g L<sup>-1</sup> of R3HBA could be obtained under microaerobic conditions from 16.4 g L<sup>-1</sup> of PHB that were accumulated under aerobic conditions using glycerol as the sole carbon and energy source. The initial concentration of the nitrogen source was 12.5 g L<sup>-1</sup> (sodium nitrate), hence the limiting nutrient was presumably different from nitrogen, although this was not clarified (Kawata et al., 2012). These conditions, when applied to cultures grown in glucose (Kawata et al., 2014) did not result in any 3HBA secretion. The glucose concentration decreased from 20 to 6% during the first 36 h of culture and then remained constant. Thus, in this experiment, a nitrogen shortage was suspected.

When extra nitrate was pulse fed at 24, 36, and 48 h to a culture of *Halomonas* sp. KM-1 with 20% (w/v) glucose, then 40.3 g L<sup>-1</sup> R3HBA were secreted with a productivity of

**TABLE 1** | Summary of studies reporting the production of 3HA in non-genetically modified organisms using several operational strategies.

Microorganism	Strategy	Hydroxy acid <sup>d</sup>	Yield <sup>a</sup> (3HA Titer, gL <sup>-1</sup> )	HA Volumetric productivity (gL <sup>-1</sup> h <sup>-1</sup> )		References
				Depolymerization <sup>b</sup>	Fermentation and depolymerization <sup>c</sup>	
<i>Azohydromonas lata</i> DSM 1123	Water, initial pH 4.0, 37°C	R3HBA	84% (117.8)	117.8	4.91	Lee et al., 1999
			96% (0.99)	1.98	0.0825	
<i>Cupriavidus necator</i> NCIMB 11599	Water, initial pH 7.0, 30°C	R3HBA	19% (5.8)	0.17	NA	Lee et al., 1999
		R3HVA	23% (0.6)	0.017	NA	
<i>Pseudomonas oleovorans</i> ATCC 29347	Water, initial pH 7.0, 30°C	R3HHx	9.2% (0.13)	0.0014	NA	Lee et al., 1999
		R3HO	9.7% (1.42)	0.015	NA	
<i>Pseudomonas aeruginosa</i> PAO1 (DSM 1707)	Water, initial pH 7.0, 30°C	R3HO	9.6% (0.34)	0.0035	NA	Lee et al., 1999
		R3HD	8.8% (1.02)	0.0106	NA	
		R3HDD	6.7% (0.08)	0.0008	NA	
		R3HO	76%(0.356)	0.059	0.022	
<i>P. putida</i> GPo1	50 mM potassium phosphate buffer, pH 11, 30°C	R3HHx	21%(0.015)	0.003	0.001	Ren et al., 2005
<i>P. putida</i> GPo1	50 mM potassium phosphate buffer, pH 10, 30°C	mcl-HAs	Average 70% (≈ 1.1)	0.14	0.058	Ruth et al., 2007
<i>P. putida</i> GPo1	Culture broth, pH-stat at pH 10, 30°C.	R3HOR3HHx	90% (0.63)	NA	0.042	Ren et al., 2007
<i>P. putida</i> Bet001	0.2MTris-HCl buffer, pH 9, I = 0.2M, 30 °C	R3HO	54% (0.06)	0.001	0.001	Anis et al., 2018
		R3HHx	69% (0.64)	0.013	0.007	
		R3HD	98% (0.73)	0.015	0.008	
		R3HDD	47% (0.18)	0.004	0.002	
<i>Halomonas</i> sp. KM-1	Shift to microaerobic conditions under nitrogen rich condition	R3HBA	55% (40.3)	1.68	0.48	Kawata et al., 2014
<i>Halomonas</i> sp. OITC1261	Aerobic culture, sucrose, sodium nitrate as limiting nutrient	R3HBA	58 g L <sup>-1</sup> R3HBA +27 g L <sup>-1</sup> PHB	NA	0.65	Yokaryo et al., 2018

<sup>a</sup>Yield refers to the mass of 3-hydroxyalkanoic acid obtained over the initial mass of polyhydroxyalkanoates in cells mass. The titer of 3HA is shown in parenthesis.

<sup>b</sup>Volumetric productivity of the depolymerization process, not accounting for the time required for PHAs production.

<sup>c</sup>Volumetric productivity of the depolymerization and fermentation process, accounting for the time required for PHAs production.

<sup>d</sup>R3HBA, (R)-3-hydroxybutyric acid; R3HVA, (R)-3-hydroxyvaleric acid; R3HHx, (R)-3-hydroxyhexanoic acid; R3HO, (R)-3-hydroxyoctanoic acid; R3HD, (R)-3-hydroxydecanoic acid; R3HDD, (R)-3-hydroxydodecanoic acid.

0.48 g L<sup>-1</sup> h<sup>-1</sup> after a shift from aerobic cultivation for 60 h to microaerobic cultivation for 24 h. No R3HBA was secreted when no extra nitrate was supplemented (Kawata et al., 2014) indicating that a regulatory mechanism was controlling the activity of the PHB depolymerase, presumably related to the stringent response (see section Accumulation and Mobilization of PHAs). Glucose concentration during the depolymerization phase under microaerobic conditions was zero and a decrease in total cell concentration was observed. This behavior is consistent with the depolymerization of the accumulated PHB with only partial use of the released R3HBA for growth (our calculations show that 79% of the depolymerized PHB was recovered as 3HBA, equivalent to 55% of the maximum recovery if all the accumulated PHB is transformed to 3HBA). This can be ascribed

to the microaerobic conditions applied that limited the use of acetyl-CoA for growth and the regeneration of NAD<sup>+</sup> from NADH. Since NAD<sup>+</sup> is the cofactor used by 3-hydroxybutyrate dehydrogenase, this could explain the high titers of R3HBA. Unfortunately, no nitrate concentrations during the growth or depolymerization phase were reported to ascertain whether it is consumed or not during the microaerobic cultivation. Moreover, PHB was not completely mobilized. Since no information regarding the pH of the culture (or its control) was presented, presumably the lack of complete depolymerization was caused by a decrease in pH.

A new species of *Halomonas*, *Halomonas* sp. OITC1261 was isolated by Yokaryo et al. (2018). Unlike *Halomonas* sp. KM-1, *Halomonas* sp. OITC1261 produces R3HBA under

aerobic conditions and, apparently, without the need to supplement with extra nitrogen source once the carbon source is exhausted to promote PHB depolymerization. In fact, the data presented by Yokaryo et al. (2018) showed that R3HBA is produced concomitantly with PHB after ~10 h of cell growth. Presumably, PHB and R3HBA started to accumulate after the exhaustion of the nitrogen source, which could also explain the increase in the dissolved oxygen concentration. It is not clear whether the production of R3HBA occurs through PHB *in-vivo* depolymerization or proceeds directly from (R)-3-hydroxybutyryl-CoA or acetoacetate.

## Production of Hydroxyalkanoates in Genetically Modified Microorganisms

### Mutants of native PHA producers

The exploration of alternative pathways for the production of R3HAs emerges from the recognition of two characteristics found in native PHA producers: (i) depolymerization products can be metabolized, for example, R3HBA is converted to acetoacetate by the 3-hydroxybutyrate dehydrogenase (HBD) enzyme (Tokiwa and Ugwu, 2007) and (ii) producing 3HA is a two-stage process where PHA is accumulated and then depolymerized in a subsequent step that often requires a change in media or process conditions. A process for the isolation of 3-hydroxybutyrate dehydrogenase null mutants was described more than 40 years ago (Lafferty, 1977), including UV mutagenesis, followed by the destruction using antibiotics of the bacteria capable of 3HBA assimilation and the selection of 3HBD null mutants by spread plating of the individuals surviving the treatment with bactericidal.

Ugwu et al. (2008), reported the production of R3HBA in *C. necator* through the acetoacetate pathway induced by random mutation using UV radiation. The mutants achieved a titer of 0.150 g L<sup>-1</sup> of R3HBA in a 5L fermenter after 48 h of cultivation using either glucose or sucrose as carbon source. The concentration of R3HBA was increased by feeding lithium acetoacetate to resting cells of the mutant strain, reaching 0.84 g L<sup>-1</sup> of R3HBA. The results were interpreted as indicative of a disruption in the *phbB* gene (coding for acetoacetyl-CoA reductase), making this strain unable of PHB accumulation (see Figure 2). Ugwu et al. (2008) reasoned that the excess of acetoacetyl-CoA produced under conditions allowing for PHB accumulation was channeled toward R3HBA via acetoacetate.

Using UV mutagenesis, Ugwu et al. (2011) obtained an R3HBA-producing mutant of *Azohydromonas lata*. When cells of this mutant were resuspended in phosphate buffer containing glucose (1% v/w), ethylacetoacetate (2% v/v), or (R,S)-1,3-butanediol (3% v/v), the resting cells produced R3HBA at concentrations of 6.5, 7.3, and 8.7 g L<sup>-1</sup>, respectively.

### Production of 3HAs in recombinant *E. coli* strains

An alternative process for the production of R3HBA is the use of recombinant methods to express PHA related genes in well-characterized non-PHA producing and fast-growing microorganisms such as *Escherichia coli* (Chen et al., 2013). Lee et al. modified *E. coli* strains by inserting two plasmid systems containing the *phaA<sub>Re</sub>*, *phbB<sub>Re</sub>*, and *phbC<sub>Re</sub>* genes) and the

*phaZ1<sub>Re</sub>* depolymerase from *Ralstonia eutropha* (Lee and Lee, 2003). This design achieved an R3HBA concentration of 9.6 g L<sup>-1</sup> in 51 h of fermentation using glucose as a carbon source.

Shiraki et al. (2006) engineered *E. coli* and *R. eutropha* to express the same enzymes leading to the production of PHB but different depolymerases. The strains compared were an *R. eutropha* null mutant for 3-hydroxybutyrate dehydrogenase and a recombinant *E. coli* strain harboring the synthetic PHB operon of *R. eutropha* and an extracellular depolymerase of *Paucimonas lemoignei*. The production of R3HBA by the 3-hydroxybutyrate dehydrogenase null mutant of *R. eutropha* was found to be dependent on the supply of oxygen, achieving an R3HBA concentration of 3.13 g L<sup>-1</sup> under anaerobic conditions and concentrations in the 0.41–1.04 g L<sup>-1</sup> range under aerobic culture conditions. The intracellular PHB content decreased concomitantly with the production of R3HBA, reaching almost zero for the experiment performed under anaerobic conditions after 50 h of depolymerization. Presumably, under aerobic conditions the accumulated PHB was depolymerized to a molecule different than R3HBA, such as 3-hydroxybutyryl-CoA, or the produced R3HBA was metabolized using pathways not using 3-hydroxybutyrate dehydrogenase (BDH). In fact, Shiraki et al. (2006) verified that no BDH was expressed and no BDH was found in the supernatant fraction of cells grown under PHB accumulation conditions, however, it was not verified whether the mutant could grow in R3HBA. On the other hand, the recombinant *E. coli* harboring the PHB operon and the *P. lemoignei* depolymerase reached a concentration of approximately 7.3 g L<sup>-1</sup> of R3HBA after 100 h. Since *E. coli* is not a native PHB producer, presumably there were no alternative pathways for R3HBA production or consumption different from the inserted genes (Shiraki et al., 2006). Interestingly, the difference between the R3HBA production pathways used by Shiraki et al. (2006) and Lee and Lee (2003) is the PHB depolymerase gene. While Shiraki used the extracellular depolymerase of *Paucimonas lemoignei* capable of hydrolyzing both native PHB granules and denaturated ones (Handrick et al., 2001), Lee and Lee used a gene from *R. eutropha*. In particular, the depolymerase *PhaZa1* used by Lee and Lee (2003) was found to secrete rather low concentrations of R3HBA when expressed in the same *E. coli* strain (Uchino et al., 2008).

Generally, the use of the *phaCAB* and *phaZ* genes requires a two-stage fermentation, accumulation of the polymer followed by depolymerization, thereby the required cultivation times are usually long. Hence, the interest in the last decades focused on the direct microbial production of extracellular 3HA monomer without going through these two stages and achieving a straightforward, less energy and time-consuming process.

The first alternative pathway was reported by Gao et al. (2002), by introducing the *phbA*, *phbB*, *buk* and *ptb* genes in recombinant *E. coli* DH5K. This pathway starts from glucose to yield acetyl-CoA, which is the key compound in glycolysis, *PhbA* catalyzes the formation of acetoacetyl-CoA from two acetyl-CoAs, which is then reduced to (R)-3-hydroxybutyryl-CoA under the action of *PhbB*. (R)-3-hydroxybutyryl-CoA is then transformed into (R)-3-hydroxybutyryl-P by *Ptb* (see Figure 2). Finally, *Buk* converts the (R)-3 hydroxybutyryl-P into R3HBA, resulting in

the production of  $12\text{ g L}^{-1}$  in fed-batch cultures (Gao et al., 2002). The direct method presents some advantages: (i) glucose is transformed without accumulation and depolymerization of PHB, (ii) R3HBA production is not associated with cell growth, and (iii) immobilization of the recombinant strain may allow a continuous R3HBA production process to be established.

Similarly to the system presented by Gao et al. (2002), (R)-3HB-CoA can be directly hydrolyzed into R3HBA using TesB, a class II thioesterase enzyme that catalyzed the hydrolysis of the CoA moiety from acyl-CoAs (Naggert et al., 1991). For example, when TesB acts on 3-hydroxybutyryl-CoA, free R3HBA monomers are obtained by cleaving coenzyme A.

Liu et al. (2007) used *E. coli* BW25113 as host for the expression of *phbA* and *phbB* genes from *R. eutropha* and *tesB* from *E. coli*. This strain produced  $3.98\text{ g L}^{-1}$  R3HBA in shake flask culture using  $11.4\text{ g L}^{-1}$  of glucose. Using a fed-batch strategy,  $12.2\text{ g L}^{-1}$  R3HBA were accumulated in 24 h. The feeding strategy consisted of pumping a solution containing glucose ( $20\text{ g L}^{-1}$ ) and ammonium sulfate ( $2\text{ g L}^{-1}$ ) each time glucose concentration in the broth was lower than  $10\text{ g L}^{-1}$ . The productivity achieved by this system ( $0.51\text{ g L}^{-1}\text{ h}^{-1}$ ) is among the highest reported so far for the direct production of R3HBA (see Table 2). Previous to this work, it was well established that TesB was capable of releasing CoA from acyl CoA of C<sub>6</sub>-C<sub>18</sub> carbon length, as well as 3-hydroxyacyl-CoA esters, to their corresponding free fatty acids (Naggert et al., 1991), but not from short-chain length hydroxyacyl-CoA. In this regard, Zheng et al. (2004) reported the production of (R)-3-hydroxydecanoic acid (R3HD) from fructose by a recombinant *E. coli*. The recombinant strain contains the *phaG* gene from *P. putida* encoding for (R)-3-hydroxydecanoyl-acyl carrier protein-coenzyme A transacylase. PhaG links fatty acid *de novo* biosynthesis and PHA production by catalyzing the conversion between (R)-3-hydroxydecanoyl-acyl carrier protein and (R)-3-hydroxydecanoyl-CoA (Rehm et al., 1998). When the *E. coli* strain containing only PhaG was cultured in shake flasks with  $20\text{ g L}^{-1}$  fructose,  $0.64\text{ g L}^{-1}$  of R3HD, and  $2.11\text{ g L}^{-1}$  of biomass were obtained. The R3HD titer was increased to  $1.02\text{ g L}^{-1}$  when a plasmid expressing *tesB* was also inserted into the strain along with *phaG*, suggesting that the activity of TesB in the strain containing only *phaG* was insufficient for efficient hydrolysis of the produced (R)-3-hydroxydecanoyl-CoA.

In *E. coli*, acetate is often produced concomitantly with R3HBA (Gao et al., 2002; Tseng et al., 2009; Guevara-Martínez et al., 2015), decreasing product yield and lowering the growth rate at concentrations as low as  $0.5\text{ g L}^{-1}$ ; thus, difficulting the use of high-cell-density cultures with high volumetric productivities (Nakano et al., 1997; Roe et al., 2002). Perez-Zabaleta et al. (2019) studied the production of R3HBA using the native *E. coli* acyl-CoA thioesterases (*fadM*, *tesA*, *tesB*, *ybgC*, *ydiI*, and *yciA*). These enzymes are also active with acetyl-CoA as substrate (McMahon and Prather, 2014), and therefore could contribute to the production of acetate. In this work, the impact of deletion of genes involved in the production of acetic acid (*poxB*, *pta*, or *iclR*) on R3HBA producing fed-batch cultures was investigated using *E. coli* AF1000. Also, several *E. coli* strains were compared including

*E. coli* AF1000 and BL21 as low acetate-forming R3HBA production platforms. All the strains carrying  $\beta$ -ketothiolase (*t3*) and acetoacetyl-CoA reductase (*rx*) from *Halomonas boliviensis* and overexpressing the glucose-6-phosphate dehydrogenase gene (*zwf*). No important reduction on acetic acid titers was found for the deletion of the aforementioned genes. The best results were obtained using strain BL21 achieving the highest R3HBA titer and volumetric productivity reported up to date (see Table 2). Interestingly, Guevara-Martínez et al. (2019) working with the same recombinant strain (*E. coli* AF1000-*t3-rx-zwf*) showed that the deletion of *tesA* or *fadM* resulted in minor decreases in R3HBA production, while deletion of *tesB* and *yciA* decreased the R3HBA titer by 11 and 33%, respectively. These results suggest that YciA, and not TesB, is the acyl-CoA thioesterase largely responsible for R3HBA production from (R)-3-hydroxybutyryl-CoA in *E. coli*.

The production of S3HBA from glucose in an engineered *E. coli* strain was reported by Lee et al. (2008). The genes coding for PhaA from *R. eutropha*, (S)-3-hydroxybutyryl-CoA dehydrogenase (HBD) from *Clostridium acetobutylicum* ATCC824, and 3-hydroxyisobutyryl-CoA hydrolase (BCH) from *Bacillus cereus* ATCC14579 were inserted in *E. coli* BL21. Under fed-batch cultivation with glucose as substrate,  $10.3\text{ g L}^{-1}$  of S3HBA and  $65\text{ g L}^{-1}$  of biomass were accumulated in 38 h. The yield of S3HBA production was low compared with that of R3HBA from glucose found by Gao et al. (2002). Lee et al. (2008) interpreted this low yield as a consequence of S3HBA-CoA being an intermediate of fatty-acid  $\beta$ -oxidation pathway; therefore, it can be degraded into acetyl-CoA. Similarly, Tseng et al. reported the production of S3HBA and R3HBA using an *E. coli* strain harboring plasmids containing genes for different thiolases (*phaA* and *bktB* from *R. eutropha* and *thl* from *C. acetobutylicum* ATCC 824), *hbd* and *phaB* genes for the production of (R) and (S) hydroxybutyryl-CoA and either *tesB* or *ptb-buk* genes to remove the CoA moiety. The impact of the thiolase in the titers of the hydroxy acids was found to be low. On the other the selection of the enzyme hydrolyzing the CoA was critical. In fact, when Ptb-Buk was used no S3HBA was detected. If TesB was included, then both R3HBA and S3HBA were produced.

Recently, (R)-3-hydroxyvalerate (R3HVA) and R3HBA were produced in a recombinant strain of *E. coli* capable of glycerol conversion (Miscovic et al., 2019). The engineered strain (P3HA31) harbors the *phaA* and *bktB* genes (from *Cupriavidus necator* ATCC 43291) to catalyze the condensation of two acetyl-CoA molecules or an acetyl-CoA and a propionyl-CoA molecule for the formation of acetoacetyl-CoA and 3-ketovaleryl-CoA, respectively. Two genes for the reduction of acetoacetyl-CoA were inserted, *phaB* from *C. necator* and *hdb* from *Clostridium acetobutylicum* ATCC 824 catalyzing the formation of (R)-3-hydroxybutyryl-CoA and its S stereoisomer, respectively. Finally, *tesB* was introduced for the production of the corresponding hydroxycarboxylic acids. The strain was further optimized to increase the propionyl-CoA pool from succinyl-CoA by deregulating the glyoxylate shunt (mutating *iclR*) and by inactivating the oxidative TCA cycle gene *sdhA*, thus blocking the conversion of succinate to fumarate. The double mutant P3HA31 $\Delta$ *sdhA* $\Delta$ *iclR* achieved a concentration

**TABLE 2** | Summary of engineered strains for the production of 3-hydroxyalkanoic acids.

Strains	Carbon substrate	3HA titer (g L <sup>-1</sup> ) <sup>a</sup>	3HA Volumetric productivity (g L <sup>-1</sup> h <sup>-1</sup> )	References
<i>E. coli</i> DH5α(phaA-phaB-buk+ ptb)	Glucose	12.0 (R3HBA)	0.25	Gao et al., 2002
<i>E. coli</i> XLI-Blue (phaA-phaB-phaC-phaZi)	Glucose	9.6 (R3HBA)	0.19	Lee and Lee, 2003
<i>E. coli</i> DH5 (phaA-phaB-phaG)	Glucose + Acrylic acid	0.7 (R3HBA)	0.01	Zhao et al., 2003
<i>E. coli</i> JM 109 (pha CAB-phaZ7)	Glucose	7.3 (R3HBA)	0.073	Shiraki et al., 2006
UV radiation mutant <i>Cupriavidus necator</i>	Glucose or sucrose + Lithium acetoacetate	0.84 (R3HBA)	0.026	Ugwu et al., 2008
UV mutant radiation <i>Azohydromonas lata</i>	Sucrose + 1,3 butanodiol	8.7 (R3HBA)	0.082	Ugwu et al., 2011
<i>E. coli</i> BW25113 (phaB- phaB - tesB)	Glucose	12.2 (R3HBA)	0.51	Liu et al., 2007
<i>Pseudomonas putida</i> KTOY07 (with pSPH09 plasmid)	Lauric acid	7.27 (96% R3HDD)	0.26	Chung et al., 2009
<i>E. coli</i> K-12 MG1655(DE3)	Glucose	2.92 (R3HBA)	0.06	Tseng et al., 2009
		2.08 (S3HBA)	0.04	
		0.50 (R3HVA)	0.007	
<i>E. coli</i> with the plasmid sets pET-PB-B, and pCDF-T-H (for (S)-3HV synthesis) or pCDF-T-P (for (R)-3HV synthesis)	Glucose	0.31 (S3HVA)	0.004	Tseng et al., 2010
		0.60 (R3HVA)	0.0084	
		0.19 (S3HVA)	0.003	
<i>E. coli</i> (phaAB-pct)	Glucose +acetate	5.2 (R3HBA)	0.22	Matsumoto et al., 2013
Mutant of <i>M. rhodesianum</i> (DlpA <sup>-</sup> Dhbd <sup>-</sup> )	Methanol	2.81(R3HBA)	0.014	Hölscher et al., 2010
<i>E. coli</i> strain AF1000 pJBG3R3X	Glucose + phosphate-limited	2.85(R3HBA)	1.5	Guevara-Martínez et al., 2015
<i>E. coli</i> (phaA-HBD-BCH)	Glucose	10.3 (S3HBA)	0.12	Lee et al., 2008
<i>Clostridium coskatii</i> [p83_tcb]	Syngas, anaerobic culture	0.1 (R3HBA)	1.4 · 10 <sup>-4</sup>	Flüchter et al., 2019
<i>Clostridium coskatii</i> [p83_tcb](thlA-ctfA/ctfB-bdhA)	Fructose, anaerobic culture	2.25 (R3HBA)	0.032	Flüchter et al., 2019
<i>S. cerevisiae</i> (ERG10- hbd-tesB)	Ethanol biotransformation under aerobic conditions	12 (S3HBA)	0.06	Yun et al., 2015
<i>Arxula adenivorans</i> (thl-phaB)	Glucose fed-batch followed by ethanol feeding	3.78 (R3HBA)	0.043	Biernacki et al., 2017
<i>E. coli</i> BL21 (t3-rx- zwf)	Nitrogen limited fed-batch cultivation with glucose as substrate	16.3 (R3HBA)	1.52	Perez-Zabaleta et al., 2019
<i>Synechocystis</i> sp. (phaA-phaB1-TesB)	Photosynthetic cultivation	1.84 (R3HBA)	7.7 · 10 <sup>-3</sup>	Wang et al., 2018
<i>E. coli</i> AF1000 (t3-rx)	Glucose, xylose and arabinose as substrate	0.54 (R3HBA)	0.029	Jarmander et al., 2015
<i>E. coli</i> (phaA -bktB-phaB-hdb-tesB-ΔsdhAΔiclR)	Glycerol as carbon and energy source, aerobic	2.0 (R3HBA)	0.042	Miscevic et al., 2019
		3.71 (R3HVA)	0.077	

<sup>a</sup>R3HBA, (R)-3-hydroxybutyric acid; R3HDD, (R)-3-hydroxydodecanoic acid; S3HBA, (S)-3-hydroxybutyric acid; S3HVA, (S)-3-hydroxyvaleric acid.

of 3.71 g L<sup>-1</sup> of R3HVA, 2.97 g L<sup>-1</sup> of propionate and nearly 2 g L<sup>-1</sup> of R3HBA. Despite the fact that *hdb* was expressed, results suggest that PhaB was catalytically more active than Hbd since higher titers in (R)-3-HB/HV than (S)-3-HB/HV were found. Alternatively, this might be the consequence of a larger abundance of NADPH compared to NADH, as PhaB and Hbd are NADPH-dependent and NADH-dependent, respectively. Tseng et al. (2010) previously reported that a similar *E. coli* engineered strain was able to produce R3HBAs and (R) and (S) 3HVAs. When glycerol was used as carbon source, 0.60 g L<sup>-1</sup> R3HVA,

0.19 g L<sup>-1</sup> S3HVA, 0.58 g L<sup>-1</sup> R3HBA, and nearly 1.2 g L<sup>-1</sup> acetate were produced.

Finally, a third alternative for the hydrolysis of CoA from (R)-3-hydroxybutyryl-CoA, besides TesB and Ptb-Buk, was designed based on the use of a propionyl CoA transferase (Pct). Pct works by transferring a CoA from (R)-3-hydroxybutyryl-CoA to another short-chain fatty acid. Matsumoto et al. (2013) engineered *E. coli* BW25113 by inserting a plasmid containing the *phaA* and *phaB* genes from *R. eutropha* and *pct* from *Clostridium propionicum*. This *pct* gene was selected since catalyzes the

transfer reaction of CoA between R3HBA and acetate (Jossek et al., 1998). Cells were cultured for 24 h in test tubes at 30°C with 10 g L<sup>-1</sup> glucose and acetate concentrations in the 0–10 g L<sup>-1</sup> range. Acetic acid enhances R3HBA production when Pct is expressed as will act as the molecule receiving the CoA moiety and will serve as substrate for the condensation reaction of two acetyl-CoAs catalyzed by PhaA. Results showed that the maximum concentration (9.0 g L<sup>-1</sup>) and volumetric productivity (0.22 g L<sup>-1</sup> h<sup>-1</sup>) were attained at a concentration of 6.6 g L<sup>-1</sup> of acetic acid. Unfortunately, no efforts were made to investigate the performance of the engineered strain using a fed-batch culture where acetic acid and glucose concentrations could be controlled independently, possibly increasing product titer and volumetric productivity.

## ALTERNATIVE SUBSTRATES AND MICROORGANISMS FOR 3HA PRODUCTION

Decreasing the cost of industrial PHA production requires the use of abundant and low-cost carbon and energy substrates such as molasses, glucose, sucrose derived from sugar cane, sugars produced from lignocellulose, one-carbon compounds (formate and methanol) and gaseous substrates (syngas, knallgas, and methane). This is also true for the production of the monomers constituting PHAs.

Regarding the use of lignocellulosic hydrolyzates, Wang and Liu (2014) discovered that in batch cultures of *B. cepacia*, the concentration of R3HBA released during growth was stimulated by nitrate and chloride ions. The concentration of R3HBA reached 16.2 g L<sup>-1</sup> in hydrolysates of *Paulownia elongate*, however, this concentration could not be achieved in model hydrolyzates. The production of 3HBA with *Halomonas* sp. KM-1 has also been shown with sugars obtained from lignocellulosic materials. Using saccharified Japanese cedar as carbon source, a concentration of 21.1 g L<sup>-1</sup> R3HBA was obtained with a yield of 89% (based on initial PHB) after shifting from an aerobic accumulation phase to a microaerobic PHB depolymerization phase (Kawata et al., 2015). Interestingly in this microorganism, the R3HBA titer obtained without the addition of urea at the onset of the microaerobic phase was lower compared to adding 7.1 g L<sup>-1</sup> of urea. Unfortunately, it is not clear whether the effect of urea is due to an increase in media pH or to its consumption.

Jarmander et al. (2015) reported the construction of an *E. coli* strain capable of producing R3HBA from xylose, glucose and arabinose harboring the acetoacetyl-CoA thiolase (*t3*) and acetoacetyl-CoA reductase (*rx*) genes from *H. boliviensis*. The conversion of 3-hydroxybutyryl-CoA to R3HBA was assumed to be catalyzed by the *E. coli* native TesB enzyme. Albeit this work represents an interesting achievement from a genetic manipulation perspective targeting the production of new compounds from lignocellulosic derived sugars, the highest R3HBA yield on mixed sugars was 0.23 g/g with a 3HBA titer of 0.54 g L<sup>-1</sup> under nitrogen depleted conditions in batch culture. On the other hand, the highest concentration of R3HBA (1.87 g

L<sup>-1</sup>) was achieved in a nitrogen fed-batch culture with an overall yield of 0.05 g R3HBA g sugars<sup>-1</sup>.

Although the accumulation of PHB from knallgas is well-documented (see section Substrates for the Production of Polyhydroxyalkanoates and Its Monomers), no evidence exists in the open literature regarding the production of 3HBA or 3HAs from knallgas, despite *A. lata* being one of the first bacteria where R3HBA production was demonstrated (Lee et al., 1999). Similarly, the accumulation of PHB in methanotrophs is well documented (for a recent review see Strong et al., 2016), however, no known organism has been reported to produce 3HBA or any other 3HA either from *in-vivo* depolymerization of the accumulated PHB, through an engineered pathway or from the *ex-vivo* depolymerization of the extracted PHB.

A notable exception regarding the use of C1 compounds for the production of 3HAs is the use of methanol for the obtention of R3HBA. *Methylobacterium rhodesianum* MB 126 was genetically modified by knocking-out the 3-hydroxybutyrate dehydrogenase gene. Since the mutant strain still exhibits growth in R3HBA, transposon mutagenesis was used to obtain a double mutant unable to grow on R3HBA. The double mutant was shown to have, along with a lack of 3-hydroxybutyrate dehydrogenase, an incomplete citric acid cycle due to a defective lipoic acid synthase (*LipA*). In fed-batch culture, using methanol as the sole carbon and energy substrate, 2.8 g L<sup>-1</sup> of R3HBA were obtained after accumulating PHB under nitrogen limitation and inducing its degradation under a carbon limited and nitrogen-rich condition (Hölscher et al., 2010).

All the aforementioned genetic modifications lead to the production of 3HBA or 3HAs under aerobic conditions. Flüchter et al. (2019) constructed a genetically modified strain of *Clostridium coskatii* harboring the thiolase A gene (*thlA*; CA\_C2873) and the acetoacetyl-CoA:acetate/butyrate CoA transferase genes (*ctfA/ctfB*; CA\_P0163/ CA\_P0164) from *C. acetobutylicum* ATCC 824 and the 3-hydroxybutyrate dehydrogenase gene (*bdhA*; CDIF630\_02933) from *Clostridium difficile* DSM 27543. The engineered pathway directs acetyl-CoA to acetoacetyl-CoA using thiolase A, which is converted into acetoacetate using the acetoacetyl-CoA:acetate/butyrate CoA transferase and the final conversion of acetoacetate to 3-hydroxybutyrate by 3-hydroxybutyrate dehydrogenase. Under heterotrophic conditions with fructose as carbon and energy source and under anaerobic condition, 2.3 g L<sup>-1</sup> of R3HBA accumulated in 60 h of batch culture and 3.9 g L<sup>-1</sup> of acetate were concomitantly produced. Under autotrophic conditions using syngas (CO 40 mol %, H<sub>2</sub> 40 mol %, CO<sub>2</sub> 10 mol % and N<sub>2</sub> 10 mol %) a concentration of 0.1 g L<sup>-1</sup> of R3HBA was obtained along with 2.1 g L<sup>-1</sup> of acetate. Although the achieved concentrations, especially under autotrophic conditions are low, this study represents an important proof of concept for the utilization of inexpensive and abundant gaseous substrates. Interestingly, although the production of acetate should be reduced, it cannot be completely eliminated as acetate is used in the reaction catalyzed by the acetoacetyl-CoA:acetate/butyrate CoA transferase to accept the CoA molecule in the step leading to the production of acetoacetate. In a previous report, Woolston et al. (2018) achieved comparable titers both under heterotrophic and

autotrophic growth. However, the product obtained by Woolston et al. was (S)-3-HBA instead of R-3-HBA due to an engineered pathway using the *phaA* gene from *C. necator*, the NADH-dependent (S)-3-hydroxybutyryl-CoA dehydrogenase from *C. acetobutylicum* and the thioesterase *tesB* from *E. coli*.

The production of (S)-3-HBA has been also demonstrated in metabolically engineered *Saccharomyces cerevisiae*, Yun et al. (2015) reported one of the few modifications in yeasts aimed at the production of hydroxyacids, where the following genes were introduced: acetyl-CoA C-acetyltransferase (*erg10p* from *S. cerevisiae* BY4741) for the condensation of two molecules of acetyl-CoA into acetoacetyl-CoA, NADH-dependent acetoacetyl-CoA reductase (ACR, *hbd* from *C. acetobutylicum* ATCC 824) converting acetoacetyl-CoA to (S)-3-hydroxybutyryl-CoA and 3-hydroxybutyryl-CoA thioesterase (*tesB* from *E. coli* K-12 MG1655) to remove the CoA molecule from (S)-3-hydroxybutyryl-CoA. Using ethanol as the substrate in fed-batch cultivation, 12 g L<sup>-1</sup> of (S)-3-HBA were accumulated in 200 h. Small amounts of glycerol were accumulated during the first half of the culture (close to 6 g L<sup>-1</sup>) but they were reduced to zero by the end of the culture. A similar strategy was used by Biernacki et al. (2017) for the production of R3HBA in *Arxula adenivorans* after inserting the *thl* gene from *C. acetobutylicum* ATCC 824 and *phbB* from *C. necator* H16. In fed-batch cultures with glucose as the carbon source, ethanol is produced under hypoxic conditions during the first 50 h of culture. A shift to aerobic conditions promotes ethanol assimilation and R3HBA production reaching a maximum of 3.78 g L<sup>-1</sup>.

Finally, the use of photosynthetic organisms for 3HA production has also been explored. Wang et al. (2018) modified the cyanobacteria *Synechocystis* sp. After inserting the genes *phaA*, *phaB1*, and *tesB* a concentration of 1.84 g L<sup>-1</sup> of R3HBA was obtained at the end of 10 days of photoautotrophic cultivation.

Most of the available literature on the direct microbial production of HAs (without accumulation of PHAs) deals with the obtention of short-chain length hydroxy acids. Notable exceptions are the engineered systems based on *Pseudomonas putida* strains. Chung et al. (2009) constructed a novel pathway in *Pseudomonas putida* KTOY01, a mutant of *P. putida* KT2440 unable to accumulate PHA due to a PHA synthesis operon knockout, by expressing the *tesB* gene and knocking the genes *fadB* and *fadA* to create a  $\beta$ -oxidation-pathway-deficient mutant. This strain accumulated 7.27 g L<sup>-1</sup> of R3HAs, with over 96% mol of (R)-3-hydroxydodecanoic acid when lauric acid was added into the culture broth. However, lauric acid is a related carbon source making this process closer to biotransformation rather than synthesis. Similar work was performed by Chung et al. using *Pseudomonas entomophila* as the host strain. When tetraoic acid and dodecanoic acid were used as related carbon sources in shake flask cultures, 6.65 g L<sup>-1</sup> 3-hydroxytetradecanoic acid and 4.6 g L<sup>-1</sup> 3-hydroxydodecanoic acid were obtained. No reports of the production of mcl-HAs are available in the literature, however, the work of Agnew et al. (2012) showing the production of C<sub>12</sub> and C<sub>14</sub> polyhydroxyalkanoates from glucose in *E. coli* could be a starting point for the introduction of a thioesterase such as *TesB*.

## SECRETION OF PHAs

A possible approach to decrease the cost of PHAs and 3HAs production is to devise simplified methods for the recovery of the accumulated polymers. Although the production of 3HAs from recovered PHAs requires more steps than the direct fermentation strategies presented in the previous section, starting from pure or partially purified PHAs could lead to a simplified downstream processing. Moreover, the production 3HAs esters, as outlined in section Chemical and Enzymatic Hydrolysis of Recovered PHAs starts from PHAs, and thus it can benefit from simplified methods for the recovery of these polymers. A recurrent strategy is the induction of cell lysis to release the PHA granules.

Resch et al. (1998) expressed the *Alcaligenes eutrophus phbCAB* genes and the cloned lysis gene E of bacteriophage PhiX174 in *E. coli* cells, which allowed to perform PHB synthesis and at the same time generate the E-lysis tunnel structure that is characterized by a small opening with edges in the transmembrane envelope (Resch et al., 1998). E-lysis produces holes approximately of equal size to the diameter of the cells (producing lysis) and releases around 90% of the PHB. The PHB granules vary in size and have the tendency of self-aggregation. Based on these facts and the structural analysis of protein E it was postulated as a way to obtain free PHB granules in the extracellular medium. Similarly, a *P. putida* KT2440 mutant was constructed by expressing two proteins from the pneumococcal bacteriophage EJ-1, an endolysin (Ejl) and a holin (Ejh) and the mutation of the *tolB* gene to reduce the integrity of the membrane and promote a lysis sensitivity. After inducing the accumulation of PHAs and the lysis of cells, 0.28 g L<sup>-1</sup> of PHAs were recovered using direct extraction of the wet biomass with ethyl acetate (Martínez et al., 2011). Using the endolysin (Ejl) and a holin (Ejh) system, but under the control of a promoter induced by xylose but inhibited by glucose, nearly two-thirds of the PHB accumulated in *Bacillus megaterium* using glucose as carbon source was released into the broth after 20 h of culture post glucose exhaustion. A fraction of the PHB remains associated with the cell debris, possible through hydrophobic interactions (Hori et al., 2002).

A different but related approach was presented by Borrero-de Acuña et al. (2017). A programmable lysis system was built based on the expression of lysozyme and tested in *Pseudomonas putida* KT2440 under conditions promoting growth or PHA accumulation. The lytic system did not affect the biomass yield or growth rate of *P. putida* under balanced growth but did reduce the biomass production by 25% when conditions permissive of PHA accumulation were applied. Notwithstanding, the PHA content was kept and after the induction of the lytic system, nearly 75% of the accumulated polymer was recovered. The released polymer was recovered by mixing the fermentation broth with chloroform at a 18:1 (v/v) ratio followed by phase separation, representing an excellent reduction in solvent and energy use.

Another strategy for the recovery of PHAs is the use of external cell lytic agents such as the *Bdellovibrio bacteriovorus*

HD100 bacterium, an obligate predator of other gram-negative bacteria which acts as a lithic agent for the recovery of intracellular bioproducts of industrial interest (Martínez et al., 2016). *B. bacteriovorus* HD100 was genetically modified by eliminating the PHA depolymerase gene in order to prevent the breakdown of the recovered PHAs. After allowing the accumulation of PHAs in *P. putida*, *C. necator*, and a recombinant *E. coli* strain, each culture was infected with a suspension of *B. bacteriovorus* cells. Sixty-five percentage of the PHA accumulated in *P. putida* could be recovered at high cell densities using this method. The polymer was directly extractable from the wet biomass of the co-cultures, thus avoiding the need for biomass drying. When *C. necator* cells were used as prey in low concentration (PHB titer less than  $1\text{ g L}^{-1}$ ), the PHB recovery yield was 80%.

Currently, efforts are focused on the creation of “leaking” bacteria for an easy “export” of PHB, this is the implementation of secretion mechanisms in which a cell breakdown is not required in a chemical or mechanical way and the biomass could be recycled to implement a semi-continuous PHB production system. Protein secretion is the main route by which bacteria not only interact with the extracellular environment, but also secrete products that are essential for cells, which include adhesion, pathogenicity, adaptation, and in some cases enzymatic degradation. Hence, the gram-negative bacteria have developed a wide variety of pathways for the secretion of different products into the extracellular matrix while maintaining the integrity of the cellular structure (Henderson and He, 2009; Costa et al., 2015).

Type I secretion systems (T1SS) or ABC transporters (ATP-binding cassette) are heterotrimeric complexes that are composed of three segments that interact with each other (Nicaud et al., 1986). Type II secretion systems (T2SS) are one of the best-known secretion systems because they are conserved in most gram-negative bacteria. Type II systems are able to transport folded proteins from the periplasm to the extracellular environment (Green and Meccas, 2016). T1SS and T2SS are the most used secretion systems in biological engineering and therefore the most studied in detail. These two systems stand out for the fact that each one of them recognizes a sequence through its peptide ends as an objective, that is, the signalized sequence can be fused with other proteins which causes the cell to target the new fusion protein for their respective secretion. Fusion proteins have been applied to indirectly secrete PHB molecules, this has been reported by Linton et al. (2012), who initially conducted a study to evaluate the efficacy and viability of the secretion systems used by *E. coli*. The signal peptides corresponded to HlyA (T1SS), TorA (T2SS, TAT), GeneIII (T2SS, Sec), and PelB (T2SS, Sec) (Linton et al., 2012). The results obtained show that the PelB system was not effective in the translocation of GFP, while the other two T2SSs successfully exported GFP to the periplasm and with respect to the HlyA system, also secrete the GFP protein to the extracellular medium (Linton et al., 2012). Based on these results, the HlyA signal peptide fusion protein and a fascine that associates with the PHB granules were used to bind the signaling sequence to

the PHB granule, leading to the secretion of PHB to the extracellular medium (Rahman et al., 2013). Results indicate that after 48 h of culture 36% of the total PHB produced by the secretory strain was collected in the secreted fraction while the remaining 64% corresponded to the internal fraction. SEM images of the PHB accumulating *E. coli* strain with and without the secretory system show that PHB is not excreted as granules, but as an amorphous material. This evidence, combined with the low secretion found, suggest that the system cannot export the intact PHB granules. Sabirova et al. (2006) constructed an *Alcanivorax borkumensis* SK2 mutant capable of PHA hyperproduction. Interestingly, this mutant release part of the produced PHA to the extracellular medium when it was cultured in alkanes without cell lysis. The secretion mechanism remains unknown.

## CONCLUSION AND PERSPECTIVES

As outlined in this review, after 20 years of the discovery of the *in-vivo* hydrolysis of PHB accumulated in *Azohydromonas lata*, and even though this system remains as the one showing the highest titer of (*R*)-3-hydroxybutyrate, a large body of knowledge have been accumulated regarding the production of other, potentially more industrially useful, 3-hydroxyalkanoic acids from diverse substrates including fatty acids and sugars derived from lignocellulosic materials. In this regard, the production of 3-hydroxyacids directly from its precursors, and without the accumulation of PHAs, in recombinant strains show the potential of transferring this production system into a wide range of hosts to expand the number of substrates that can be used for the production of these valuable compounds.

Thanks to the availability of techniques for genetic manipulation, *E. coli* served as the preferred host for the introduction of new pathways for the direct production of 3HAs. Since the first reports dealing with the production of R3HBA using the native *E. coli* thioesterases, significant efforts were performed to increase titer, yield, and productivities and to expand the range of 3HAs that can be obtained in *E. coli*.

However, more research is needed for bacterial production of these hydroxy acids to reach a level of industrial use. Research needs include increasing titer and productivities in *E. coli* from sugars and other readily available substrates, as well as achieving its production from inexpensive gaseous substrates such as methane, syngas, and knallgas. Up to date, only the production of 3-hydroxybutyrate has been demonstrated from syngas, remaining the production of this acid from knallgas and methane, as well as the production of *mcl*-hydroxy acids a completely unexplored area of research.

Finally, the secretion and lytic systems, mainly developed during the last two decades, open the possibility of a facile and inexpensive PHA recovery, combined with efficient chemical or enzymatic hydrolysis methods, they can constitute a powerful combination for gaining access to a wide range of 3-hydroxy acids.

## AUTHOR CONTRIBUTIONS

All the authors performed literature search and drafted sections of the manuscript. LY, RC, and FS drafted most of the sections dealing with PHA accumulation, 3HA production and alternative PHA recovery strategies. AV-F drafted sections dealing with the different substrates used for PHA production and created **Figure 1**. All authors revised the manuscript and approved the final version.

## REFERENCES

- Adkins, J., Pugh, S., McKenna, R., and Nielsen, D. R. (2012). Engineering microbial chemical factories to produce renewable “biomonomers.” *Front. Microbiol.* 3:313. doi: 10.3389/fmicb.2012.00313
- Agarwal, A. S., Zhai, Y., Hill, D., and Sridhar, N. (2011). The electrochemical reduction of carbon dioxide to formate/formic acid: engineering and economic feasibility. *ChemSusChem* 4, 1301–1310. doi: 10.1002/cssc.201100220
- Agnew, D. E., Stevermer, A. K., Youngquist, J. T., and Pflieger, B. F. (2012). Engineering *Escherichia coli* for production of C12–C14 polyhydroxyalkanoate from glucose. *Metab. Eng.* 14, 705–713. doi: 10.1016/j.ymben.2012.08.003
- Alves, M. I., Macagnan, K. L., Rodrigues, A. A., de Assis, D. A., Torres, M. M., de Oliveira, P. D., et al. (2017). Poly(3-hydroxybutyrate)-P(3HB): review of production process technology. *Ind. Biotechnol.* 13, 192–208. doi: 10.1089/ind.2017.0013
- Amulya, K., Jukuri, S., and Venkata Mohan, S. (2015). Sustainable multistage process for enhanced productivity of bioplastics from waste remediation through aerobic dynamic feeding strategy: process integration for up-scaling. *Bioresour. Technol.* 188, 231–239. doi: 10.1016/j.biortech.2015.01.070
- Anis, S. N. S., Annur, M. S. M., and Simarani, K. (2018). Microbial biosynthesis and *in vivo* depolymerization of intracellular medium-chain-length poly-3-hydroxyalkanoates as potential route to platform chemicals. *Biotechnol. Appl. Biochem.* 65, 784–796. doi: 10.1002/bab.1666
- Bera, A., Dubey, S., Bhayani, K., Mondal, D., Mishra, S., and Ghosh, P. K. (2015). Microbial synthesis of polyhydroxyalkanoate using seaweed-derived crude levulinic acid as co-nutrient. *Int. J. Biol. Macromol.* 72, 487–494. doi: 10.1016/j.ijbiomac.2014.08.037
- Bhati, R., and Mallick, N. (2016). Carbon dioxide and poultry waste utilization for production of polyhydroxyalkanoate biopolymers by *Nostoc muscorum* Agardh: a sustainable approach. *J. Appl. Phycol.* 28, 161–168. doi: 10.1007/s10811-015-0573-x
- Biddy, M. J., Scarlata, C. J., and Kinchin, C. M. (2016). *Chemicals From Biomass: A Market Assessment of Bioproducts With Near-Term Potential*. Golden, CO: NREL.
- Biernacki, M., Riechen, J., Hähnel, U., Roick, T., Baronian, K., Bode, R., et al. (2017). Production of (R)-3-hydroxybutyric acid by *Arxula adenivorans*. *AMB Express* 7, 1–12. doi: 10.1186/s13568-016-0303-z
- Borrero-de Acuña, J. M., Aravena-Carrasco, C., Gutierrez-Urrutia, I., Duchens, D., and Poblete-Castro, I. (2019). Enhanced synthesis of medium-chain-length poly(3-hydroxyalkanoates) by inactivating the tricarboxylate transport system of *Pseudomonas putida* KT2440 and process development using waste vegetable oil. *Process Biochem.* 77, 23–30. doi: 10.1016/j.procbio.2018.10.012
- Borrero-de Acuña, J. M., Hidalgo-Dumont, C., Pacheco, N., Cabrera, A., and Poblete-Castro, I. (2017). A novel programmable lysozyme-based lysis system in *Pseudomonas putida* for biopolymer production. *Sci. Rep.* 7:4373. doi: 10.1038/s41598-017-04741-2
- Brämer, C. O., Vandamme, P., da Silva, L. F., Gomez, J. G., and Steinbüchel, A. (2001). Polyhydroxyalkanoate-accumulating bacterium isolated from soil of a sugar-cane plantation in Brazil. *Int. J. Syst. Evol. Microbiol.* 51, 1709–1713. doi: 10.1099/00207113-51-5-1709
- Braunegg, G., Bona, R., and Koller, M. (2004). Sustainable polymer production. *Polym. Plast. Technol. Eng.* 43, 1779–1793. doi: 10.1081/PPT-200040130

## FUNDING

FS gratefully acknowledges financial support from CONICYT – Chile (National Commission for Scientific and Technological Research), grants Fondecyt Iniciación 11170081 and Proyectos REDES ETAPA INICIAL, Convocatoria 2017, REDI170254. LY, AV-F, and FS acknowledge financial support from grant Apoyo a la Formación de Redes Internacionales entre Centros de Investigación REDES190137, CONICYT-PCI.

- Bresan, S., Sznajder, A., Hauf, W., Forchhammer, K., Pfeiffer, D., and Jendrossek, D. (2016). Polyhydroxyalkanoate (PHA) granules have no phospholipids. *Sci. Rep.* 6:26612. doi: 10.1038/srep26612
- Brigham, C. (2019). Perspectives for the biotechnological production of biofuels from CO<sub>2</sub> and H<sub>2</sub> using *Ralstonia eutropha* and other ‘Knallgas’ bacteria. *Appl. Microbiol. Biotechnol.* 103, 2113–2120. doi: 10.1007/s00253-019-09636-y
- Brigham, C. J., Speth, D. R., Rha, C., and Sinskey, A. J. (2012). Whole-genome microarray and gene deletion studies reveal regulation of the polyhydroxyalkanoate production cycle by the stringent response in *Ralstonia eutropha* H16. *Appl. Environ. Microbiol.* 78, 8033–8044. doi: 10.1128/AEM.01693-12
- Bugnicourt, E., Cinelli, P., Lazzeri, A., and Alvarez, V. (2014). Polyhydroxyalkanoate (PHA): review of synthesis, characteristics, processing and potential applications in packaging. *Express Polym. Lett.* 8, 791–808. doi: 10.3144/expresspolymlett.2014.82
- Cao, Q., Zhang, J., Liu, H., Wu, Q., Chen, J., and Chen, G.-Q. (2014). The mechanism of anti-osteoporosis effects of 3-hydroxybutyrate and derivatives under simulated microgravity. *Biomaterials* 35, 8273–8283. doi: 10.1016/j.biomaterials.2014.06.020
- Chen, G.-Q. (2009). A microbial polyhydroxyalkanoates (PHA) based bio- and materials industry. *Chem. Soc. Rev.* 38:2434. doi: 10.1039/b812677c
- Chen, G.-Q., König, K.-H., Lafferty, and R. M. (1991). Production of poly-D(-)-3-hydroxybutyrate and poly-D(-)-3-hydroxyvalerate by strains of *Alcaligenes latus*. *Anton. Leeuwen.* 60, 61–66. doi: 10.1007/BF00580443
- Chen, G.-Q., and Patel, M. K. (2012). Plastics derived from biological sources: present and future: a technical and environmental review. *Chem. Rev.* 112, 2082–2099. doi: 10.1021/cr200162d
- Chen, X., Tao, L., Shekiri, J., Mohaghghi, A., Decker, S., Wang, W., et al. (2012). Improved ethanol yield and reduced Minimum Ethanol Selling Price (MESP) by modifying low severity dilute acid pretreatment with deacetylation and mechanical refining: 1) experimental. *Biotechnol. Biofuels* 5:60. doi: 10.1186/1754-6834-5-60
- Chen, X., Zhou, L., Tian, K., Kumar, A., Singh, S., Prior, B. A., et al. (2013). Metabolic engineering of *Escherichia coli*: a sustainable industrial platform for bio-based chemical production. *Biotechnol. Adv.* 31, 1200–1223. doi: 10.1016/j.biotechadv.2013.02.009
- Choi, J., and Lee, S. Y. (1999). Factors affecting the economics of polyhydroxyalkanoate production by bacterial fermentation. *Appl. Microbiol. Biotechnol.* 51, 13–21. doi: 10.1007/s002530051357
- Choi, M. H., Yoon, S. C., and Lenz, R. W. (1999). Production of poly(3-hydroxybutyric acid-co-4-hydroxybutyric acid) and poly(4-hydroxybutyric acid) without subsequent degradation by *Hydrogenophaga pseudoflava*. *Appl. Environ. Microbiol.* 65, 1570–1577.
- Chung, A., Liu, Q., Ouyang, S. P., Wu, Q., and Chen, G. Q. (2009). Microbial production of 3-hydroxydodecanoic acid by *pha* operon and *fadBA* knockout mutant of *Pseudomonas putida* KT2442 harboring *tesB* gene. *Appl. Microbiol. Biotechnol.* 83, 513–519. doi: 10.1007/s00253-009-1919-6
- Costa, T. R. D., Felisberto-rodrigues, C., Meir, A., Prevost, M. S., Redzej, A., Trokter, M., et al. (2015). Secretion systems in Gram-negative insights. *Nat. Publ. Gr.* 13, 343–359. doi: 10.1038/nrmicro3456
- Cruz, M. V., Freitas, F., Paiva, A., Mano, F., Dionísio, M., Ramos, A. M., et al. (2016). Valorization of fatty acids-containing wastes and byproducts into short- and medium-chain length polyhydroxyalkanoates. *N. Biotechnol.* 33, 206–215. doi: 10.1016/j.nbt.2015.05.005

- Cruz, M. V., Paiva, A., Lisboa, P., Freitas, F., Alves, V. D., Simões, P., et al. (2014). Production of polyhydroxyalkanoates from spent coffee grounds oil obtained by supercritical fluid extraction technology. *Bioresour. Technol.* 157, 360–363. doi: 10.1016/j.biortech.2014.02.013
- de Paula, F. C., Kakazu, S., de Paula, C. B. C., Gomez, J. G. C., and Contiero, J. (2017). Polyhydroxyalkanoate production from crude glycerol by newly isolated *Pandoraea* sp. *J. King Saud Univ. Sci.* 29, 166–173. doi: 10.1016/j.jksus.2016.07.002
- de Roo, G., Kellerhals, M. B., Ren, Q., Witholt, B., and Kessler, B. (2002). Production of chiral R-3-hydroxyalkanoic acids and R-3-hydroxyalkanoic acid methylesters via hydrolytic degradation of polyhydroxyalkanoate synthesized by pseudomonads. *Biotechnol. Bioeng.* 77, 717–722. doi: 10.1002/bit.10139
- Dietrich, D., Illman, B., and Crooks, C. (2013). Differential sensitivity of polyhydroxyalkanoate producing bacteria to fermentation inhibitors and comparison of polyhydroxybutyrate production from *Burkholderia cepacia* and *Pseudomonas pseudoflava*. *BMC Res. Notes* 6:219. doi: 10.1186/1756-0500-6-219
- Dietrich, K., Dumont, M.-J. J., Del Rio, L. F., and Orsat, V. V. (2016). Producing PHAs in the bioeconomy - Towards a sustainable bioplastic. *Sustain. Prod. Consum.* 9, 58–70. doi: 10.1016/j.spc.2016.09.001
- Doi, Y. (1990). Cyclic nature of poly(3-hydroxyalkanoate) metabolism in *Alcaligenes eutrophus*. *FEMS Microbiol. Lett.* 67, 165–169. doi: 10.1016/0378-1097(90)90188-V
- Fei, T., Cazeneuve, S., Wen, Z., Wu, L., and Wang, T. (2016). Effective recovery of poly-β-hydroxybutyrate (PHB) biopolymer from *Cupriavidus necator* using a novel and environmentally friendly solvent system. *Biotechnol. Prog.* 32, 678–685. doi: 10.1002/btpr.2247
- Flüchter, S., Follonier, S., Schiel-Bengelsdorf, B., Bengelsdorf, F. R., Zinn, M., and Dürre, P. (2019). Anaerobic production of poly(3-hydroxybutyrate) and its precursor 3-hydroxybutyrate from synthesis gas by autotrophic clostridia. *Biomacromolecules* 20, 3271–3282. doi: 10.1021/acs.biomac.9b00342
- Follonier, S. (2015). Pilot-scale production of functionalized mcl-PHA from grape pomace supplemented with fatty acids. *Chem. Biochem. Eng. Q.* 29, 113–121. doi: 10.15255/CABEQ.2014.2251
- Fuhrmann, E., and Talbiersky, J. (2005). Synthesis of alkyl aryl ethers by catalytic williamson ether synthesis with weak alkylation agents. *Org. Process Res. Dev.* 9, 206–211. doi: 10.1021/op050001h
- Gao, H. J., Wu, Q., and Chen, G. Q. (2002). Enhanced production of D-(-)-3-hydroxybutyric acid by recombinant *Escherichia coli*. *FEMS Microbiol. Lett.* 213, 59–65. doi: 10.1016/S0378-1097(02)00788-7
- Gao, X., Chen, J.-C. C., Wu, Q., and Chen, G.-Q. Q. (2011). Polyhydroxyalkanoates as a source of chemicals, polymers, and biofuels. *Curr. Opin. Biotechnol.* 22, 768–774. doi: 10.1016/j.copbio.2011.06.005
- Gebauer, B., and Jendrossek, D. (2006). Assay of poly(3-hydroxybutyrate) depolymerase activity and product determination. *Appl. Environ. Microbiol.* 72, 6094–6100. doi: 10.1128/AEM.01184-06
- Geyer, R., Jambeck, J. R., and Law, K. L. (2017). Production, use, and fate of all plastics ever made. *Sci. Adv.* 3:e1700782. doi: 10.1126/sciadv.1700782
- Gómez Cardozo, J. R., Mora Martínez, A. L., Yepes Pérez, M., and Correa Londoño, G. A. (2016). Production and characterization of polyhydroxyalkanoates and native microorganisms synthesized from fatty waste. *Int. J. Polym. Sci.* 2016, 1–12. doi: 10.1155/2016/6541718
- Gorenflo, V., Schmack, G., Vogel, R., and Steinbüchel, A. (2001). Development of a process for the biotechnological large-scale production of 4-hydroxyvalerate-containing polyesters and characterization of their physical and mechanical properties. *Biomacromolecules* 2, 45–57. doi: 10.1021/bm0000992
- Green, E. R., and Mecsas, J. (2016). Bacterial secretion systems: an overview. *Microbiol. Spectr.* 4, 215–239. doi: 10.1128/microbiolspec.vmbf-0012-2015
- Grousseau, E., Blanchet, E., Délérès, S., Albuquerque, M. G. E., Paul, E., and Uribe Larrea, J. L. (2013). Impact of sustaining a controlled residual growth on polyhydroxybutyrate yield and production kinetics in *Cupriavidus necator*. *Bioresour. Technol.* 148, 30–38. doi: 10.1016/j.biortech.2013.08.120
- Guevara-Martínez, M., Gällnö, K. S., Sjöberg, G., Jarmander, J., Perez-Zabaleta, M., Quillaguamán, J., et al. (2015). Regulating the production of (R)-3-hydroxybutyrate in *Escherichia coli* by N or P limitation. *Front. Microbiol.* 6, 844. doi: 10.3389/fmicb.2015.00844
- Guevara-Martínez, M., Perez-Zabaleta, M., Gustavsson, M., Quillaguamán, J., Larsson, G., and van Maris, A. J. A. (2019). The role of the acyl-CoA thioesterase “YciA” in the production of (R)-3-hydroxybutyrate by recombinant *Escherichia coli*. *Appl. Microbiol. Biotechnol.* 103, 3693–3704. doi: 10.1007/s00253-019-09707-0
- Haas, C. (2015). Production of PHB from chicory roots – Comparison of three *Cupriavidus necator* strains. *Chem. Biochem. Eng. Q.* 29, 99–112. doi: 10.15255/CABEQ.2014.2250
- Hahn, S. K., Chang, Y. K., Kim, B. S., and Chang, H. N. (1994). Optimization of microbial poly(3-hydroxybutyrate) recover using dispersions of sodium hypochlorite solution and chloroform. *Biotechnol. Bioeng.* 44, 256–261. doi: 10.1002/bit.260440215
- Hamilton, L. A., Feilt, S., Muffett, C., Kelso, M., Rubright, S., Bernhardt, C., et al. (2019). *The Hidden Costs of a Plastic Planet*. Available online at: www.ciel.org/plasticandclimate
- Handrick, R., Reinhardt, S., Focarete, M. L., Scandola, M., Adamus, G., Kowalczyk, M., et al. (2001). A new type of thermoalkalophilic hydrolase of *Paucimonas lemoignei* with high specificity for amorphous polyesters of short chain-length hydroxyalkanoic acids. *J. Biol. Chem.* 276, 36215–36224. doi: 10.1074/jbc.M101106200
- Hänggi, U. J. (2012). Pilot scale production of PHB with *Alcaligenes latus*. *Nov. Biograd. Microb. Polym.* 65–70. doi: 10.1007/978-94-009-2129-0\_6
- Hazer, D. B., Kiliçay, E., and Hazer, B. (2012). Poly(3-hydroxyalkanoate)s: diversification and biomedical applications. *Mater. Sci. Eng. C* 32, 637–647. doi: 10.1016/j.msec.2012.01.021
- Heinrich, D., Madkour, M. H., Al-Ghamdi, M. A., Shabbaj, I. L., and Steinbüchel, A. (2012). Large scale extraction of poly(3-hydroxybutyrate) from *Ralstonia eutropha* H16 using sodium hypochlorite. *AMB Express* 2, 1–6. doi: 10.1186/2191-0855-2-59
- Henderson, I. R., and He, M. (2009). Secretion and subcellular localizations of bacterial proteins: a semantic awareness issue. *Trends Microbiol.* 17, 139–145. doi: 10.1016/j.tim.2009.01.004
- Henderson, R. A., and Jones, C. W. (1997). Physiology of poly-3-hydroxybutyrate (PHB) production by *Alcaligenes eutrophus* growing in continuous culture. *Microbiology* 143, 2361–2371. doi: 10.1099/00221287-143-7-2361
- Hiroe, A., Chek, M. F., Hakoshima, T., Sudesh, K., and Taguchi, S. (2019). “Synthesis of polyesters III: acyltransferase as catalyst,” in *Enzymatic Polymerization towards Green Polymer Chemistry*, eds S. Kobayashi, H. Uyama, K.J. Singapore: Springer, 199–231. doi: 10.1007/978-981-13-3813-7\_7
- Hodge, D. B., Karim, M. N., Schell, D. J., McMillan, J. D. (2008). Soluble and insoluble solids contributions to high-solids enzymatic hydrolysis of lignocellulose. *Bioresour. Technol.* 99, 8940–8948. doi: 10.1016/j.biortech.2008.05.015
- Hölscher, T., Breuer, U., Adrian, L., Harms, H., and Maskow, T. (2010). Production of the chiral compound (R)-3-hydroxybutyrate by a genetically engineered methylotrophic bacterium. *Appl. Environ. Microbiol.* 76, 5585–5591. doi: 10.1128/AEM.01065-10
- Hori, K., Kaneko, M., Tanji, Y., Xing, X.-H., and Unno, H. (2002). Construction of self-disruptive *Bacillus megaterium* in response to substrate exhaustion for polyhydroxybutyrate production. *Appl. Microbiol. Biotechnol.* 59, 211–216. doi: 10.1007/s00253-002-0986-8
- James, B. W., Mauchline, W. S., Dennis, P. J., Keevil, C. W., and Wait, R. (1999). Poly-3-hydroxybutyrate in *Legionella pneumophila*, an energy source for survival in low-nutrient environments. *Appl. Environ. Microbiol.* 65, 822–827.
- Jarmander, J., Belotserkovsky, J., Sjöberg, G., Guevara-Martínez, M., Pérez-Zabaleta, M., Quillaguamán, J., et al. (2015). Cultivation strategies for production of (R)-3-hydroxybutyric acid from simultaneous consumption of glucose, xylose and arabinose by *Escherichia coli*. *Microb. Cell Fact.* 14:51. doi: 10.1186/s12934-015-0236-2
- Jers, C., Kalantari, A., Garg, A., and Mijakovic, I. (2019). Production of 3-hydroxypropanoic acid from glycerol by metabolically engineered bacteria. *Front. Bioeng. Biotechnol.* 7:124. doi: 10.3389/fbioe.2019.00124
- Jiang, G., Hill, D., Kowalczyk, M., Johnston, B., Adamus, G., Irorere, V., et al. (2016). Carbon sources for polyhydroxyalkanoates and an integrated biorefinery. *Int. J. Mol. Sci.* 17:1157. doi: 10.3390/ijms17071157
- Jiang, G., Johnston, B., Townrow, D., Radecka, I., Koller, M., Chaber, P., et al. (2018). Biomass extraction using non-chlorinated solvents for

- biocompatibility improvement of polyhydroxyalkanoates. *Polymers* 10:731. doi: 10.3390/polym10070731
- Jossek, R., Reichelt, R., and Steinbüchel, A. (1998). *In vitro* biosynthesis of poly(3-hydroxybutyric acid) by using purified poly(hydroxyalkanoic acid) synthase of *Chromatium vinosum*. *Appl. Microbiol. Biotechnol.* 49, 258–266. doi: 10.1007/s002530051166
- Jossek, R., and Steinbüchel, A. (1998). *In vitro* synthesis of poly(3-hydroxybutyric acid) by using an enzymatic coenzyme A recycling system. *FEMS Microbiol. Lett.* 168, 319–324. doi: 10.1111/j.1574-6968.1998.tb13290.x
- Juengert, J. R., Borisova, M., Mayer, C., Wolz, C., Brigham, C. J., Sinskey, A. J., et al. (2017). Absence of ppGpp leads to increased mobilization of intermediately accumulated poly(3-hydroxybutyrate) in *Ralstonia eutropha* H16. *Appl. Environ. Microbiol.* 83:AEM.00755–00717. doi: 10.1128/AEM.00755-17
- Juengert, J. R., Patterson, C., and Jendrossek, D. (2018). Poly(3-hydroxybutyrate) (PHB) polymerase PhaC1 and PHB depolymerase PhaZa1 of *Ralstonia eutropha* are phosphorylated *in vivo*. *Appl. Environ. Microbiol.* 84, 1–12. doi: 10.1128/AEM.00604-18
- Kawata, Y., Ando, H., Matsushita, I., and Tsubota, J. (2014). Efficient secretion of (R)-3-hydroxybutyric acid from *Halomonas* sp. KM-1 by nitrate fed-batch cultivation with glucose under microaerobic conditions. *Bioresour. Technol.* 156, 400–403. doi: 10.1016/j.biortech.2014.01.073
- Kawata, Y., Kawasaki, K., and Shigeri, Y. (2012). Efficient secreted production of (R)-3-hydroxybutyric acid from living *Halomonas* sp. KM-1 under successive aerobic and microaerobic conditions. *Appl. Microbiol. Biotechnol.* 96, 913–920. doi: 10.1007/s00253-012-4218-6
- Kawata, Y., Nojiri, M., Matsushita, I., and Tsubota, J. (2015). Improvement of (R)-3-hydroxybutyric acid secretion during *Halomonas* sp. KM-1 cultivation with saccharified Japanese cedar by the addition of urea. *Let. Appl. Microbiol.* 61, 397–402. doi: 10.1111/lam.12473
- Keenan, T. M., Nakas, J. P., and Tanenbaum, S. W. (2006). Polyhydroxyalkanoate copolymers from forest biomass. *J. Ind. Microbiol. Biotechnol.* 33, 616–626. doi: 10.1007/s10295-006-0131-2
- Khosravi-Darani, K. (2015). Application of Poly(hydroxyalkanoate) In food packaging: improvements by nanotechnology. *Chem. Biochem. Eng. Q.* 29, 275–285. doi: 10.15255/CABEQ.2014.2260
- Khosravi-Darani, K., Mokhtari, Z. B., Amari, T., and Tanaka, K. (2013). Microbial production of poly(hydroxybutyrate) from C1 carbon sources. *Appl. Microbiol. Biotechnol.* 97, 1407–1424. doi: 10.1007/s00253-012-4649-0
- Kim, B. S., Lee, S. C., Lee, S. Y., Chang, H. N., Chang, Y. K., and Woo, S. I. (1994). Production of poly(3-hydroxybutyric acid) by fed-batch culture of *Alcaligenes eutrophus* with glucose concentration control. *Biotechnol. Bioeng.* 43, 892–898. doi: 10.1002/bit.260430908
- Kim, M., Cho, K. S., Ryu, H. W., Lee, E. G., and Chang, Y. K. (2003). Recovery of poly(3-hydroxybutyrate) from high cell density culture of *Ralstonia eutropha* by direct addition of sodium dodecyl sulfate. *Biotechnol. Lett.* 25, 55–59. doi: 10.1023/A:1021734216612
- Kim, T. W., Park, J. S., and Lee, Y. H. (1996). Enzymatic characteristics of biosynthesis and degradation of poly-β-hydroxybutyrate of *Alcaligenes latus*. *J. Microbiol. Biotechnol.* 6, 425–431.
- Knoll, M., Hamm, T. M., Wagner, F., Martinez, V., and Pleiss, J. (2009). The PHA depolymerase engineering database: a systematic analysis tool for the diverse family of polyhydroxyalkanoate (PHA) depolymerases. *BMC Bioinformatics* 10:89. doi: 10.1186/1471-2105-10-89
- Koller, M. (2014). Poly(hydroxyalkanoates) for food packaging: application and attempts towards implementation. *Appl. Food Biotechnol.* 1, 3–15.
- Kosseva, M. R., and Rusbandi, E. (2018). Trends in the biomanufacture of polyhydroxyalkanoates with focus on downstream processing. *Int. J. Biol. Macromol.* 107, 762–778. doi: 10.1016/j.ijbiomac.2017.09.054
- Kubowicz, S., and Booth, A. M. (2017). Biodegradability of plastics: challenges and misconceptions. *Environ. Sci. Technol.* 51, 12058–12060. doi: 10.1021/acs.est.7b04051
- Kumar, P., Ray, S., and Kalia, V. C. (2016). Production of co-polymers of polyhydroxyalkanoates by regulating the hydrolysis of biowastes. *Bioresour. Technol.* 200, 413–419. doi: 10.1016/j.biortech.2015.10.045
- Kunasundari, B., and Sudesh, K. (2011). Isolation and recovery of microbial polyhydroxyalkanoates. *Express Polym. Lett.* 5, 620–634. doi: 10.3144/expresspolymlett.2011.60
- Lafferty, R. M. (1977). *Process for the Manufacture of D(-)-3-Hydroxybutyric Acid and D(-)-3-Hydroxybutyric Acid Producing Mutants*. US4211846A.
- Lafferty, R. M., and Heinzle, E. (1977). *Cyclic Carbonic Acid Esters as Solvents for Poly-β-Hydroxybutyric Acid*. US4101533A.
- Lawrence, A. G., Schoenheit, J., He, A., Tian, J., Liu, P., Stubbe, J., et al. (2005). Transcriptional analysis of *Ralstonia eutropha* genes related to poly-(R)-3-hydroxybutyrate homeostasis during batch fermentation. *Appl. Microbiol. Biotechnol.* 68, 663–672. doi: 10.1007/s00253-005-1969-3
- Lee, I. (1995). Regulation of poly-β-hydroxybutyrate biosynthesis by nicotinamide nucleotide in *Alcaligenes eutrophus*. *FEMS Microbiol. Lett.* 131, 35–39. doi: 10.1016/0378-1097(95)00231-S
- Lee, S.-H., Park, S. J., Lee, S. Y., and Hong, S. H. (2008). Biosynthesis of enantiopure (S)-3-hydroxybutyric acid in metabolically engineered *Escherichia coli*. *Appl. Microbiol. Biotechnol.* 79, 633–641. doi: 10.1007/s00253-008-1473-7
- Lee, S. Y., and Lee, Y. (2003). Metabolic engineering of *Escherichia coli* for production of enantiomerically pure (R)-(-)-hydroxycarboxylic acids. *Appl. Environ. Microbiol.* 69, 3421–3426. doi: 10.1128/AEM.69.6.3421
- Lee, S. Y., Lee, Y., and Wang, F. (1999). Chiral compounds from bacterial polyesters: sugars to plastics to fine chemicals. *Biotechnol. Bioeng.* 65, 363–368. doi: 10.1002/(SICI)1097-0290(19991105)65:3<363::AID-BIT15>3.0.CO;2-1
- Lee, Y., Park, S. H., Lim, I. T., Han, K., and Lee, S. Y. (2000). Preparation of alkyl (R)-(-)-3-hydroxybutyrate by acidic alcoholysis of poly-(R)-(-)-3-hydroxybutyrate. *Enzyme Microb. Technol.* 27, 33–36. doi: 10.1016/S0141-0229(00)00146-0
- Levett, I., Birkett, G., Davies, N., Bell, A., Langford, A., Laycock, B., et al. (2016). Techno-economic assessment of poly-3-hydroxybutyrate (PHB) production from methane—The case for thermophilic bioprocessing. *J. Environ. Chem. Eng.* 4, 3724–3733. doi: 10.1016/j.jece.2016.07.033
- Li, F., Zhang, C., Liu, Y., Liu, D., Xia, H., and Chen, S. (2016). Efficient production of (R)-3-hydroxybutyric acid by *Pseudomonas* sp. DS1001a and its extracellular poly(3-hydroxybutyrate) depolymerase. *Process Biochem.* 51, 369–373. doi: 10.1016/j.procbio.2015.12.016
- Liddell, J. M. (1999). Process for the recovery of Polyhydroxyalkanoic acid. *U.S. Pat.* 5, 12–14.
- Linton, E., Walsh, M. K., Sims, R. C., and Miller, C. D. (2012). Translocation of green fluorescent protein by comparative analysis with multiple signal peptides. *Biotechnol. J.* 7, 667–676. doi: 10.1002/biot.201100158
- Listewnik, H.-F., Wendlandt, K.-D., Jechorek, M., and Mirschel, G. (2007). Process design for the microbial synthesis of poly-β-hydroxybutyrate (PHB) from natural gas. *Eng. Life Sci.* 7, 278–282. doi: 10.1002/elsc.200620193
- Liu, Q., Ouyang, S. P., Chung, A., Wu, Q., and Chen, G. Q. (2007). Microbial production of R-3-hydroxybutyric acid by recombinant *E. coli* harboring genes of phbA, phbB, and tesB. *Appl. Microbiol. Biotechnol.* 76, 811–818. doi: 10.1007/s00253-007-1063-0
- Lo, C.-Y., Lee, W.-H., Tsuge, T., Doi, Y., and Sudesh, K. (2005). Biosynthesis and characterization of poly(3-hydroxybutyrate-co-3-hydroxyhexanoate) from palm oil products in a *Wautersia eutropha* mutant. *Biotechnol. Lett.* 27, 1405–1410. doi: 10.1007/s10529-005-0690-8
- Loow, Y.-L., Wu, T. Y., Md. Jahim, J., Mohammad, A. W., and Teoh, W. H. (2016). Typical conversion of lignocellulosic biomass into reducing sugars using dilute acid hydrolysis and alkaline pretreatment. *Cellulose* 23, 1491–1520. doi: 10.1007/s10570-016-0936-8
- Lu, J., Brigham, C. J., Li, S., and Sinskey, A. J. (2016). *Ralstonia eutropha* H16 as a platform for the production of biofuels, biodegradable plastics, and fine chemicals from diverse carbon resources. *Biotechnol. Biofuel Prod. Optim.* 2016, 325–351. doi: 10.1016/B978-0-444-63475-7.00012-1
- Lu, J., Tappel, R. C., and Nomura, C. T. (2009). Mini-review: biosynthesis of poly(hydroxyalkanoates). *Polym. Rev.* 49, 226–248. doi: 10.1080/15583720903048243
- Martínez, V., García, P., García, J. L., and Prieto, M. A. (2011). Controlled autolysis facilitates the polyhydroxyalkanoate recovery in *Pseudomonas putida* KT2440. *Microb. Biotechnol.* 4, 533–547. doi: 10.1111/j.1751-7915.2011.00257.x
- Martínez, V., Herencias, C., Jurkevitch, E., and Prieto, M. A. (2016). Engineering a predatory bacterium as a proficient killer agent for intracellular bio-products recovery: the case of the polyhydroxyalkanoates. *Sci. Rep.* 6:24381. doi: 10.1038/srep24381

- Matsumoto, K., Okei, T., Honma, I., Ooi, T., Aoki, H., and Taguchi, S. (2013). Efficient (R)-3-hydroxybutyrate production using acetyl CoA-regenerating pathway catalyzed by coenzyme A transferase. *Appl. Microbiol. Biotechnol.* 97, 205–210. doi: 10.1007/s00253-012-4104-2
- Matsuyama, A., Yamamoto, H., Kawada, N., and Kobayashi, Y. (2001). Industrial production of (R)-1,3-butanediol by new biocatalysts. *J. Mol. Catal. B Enzym.* 11, 513–521. doi: 10.1016/S1381-1177(00)00032-1
- McMahon, M. D., and Prather, K. L. J. (2014). Functional screening and *in vitro* analysis reveal thioesterases with enhanced substrate specificity profiles that improve short-chain fatty acid production in *Escherichia coli*. *Appl. Environ. Microbiol.* 80, 1042–1050. doi: 10.1128/AEM.03303-13
- Melih Tamer, I., Moo-Young, M., and Chisti, Y. (1998). Disruption of *Alcaligenes latus* for recovery of poly( $\beta$ -hydroxybutyric acid): comparison of high-pressure homogenization, bead milling, and chemically induced lysis. *Ind. Eng. Chem. Res.* 37, 1807–1814.
- Mikkilä, I., Karlapudi, A. P., Venkateswarulu, T. C., D. J. B., Nath, S. B., and Kodali, V. P. (2014). Isolation, screening and extraction of polyhydroxybutyrate (PHB) producing bacteria from sewage sample. *Int. J. Pharm. Tech. Res.* 6, 850–857.
- Miscevic, D., Srirangan, K., Kefale, T., Kilpatrick, S., Chung, D. A., Moo-Young, M., et al. (2019). Heterologous production of 3-hydroxyvalerate in engineered *Escherichia coli*. *Metab. Eng.* doi: 10.1016/j.mben.2019.11.005. [Epub ahead of print].
- Misra, S. K., Valappil, S. P., Roy, I., and Boccaccini, A. R. (2006). Polyhydroxyalkanoate (PHA)/inorganic phase composites for tissue engineering applications. *Biomacromolecules* 7, 2249–2258. doi: 10.1021/bm060317c
- Mothes, G., Schnorpfel, C., and Ackermann, J.-U. (2007). Production of PHB from crude glycerol. *Eng. Life Sci.* 7, 475–479. doi: 10.1002/elsc.200620210
- Mozejko-Ciesielska, J., Dabrowska, D., Szalewska-Palasz, A., and Ciesielski, S. (2017). Medium-chain-length polyhydroxyalkanoates synthesis by *Pseudomonas putida* KT2440 relA/spoT mutant: bioprocess characterization and transcriptome analysis. *AMB Express* 7:92. doi: 10.1186/s13568-017-0396-z
- Mozejko-Ciesielska, J., and Kiewisz, R. (2016). Bacterial polyhydroxyalkanoates: still fabulous? *Microbiol. Res.* 192, 271–282. doi: 10.1016/j.micres.2016.07.010
- Naggert, J., Narasimhan, M. L., DeVeaux, L., Cho, H., Randhawa, Z. I., Cronan, J. E., et al. (1991). Cloning, sequencing, and characterization of *Escherichia coli* thioesterase II. *J. Biol. Chem.* 266, 11044–11050.
- Nakano, K., Rischke, M., Sato, S., and Märkl, H. (1997). Influence of acetic acid on the growth of *Escherichia coli* K12 during high-cell-density cultivation in a dialysis reactor. *Appl. Microbiol. Biotechnol.* 48, 597–601. doi: 10.1007/s002530051101
- Naranjo, J. M., Posada, J. A., Higuera, J. C., and Cardona, C. A. (2013). Valorization of glycerol through the production of biopolymers: the PHB case using *Bacillus megaterium*. *Bioresour. Technol.* 133, 38–44. doi: 10.1016/j.biortech.2013.01.129
- Nicaud, J. M., Mackman, N., Gray, L., and Holland, I. B. (1986). The C-terminal, 23 kDa peptide of *E. coli* haemolysin 2001 contains all the information necessary for its secretion by the haemolysin (Hly) export machinery. *FEBS Lett.* 204, 331–335. doi: 10.1016/0014-5793(86)80838-9
- Nozawa, T., Sato, S., and Takahashi, R. (2009). Vapor-phase dehydration of 1,3-butanediol over CeO<sub>2</sub>-ZrO<sub>2</sub> catalysts. *Top. Catal.* 52, 609–617. doi: 10.1007/s11244-009-9198-0
- Obruca, S., Sedlacek, P., Mravec, F., Samek, O., and Marova, I. (2016). Evaluation of 3-hydroxybutyrate as an enzyme-protective agent against heating and oxidative damage and its potential role in stress response of poly(3-hydroxybutyrate) accumulating cells. *Appl. Microbiol. Biotechnol.* 100, 1365–1376. doi: 10.1007/s00253-015-7162-4
- Oh, Y. H., Lee, S. H., Jang, Y.-A., Choi, J. W., Hong, K. S., Yu, J. H., et al. (2015). Development of rice bran treatment process and its use for the synthesis of polyhydroxyalkanoates from rice bran hydrolysate solution. *Bioresour. Technol.* 181, 283–290. doi: 10.1016/j.biortech.2015.01.075
- Pan, W., Nomura, C. T., and Nakas, J.P. (2012). Estimation of inhibitory effects of hemicellulosic wood hydrolysate inhibitors on PHA production by *Burkholderia cepacia* ATCC 17759 using response surface methodology. *Bioresour. Technol.* 125, 275–282. doi: 10.1016/j.biortech.2012.08.107
- Peña, C., Castillo, T., García, A., Millán, M., and Segura, D. (2014). Biotechnological strategies to improve production of microbial poly-(3-hydroxybutyrate): a review of recent research work. *Microb. Biotechnol.* 7, 278–293. doi: 10.1111/1751-7915.12129
- Pérez-Fortes, M., Schöneberger, J. C., Boulamanti, A., and Tzimas, E. (2016). Methanol synthesis using captured CO<sub>2</sub> as raw material: techno-economic and environmental assessment. *Appl. Energy* 161, 718–732. doi: 10.1016/j.apenergy.2015.07.067
- Perez-Zabaleta, M., Guevara-Martínez, M., Gustavsson, M., Quillaguamán, J., Larsson, G., and van Maris, A. J. A. (2019). Comparison of engineered *Escherichia coli* AF1000 and BL21 strains for (R)-3-hydroxybutyrate production in fed-batch cultivation. *Appl. Microbiol. Biotechnol.* 103, 5627–5639. doi: 10.1007/s00253-019-09876-y
- Poblete-Castro, I., Binger, D., Oehlert, R., and Rohde, M. (2014). Comparison of mcl-Poly(3-hydroxyalkanoates) synthesis by different *Pseudomonas putida* strains from crude glycerol: citrate accumulates at high titer under PHA-producing conditions. *BMC Biotechnol.* 14:962. doi: 10.1186/s12896-014-0110-z
- Poirier, Y., Nawrath, C., and Somerville, C. (1995). Production of polyhydroxyalkanoates, a family of biodegradable plastics and elastomers, in bacteria and plants. *Nat. Biotechnol.* 13, 142–150. doi: 10.1038/nbt0295-142
- Polyák, P., Dohovits, E., Nagy, G. N., Vértessy, B. G., Vörös, G., and Pukánszky, B. (2018). Enzymatic degradation of poly-((R)-3-hydroxybutyrate): mechanism, kinetics, consequences. *Int. J. Biol. Macromol.* 112, 156–162. doi: 10.1016/j.ijbiomac.2018.01.104
- Posada, J. A., Naranjo, J. M., López, J. A., Higuera, J. C., and Cardona, C. A. (2011). Design and analysis of poly-3-hydroxybutyrate production processes from crude glycerol. *Process Biochem.* 46, 310–317. doi: 10.1016/j.procbio.2010.09.003
- Rahman, A., Linton, E., Hatch, A. D., Sims, R. C., and Miller, C. D. (2013). Secretion of polyhydroxybutyrate in *Escherichia coli* using a synthetic biological engineering approach. *J. Biol. Eng.* 7:24. doi: 10.1186/1754-1611-7-24
- Ramsay, J. A., Berger, E., Ramsay, B., and Chavarie, C. (1990). Poly-3-hydroxyalpoic acid granules by a surfactant-hypochlorite treatment. *J. Biotechnol. Technol.* 4, 221–226.
- Ramsay, J. A., Berger, E., Voyer, R., and Chavarie, C. (1994). Extraction of poly-3-hydroxybutyrate using chlorinated solvents. *Biotechnol. Techn.* 8, 589–594.
- Raposo, R. S., de Almeida, M. C. M. D., de Oliveira, M., da, C. M. A., da Fonseca, M. M., and Cesário, M. T. (2017). A *Burkholderia sacchari* cell factory: production of poly-3-hydroxybutyrate, xylitol and xylonic acid from xylose-rich sugar mixtures. *N. Biotechnol.* 34, 12–22. doi: 10.1016/j.nbt.2016.10.001
- Rathbone, S., Furrer, P., Lübber, J., Zinn, M., and Cartmell, S. (2010). Biocompatibility of polyhydroxyalkanoate as a potential material for ligament and tendon scaffold material. *J. Biomed. Mater. Res. Part A* 93A, 1391–1403. doi: 10.1002/jbm.a.32641
- Rehm, B. H. A., Krüger, N., and Steinbüchel, A. (1998). A new metabolic link between fatty acid *de novo* synthesis and polyhydroxyalkanoic acid synthesis. *J. Biol. Chem.* 273, 24044–24051. doi: 10.1074/jbc.273.37.24044
- Reinecke, F., and Steinbüchel, A. (2008). *Ralstonia eutropha* strain H16 as model organism for PHA metabolism and for biotechnological production of technically interesting biopolymers. *J. Mol. Microbiol. Biotechnol.* 16, 91–108. doi: 10.1159/000142897
- Ren, Q., Grubelnik, A., Hoerler, M., Ruth, K., Hartmann, R., Felber, H., et al. (2005). Bacterial poly(hydroxyalkanoates) as a source of chiral hydroxyalkanoic acids. *Biomacromolecules* 6, 2290–2298. doi: 10.1021/bm050187s
- Ren, Q., Ruth, K., Thöny-Meyer, L., and Zinn, M. (2007). Process engineering for production of chiral hydroxycarboxylic acids from bacterial polyhydroxyalkanoates. *Macromol. Rapid Commun.* 28, 2131–2136. doi: 10.1002/marc.200700389
- Ren, Q., Ruth, K., Thöny-Meyer, L., and Zinn, M. (2010). Enantiomerically pure hydroxycarboxylic acids: current approaches and future perspectives. *Appl. Microbiol. Biotechnol.* 87, 41–52. doi: 10.1007/s00253-010-2530-6
- Resch, S., Gruber, K., Wanner, G., Slater, S., Dennis, D., and Lubitz, W. (1998). Aqueous release and purification of poly( $\beta$ -hydroxybutyrate) from *Escherichia coli*. 65, 173–182.
- Roe, A. J., O'Byrne, C., McLaggan, D., and Booth, I. R. (2002). Inhibition of *Escherichia coli* growth by acetic acid: a problem with methionine biosynthesis and homocysteine toxicity. *Microbiology* 148, 2215–2222. doi: 10.1099/00221287-148-7-2215

- Roohi, Z. M. R., and Kuddus, M. (2018). PHB (poly- $\beta$ -hydroxybutyrate) and its enzymatic degradation. *Polym. Adv. Technol.* 29, 30–40. doi: 10.1002/pat.4126
- Ruth, K., Grubelnik, A., Hartmann, R., Egli, T., Zinn, M., and Ren, Q. (2007). Efficient production of (R)-3-hydroxycarboxylic acids by biotechnological conversion of polyhydroxyalkanoates and their purification. *Biomacromolecules* 8, 279–286. doi: 10.1021/bm060585a
- Sabirova, J. S., Ferrer, M., Lunsdorf, H., Wray, V., Kalscheuer, R., Steinbüchel, A., et al. (2006). Mutation in a “tesB-Like” hydroxyacyl-coenzyme A-specific thioesterase gene causes hyperproduction of extracellular polyhydroxyalkanoates by *Alcanivorax borkumensis* SK2. *J. Bacteriol.* 188, 8452–8459. doi: 10.1128/JB.01321-06
- Schweitzer, D., Mullen, C. A., Boateng, A. A., and Snell, K. D. (2015). Biobased n-butanol prepared from poly-3-hydroxybutyrate: optimization of the reduction of n-butyl crotonate to n-butanol. *Org. Process Res. Dev.* 19, 710–714. doi: 10.1021/op500156b
- Seebach, D., Beck, A. K., Breitschuh, R., and Job, K. (2003). “Direct degradation of the biopolymer poly[(R)-3-hydroxybutyric acid] to (R)-3-hydroxybutanoic acid and its methyl ester,” in *Organic Syntheses* (Hoboken, NJ: John Wiley & Sons, Inc.), 39–39. doi: 10.1002/0471264180.os071.05
- Seebach, D., Chow, H.-F., Jackson, R. F. W., Sutter, M. A., Thaisrivongs, S., and Zimmermann, J. (1986). (+)-11,11'-Di-O-methylelaioophylidene – preparation from elaiophylin and total synthesis from (R)-3-hydroxybutyrate and (S)-malate. *Liebigs Ann. der Chemie* 1986, 1281–1308. doi: 10.1002/jlac.198619860714
- Shah, M., Naseer, M. I., Choi, M. H., Kim, M. O., and Yoon, S. C. (2010). Amphiphilic PHA-mPEG copolymeric nanocontainers for drug delivery: preparation, characterization and *in vitro* evaluation. *Int. J. Pharm.* 400, 165–175. doi: 10.1016/j.ijpharm.2010.08.008
- Shiraki, M., Endo, T., and Saito, T. (2006). Fermentative production of (R)-(-)-3-hydroxybutyrate using 3-hydroxybutyrate dehydrogenase null mutant of *Ralstonia eutropha* and recombinant *Escherichia coli*. *J. Biosci. Bioeng.* 102, 529–534. doi: 10.1263/jbb.102.529
- Silva, L. F., Taciro, M. K., Michelin Ramos, M. E., Carter, J. M., Pradella, J. G. C., and Gomez, J. G. C. (2004). Poly-3-hydroxybutyrate (P3HB) production by bacteria from xylose, glucose and sugarcane bagasse hydrolysate. *J. Ind. Microbiol. Biotechnol.* 31, 245–254. doi: 10.1007/s10295-004-0136-7
- Srivatsan, A., and Wang, J. D. (2008). Control of bacterial transcription, translation and replication by (p)ppGpp. *Curr. Opin. Microbiol.* 11, 100–105. doi: 10.1016/j.mib.2008.02.001
- Steinbüchel, A., Hein, S. (2001). “Biochemical and molecular basis of microbial synthesis of polyhydroxyalkanoates in microorganisms,” in: *Biopolyesters. Advances in Biochemical Engineering/Biotechnology*, Vol. 71, eds W. Babel and A. Steinbüchel (Berlin; Heidelberg: Springer), 81–123. doi: 10.1007/3-540-40021-4\_3
- Steinbüchel, A., and Valentin, H. E. (1995). Diversity of bacterial polyhydroxyalkanoic acids. *FEMS Microbiol. Lett.* 128, 219–228. doi: 10.1111/j.1574-6968.1995.tb07528.x
- Strong, P., Laycock, B., Mahamud, S., Jensen, P., Lant, P., Tyson, G., et al. (2016). The opportunity for high-performance biomaterials from methane. *Microorganisms* 4:11. doi: 10.3390/microorganisms4010011
- Suriyamongkol, P., Weselake, R., Narine, S., Moloney, M., and Shah, S. (2007). Biotechnological approaches for the production of polyhydroxyalkanoates in microorganisms and plants — A review. *Biotechnol. Adv.* 25, 148–175. doi: 10.1016/j.biotechadv.2006.11.007
- Sznajder, A., Pfeiffer, D., and Jendrossek, D. (2015). Comparative proteome analysis reveals four novel polyhydroxybutyrate (PHB) granule-associated proteins in *Ralstonia eutropha* H16. *Appl. Environ. Microbiol.* 81, 1847–1858. doi: 10.1128/AEM.03791-14
- Taidi, B., Mansfield, D. A., and Anderson, A. J. (1995). Turnover of poly(3-hydroxybutyrate) (PHB) and its influence on the molecular mass of the polymer accumulated by *Alcaligenes eutrophus* during batch culture. *FEMS Microbiol. Lett.* 129, 201–205. doi: 10.1111/j.1574-6968.1995.tb07580.x
- Tajima, K., Han, X., Hashimoto, Y., Satoh, Y., Satoh, T., and Taguchi, S. (2016). *In vitro* synthesis of polyhydroxyalkanoates using thermostable acetyl-CoA synthetase, CoA transferase, and PHA synthase from the thermotolerant bacteria. *J. Biosci. Bioeng.* 122, 660–665. doi: 10.1016/j.jbiosc.2016.06.001
- Tajima, K., Han, X., Satoh, Y., Ishii, A., Araki, Y., Munekata, M., et al. (2012). *In vitro* synthesis of polyhydroxyalkanoate (PHA) incorporating lactate (LA) with a block sequence by using a newly engineered thermostable PHA synthase from *Pseudomonas* sp. SG4502 with acquired LA-polymerizing activity. *Appl. Microbiol. Biotechnol.* 94, 365–376. doi: 10.1007/s00253-011-3840-z
- Tanaka, K., Ishizaki, A., Kanamaru, T., and Kawano, T. (1995). Production of poly (D-3-hydroxybutyrate) from CO<sub>2</sub>, H<sub>2</sub>, and O<sub>2</sub> by high cell density autotrophic cultivation of *Alcaligenes eutrophus*. *Biotechnol. Bioeng.* 45, 268–275.
- Tanaka, K., Miyawaki, K., Yamaguchi, A., Khosravi-Darani, K., and Matsusaki, H. (2011). Cell growth and P(3HB) accumulation from CO<sub>2</sub> of a carbon monoxide-tolerant hydrogen-oxidizing bacterium, *Ideonella* sp. O-1. *Appl. Microbiol. Biotechnol.* 92, 1161–1169. doi: 10.1007/s00253-011-3420-2
- Tieu, K., Perier, C., Caspersen, C., Teismann, P., Wu, D.-C., Yan, S.-D., et al. (2003). D- $\beta$ -Hydroxybutyrate rescues mitochondrial respiration and mitigates features of Parkinson disease. *J. Clin. Invest.* 112, 892–901. doi: 10.1172/JCI18797
- Tokiwa, Y., and Ugwu, C. U. (2007). Biotechnological production of (R)-3-hydroxybutyric acid monomer. *J. Biotechnol.* 132, 264–272. doi: 10.1016/j.jbiotec.2007.03.015
- Tseng, H.-C. C., Harwell, C. L., Martin, C. H., and Prather, K. L. J. L. (2010). Biosynthesis of chiral 3-hydroxyvalerate from single propionate-unrelated carbon sources in metabolically engineered *E. coli*. *Microb. Cell Fact.* 9:96. doi: 10.1186/1475-2859-9-96
- Tseng, H. C., Martin, C. H., Nielsen, D. R., and Prather, K. L. J. (2009). Metabolic engineering of *Escherichia coli* for enhanced production of (R)- and (S)-3-hydroxybutyrate. *Appl. Environ. Microbiol.* 75, 3137–3145. doi: 10.1128/AEM.02667-08
- Tsuge, Y., Kawaguchi, H., Sasaki, K., and Kondo, A. (2016). Engineering cell factories for producing building block chemicals for bio-polymer synthesis. *Microb. Cell Fact.* 15:19. doi: 10.1186/s12934-016-0411-0
- Uchino, K., Saito, T., Gebauer, B., and Jendrossek, D. (2007). Isolated poly(3-hydroxybutyrate) (PHB) granules are complex bacterial organelles catalyzing formation of PHB from acetyl coenzyme A (CoA) and degradation of PHB to acetyl-CoA. *J. Bacteriol.* 189, 8250–8256. doi: 10.1128/JB.00752-07
- Uchino, K., Saito, T., and Jendrossek, D. (2008). Poly(3-hydroxybutyrate) (PHB) depolymerase PhaZa1 is involved in mobilization of accumulated PHB in *Ralstonia eutropha* H16. *Appl. Environ. Microbiol.* 74, 1058–1063. doi: 10.1128/AEM.02342-07
- Ueda, H., and Tabata, Y. (2003). Polyhydroxyalkanoate derivatives in current clinical applications and trials. *Adv. Drug Deliv. Rev.* 55, 501–518. doi: 10.1016/S0169-409X(03)00037-1
- Ugwu, C. U., Tokiwa, Y., Aoyagi, H., Uchiyama, H., and Tanaka, H. (2008). UV mutagenesis of *Cupriavidus necator* for extracellular production of (R)-3-hydroxybutyric acid. *J. Appl. Microbiol.* 105, 236–242. doi: 10.1111/j.1365-2672.2008.03774.x
- Ugwu, C. U., Tokiwa, Y., and Ichiba, T. (2011). Production of (R)-3-hydroxybutyric acid by fermentation and bioconversion processes with *Azohydromonas lata*. *Bioresour. Technol.* 102, 6766–6768. doi: 10.1016/j.biortech.2011.03.073
- Volova, T., Shishatskaya, E., Sevastianov, V., Efremov, S., and Mogilnaya, O. (2003). Results of biomedical investigations of PHB and PHB/PHV fibers. *Biochem. Eng. J.* 16, 125–133. doi: 10.1016/S1369-703X(03)00038-X
- Wang, B., Xiong, W., Yu, J., Maness, P.-C., and Meldrum, D. R. (2018). Unlocking the photobiological conversion of CO<sub>2</sub> to (R)-3-hydroxybutyrate in cyanobacteria. *Green Chem.* 20, 3772–3782. doi: 10.1039/C8GC01208C
- Wang, F., and Lee, S. (1997). Poly(3-Hydroxybutyrate) production with high productivity and high polymer content by a fed-batch culture of *Alcaligenes latus* under nitrogen limitation. *Appl. Environ. Microbiol.* 63, 3703–3706.
- Wang, L., Armbruster, W., and Jendrossek, D. (2007). Production of medium-chain-length hydroxyalkanoic acids from *Pseudomonas putida* in pH stat. *Appl. Microbiol. Biotechnol.* 75, 1047–1053. doi: 10.1007/s00253-007-0920-1
- Wang, S. Y., Wang, Z., Liu, M. M., Xu, Y., Zhang, X. J., and Chen, G.-Q. (2010). Properties of a new gasoline oxygenate blend component: 3-Hydroxybutyrate methyl ester produced from bacterial poly-3-hydroxybutyrate. *Biomass Bioenergy* 34, 1216–1222. doi: 10.1016/j.biombioe.2010.03.020
- Wang, Y., and Liu, S. (2014). Production of (R)-3-hydroxybutyric acid by *Burkholderia cepacia* from wood extract hydrolysates. *AMB Express* 4:28. doi: 10.1186/s13568-014-0028-9
- Wang, Y.-W., Wu, Q., Chen, J., and Chen, G.-Q. (2005). Evaluation of three-dimensional scaffolds made of blends of hydroxyapatite and poly(3-hydroxybutyrate-co-3-hydroxyhexanoate) for bone

- reconstruction. *Biomaterials* 26, 899–904. doi: 10.1016/j.biomaterials.2004.03.035
- Windhorst, C., and Gescher, J. (2019). Efficient biochemical production of acetoin from carbon dioxide using *Cupriavidus necator* H16. *Biotechnol. Biofuels* 12:163. doi: 10.1186/s13068-019-1512-x
- Witholt, B., and Kessler, B. (1999). Perspectives of medium chain length poly(hydroxyalkanoates), a versatile set of bacterial bioplastics. *Curr. Opin. Biotechnol.* 10, 279–285. doi: 10.1016/S0958-1669(99)80049-4
- Woolston, B. M., Emerson, D. F., Currie, D. H., and Stephanopoulos, G. (2018). Redirecting carbon flux in *Clostridium ljungdahlii* using CRISPR interference (CRISPRi). *Metab. Eng.* 48, 243–253. doi: 10.1016/j.ymben.2018.06.006
- Worm, B., Lotze, H. K., Jubinville, I., Wilcox, C., and Jambeck, J. (2017). Plastic as a persistent marine pollutant. *Annu. Rev. Environ. Resour.* 42, 1–26. doi: 10.1146/annurev-environ-102016-060700
- Yamanashi, T., Iwata, M., Kamiya, N., Tsunetomi, K., Kajitani, N., Wada, N., et al. (2017). Beta-hydroxybutyrate, an endogenous NLRP3 inflammasome inhibitor, attenuates stress-induced behavioral and inflammatory responses. *Sci. Rep.* 7:7677. doi: 10.1038/s41598-017-08055-1
- Yamane, T., Fukunaga, M., Lee, Y. W. (1996). Increased PHB productivity by high-cell-density fed-batch culture of *Alcaligenes latus*, a growth-associated PHB producer. *Biotechnol. Bioeng.* 50, 197–202. doi: 10.1002/(SICI)1097-0290(19960420)50:2<197::AID-BIT8>3.0.CO;2-H
- Yishai, O., Lindner, S. N., Gonzalez de la Cruz, J., Tenenboim, H., and Bar-Even, A. (2016). The formate bio-economy. *Curr. Opin. Chem. Biol.* 35, 1–9. doi: 10.1016/j.cbpa.2016.07.005
- Yokaryo, H., Teruya, M., Hanashiro, R., Goda, M., and Tokiwa, Y. (2018). Direct production of (R)-3-hydroxybutyric acid of high optical purity by *Halomonas* sp. OITC1261 under aerobic conditions. *Biotechnol. J.* 13, 1–6. doi: 10.1002/biot.201700343
- Yun, E. J., Kwak, S., Kim, S. R., Park, Y. C., Jin, Y. S., and Kim, K. H. (2015). Production of (S)-3-hydroxybutyrate by metabolically engineered *Saccharomyces cerevisiae*. *J. Biotechnol.* 209, 23–30. doi: 10.1016/j.jbiotec.2015.05.017
- Zhang, J., Cao, Q., Li, S., Lu, X., Zhao, Y., Guan, J.-S., et al. (2013). 3-Hydroxybutyrate methyl ester as a potential drug against Alzheimer's disease via mitochondria protection mechanism. *Biomaterials* 34, 7552–7562. doi: 10.1016/j.biomaterials.2013.06.043
- Zhang, X., Luo, R., Wang, Z., Deng, Y., and Chen, G.-Q. (2009). Application of (R)-3-hydroxyalkanoate methyl esters derived from microbial polyhydroxyalkanoates as novel biofuels. *Biomacromolecules* 10, 707–711. doi: 10.1021/bm801424e
- Zhao, K., Tian, G., Zheng, Z., Chen, J. C., and Chen, G. Q. (2003). Production of D-(-)-3-hydroxyalkanoic acid by recombinant *Escherichia coli*. *FEMS Microbiol. Lett.* 218, 59–64. doi: 10.1016/S0378-1097(02)01108-4
- Zheng, J., and Suh, S. (2019). Strategies to reduce the global carbon footprint of plastics. *Nat. Clim. Change* 9, 374–378. doi: 10.1038/s41558-019-0459-z
- Zheng, Z., Gong, Q., and Chen, G. (2004). Novel method for production of 3-hydroxydecanoic acid by recombinant *Escherichia coli* and *Pseudomonas putida*. *Chinese J. Chem. Eng.* 12, 550–555.

**Conflict of Interest:** The authors declare that the research was conducted in the absence of any commercial or financial relationships that could be construed as a potential conflict of interest.

Copyright © 2020 Yañez, Conejeros, Vergara-Fernández and Scott. This is an open-access article distributed under the terms of the Creative Commons Attribution License (CC BY). The use, distribution or reproduction in other forums is permitted, provided the original author(s) and the copyright owner(s) are credited and that the original publication in this journal is cited, in accordance with accepted academic practice. No use, distribution or reproduction is permitted which does not comply with these terms.



## Two internal bottlenecks cause the overflow metabolism leading to poly (3-hydroxybutyrate) production in *Azohydromonas lata* DSM1123

Felipe Scott<sup>a,\*</sup>, Luz Yañez<sup>a</sup>, Raúl Conejeros<sup>b</sup>, Blanca Araya<sup>a</sup>, Alberto Vergara-Fernández<sup>a</sup>

<sup>a</sup> Universidad de los Andes, Facultad de Ingeniería y Ciencias Aplicadas, Green Technology Research Group, Chile

<sup>b</sup> Escuela de Ingeniería Bioquímica, Facultad de Ingeniería, Pontificia Universidad Católica de Valparaíso, Chile

### ARTICLE INFO

Editor: Dr. Z. Wen

#### Keywords:

Polyhydroxybutyrate  
Overflow metabolism  
Flux balance analysis  
*Azohydromonas lata*  
Biopolymers

### ABSTRACT

Polyhydroxybutyrate production in the bacteria *Azohydromonas lata* DSM1123 has been regarded as growth-associated based on batch experiments. However, growth association can only be confirmed under chemostat culture. In this work, an experimental approach followed by Flux Balance Analysis (FBA) modeling was used to analyze the behavior of this strain under glucose, oxygen, and nitrogen-limited conditions. The model allowed the identification of candidate enzymes constraining the flux through the tricarboxylic acid cycle, and the role of ATP synthase as the key flux controlling enzyme for the respiratory metabolism, in terms of its share of the total metabolically active protein. The results presented in this work and the model developed could assist in the economic and environmental assessment of new continuous processes to produce PHB and other metabolites in *A. lata* DSM1123, a strain capable of hydrogen use and CO<sub>2</sub> fixation.

### 1. Introduction

Synthetic polymers, such as polyolefins mainly produced from petroleum-based monomers, are non-biodegradable and non-renewable materials. As a result, plastics accumulate, rather than decompose, and close to 60% of all plastics produced from 1950 to 2015 can be found in landfills or the natural environment, amounting to approximately 4900 metric tons [1]. Emissions of greenhouse gases related to the plastics' life cycle contribute to global warming. Estimates point to cumulative emissions from plastics production and use reaching 56 gigatons of carbon by 2050, being equivalent to 10–13% of the remaining carbon budget to stay below 2 °C [2].

Polyhydroxyalkanoates (PHAs) are a family of renewable bio-based and biodegradable polymers that are expected to reduce -along with other biopolymers and monomers such as lactic, succinic, and caproic acids- the impacts of plastic production and use, including greenhouse gas emissions [3]. Poly-(3-hydroxybutyrate), PHB, is the most widespread and best-characterized PHA and accumulates in many bacteria as a carbon and energy reservoir [4] from a wide range of carbohydrates and lipids including sucrose [5]. From an environmental perspective, the use of methane [6] or H<sub>2</sub>:CO<sub>2</sub>:O<sub>2</sub> [7] (knallgas) mixtures could tackle both environmental and economic issues by using abundant resources and fixing CO<sub>2</sub> into useful products. Mechanical properties of PHB are

similar to those of polypropylene, and it has been used in medical applications, controlled release of drugs, and food packaging among others, for a recent review see Yañez et al. [8].

The most characterized PHB producer is the Gram-negative and obligate aerobe *Ralstonia eutropha* (*Cupriavidus necator*). *R. eutropha* growth and PHB accumulation can be achieved using knallgas or sugars and organic acids as substrates. PHB accumulation in *R. eutropha* follows a non-growth associated pattern: the specific PHB productivity decreases as the growth rate increases in a chemostat culture [9].

*Azohydromonas lata* (formerly *Alcaligenes latus*) is a Gram-negative facultative autotroph, capable of using knallgas and organic molecules (including sucrose and glucose) for growth and PHB production, having the highest volumetric productivity of PHB accumulation reported up-to-date [10]. Interestingly, the production of PHB in *A. lata* in batch cultures has been reported as growth associated [5]. The counterintuitive production of PHB during balanced growth, instead of producing biomass only, has been only reported in *Methylobacterium rhodesianum* MB126 [11], and a respiratory mutant of *Azotobacter vinelandii* [12]. A growth-associated product should display a proportionality between the specific PHB accumulation rate and the growth rate [13]. Since the data obtained in batch cultures only represent a narrow range of growth rates and under balanced growth conditions, it is unclear under which conditions this positive correlation occurs. In this regard, chemostat

\* Corresponding author.

E-mail address: [fscott@miuandes.cl](mailto:fscott@miuandes.cl) (F. Scott).

<https://doi.org/10.1016/j.jece.2021.105665>

Received 14 February 2021; Received in revised form 15 April 2021; Accepted 8 May 2021

Available online 14 May 2021

2213-3437/© 2021 Elsevier Ltd. All rights reserved.

cultivation is an ideal technique for the study of this relationship, as it enables the investigation of the effect of varying dilution rates (hence specific growth rates) over the rates of product formation under different nutrient limitations.

Although relevant for industrial process design and optimization, the descriptions of specific product formation rates as a function of the specific growth rate ( $\mu$ ) are of a phenomenological nature. Hence, they do not shed light on the metabolic processes upon which the mechanistic explanations lie. Conversely, constraint-based modeling of cell metabolism, such as Flux Balance Analysis (FBA), has allowed the explanation of the counterintuitive occurrence of overflow metabolism [14], specially using reduced metabolic networks dealing with the central carbon metabolism [15]. FBA entails a set of equality constraints derived from mass conservation equations relating reaction rates (fluxes) for all metabolites in a metabolic network under steady-state. Additionally, fluxes are constrained by physiologically feasible lower and upper bounds. Given that the number of equality constraints is always less than the number of fluxes, an objective function is used to obtain a linear optimization problem.

FBA models have been used to provide explanations to the overflow metabolism by mathematically expressing a simple principle: if respiration or other internal process is limited in the high energy-efficiency pathway, by-product formation through a less energy-efficient pathway can lead to extra ATP production and higher  $\mu$  [16]. This requires that the byproduct can be generated with a net gain of ATP.

This work aims at determining under which conditions PHB production is associated with growth considering oxygen, nitrogen, and carbon limited chemostat cultures and to shed light into the growth associated PHB accumulation in *A. lata* DSM1123 considering the metabolic processes involved.

For the first time, a complete characterization of this strain under chemostat culture and a calibrated metabolic model of the central carbon metabolism are provided. The Flux Balance Analysis Model (FBA) was constructed after an extensive analysis of the genome of *A. lata* and available literature. The FBA model provides a feasible set of intracellular fluxes, including growth associated and non-growth associated energy requirements, that is consistent with the extracellular fluxes calculated from the chemostat experimental data. The model could be utilized for the assessment of economically and environmentally sound processes to produce PHB or other metabolites using *A. lata* and its extensive repertoire of substrates –including hydrogen– and its ability to fix CO<sub>2</sub>.

## 2. Materials and methods

### 2.1. Microorganism

The strain *Azohydromonas lata* DSM 1123 (strain H-1) was obtained from DSMZ (Germany). The strain was stored at  $-80\text{ }^{\circ}\text{C}$  in nutrient broth (Merck) with 25% w/v glycerol. Strain DSM 1123 is a reference strain while *Azohydromonas lata* DSM 1122 (strain H-4) is the type strain.

### 2.2. Seed cultures

One glycerol stock was streaked on a nutrient agar petri dish and incubated at  $30\text{ }^{\circ}\text{C}$ . After 24–48 h one colony was used to inoculate a 100 mL shake flask with 20 mL of AL1 mineral medium [10] and incubated for 15–20 h. This seed culture was utilized to inoculate a 500 mL shake flask with 100 mL AL1. Between 50 and 100 mL of the second seed culture was transferred to the bioreactor to reach an initial OD<sub>600</sub> between 0.1 and 0.2. In the aforementioned cultures,  $10\text{ gL}^{-1}$  glucose and  $2\text{ gL}^{-1}$  ammonium sulfate were used and the shake flasks were cultured in a shaking incubator at 200 RPM and  $30\text{ }^{\circ}\text{C}$ .

### 2.3. Chemostat cultivations

Chemostats were performed in a 3.6 L (total volume, 2.3 L working volume) fermenter (Labfors 5, Infors-HT, Basel, Switzerland) equipped with pH, dissolved oxygen (DO), and temperature controllers. Temperature was maintained at  $30\text{ }^{\circ}\text{C}$  and water evaporated from the broth was condensed using a water-cooled condenser. DO was controlled above 40% of oxygen saturation in air (except for the oxygen-limited cultures where 1.0 vvm air and 250 RPM were used) by varying the stirring speed between 300 and 600 RPM and the gas mixture between air and pure oxygen in a cascade control at 2 vvm. Gas flows were controlled by mass flow controllers and refer to normal conditions. The pH was maintained at 6.8 by the addition of a 2 M NaOH solution. The culture medium was the mineral salt medium AL2 [10] with  $10\text{ gL}^{-1}$  glucose as the carbon and energy source.

Nitrogen-limited, oxygen-limited, and glucose-limited chemostats were performed by altering the inlet medium composition or the oxygen transfer rate. The nitrogen-limited feeding medium contains  $0.5\text{ gL}^{-1}$  ammonium sulfate while  $3\text{ gL}^{-1}$  was used for the glucose and oxygen-limited conditions. Dilution rates ranging from 0.05 to  $0.4\text{ h}^{-1}$  were applied under each nutrient limitation campaign. Changes between dilution rates were randomized. Cultures were sampled after achieving steady-state (at least after 4 residence times) and checking for signs of contamination using optical microscopy and Raman spectroscopy.

### 2.4. Analytical procedures

CO<sub>2</sub> in the exhaust gases from the bioreactor was measured using an in-line CO<sub>2</sub> IR detector (CoZIR® CM-0188, CO2Meter, USA). The sensor was calibrated using nitrogen and air before each measurement. Oxygen consumption rate was estimated off-line using an oxygen mass balance after the determination of the volumetric oxygen mass transfer coefficient. The procedure is detailed in the [Supplementary Material Section S1](#).

#### 2.4.1. Culture supernatant collection and analysis

Culture supernatants were obtained by centrifuging broth samples in Eppendorf tubes at 17000 RCF for 1 min at  $4\text{ }^{\circ}\text{C}$  and used immediately or stored at  $-20\text{ }^{\circ}\text{C}$ . Glucose concentration was determined in culture supernatants and feed media using an enzymatic assay (D-glucose assay kit GOPOD, Megazyme, Ireland) according to the manufacturer's instructions. The concentration of NH<sub>4</sub><sup>+</sup> was determined using an ammonium-ion electrode (EW-27504-00, Cole-Parmer, USA).

Citrate, malate, pyruvate, 3-hydroxybutyrate, acetate, succinate, and glucose were quantified in half of the culture supernatants to check for organic acids production by HPLC with a UV-Vis detector at 210 nm and a refractive index detector (Prominence, Shimadzu). Samples (20  $\mu\text{L}$ ) were separated in an Aminex HPX-87H ion-exclusion column (300 x 7.8 mm, Bio-Rad) at  $40\text{ }^{\circ}\text{C}$ , using  $1.7\text{ mM H}_2\text{SO}_4$  at a flow rate of 0.6 mL/min as the mobile phase. Glucose concentrations measured using the enzymatic kit and HPLC were in good agreement, as well as the concentration of 3-hydroxybutyric acid when quantified using an enzymatic kit specific for (R)-3-hydroxybutyrate (K-HDBA, Megazyme, Ireland).

#### 2.4.2. Biomass, protein, and PHB quantification

For the estimation of biomass concentration, aliquots of culture were centrifuged (2470 RCF, 10 min) to separate a cell-free supernatant and a biomass pellet. The pellet was washed twice with Type II water, dried, and used to determine the cell dry weight concentration. Protein estimation was performed in washed pellets resuspended in Type I water at a concentration of approximately  $1\text{ gL}^{-1}$ . The cell suspension was extracted with 0.1 M NaOH for 1 h at  $90\text{ }^{\circ}\text{C}$  and the protein content was determined using the Pierce™ BCA Protein Assay Kit (ThermoFisher Scientific).

PHB was determined in washed and dried pellets, obtained as previously described, by a standard gas chromatography technique [17].

Briefly, a weighted sample of dried cells (10–40 mg) was mixed with 2 mL of HCl and 1-propanol (1:4 v/v) and 2 mL of dichloroethane in closed tubes. 1 mg of benzoic acid in 1-propanol was added as the internal standard. Tubes were heated for 3 h at 100 °C. After cooling, residues were extracted from the organic phase with 4 mL of water and 500  $\mu$ L of the organic phase were collected. 5  $\mu$ L of the organic phase were injected into a GC equipped with an FID detector (Shimadzu GC-2014) and an Agilent J&W DB-624 UI column. The initial oven temperature was 90 °C, increasing up to 180 °C at a rate of 15 °C min<sup>-1</sup>. Helium was used as carrier gas at 2.0 mL/min with a 5:1 split ratio (linear velocity of 35.8 cm s<sup>-1</sup>). The FID detector temperature was set to 250 °C and the injection port to 275 °C. A calibration curve using an external PHB standard (sc-255438, Santa Cruz Biotechnology) was prepared in the 0–40 mg of PHB range.

#### 2.4.3. Exopolysaccharides (EPS) quantification

The method for EPS quantification was adapted from literature [18]. Briefly, 15 mL of culture supernatant obtained by centrifugation at 2470 RCF for 20 min. Next, EPS were precipitated from the supernatant using three volumes of cold (-20 °C) pure ethanol. After an incubation period of 24 h at -20 °C the precipitate was centrifuged, washed two times with pure cold ethanol, and dried until constant weight. The total EPS concentration was calculated as the difference between the dried weight and the weight of the residue left after calcination in a muffle oven at 450 °C for 24 h divided by the initial sample volume.

#### 2.4.4. Raman spectroscopy

Raman analyses of dry biomass harvested from the cultures, washed twice with Type II water and dried at 70 °C on a Raman grade CaF<sub>2</sub> supports (Crystan, UK) were performed using a Horiba XploRA™ PLUS Raman microscope with a 50x objective lens. A diode laser of 532 nm was used, and the collected Raman radiation was dispersed with a 1200 lines (750 nm) grating. All spectra were obtained in the spectral window of 600–1800 cm<sup>-1</sup> using 60 s of acquisition time and 2 accumulations. The Raman spectra were baseline corrected and normalized using the LabSpec 6 suite. The analysis of the characteristic frequencies and intensities was performed using previously reported Raman spectra [19] and the spectra of pure PHB (sc-255438, Santa Cruz Biotechnology).

### 2.5. Presentation of results

Each chemostat culture is presented as a single data point corresponding to the mean of two or three analytical determinations, along with its standard deviation. Therefore, each data point at a given dilution rate is a biological replicate. When calculating specific rates and fluxes, the error was propagated using standard formulas (see [Supplementary Material, Section S2](#)). Unless stated otherwise, percentages are mass-based, and cell dry weights (CDW) refer to residual (active or PHB free) biomass.

### 2.6. Metabolic model and calculations

#### 2.6.1. Metabolic model of the central carbon metabolism of *A. lata* DSM1123

The Core *Escherichia coli* (e\_coli\_core) metabolic model [20] obtained from the BiGG Models platform [21] was utilized as a template of the central carbon metabolism in bacteria. The genome of *A. lata* NBRC 102462 (Accession Number PRJDB1079: <https://www.ncbi.nlm.nih.gov/bioproject/196452>) was used. An initial draft of the network was constructed by compiling annotated metabolic genes and relevant reactions were added (or deleted) from the e\_coli\_core template with the respective gene-protein-reaction (GPR) assignment [22] using information from BRENDA [23], MetaCyc [24], KEGG [25] and KBase [26]. The model was manually curated. Only one reaction was added during gap-filling: 6-phosphogluconolactonase (PGL) to complete the Entner-Doudoroff (ED) pathway. Kim et al. [27] reported

glucose-6-phosphate dehydrogenase activity with sucrose in the closely related *A. australica* DSM1124. Therefore, a PGL negative phenotype can be ruled out, since glucose-6-phosphate dehydrogenase would produce 6-phospho-D-glucono-1,5-lactone without the use of this intermediary. Finally, reaction directionality was manually curated to avoid a thermodynamically infeasible production of ATP or proton excretion without energy expenditure, and the model was charge and mass balance checked using the CobraToolbox [28]. A metabolic map of the active reactions is presented in [Supplementary Material S5](#). The biomass formation equation was adapted from the e\_coli\_core model to yield exactly 1.00 gCDW and an elemental composition close to previously reported values [5] ([Supplementary Material, Section S3](#)).

#### 2.6.2. Flux balance analysis (FBA) and Flux variability analysis (FVA)

After a manually curated model was obtained, manipulations (addition of constraints, changes in reaction bounds and directionality, etc.), as well as FBA and VFA simulations were performed using the COBRA Toolbox [28] in MATLAB™.

Additionally to the standard FBA model, the total enzyme mass was estimated and constrained using an approach previously reported [29]. The mass of each enzyme was estimated by dividing the predicted flux ( $v_i$ ) by the maximum reported *in vitro* activity ( $a_i$ ) and a saturation factor ( $\sigma$ ) that was fixed to 0.5 for all reactions. Although the saturation factor will depend on allosteric regulation and internal substrate concentrations among other factors, this assumption stems from the observation that in *E. coli* most of the glycolytic enzymes are half-saturated [30]. All enzyme masses need to be positive, therefore each reversible reaction was split into two irreversible reactions. The *in-vitro* activities were collected from the literature and the complete problem formulation can be found in the [Supplementary Material \(section S3\)](#). Due to the lack of information regarding enzymes from *A. lata*, information from other Gram-negative bacteria was used.

Lexicographic optimization [31] was used to select between competing product fluxes that are equally optimal from a biomass maximization perspective.  $\mu$  was used as the first FBA objective function; then the optimum value of the biomass flux is added as a constraint and PHB accumulation is maximized instead.

## 3. Results and discussion

### 3.1. Effects of nutrient limitation and dilution rate on PHB accumulation and biomass concentration

*Azohydromonas lata* DSM 1123 was grown in chemostat culture at dilution rates ranging from 0.05 to 0.4 h<sup>-1</sup> with mineral medium and glucose as the sole carbon and energy source. Panels A-F in [Fig. 1](#) show culture parameters and their relationship with the dilution rate under nitrogen, oxygen, or glucose limiting conditions.

#### 3.1.1. Nitrogen limited-chemostat culture

The PHB content under nitrogen limitation slightly decreases from an average of 75% at a dilution rate of 0.05 h<sup>-1</sup> to 65% at the maximum dilution rate of 0.4 h<sup>-1</sup> ([Fig. 1](#), Panel A), a slight decrease in sharp contrast to nitrogen-limited chemostats of *R. eutropha* where a linear decrease from a PHB content of 80% to less than 10% was reported as the dilution rate increases from 0.025 to 0.4 h<sup>-1</sup> [9]. The glucose and ammonium sulfate concentration in the chemostat runs ([Fig. 1](#), panels C and D) is consistent with an ammonium limited condition: glucose was present at every dilution rate and the titer of ammonium sulfate was negligible at dilution rates lower than 0.2 h<sup>-1</sup>. As the growth rate increases, the overall PHB yield on glucose decreases from 0.41  $\pm$  0.02 (D=0.05 h<sup>-1</sup>) to 0.30  $\pm$  0.03 gg<sup>-1</sup> (D=0.4 h<sup>-1</sup>). A carbon-mole yield analysis is presented in the [Supplementary Material \(Section S4\)](#).

The maximum specific PHB accumulation rate ([Fig. 1](#), Panel F) was found under nitrogen limitation at a dilution rate of 0.4 h<sup>-1</sup> corresponding to 7.9  $\pm$  0.14 mmol gCDW<sup>-1</sup> h<sup>-1</sup> (equivalent to 0.69 gPHB

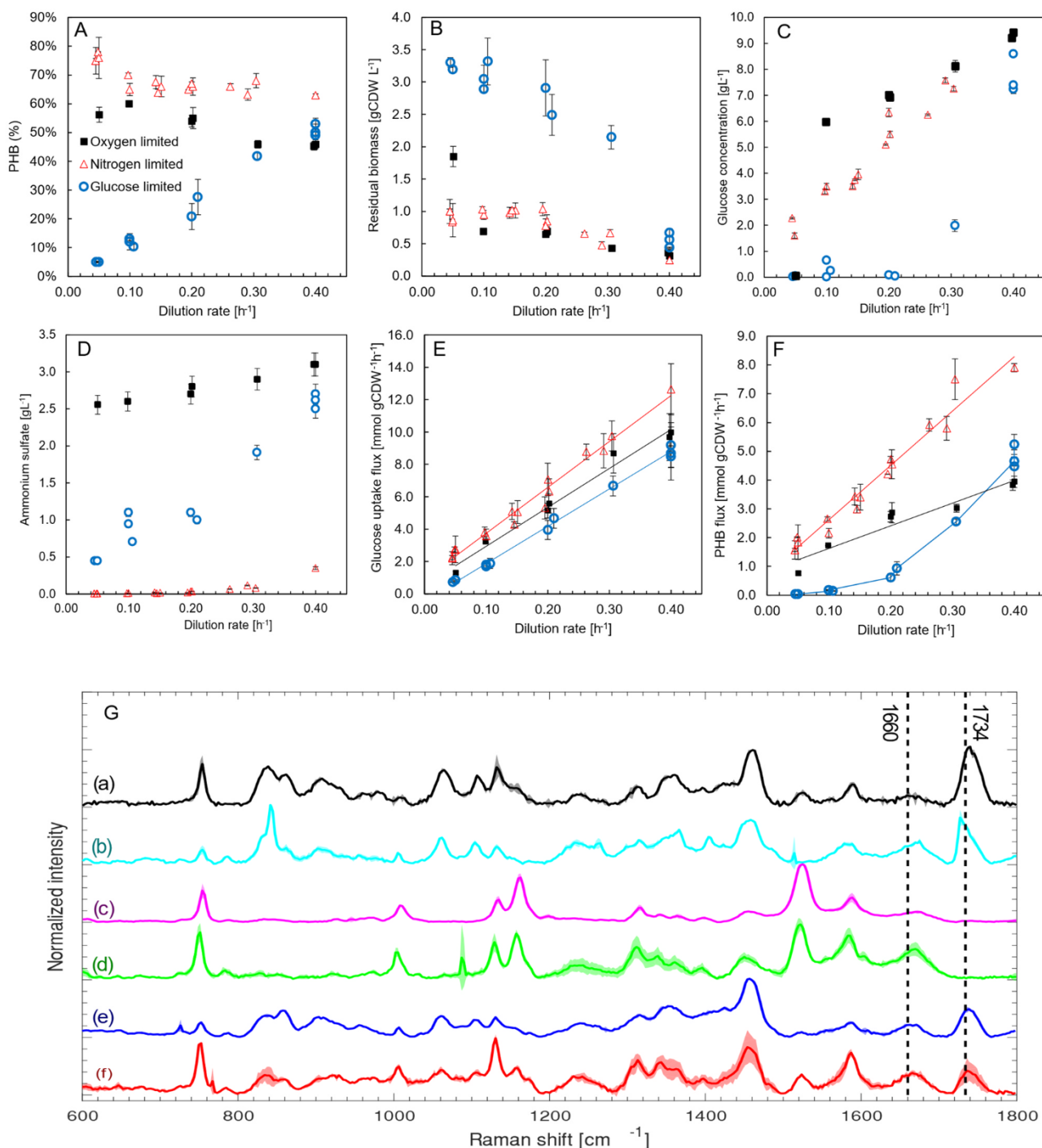


**Fig. 1.** Effects of the dilution rate in chemostat culture (equivalent to the specific growth rate) on PHB content (A), residual (PHB free) biomass (B), glucose (C) and ammonium sulfate (D) concentration in the bioreactor, specific glucose uptake rate per gram of residual biomass (E), and specific PHB accumulation rate per gram of residual biomass (F). Red triangles correspond to nitrogen-limited chemostats, black squares to oxygen-limited chemostats, and blue circles to glucose-limited chemostats. Raman spectra of washed and dried biomass samples withdrawn from (G): (a) nitrogen-limited chemostat at a dilution rate of 0.05 h<sup>-1</sup>, (b), (c) and (d) oxygen-limited chemostat at dilution rates of 0.3 h<sup>-1</sup>, 0.05 h<sup>-1</sup> and 0.1 h<sup>-1</sup>, respectively Batch cultures with glucose (e) and glucose and formate (f) as carbon sources. The shaded area represents the standard deviation. (For interpretation of the references to colour in this figure legend, the reader is referred to the web version of this article.)

gCDW<sup>-1</sup> h<sup>-1</sup>). This value agrees with the instantaneous specific PHB synthesis rate reported by Wang and Lee [10], with a maximum of 0.87 gPHB gCDW<sup>-1</sup> h<sup>-1</sup> after the onset of nitrogen limitation in a batch culture of *A. lata* DSM1123 using sucrose as carbon and energy source. The difference can be explained by the increased specific sucrose uptake rate compared to the glucose uptake rate reported for this microorganism [10]. Comparatively, the PHB flux values found in this work are

much higher, especially for the nitrogen-limited cultures, than for those found in nitrogen-limited chemostats with glucose as the carbon source for *R. eutropha* (0.15 gPHB gCDW<sup>-1</sup> h<sup>-1</sup> [32] or 0.23 gPHB gCDW<sup>-1</sup> h<sup>-1</sup>). A maximum of 10.6 mM of succinic acid was measured at a dilution rate of 0.1 h<sup>-1</sup> and 2.0 mM of malic acid at a dilution rate of 0.2 h<sup>-1</sup> (the complete set of organic acid measurements is presented in the [Supplementary Material Table S6](#)).

### 3.1.2. Oxygen limited-chemostat cultures

PHB accumulation in chemostats under oxygen limitation showed a decrease of the PHB fraction at low dilution rates compared with the results obtained under ammonia-limited conditions (Fig. 1, panel A). Glucose and ammonium sulfate titers are consistent with an oxygen limited chemostat. PHB yield on glucose was  $0.27 \pm 0.03 \text{ g g}^{-1}$ , irrespective of the dilution rate. PHB content reached a maximum of 60% at a dilution rate of  $0.1 \text{ h}^{-1}$  decreasing to 46% at a dilution rate of  $0.4 \text{ h}^{-1}$ . Using a kinetic model for PHB production and cell growth in *A. lata* DSM 1123, Papapostolou [33] reported an intracellular PHB content of 43.3% at the end of a 43 h fed-batch culture, where the dissolved oxygen concentration was maintained at 6% of its saturation value. A maximum of 7.9 mM succinic acid at a dilution rate of  $0.2 \text{ h}^{-1}$  and 1.6 mM of malic acid at a dilution rate of  $0.1 \text{ h}^{-1}$  were measured (see Table S6, Supplementary Material).

### 3.1.3. Glucose-limited chemostat culture

The trends of PHB accumulation under oxygen and nitrogen are in general accord with the general behavior of PHB accumulation in other organisms: PHB accumulation triggers when a nutrient, different than the carbon source is limiting [4]. On the other hand, PHB accumulation in glucose limiting chemostats showed a completely different trend (Fig. 1. A). At a dilution rate of  $0.05 \text{ h}^{-1}$  the PHB percentage was as low as  $4.85 \pm 0.35\%$ , increasing linearly to  $50.7 \pm 2.1\%$  at a dilution rate of  $0.4 \text{ h}^{-1}$ . The PHB accumulation obtained at dilution rates of 0.3 and  $0.4 \text{ h}^{-1}$  were in good agreement with the PHB content of exponentially growing batch cultures (and of the exponential growth zone of fed-batch cultures) where the carbon source is the limiting nutrient, with reported values close to 50% PHB [5,10] and 53% [34]. To the best of our knowledge, this is the first report where a low PHB content is described in a culture of *A. lata* under glucose-limiting conditions. To confirm this result, samples of biomass were analyzed using Raman spectroscopy (Fig. 1G). The Raman spectrum revealed characteristic emission lines attributable to proteins (amide I at  $1660\text{--}1662 \text{ cm}^{-1}$ ) and PHB ( $1734\text{--}1736 \text{ cm}^{-1}$ ) [19]. A PHB standard (data now shown) shows several Raman peaks being the most intense found at  $837$  and  $1734\text{--}1736 \text{ cm}^{-1}$ . Samples from a nitrogen-limited chemostat at a dilution rate of  $0.05 \text{ h}^{-1}$  (Fig. 1G, spectrum a) and glucose-limited chemostat at a dilution rate of  $0.3 \text{ h}^{-1}$  showed clear PHB peak at  $1734 \text{ cm}^{-1}$  with PHB to amide I peak heights ratios of 5.5 and 2.2, respectively. These results agree with the PHB content of the samples, 42% ( $D=0.3 \text{ h}^{-1}$ , glucose-limited) and 75% ( $D=0.05 \text{ h}^{-1}$ , nitrogen-limited) assuming that a positive linear correlation exists between the PHB/Amide I ratio and PHB content [19]. The analysis of the glucose-limited chemostats at dilution rates of  $0.05$  and  $0.1 \text{ h}^{-1}$  (Fig. 1. E, spectrums c and d) show a nearly absent PHB peak at  $1734 \text{ cm}^{-1}$ , confirming the results of the GC analysis. The accumulation of PHA under unrestricted growth conditions at high dilution rates was also observed in cultures of *Ps. oleovorans*, although the maximum content was 10% [35].

Fig. 1E shows the calculated glucose uptake rates in  $\text{mmol gCDW}^{-1} \text{ h}^{-1}$ . Glucose uptake rates under oxygen and nitrogen limitation were found to be higher than those obtained under glucose limiting conditions at every dilution rate. The specific glucose uptake rates in chemostats of *R. eutropha* operated at  $D=0.1 \text{ h}^{-1}$  were found to be similar and to decrease in the same order as the one found in our work: ammonia limited ( $4.2 \text{ mmol gCDW}^{-1} \text{ h}^{-1}$ ) followed by oxygen-limited ( $3.1 \text{ mmol gCDW}^{-1} \text{ h}^{-1}$ ) and glucose-limited ( $2.0 \text{ mmol gCDW}^{-1} \text{ h}^{-1}$ ) conditions [9]. The production of organic acids was negligible (see Table S6, Supplementary Material).

The PHB flux; this is, the specific PHB productivity based on the residual biomass is shown in Fig. 1F. A linear trend was found between PHB flux and the dilution rate for the ammonia limited and oxygen-limited chemostat. For the glucose-limited cultures, the relationship between PHB flux and dilution rate is best described considering two linear zones, with an almost negligible PHB accumulation rate at

dilution rates below  $0.1 \text{ h}^{-1}$ . Interestingly, *Azohydromonas australica* DSM1124, a species closely related to *A. lata* DSM1123, showed no PHB accumulation during the growth phase in batch culture (before ammonium exhaustion) using glycerol as the sole carbon and energy source [36]. The authors attributed this change in the behavior of a strain known for PHB accumulation during exponential growth to the use of a carbon source other than glucose [36]. However, since the cells grew at a  $\mu = 0.075 \text{ h}^{-1}$ , our results indicate that the reduced PHB accumulation it is not related to the nature of the substrate, but to the failure of glycerol to produce an uptake rate of carbon compatible with a  $\mu$  sufficiently high as to promote the accumulation of PHB (see Section 3.2).

### 3.2. Calibration and predictions of the central carbon metabolism model of *A. lata* DSM1123

The model of the central metabolism of *A. lata* DSM1123 under heterotrophic conditions accounts for 137 genes, 86 intracellular reactions, 22 cellular exchange reactions, and 80 metabolites segregated into two compartments (intracellular and extracellular). Model fit, particularly the growth rate, depends on two key parameters relating energy requirements with carbon substrate consumption: Non-growth associated maintenance energy (NGAME) and growth-associated maintenance energy (GAME). NGAME requirements were assumed to be constant under glucose, oxygen, or nitrogen-limiting conditions, and a value of  $5.25 \text{ mmol ATP gCDW}^{-1} \text{ h}^{-1}$  was estimated from our chemostat data. GAME was stipulated as a condition-specific parameter depending on the nutrient limiting growth. For nitrogen and oxygen-limited chemostats, a GAME value of  $80 \text{ mmol ATP gCDW}^{-1}$  was found to provide the best fit while  $105 \text{ mmol ATP gCDW}^{-1}$  was found for the glucose-limited experiments. Details regarding GAME and NGAME estimation and its comparison with published data can be found in the Supplementary Material (section S3).

EPS were detected under every experimental condition. A mean value of EPS concentrations of  $0.29 \pm 0.05 \text{ gL}^{-1}$  was found irrespective of the nutrient limiting growth. EPS production was accounted for in the model by means of a linear constraint relating the flux of EPS production to the glucose uptake flux (Supplementary Material, section S4). Similar values have been found for chemostat cultivation of *Clostridium acetobutylicum* [15].

When PHB production is maximized at zero growth rate, the model predicts a maximum yield equal to  $1.0 \text{ mol PHB (mol glucose)}^{-1}$  or  $0.48 \text{ gPHB (g glucose)}^{-1}$ . PHB yield is essentially the same as those reported by Yamane [37] and Bormann [38]. Concomitant with PHB production  $5.5 \text{ mol ATP}$  are produced per mol of glucose, a value already predicted for a P/O ratio of 1.5 using the Entner-Doudoroff pathway as assumed in our work [37]. The maximum biomass yield corresponds to  $0.0789 \text{ g biomass per mmol glucose}$ , equivalent to  $0.438 \text{ gCDW (g glucose)}^{-1}$ . This value does not include the glucose consumption required for maintenance energy generation. If NGAME is included, a yield of  $0.291 \text{ gCDW (g glucose)}^{-1}$  is obtained at a growth rate of  $0.05 \text{ h}^{-1}$  and  $0.363 \text{ gCDW (g glucose)}^{-1}$  at a growth rate of  $0.1 \text{ h}^{-1}$ .

#### 3.2.1. An overflow metabolism leads to PHB accumulation under glucose-limited conditions

Fig. 2 shows the fitting between the exchange fluxes of  $\text{CO}_2$ ,  $\text{O}_2$ , glucose, ammonia, PHB and  $\mu$  predicted by the calibrated model and the values calculated from the chemostat experiments. To achieve the fit shown in Fig. 2, a systematic screening was carried out to identify possible internal bottlenecks in fluxes, besides the already included total metabolically active protein constraints and GAME and NGAME parameters, that could explain the overflow of PHB observed during glucose-limited chemostat cultures. Reactions downstream citrate synthase were identified as probable bottlenecks by imposing an upper limit below the flux of the reaction calculated in the base case scenario. Constraining reaction in the glycolytic or oxidative phosphorylation pathways did not fit the data. The upper limit of the aconitase (ACONTa)

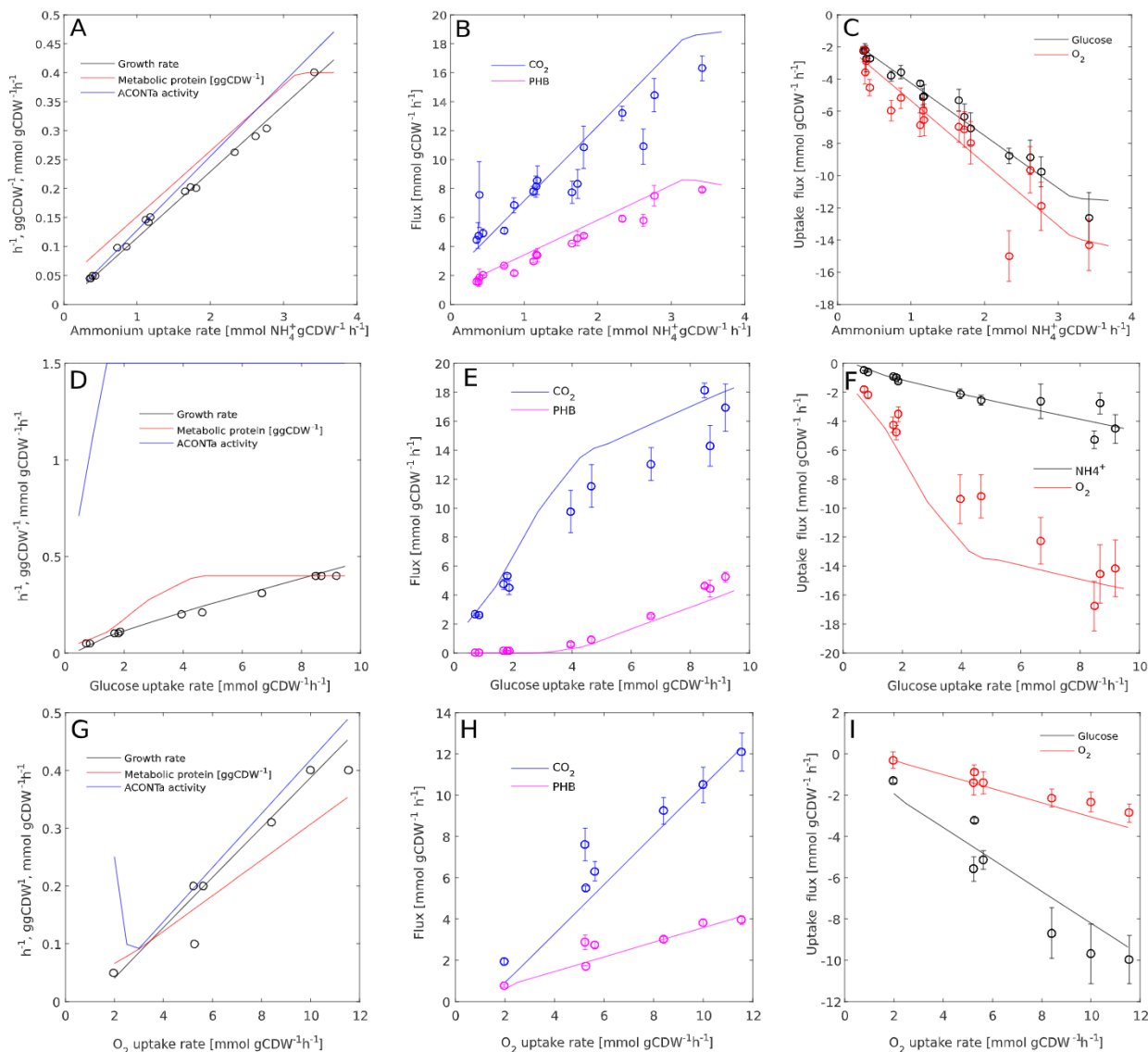


**Fig. 2.** Experimental values for the uptake and production fluxes found in chemostat cultures of *A. lata* DSM1123. Circles correspond to experimental data points while continuous lines represent the prediction of the calibrated central carbon metabolism model. Panels A-C correspond to nitrogen-limited, panels D-F to glucose-limited and G-I to oxygen-limited cultures.

reaction was estimated after fixing the NGAME and GAME values. Fig. 2 shows that the constraint imposed over the ACONTa flux ( $\leq 1.5$  mmol gCDW<sup>-1</sup> h<sup>-1</sup>) is inactive during the nitrogen-limited and oxygen-limited chemostats, but it is active (the ACONTa flux reached the allowed upper limit) during most of the glucose-limited cultures. The upper limit of 1.5 mmol gCDW<sup>-1</sup> h<sup>-1</sup> was imposed based on model fitting and the fact that the sum of organic acids derived from the tricarboxylic acid cycle measured in the oxygen-limited chemostats was close to this value. Similarly, the constraint imposed over the total metabolically active protein, with an upper bound of 400 mg protein gCDW<sup>-1</sup>, is active chiefly in the glucose-limited cultures above a glucose uptake flux of 5.2 mmol gCDW<sup>-1</sup> h<sup>-1</sup> (Fig. 2, panels A, D and G).

When the ACONTa flux constraint is not imposed, the fitting between the model and the nitrogen and oxygen-limited chemostat is unchanged. On the contrary, under glucose-limited conditions, the PHB accumulation flux is equal to zero until the total active protein constraint activates and the predicted growth rate is increased up to 0.5 h<sup>-1</sup> at a glucose uptake rate of 7.0 mmol gCDW<sup>-1</sup> h<sup>-1</sup>, remaining almost constant at higher glucose uptakes, due to the total active protein constraint being

enforced. Consequently, the ACONTa flux constraint is required to produce the model fitting shown in Fig. 2. Restricting the upper bounds of the citrate synthase, isocitrate dehydrogenase or 2-oxoglutarate dehydrogenase reactions produces the same model fit.

### 3.2.2. PHB accumulation contributes with ATP generation for growth under glucose and oxygen limited conditions

The model fit shown in Fig. 2 for the oxygen-limited and glucose limited chemostat cultures was obtained after maximizing the biomass flux in the FBA problem; no lexicographic optimization was therefore required. This indicates that PHB production contributes to the maximization of growth by providing ATP (see Section 3.2) under oxygen limitation, where oxidative phosphorylation is limited. Similarly, under glucose-limited cultures the internal bottleneck in the TCA constrains the generation of NADH, thus PHB production concomitantly generates ATP required for growth. In nitrogen-limited chemostat simulations, since glucose uptake was only constrained to be lower than the experimental values, FBA -without lexicographic optimization- fits PHB flux and glucose uptake rates only up to a  $\mu = 0.2$  h<sup>-1</sup>. Meaning that

predicted glucose uptake is reduced to nearly 50% of the experimental value; or if the glucose uptake is constrained to the experimental values, organic acids are excreted along with PHB accumulation. Thus, without a lexicographic maximization of PHB production the model fit is not possible. Results are consistent with growth being constrained by the limited supply of the nitrogen source, and not by the generation of energy as in the oxygen (reduced oxidative phosphorylation) and glucose-limited (reduced generation of NADH by the TCA internal bottleneck) conditions.

In *R. eutropha*, the levels of NAD(P)H and the ratios of NAD(P)H/NAD(P) are higher under nitrogen-limited conditions as compared to balanced growth conditions, inhibiting the activity of citrate synthase, and increasing the activity of the acetoacetyl-CoA reductase towards PHB synthesis [39], thus preventing the formation of organic acids derived from the TCA.

Since this regulatory mechanism cannot be captured in a classical FBA formulation, the lexicographic optimization of PHB production could be interpreted as a proxy of the regulation of PHB synthesis under nitrogen-limited conditions.

### 3.2.3. The high contribution of the ATP synthase complex to the total active protein limits ATP generation at high growth rates under glucose-limited conditions

The upper limit on the total metabolically active protein ( $P_{lim}$ ) was estimated as 400 mg gCDW<sup>-1</sup>, representing nearly 50% of the total protein ( $76.2 \pm 5\%$  of the cell dry weight under glucose-limited conditions without an influence of the dilution rate). At a growth rate of 0.4 h<sup>-1</sup> under glucose-limited conditions, the mass of the ATP synthase complex represented 58% of the total proteome accounted in the model, followed by the NADH dehydrogenase with less than 5%.

Considering that only 20.5% of the proteome is devoted to the central carbon metabolism and energy metabolism in *E. coli* grown in chemostat culture at 0.48 h<sup>-1</sup> in mineral medium with glucose [40], the coarse approach for protein mass estimation taken in our work overestimates the fraction of the proteome used by the ATPase complex by underestimating the turnover number for ATP synthesis at 50 s<sup>-1</sup> [41]. Since increasing the specific activity of the ATPase complex and decreasing the maximum metabolic protein content preserves the fitting of the model, the constraint on total metabolically active protein is still meaningful, especially when considering that turnover values as high as 270 s<sup>-1</sup> have been reported for the *E. coli* F<sub>0</sub>F<sub>1</sub> for the synthesis of ATP [42]. Using this value, the total metabolically active protein constraint that preserves the model fit is 210 mg gCDW<sup>-1</sup>, equivalent to 26% of the total protein.

A similar approach was followed by Nilsson and Nielsen [29] who reported that the F<sub>0</sub>F<sub>1</sub>-ATP synthase complex creates a trade-off in *S. cerevisiae* metabolism that explains the Crabtree effect. The high contribution of the ATP synthase complex towards the total proteome makes fermentation more catalytically efficient than respiration under a constrained total proteome, producing more ATP per protein mass. Considering that this enzyme is evolutionarily conserved [43], our results coincide with the interpretation of the PHB pathway as being analogous to a fermentative pathway, with a higher protein efficiency than respiration towards the production of ATP [11]. Indeed, in the FBA model maximum production of ATP from glucose without constraining  $P_{lim}$  requires 7.7 mg protein (mmol ATP)<sup>-1</sup> of which 65% corresponds to the ATP synthase complex. On the other hand, maximizing ATP generation at increasing  $P_{lim}$  values (50–400 mg gCDW<sup>-1</sup>) resulted in 4.67–4.84 mg protein (mmol ATP)<sup>-1</sup>. As the maximum allowed protein fraction increases, more glucose is utilized for PHB production (the PHB carbon yield increases from 8% to 53%) while the share of the ATP synthase complex slightly increases from 37.4% to 40.1% of the total active protein. Therefore, in a scenario of constrained protein synthesis, one gram of metabolically active protein can generate 130 mmol ATP if PHB is not produced, while the same amount of protein yields a maximum of 214 mmol ATP if PHB production is allowed.

### 3.3. Observed and predicted organic acids production

Under glucose-limited conditions, HPLC analysis of supernatants indicate negligible organic acids excretion with less than 0.01, 0.01, 0.01 and 0.02 mmol gCDW<sup>-1</sup> h<sup>-1</sup> citrate, malate, 3HBA and succinate, respectively (see [Supplementary Material, Section S4](#)). Under glucose-limited conditions, the FBA of the central carbon metabolism model does not predict acids production, consistent with the very low acid fluxes found experimentally.

Under nitrogen and oxygen limited conditions, the experimental maximum excretion of organic acids found was 0.23, 0.48, 1.24 and 0.05 mmol gCDW<sup>-1</sup> h<sup>-1</sup> for citric, malic, succinic, and 3-hydroxybutyric acid, respectively. The FBA model predicts zero acid fluxes under nitrogen limited conditions when PHB production is maximized in a lexicographic optimization problem constrained by the optimal biomass flux. FVA reveals that succinate can be produced (1.43 mmol gCDW<sup>-1</sup> h<sup>-1</sup>) under nitrogen-limited conditions if succinate, instead of PHB, is used as the objective function in the lexicographic optimization problem constrained to the optimal biomass flux values. FVA of the remaining organic acids reveals that pyruvate and citrate production is also allowed by the model.

Under oxygen limited conditions, the model predicts pyruvate excretion at a flux of 1.5 mmol gCDW<sup>-1</sup> h<sup>-1</sup> along with PHB accumulation. If the pyruvate transport PYRt2 is deleted *in-silico*, fumarate, malate and 3-hydroxybutyrate are excreted and a FVA indicates that fumarate, malate and 3HBA fluxes can be individually maximized up to 1.5 mmol gCDW<sup>-1</sup> h<sup>-1</sup>. Succinate flux reached 1.36 mmol gCDW<sup>-1</sup> h<sup>-1</sup> in the VFA analysis.

FVA and essentiality analysis (see [Supplementary Material, Section S4](#)) indicate that organic acid excretion is not essential for growth under the studied conditions. Under oxygen limitation and at the lower glucose uptake rates, *in-silico* deletion of all organic acid transporters ( $\Delta$ PYRt2- $\Delta$ FUMt2- $\Delta$ MALt2- $\Delta$ 3HBA- $\Delta$ SUCt2) reduced glucose uptake and growth rate by up to 24% and 21%, doubles the PHB accumulation flux and CO<sub>2</sub> production.

### 3.4. Effects of PHB polymerase in-silico deletion

The essentiality of PHB production was analyzed *in-silico* by generating PHB synthase deletion mutants. Since the PHB polymerization and depolymerization cycle also serves as a pathway for the conversion of one mol of NADPH into NADH (see [Section S5 in the Supplementary Material](#)), the effect of an active NAD transhydrogenase reaction (NADTRHD) was investigated in the direction of NADH formation from NAD and NADPH. Under nitrogen and oxygen-limited conditions, deletion of PHB synthase reduced  $\mu$  to a maximum of 0.25 h<sup>-1</sup>. Growth at higher growth rates can be restored by allowing organic acids production at fluxes higher than 1.5 mmol gCDW<sup>-1</sup> h<sup>-1</sup>, chiefly pyruvate under nitrogen limiting conditions and citrate, fumarate, malate, and succinate under oxygen-limited cultures. The activation of NADTRHD under these conditions allows for normal growth with reduced acid production (below 1.5 mmol gCDW<sup>-1</sup> h<sup>-1</sup>) and a reduced glucose uptake. If acid excretion is unconstrained, glucose uptake is restored.

On the other hand, under glucose-limited cultures, no growth was predicted when NADTRHD is inactive. When activated, growth was restored with a maximum  $\mu = 0.357$  h<sup>-1</sup>. No organic acid excretion was predicted.

Taken together, the results presented in [Sections 3.3 and 3.4](#) indicate that neither PHB nor organic acids production is essential for the growth of *A. lata* DSM11123. However, to account for the experimentally observed growth rates and glucose uptakes, a sink for the excess of carbon and energy (with respect to the glucose uptake solely required for growth) is required, being PHB accumulation the preferred sink in terms of growth rate maximization under oxygen and glucose-limited conditions. If the PHB accumulation ability is disrupted, the FBA model predicts that the maximum growth rate and glucose uptake is

reduced and can only be restored by allowing for the production of copious amounts of organic acids (chiefly pyruvate). Interestingly, pyruvate excretion in large amounts was reported in a PHB deletion mutant of *R. eutropha* under oxygen, ammonia and sulfate limitation, among other nutrients [44].

### 3.5. Effect of an additional energy source during growth on glucose

A verifiable hypothesis of the model put forward in this work is the reduction of the PHB content in a glucose-limited culture if a second source of NADH is provided to the cells. An NADH flux should reduce the overflow of carbon to PHB caused by the ACONTa bottleneck in the TCA, a bottleneck that also constrains NADH and ATP production. To test this hypothesis, a batch culture of *A. lata* with glucose ( $10 \text{ gL}^{-1}$ ) as the main carbon source, formate ( $1 \text{ gL}^{-1}$ ) as an auxiliary substrate and  $2 \text{ gL}^{-1}$  ammonium sulfate was performed in 500 mL Erlenmeyer flask with 100 mL AL1 medium. As a control, a culture without formate was also included. Each condition was assayed in triplicates. After 24 h, the glucose cultures contained  $59.9 \pm 1.3\%$  PHB while for the formate and glucose cultures the PHB content was  $28 \pm 6.0\%$ . Raman analyses (Fig. 1. E, spectrums e and f) confirm the higher PHB content in the control. Although a more detailed investigation of the use of formate as an auxiliary substrate for the provision of NADH requires further investigation, this preliminary result supports our hypothesis of a constrained TCA.

## 4. Conclusion

A complementary experimental and modeling approach was used to analyze the production of PHB in chemostat cultures of *A. lata* DSM1123. Results showed that significant PHB accumulation occurred not only under nitrogen and oxygen-limited conditions, but also under glucose-limited chemostat cultures but only after a threshold dilution rate, mimicking the overflow metabolism observed in other bacteria. The counterintuitive PHB accumulation under glucose-limited conditions, a situation where only biomass production should be observed, could be explained by a Flux Balance Model incorporating two internal metabolic constraints: a limited flow through the Krebs cycle and a maximum metabolically active protein.

The characterization of this strain in chemostat culture and the model developed can be used for the design and environmental and economic assessment of processes to produce PHB and other metabolites, where the constraints leading to a growth associated production can boost the process productivity, such as continuous or fed-batch cultures.

### CRedit authorship contribution statement

**Felipe Scott:** Conceptualization, Investigation, Formal analysis, Software, Writing - original draft, Writing - review & editing, Funding acquisition, Supervision, Project administration. **Luz Yañez:** Investigation, Software, Visualization. **Raúl Conejeros:** Conceptualization, Formal analysis, Software, Writing - review & editing. **Blanca Araya:** Investigation, Formal analysis, Writing - review & editing. **Alberto Vergara-Fernández:** Writing - review & editing, Funding acquisition.

### Declaration of Competing Interest

The authors declare that the research was conducted in the absence of any commercial or financial relationships that could be construed as a potential conflict of interest.

### Data Availability

Datasets related to this article can be found at <https://doi.org/10.17632/ykvpj42jw.3>, an open-source online data repository

hosted at Mendeley Data.

## Acknowledgments

The present work has been financially supported by the National Agency for Research and Development, Chile (ANID) grants CONICYT-FONDECYT iniciación 11170081 and CONICYT-PCI REDES190137.

## Appendix A. Supporting information

Supplementary data associated with this article can be found in the online version at [doi:10.1016/j.jece.2021.105665](https://doi.org/10.1016/j.jece.2021.105665).

## References

- [1] R. Geyer, J.R. Jambeck, K.L. Law, Production, use, and fate of all plastics ever made, *Sci. Adv.* 3 (2017), 1700782.
- [2] Hamilton, L.A. et al. *The Hidden Costs of a Plastic Planet.* ([www.ciel.org/plasticandclimate](http://www.ciel.org/plasticandclimate)) (2019).
- [3] J. Zheng, S. Suh, Strategies to reduce the global carbon footprint of plastics, *Nat. Clim. Change* 9 (2019) 374–378.
- [4] A. Steinbüchel, S. Hein, Biochemical and molecular basis of microbial synthesis of polyhydroxyalkanoates in microorganisms, in: W. Babel, A. Steinbüchel (Eds.), *Biopolymers. Advances in Biochemical Engineering/Biotechnology*, vol. 71, Springer Berlin, Heidelberg, 2001, pp. 81–123.
- [5] T. Yamane, M. Fukunaga, Y.W. Lee, Increased PHB productivity by high-cell-density fed-batch culture of *Alcaligenes latus*, a growth-associated PHB producer, *Biotechnol. Bioeng.* 50 (1996) 197–202.
- [6] F. Ghodossi, H. Golzar, F. Yazdian, K. Khosravi-Darani, E. Vasheghani-Farahani, Effect of carbon sources for PHB production in bubble column bioreactor: emphasis on improvement of methane uptake, *J. Environ. Chem. Eng.* 7 (2019), 102978.
- [7] C. Brigham, Perspectives for the biotechnological production of biofuels from CO<sub>2</sub> and H<sub>2</sub> using *Ralstonia eutropha* and other ‘Knallgas’ bacteria, *Appl. Microbiol. Biotechnol.* 103 (2019) 2113–2120.
- [8] L. Yañez, R. Conejeros, A. Vergara-Fernández, F. Scott, Beyond intracellular accumulation of polyhydroxyalkanoates: chiral hydroxyalkanoic acids and polymer secretion, *Front. Bioeng. Biotechnol.* 8 (2020) 248.
- [9] R.A. Henderson, C.W. Jones, Physiology of poly-3-hydroxybutyrate (PHB) production by *Alcaligenes eutrophus* growing in continuous culture, *Microbiology* 143 (1997) 2361–2371.
- [10] F. Wang, S. Lee, Poly(3-Hydroxybutyrate) production with high productivity and high polymer content by a fed-batch culture of *Alcaligenes latus* under nitrogen limitation, *Appl. Environ. Microbiol.* 63 (1997) 3703–3706.
- [11] J.U. Ackermann, W. Babel, Growth-associated synthesis of poly(hydroxybutyric acid) in *Methylobacterium rhodesianum* as an expression of an internal bottleneck, *Appl. Microbiol. Biotechnol.* 47 (1997) 144–149.
- [12] W.J. Page, O. Knosp, Hyperproduction of poly-beta-hydroxybutyrate during exponential growth of *azotobacter vinelandii* UWD, *Appl. Environ. Microbiol.* 55 (1989) 1334–1339.
- [13] J.A. De Hollander, Kinetics of microbial product formation and its consequences for the optimization of fermentation processes, *Antonie Van Leeuwenhoek* 63 (1993) 375–381.
- [14] D.H. de Groot, J. Lischke, R. Muolo, R. Planqué, F.J. Bruggeman, B. Teusink, The common message of constraint-based optimization approaches: overflow metabolism is caused by two growth-limiting constraints, *Cell. Mol. Life Sci.* 77 (2020) 441–453.
- [15] J. Wallenius, H. Maaheimo, T. Eerikäinen, Carbon 13-metabolic flux analysis derived constraint-based metabolic modelling of *Clostridium acetobutylicum* in stressed chemostat conditions, *Bioresour. Technol.* 219 (2016) 378–386.
- [16] K.B. Andersen, K. von Meyenburg, Are growth rates of *Escherichia coli* in batch cultures limited by respiration? *J. Bacteriol.* 144 (1980) 114–123.
- [17] V. Riis, W. Mai, Gas chromatographic determination of poly-β-hydroxybutyric acid in microbial biomass after hydrochloric acid propanolysis, *J. Chromatogr. A* 445 (1988) 285–289.
- [18] N. Pacheco, M. Orellana-Saez, M. Pepczynska, J. Enrione, M. Bassas-Galia, J. M. Borrero-de Acuña, F.C. Zacconi, A.E. Marcoleta, I. Poblete-Castro, Exploiting the natural poly(3-hydroxyalkanoates) production capacity of Antarctic *Pseudomonas* strains: from unique phenotypes to novel biopolymers, *J. Ind. Microbiol. Biotechnol.* 46 (2019) 1139–1153.
- [19] O. Samek, S. Obruča, M. Šiler, P. Sedláček, P. Benešová, D. Kučera, I. Márova, J. Ježek, S. Bernatová, P. Zemánek, Quantitative Raman spectroscopy analysis of polyhydroxyalkanoates produced by *Cupriavidus necator* H16, *Sensors* 16 (2016) 1808.
- [20] J.D. Orth, B.Ø. Palsson, R.M.T. Fleming, Reconstruction and use of microbial metabolic networks: the core *Escherichia coli* metabolic model as an educational guide, *EcoSal* 4 (2010).
- [21] Z.A. King, J. Lu, A. Dräger, P. Miller, S. Federowicz, J.A. Lerman, A. Ebrahim, B. O. Palsson, N.E. Lewis, BiGG models: a platform for integrating, standardizing and sharing genome-scale models, *Nucleic Acids Res.* 44 (2016) D515–D522.
- [22] I. Thiele, B.Ø. Palsson, A protocol for generating a high-quality genome-scale metabolic reconstruction, *Nat. Protoc.* 5 (2010) 93–121.

- [23] L. Jeske, S. Placzek, I. Schomburg, A. Chang, D. Schomburg, BRENDA in 2019: a European ELIXIR core data resource, *Nucleic Acids Res.* 47 (2019) D542–D549.
- [24] R. Caspi, R. Billington, C.A. Fulcher, I.M. Keseler, A. Kothari, M. Krummenacker, M. Latendresse, P.E. Midford, Q. Ong, W.K. Ong, S. Paley, P. Subhraveti, P.D. Karp, The MetaCyc database of metabolic pathways and enzymes, *Nucleic Acids Res.* 46 (2018) D633–D639.
- [25] M. Kanehisa, KEGG: Kyoto Encyclopedia of Genes and Genomes, *Nucleic Acids Res.* 28 (2000) 27–30.
- [26] A.P. Arkin, R.W. Cottingham, C.S. Henry, N.L. Harris, R.L. Stevens, S. Maslov, P. Dehal, D. Ware, F. Perez, S. Canon, M.W. Sneddon, M.L. Henderson, W.J. Riehl, D. Murphy-Olson, S.Y. Chan, R.T. Kamimura, S. Kumari, M.M. Drake, T.S. Brettin, E.M. Glass, D. Chivian, D. Gunter, D.J. Weston, B.H. Allen, J. Baumohl, A.A. Best, M. Gerstein, A. Greiner, J. Gurtowski, H.L. Haun, F. He, R. Jain, M.P. Joachimiak, K.P. Keegan, S. Kondo, V. Kumar, M.L. Land, F. Meyer, M. Mills, P.S. Novichkov, T. Oh, G.J. Olsen, R. Olson, B. Parrello, S. Pasternak, E. Pearson, S.S. Poon, G. A. Price, S. Ramakrishnan, P. Ranjan, P.C. Ronald, M.C. Schatz, S. Seaver, M. Shukla, R.A. Sutormin, M.H. Syed, J. Thomason, N.L. Tintle, D. Wang, F. Xia, H. Yoo, S. Yoo, D. Yu, KBase: The United States department of energy systems biology knowledgebase, *Nat. Biotechnol.* 36 (2018) 566–569.
- [27] T.W. Kim, J.S. Park, Y.H. Lee, Enzymatic characteristics of biosynthesis and degradation of poly- $\beta$ -hydroxybutyrate of *Alcaligenes latus*, *J. Microbiol. Biotechnol.* 6 (1996) 425–431.
- [28] L. Heirendt, S. Arreckx, T. Pfau, S.N. Mendoza, A. Richelle, A. Heinken, H. S. Haraldsdóttir, J. Wachowiak, S.M. Keating, V. Vlasov, S. Magnúsdóttir, C.Y. Ng, G. Preciat, A. Żagare, S. Chan, M.K. Aurich, C.M. Clancy, J. Modamio, J.T. Sauls, A. Noronha, A. Bordbar, B. Cousins, D.C. El Assal, L.V. Valcarcel, I. Apaolaza, S. Ghaderi, M. Ahooshoh, M. Ben Guebila, A. Kostromins, N. Sompairac, H.M. Le, D. Ma, Y. Sun, L. Wang, J.T. Yurkovich, M. Oliveira, P.T. Vuong, L.P. El Assal, I. Kuperstein, A. Zinovyev, H.S. Hinton, W.A. Bryant, F.J. Aragón Artacho, F. J. Planes, E. Stalidzans, A. Maass, S. Vempala, M. Hucka, M.A. Saunders, C. D. Maranas, N.E. Lewis, T. Sauter, B.Ø. Pálsson, I. Thiele, R. Fleming, Creation and analysis of biochemical constraint-based models using the COBRA Toolbox v.3.0, *Nat. Protoc.* 14 (2019) 639–702.
- [29] A. Nilsson, J. Nielsen, Metabolic trade-offs in yeast are caused by F1F0-ATP synthase, *Sci. Rep.* 6 (2016) 22264.
- [30] B.D. Bennett, E.H. Kimball, M. Gao, R. Osterhout, S.J. Van Dien, J.D. Rabinowitz, Absolute metabolite concentrations and implied enzyme active site occupancy in *Escherichia coli*, *Nat. Chem. Biol.* 5 (2009) 593–599.
- [31] J.A. Gomez, K. Höffner, P.I. Barton, DFBALab: a fast and reliable MATLAB code for dynamic flux balance analysis, *BMC Bioinform.* 15 (2014) 409.
- [32] A. Atlič, M. Koller, D. Scherzer, C. Kutschera, E. Grillo-Fernandes, P. Horvat, E. Chiellini, G. Braunege, Continuous production of poly([R]-3-hydroxybutyrate) by *Cupriavidus necator* in a multistage bioreactor cascade, *Appl. Microbiol. Biotechnol.* 91 (2011) 295–304.
- [33] A. Papapostolou, E. Karasavvas, C. Chatzidoukas, Oxygen mass transfer limitations set the performance boundaries of microbial PHA production processes – a model-based problem investigation supporting scale-up studies, *Biochem. Eng. J.* 148 (2019) 224–238.
- [34] B.A. Ramsay, K. Lomaliza, C. Chavarie, B. Dubé, P. Bataille, J.A. Ramsay, Production of poly-(beta-hydroxybutyric-co-beta-hydroxyvaleric) acids, *Appl. Environ. Microbiol.* 56 (1990) 2093–2098.
- [35] R. Durner, B. Witholt, T. Egli, Accumulation of poly[(R)-3-hydroxyalkanoates] in *Pseudomonas oleovorans* during growth with octanoate in continuous culture at different dilution rates, *Appl. Environ. Microbiol.* 66 (2000) 3408–3414.
- [36] G. Haage, E. Wallner, R. Bona, F. Schellauf, G. Braunege, Production of Poly-3-hydroxybutyrate-co-3-hydroxy-valerate with *Alcaligenes latus* DSM 1124 on Various Carbon Sources. *Biorelated Polymers*, Springer, US, 2001, pp. 147–155, [https://doi.org/10.1007/978-1-4757-3374-7\\_13](https://doi.org/10.1007/978-1-4757-3374-7_13).
- [37] T. Yamane, Yield of poly-D(-)-3-hydroxybutyrate from various carbon sources: a theoretical study, *Biotechnol. Bioeng.* 41 (1993) 165–170.
- [38] E.J. Bormann, Stoichiometrically calculated yields of the growth-associated production of polyhydroxybutyrate in bacteria, *Biotechnol. Lett.* 22 (2000) 1437–1442.
- [39] I. Lee, M.K. Kim, H.N. Chang, Y.H. Park, Regulation of poly- $\beta$ -hydroxybutyrate biosynthesis by nicotinamide nucleotide in *Alcaligenes eutrophus*, *FEMS Microbiol. Lett.* 131 (1995) 35–39.
- [40] W. Liebermeister, E. Noor, A. Flamholz, D. Davidi, J. Bernhardt, R. Milo, Visual account of protein investment in cellular functions, *Proc. Natl. Acad. Sci. U.S.A.* 111 (2014) 8488–8493.
- [41] R. Iino, R. Hasegawa, K.V. Tabata, H. Noji, Mechanism of Inhibition by C-terminal  $\alpha$ -Helices of the  $\epsilon$  Subunit of *Escherichia coli* FoF1-ATP Synthase, *J. Biol. Chem.* 284 (2009) 17457–17464.
- [42] C. Etzold, G. Deckers-Hebestreit, K. Altendorf, Turnover number of *Escherichia coli* FoF1 ATP synthase for ATP synthesis in membrane vesicles, *Eur. J. Biochem.* 243 (1997) 336–343.
- [43] M. Yoshida, E. Muneyuki, T. Hisabori, ATP synthase — A marvellous rotary engine of the cell, *Nat. Rev. Mol. Cell Biol.* 2 (2001) 669–677.
- [44] A. Steinbüchel, H.G. Schlegel, Excretion of pyruvate by mutants of *Alcaligenes eutrophus*, which are impaired in the accumulation of poly( $\beta$ -hydroxybutyric acid) (PHB), under conditions permitting synthesis of PHB, *Appl. Microbiol. Biotechnol.* 31 (1989) 168–175.



# Production of (R)-3-hydroxybutyric acid from methane by *in vivo* depolymerization of polyhydroxybutyrate in *Methylocystis parvus* OBBP

Luz Yáñez<sup>a,b</sup>, Yadira Rodríguez<sup>a</sup>, Felipe Scott<sup>b</sup>, Alberto Vergara-Fernández<sup>b</sup>, Raúl Muñoz<sup>a,\*</sup>

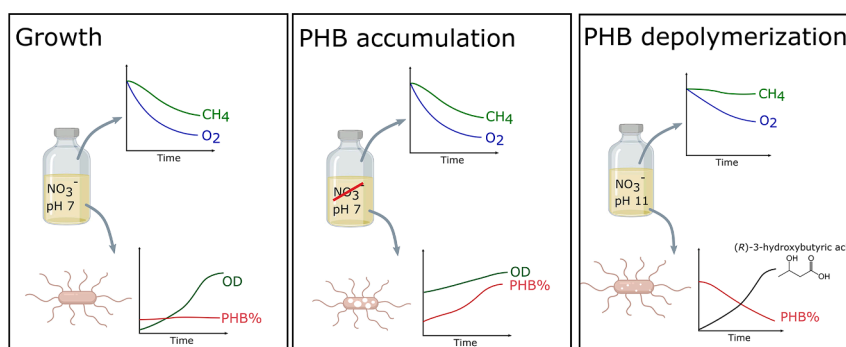
<sup>a</sup> Institute of Sustainable Processes, Universidad de Valladolid, Doctor Mergelina s/n, 47011, Spain

<sup>b</sup> Green Technology Research Group, Facultad de Ingeniería y Ciencias Aplicadas, Universidad de Los Andes, 7550000, Chile

## HIGHLIGHTS

- PHB accumulated in *M. parvus* was depolymerized under alkaline conditions.
- The depolymerization produced (R)-3-hydroxybutyrate with a 77% conversion.
- The presence of a nitrogen source promoted depolymerization and monomer release.
- Low O<sub>2</sub> supply rates and high monomers concentration reduced PHB depolymerization.

## GRAPHICAL ABSTRACT



## ARTICLE INFO

### Keywords:

(R)-3-hydroxybutyrate  
Chiral compounds  
Greenhouse gas valorization  
Methanotrophic bacteria  
Polyhydroxybutyrate

## ABSTRACT

*Methylocystis parvus* OBBP accumulates polyhydroxybutyrate (PHB) using methane as the sole carbon and energy source. In this work, the feasibility of producing (R)-3-hydroxybutyric acid (R3HBA) via intracellularly accumulated PHB through depolymerization (*in-vivo*) was investigated. Results showed that a PHB to R3HBA conversion of  $77.2 \pm 0.9\%$  (R3HBA titer of  $0.153 \pm 0.002 \text{ g L}^{-1}$ ) can be attained in a mineral medium containing  $1 \text{ g L}^{-1} \text{ KNO}_3$  at  $30 \text{ }^\circ\text{C}$  with shaking at 200 rpm and a constant pH of 11 for 72 h. Nitrogen deprivation and neutral or acidic pHs strongly reduced the excreted R3HBA concentration. Reduced oxygen availability negatively affected the R3HBA yield, which decreased to  $73.6 \pm 4.9\%$  (titer of  $0.139 \pm 0.01 \text{ g L}^{-1}$ ) under microaerobic conditions. Likewise, the presence of increasing concentrations of R3HBA in the medium before the onset of PHB depolymerization reduced the initial R3HBA release rate and R3HBA yield.

## 1. Introduction

Methane (CH<sub>4</sub>) is an inexpensive, colorless, odorless, and abundant gas that represents a widely available carbon and energy source. In

2019, CH<sub>4</sub> accounted for nearly 10 % of all U.S. anthropogenic greenhouse gas emissions (Jackson et al., 2020). The largest CH<sub>4</sub> sources included anthropogenic emissions from agriculture, waste and the extraction and use of fossil fuels (Kirschke et al., 2013; Saunio et al.,

\* Corresponding author.

E-mail addresses: [lfyanez@miuandes.cl](mailto:lfyanez@miuandes.cl) (L. Yáñez), [yadira.rodriguez@uva.es](mailto:yadira.rodriguez@uva.es) (Y. Rodríguez), [fscott@miuandes.cl](mailto:fscott@miuandes.cl) (F. Scott), [aovergara@miuandes.cl](mailto:aovergara@miuandes.cl) (A. Vergara-Fernández), [mutora@iq.uva.es](mailto:mutora@iq.uva.es) (R. Muñoz).

<https://doi.org/10.1016/j.biortech.2022.127141>

Received 9 March 2022; Received in revised form 6 April 2022; Accepted 7 April 2022

Available online 9 April 2022

0960-8524/© 2022 The Authors. Published by Elsevier Ltd. This is an open access article under the CC BY license (<http://creativecommons.org/licenses/by/4.0/>).

2016). The Global Methane Assessment report shows that decreasing methane emission by 45% during this decade would avoid 0.3 °C of global warming by 2045. Moreover, nearly a quarter-million premature deaths and 25 million tons of crop losses could be prevented annually (Ravishankara et al., 2021). CH<sub>4</sub> emissions contribute to almost one-quarter of the cumulative radiative forcing of carbon dioxide (CO<sub>2</sub>), CH<sub>4</sub> and nitrous oxide (N<sub>2</sub>O) combined since 1750 (Etminan et al., 2016). Although the lifetime of CH<sub>4</sub> in the atmosphere is much shorter than that of CO<sub>2</sub>, it absorbs thermal infrared radiation much more efficiently. Indeed, CH<sub>4</sub> exhibits a global warming potential 86 times stronger per unit of mass than CO<sub>2</sub> on a 20-year timescale and approximately 28 times more powerful on a 100-year time scale (Edenhofer, 2014). Today, CH<sub>4</sub> can be captured from landfills (38 Mt/year), wastewater treatment (21 Mt/year), agriculture (11–30 Mt/year), biomass (10 Mt/year), and natural gas production (92 Mt/year) (Strong et al., 2015). This methane can be valorized as an energy vector or as a feedstock for the biological production of products such as ectoine, biopolymers, and single cell proteins, among others (Jawaharraj et al., 2020) or for the catalytic production of methanol (Latimer et al., 2018). In this context, CH<sub>4</sub> represents a carbon and energy source for a group of gram-negative bacteria known as methanotrophs. These bacteria are classified according to the pathways used for the assimilation of the formaldehyde directly derived from CH<sub>4</sub> into type I and type II methanotrophs. Type I using the ribulose monophosphate pathway for formaldehyde assimilation, and type II methanotrophs using the serine pathway (Nguyen et al., 2021). *Methylocystis parvus* is a type II methanotroph that shows a higher specific growth rate compared to other species of the *Methylocystis* genera (Bordel et al., 2019) and the ability to synthesize the biopolymer polyhydroxybutyrate (PHB) under nitrogen-limited conditions (Rostkowski et al., 2013). *M. parvus* has been reported to accumulate more than 50% (Pieja et al., 2011; Wendlandt et al., 2001) of its dry weight as PHB, which renders it a suitable industrial biopolymer producer.

In *M. parvus*, PHB synthesis starts with the condensation of two acetyl-CoA molecules, see Fig. 2A (Bordel et al., 2019). This pathway is conserved in many bacteria such as *Ralstonia eutropha*, *Azohydromonas* spp., *Azotobacter* spp., among others (McAdam et al., 2020), where acetyl-CoA molecules can be supplied from a wide range of carbon sources. These include simple sugars and organic acids (Sirohi et al., 2020), food residues, and industrial by-products (Liu et al., 2021). Bacteria rely on PHB depolymerases (PhaZ), located intracellularly, to catabolize this stored reserve of carbon and energy (Müller-Santos et al., 2021), yielding the monomer (*R*)-3-hydroxybutyric acid (R3HBA) and dimers (Jendrossek and Handrick, 2002). If conditions are permissive for growth, the released R3HBA will act as a source of carbon and energy (Donoso et al., 2011), starting with the conversion of R3HBA to acetoacetate by the NADH-dependent enzyme (*R*)-3-hydroxybutyrate dehydrogenase (Bdh) (Tokiwa and Ugwu, 2007). If environmental conditions do not support growth, or part of the R3HBA consumption pathway is blocked, the monomer is excreted to the media (Lee et al., 1999). This strategy has been implemented in non-methanotrophic PHB producers to obtain R3HBA in the cultivation broth during PHB depolymerization. While for *Azohydromonas lata* a pH of 4.0 produced the highest titer and yield of R3HBA, a pH of 9.2 was required for the liberation of hydroxyalkanoic acids from polyhydroxyalkanoates in *Pseudomonas putida* (Ruth et al., 2007).

R3HBA is a chiral molecule that can be applied as a building block in the synthesis of fine chemicals and pharmaceutical products such as biopolymers, antibiotics (Ren et al., 2005), insecticides and fragrances (Matsuyama et al., 2001; Yáñez et al., 2020). R3HBA and its derivatives have been also used as potential drugs. For example, the infusion of R3HBA improved ATP production in mitochondria and confers partial protection against neurodegenerative disease in a Parkinson mice model (Tieu et al., 2003). Outcomes of depression (Yamanashi et al., 2017), osteoporosis (Cao et al., 2014), Alzheimer (Zhang et al., 2013), and cardiovascular diseases (Nielsen et al., 2019) have been shown to

improve using a 3HBA infusion. As a dietary supplement, the price of 3HBA is within 130–160 USD/kg (Fruggo, 2021). However, the conventional synthesis, extraction and purification of R3HBA from PHB produced from sugar-based bacterial processes is nowadays expensive (Pérez-Rivero et al., 2019), which requires alternative PHB production pathways with streamlined downstream processes in order to enhance process economics.

This work aims at determining the environmental conditions (presence or absence of carbon and nitrogen sources, pH, temperature) that lead to the production of R3HBA in the culture supernatant using the native PHB depolymerization pathway in *M. parvus*. The underlying hypothesis is that a combination of these variables would result in an active PHB depolymerase and an inactive or inhibited (*R*)-3-hydroxybutyrate dehydrogenase, as previously shown for other gram negative bacteria (Lee et al., 1999; Ren et al., 2005, 2007; Ruth et al., 2007).

## 2. Materials and methods

### 2.1. Mineral salt medium

Nitrate mineral salt (NMS) medium (pH 6.8) was composed of (g L<sup>-1</sup>): 1.0 KNO<sub>3</sub>, 1.1 MgSO<sub>4</sub>·7H<sub>2</sub>O, 0.8 Na<sub>2</sub>HPO<sub>4</sub>·12H<sub>2</sub>O, 0.26 KH<sub>2</sub>PO<sub>4</sub> and 0.2 CaCl<sub>2</sub>·2H<sub>2</sub>O; and 1 mL of trace element solution (g L<sup>-1</sup>): 0.3 Na<sub>2</sub>MoO<sub>4</sub>·2H<sub>2</sub>O, 0.3 Na<sub>2</sub>EDTA·2H<sub>2</sub>O, 1 CuSO<sub>4</sub>·5H<sub>2</sub>O, 0.5 FeSO<sub>4</sub>·7H<sub>2</sub>O, 0.4 ZnSO<sub>4</sub>·7H<sub>2</sub>O, 0.03 CoCl<sub>2</sub>, 0.02 MnCl<sub>2</sub>·4H<sub>2</sub>O, 0.015 H<sub>3</sub>BO<sub>3</sub>, 0.01 NiCl<sub>2</sub>·6H<sub>2</sub>O and 0.38 Fe-EDTA. Nitrate-free mineral salt (NFMS) medium was identical to NMS medium except that potassium nitrate was omitted. The reagents were acquired from PanReac AppliChem (Spain), except KNO<sub>3</sub>, which was purchased from COFARCAS (Spain).

### 2.2. Inocula preparation

The methanotrophic strain *Methylocystis parvus* OBBP, kindly provided by Biopolis S.L. (Valencia, Spain), was inoculated (10% v/v) under sterile conditions in 125-mL crimp-sealed serum bottles containing 50 mL of (NMS) medium. The headspace (75 mL) of the bottles was flushed under sterile conditions for 5 min with filtered oxygen (0.22 μm, Millex GP, Merck). Then, 25 mL of the oxygen headspace atmosphere was replaced with sterile methane, resulting in an O<sub>2</sub>:CH<sub>4</sub> concentration ratio of 66.7:33.3% (v/v). The cultures were incubated at 30 °C and 230 rpm in an orbital shaker (MaxQ 4000; Thermo Scientific, USA) for 5 days, unless otherwise stated. The headspace atmosphere of the bottles was replaced 6 times upon CH<sub>4</sub> depletion.

Then, biomass was collected and transferred into 2.2 L serum bottles containing 0.4 L of NMS, crimp sealed under a O<sub>2</sub>:CH<sub>4</sub> atmosphere of 66.7%:33.3% until complete methane depletion (~10 days). The headspace atmosphere was obtained by flushing for 3 min a gas mixture as described above from a 100 L-Tedlar gas sampling bag (Sigma-Aldrich, USA). The cultures were grown at 25 °C (thermostated room) with an initial pH of 6.9 and magnetically stirred at 300 rpm (Poly 15 Variomag, Thermo Fisher Scientific).

When methane was depleted, the biomass was collected by centrifugation at 10000 rpm for 8 min (Sorvall Legend RT+; Thermo Scientific, USA) and re-suspended into 0.4 L of NFMS medium to promote PHB accumulation for ~ 10 days under similar incubation conditions.

### 2.3. Optimization of PHB depolymerization in *M. Parvus*

Unless otherwise indicated, the experiments were performed batch wise using PHB containing biomass in 125 mL serum bottles (working volume of 45 mL) crimp sealed (three biological replicates). The bottles were incubated at 30 °C (except Test 3) and 230 rpm in an orbital shaker.

### 2.3.1. Test 1. Influence of the presence of nitrate and O<sub>2</sub>, and pH on PHB depolymerization

The assays were performed with NMS and NFMS media at both pH 4 and pH 11 in triplicate for 48 h. All cultures were inoculated with 10 mL of concentrated *M. parvus* culture previously grown in NFMS for 10 days (1.3 gTSS L<sup>-1</sup> with 51.4% of PHB) and were incubated for two days under an O<sub>2</sub>:CH<sub>4</sub> headspace (66.7%:33.3%) and a He:CH<sub>4</sub> atmosphere (66.7%:33.3%). A control test at pH 7 under a O<sub>2</sub>:CH<sub>4</sub> headspace (66.7%:33.3%) and NMS media was also carried out. Culture samples were collected periodically for the quantification of the R3HBA concentration. Total suspended solids (TSS), total nitrogen, PHAs, and pH were determined at the beginning and end of the experiment.

### 2.3.2. Test 2. Optimization of pH during PHB depolymerization

PHB depolymerization under an O<sub>2</sub>:CH<sub>4</sub> atmosphere (66.7%:33.3%) was assessed in triplicate at pH 10, pH 11 and pH 12 with NMS medium as above described for 48 h. The pH of the cultures was monitored three times per day and manually adjusted using 5 M NaOH, while the concentration of extracellular R3HBA was quantified once per day. The biomass concentration (estimated as TSS) and PHB cells content were determined at the beginning and the end of the experiment.

### 2.3.3. Test 3. Influence of temperature on the kinetic of PHB depolymerization

PHB depolymerization at pH 11 on NMS medium was assessed in triplicate at 25 and 35 °C for 3 h using fresh *M. parvus* with a concentration and PHB cell content of 4.17 gTSS L<sup>-1</sup> and 44.7%. The determination of extracellular R3HBA concentration was conducted at 15, 30, 60, 120 and 180 min. At the end of the experiment, cell viability was evaluated using the pellets obtained after centrifugation of the biomass from depolymerized cells. Cell viability tests were performed at 25 °C in 2.2 L serum bottles with a working volume of 0.4 L of both NMS and NFMS medium. The bottles were capped with aluminum caps and chlorobutyl rubber stoppers under and O<sub>2</sub>:CH<sub>4</sub> atmosphere (66.7%:33.3%) and incubated as above described (section 2.2) until complete CH<sub>4</sub> depletion. TSS, CH<sub>4</sub>, O<sub>2</sub> and CO<sub>2</sub> concentrations were periodically measured.

### 2.3.4. Test 4. Influence of the initial R3HBA concentration and aeration rate on PHB depolymerization

The influence of the oxygen mass transfer rate on PHB depolymerization and R3HBA yield was investigated in Erlenmeyer flasks (E-flasks) incubated at 200 rpm and 30 °C in an orbital shaker for 72 h. The lowest oxygen mass transfer rate was achieved in 100 mL E-flasks containing 100 mL of medium, while the highest oxygen transfer rate was reached in 250 mL E-flasks containing 50 mL of cultivation broth. An intermediate condition was tested in 100 mL E-flasks containing 50 mL of cultivation broth. The initial biomass concentration and PHB content of the cell suspension was 0.51 ± 0.005 gTSS L<sup>-1</sup> and 31.9 ± 1.88% PHB, respectively. The experiments were conducted in duplicate.

The potential inhibitory effect of extracellular R3HBA over PHB depolymerization was investigated using R3HBA produced *in-house* following the procedure described by Lee et al. (1999). Briefly, *Azohydromonas lata* (DSM 1123, Leibniz Institute, Germany) was cultivated from a frozen stock culture in a nutrient agar plate. A single colony was picked and used to inoculate a 500 mL E-flask with 100 mL of AL1 medium (Wang and Lee, 1997). This culture served as the inoculum for a batch bioreactor cultivation of this bacterium in a Labfors 5 bioreactor (Infors HT, Switzerland). The bioreactor was operated with 1 L of AL2 medium containing an initial glucose concentration of 30 g L<sup>-1</sup> and an initial ammonium sulfate concentration of 2 g L<sup>-1</sup>. Dissolved oxygen was maintained above 40% saturation by varying the stirring speed up to 700 rpm at 1 vvm air. When necessary, pure oxygen was automatically mixed with the inlet air flow under a cascade control. After 24 h of cultivation, approximately 12.0 g L<sup>-1</sup> of biomass were retrieved containing a PHB cell content of 75%. Cells were collected by

centrifugation, washed twice with distilled water, and resuspended in water at a concentration of approximately 120 gTSS L<sup>-1</sup>. PHB depolymerization was started by adjusting the pH to 4.0 with HCl and lasted for 1 h. The pH was controlled at 4.0 using 2 M NaOH. Following the purification procedure outlined in Lee et al. (1999), a solution containing 34.2 g L<sup>-1</sup> of sodium (*R*)-3-hydroxybutyrate was obtained. HPLC analysis indicated that the solution contained trace levels of other unidentified compounds and crotonic acid. Finally, *M. parvus* cells containing PHB were washed and resuspended in NMS medium at pH 11 supplemented with R3HBA at concentrations of 0, 120, 330 and 650 mg L<sup>-1</sup>. Cell incubation was performed in 100 mL E-flasks containing 50 mL of cell suspension with the corresponding R3HBA concentration at 30 °C and 200 rpm in an orbital shaker.

Culture samples were collected at 0, 3, 6, 48 and 72 h for R3HBA and crotonic acid quantification. The biomass and PHB cell content were monitored at the beginning and the end of experiments.

## 2.4. PHB depolymerization and R3HBA yields calculation

The PHB depolymerization percentage conversion (%) was calculated according to Eq. (1):

$$C_{PHB} = 100 \times \frac{X_{PHB}^i - X_{PHB}^f}{X_{PHB}^i} \quad (1)$$

The R3HBA molar yield was calculated as the ratio of the moles of R3HBA excreted and the moles of PHB consumed, considering that PHB hydrolysis consumes one mol of water per mol of R3HBA produced (Eq. (2)):

$$Y_{R3HBA} = 100 \left( \frac{104.10 - 18.01}{104.10} \right) \frac{X_{R3HBA}^f - X_{R3HBA}^i}{X_{PHB}^i - X_{PHB}^f} \quad (2)$$

where  $X_{PHB}^i$  and  $X_{PHB}^f$  correspond to the initial and final PHB concentrations (g L<sup>-1</sup>), and  $X_{R3HBA}^i$  and  $X_{R3HBA}^f$  represent the initial and final concentrations of R3HBA (g L<sup>-1</sup>). A similar calculation was used for the crotonic acid yield ( $Y_{croton}$ ). The conversion of PHB to R3HBA can be calculated as the product  $0.01 \cdot Y_{R3HBA} \cdot C_{PHB}$ .

Finally, the specific R3HBA release rate per gram of initial intracellular PHB ( $q_{R3HBA}$ ) was calculated as follows.

$$q_{R3HBA} = \frac{m}{X_{PHB}^i} \quad (3)$$

Where  $m$  is the slope of the line whose independent and dependent variables are the depolymerization time and R3HBA concentration (in mg L<sup>-1</sup>), respectively.

## 2.5. Analytical procedures

CH<sub>4</sub>, CO<sub>2</sub> and O<sub>2</sub> gas concentrations were measured in gas chromatograph coupled with a thermal conductivity detector (Bruker 430 GC-TCD, Bruker Corporation, USA) following the method described by Estrada et al. (2014). The optical density of the cultures samples was measured by spectrophotometry at 600 nm (UV-2550, Shimadzu, Japan). TSS and pH were analyzed according to Rodríguez et al. (2020). PHB was quantified via gas chromatography-mass spectrometry (GC-MS) (Rodríguez et al., 2020) or GC-FID (Scott et al., 2021). The concentration of R3HBA was determined using a commercial (*R*)-3-Hydroxybutyric Acid Assay Kit (Megazyme, Ireland) according to manufacturer's protocol or using HPLC with a UV-Vis detector at 210 nm and a refractive index detector (Prominence, Shimadzu) according to Scott et al. (2021). Citrate, succinate, malate and crotonic acids (Sigma-Aldrich catalog number, 113018) were quantified using the HPLC-UV-IR method described by Scott et al. (2021). The organic acids standard was purchased from Biorad (catalog number, 125-0586).

### 3. Results and discussion

#### 3.1. Influence of the presence of nitrate and O<sub>2</sub> and pH on PHB depolymerization

Fig. 1 shows the methane and oxygen consumption for the 48 h depolymerization experiments performed with NMS (Fig. 1A and B) and NFMS (Fig. 1C and D) at pH 4, 7 and 11. Consumption of methane and oxygen was faster in the control experiment with NMS at pH 7 compared to that in NFMS medium, an expected result considering that NMS allows for balanced growth. In the absence of oxygen at pH 7, methane consumption was negligible in NFMS medium and close to 10% in the NMS cultures. In this regard, Bordel et al., (2019) showed that *M. parvus* can use stored PHB as an energy source under anoxic conditions only when nitrate is available in the cultivation broth. The annotated genome of *M. parvus* contains the genes involved in nitrate reduction and revealed that denitrification is the only mechanism supporting the use of methane or PHB as an energy source in the absence of oxygen (Bordel et al., 2019).

Both pHs of 11 and 4 induced an important reduction in the consumption of methane and oxygen compared to the control tests. Thus, methane consumption was negligible at pH 11 in NMS medium, while the final consumption of oxygen accounted for 64.8 ± 9.54% of the initial O<sub>2</sub> present in the headspace (compared to 87.8 ± 0.82% of the control), suggesting the occurrence of a respiratory metabolism fueled by a substrate different than methane. pH 4 supported an oxygen and methane final consumption of 33.4 ± 12.67 and 30.6 ± 14.14%, respectively. On the other hand, neither methane nor oxygen consumption was recorded at pH 4 in NFMS medium. Similarly, at pH 11 the final consumption of CH<sub>4</sub> (37.41 ± 6.81%) and the O<sub>2</sub> uptake (30.14 ±

4.65) were reduced compared to the control.

In NMS, nitrate was consumed only in the control assays at pH 7 from the initial 130.1 mgN L<sup>-1</sup> (measured as total nitrogen) to 47.8 ± 11.5 mgN L<sup>-1</sup> at the end of the 48 h incubation period. Nitrate consumption at pHs 4.0 and 11.0 was lower than 2.6 mgN L<sup>-1</sup> during the same period, and only 0.3 mgN L<sup>-1</sup> was consumed in the assay at pH 7 in the absence of oxygen. Therefore, no significant cell growth occurred except in the control assay at neutral pH.

Interestingly, extracellular R3HBA was only detected at pH 11 in both NMS and NFMS medium (Fig. 1E). At pH 11 in NMS, 80.6 ± 0.8% of PHB was depolymerized and R3HBA secretion reached 205.8 ± 1.2 mg L<sup>-1</sup>, a higher concentration compared with the assay in NFMS, where 25.7 ± 7.9% of PHB was depolymerized and a R3HBA titer of 60.1 ± 12.9 mg L<sup>-1</sup> was measured after 48 h. The mechanisms by which nitrogen influences the depolymerization extent and rate seem to be related to the alleviation of the stringent response. In amino acid starved cells, the alarmone ppGpp accumulates and destabilizes the RNA polymerase  $\sigma^{70}$ , resulting in an induction of genes under the control of alternative sigma  $\sigma$  factors, such as  $\sigma^{54}$  (Brigham et al., 2012). ppGpp has also been implicated in the inhibition of translation (Irving et al., 2021). In *Ralstonia eutropha* H16, PHB mobilization occurs in the absence of the alarmone ppGpp, which in turn requires the presence of a source of nitrogen (Juengert et al., 2017). As further evidence of this mechanism, the genome of *M. parvus* OBBP contains the necessary bifunctional (p) ppGpp synthetase/hydrolase (WP\_016921527.1) required for the synthesis and degradation of ppGpp.

PHB depolymerization at pH 4 and pH 7 (with or without O<sub>2</sub>) in NMS supported extracellular R3HBA concentrations of 5.42 ± 0.67 mg L<sup>-1</sup>, 4.83 ± 0.37 mg L<sup>-1</sup> and 4.01 ± 0.15 mg L<sup>-1</sup>, respectively. Similarly, extracellular R3HBA concentrations of 4.68 ± 0.37 mg L<sup>-1</sup>, 6.17 ± 0.22

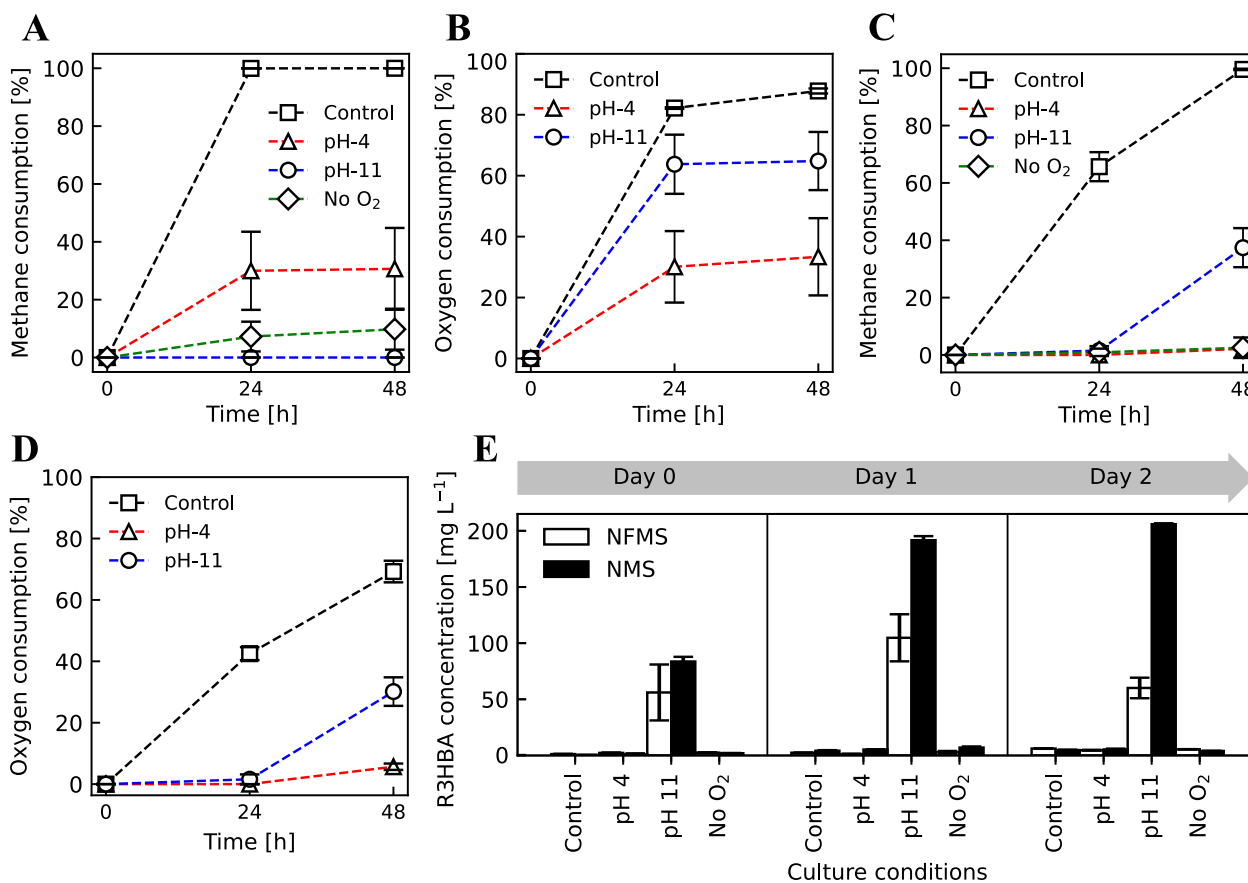


Fig. 1. CH<sub>4</sub> and O<sub>2</sub> consumption during PHB depolymerization in *M. parvus* cultivated in NMS (A, B) and NFMS (C, D) medium at pH 4 (triangles), pH 11 (circles), pH 7 (squares) and without oxygen at pH 7 (diamonds). (E) R3HBA released in *M. parvus* cultures at pH 4, pH 11, pH 7 (with and without oxygen) in NMS (black bars) and NFMS (white bars) medium.

mg L<sup>-1</sup> and 5.50 ± 0.15 mg L<sup>-1</sup> were measured after 48 h in NFMS at pH 4 and pH 7 with or without oxygen, respectively. The final pH of the culture broth in the assays initially adjusted to pH 11 in NMS and NFMS media decreased to 8.28 and 6.23, respectively, confirming the secretion of the acidic R3HBA. No significant changes in pH were measured in the rest of the experiments, which agreed with the limited R3HBA release. The estimated Y<sub>R3HBA</sub> are 31.5 ± 0.08% and 28.9 ± 0.91%, which equates to a PHB to R3HBA conversion of 25.4 ± 0.03% and 7.4 ± 2.1%, for the experiments at initial pH of 11 in NMS and NFMS, respectively.

The *in-vivo* depolymerization of the intracellularly accumulated PHAs to hydroxy acids has been reported in several bacterial strains. For instance, the depolymerization process in *Azohydromonas lata* was carried out in water without shaking to minimize oxygen transfer, at 37 °C and pH 4.0, and achieved a depolymerization efficiency of 96% of the initial PHB to R3HBA in only 30 min (Lee et al., 1999). These authors also evaluated PHB depolymerization in *Pseudomonas aeruginosa* PAO1 (DSM 1707), *Pseudomonas oleovorans* (ATCC 29347) and *Cupriavidus necator*

(NCIMB 11599) at pH values below 7.0 (Lee et al., 1999). The PHA to hydroxyacids conversion was 20% for *C. necator* and less than 10% for *Pseudomonas* species (Lee et al., 1999).

The conversion of PHA to hydroxyacids in *Pseudomonas putida* GPo1 was improved by changing the depolymerization conditions to an alkaline medium. This strain excreted (*R*)-3-hydroxyoctanoic (R3HO) acid and (*R*)-3-hydroxyhexanoic acid (R3HHx) at pH 11 in citrate buffer for 6 h with a PHA degradation efficiency and monomer production yields above 90% (w/w) (Ren et al., 2005). Ruth et al., (2007) engineered a depolymerization strategy at pH 10 in *P. putida* GPo1 under continuous mode with a production of R3HO, R3HHx, (*R*)-3-hydroxy-10 undecenoic acid, (*R*)-3-hydroxy-8-nonenoic acid, (*R*)-3-hydroxy-6-heptenoic acid, (*R*)-3-hydroxyundecanoic acid, (*R*)-3-hydroxynonanoic acid, and (*R*)-3-hydroxyheptanoic acid. The study herein presented confirmed the key role of high pH on PHA depolymerization, which is a common feature in *Pseudomonas* species. Hence, *P. putida* GPo1 released 3-hydroxyoctanoic acid and 3-hydroxyhexanoic acid from intracellular

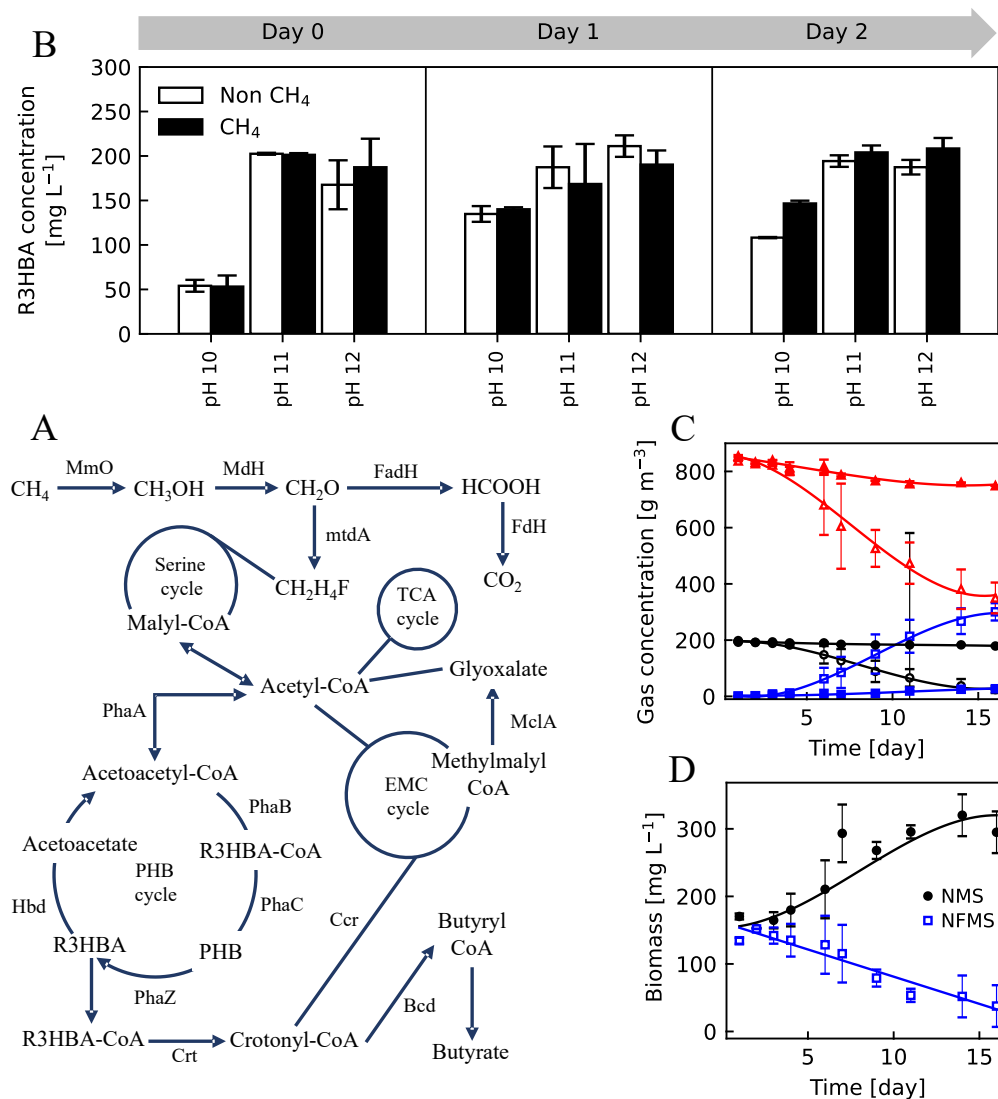


**Fig. 2.** Schematic representation of the metabolic pathways involved in the polymerization and depolymerization of PHB in *M. parvus* OBBP. MmO, methane monooxygenase; MdH, methanol dehydrogenase; FadH, formaldehyde dehydrogenase; FdH, formate dehydrogenase; MtdA, methylene tetrahydromethanopterin dehydrogenase; PhaA, β-ketothiolase; PhaB, acetoacetyl-CoA reductase; PhaC, PHB polymerase; Hbd, (*R*)-3-hydroxybutyrate dehydrogenase, Crt, 3-hydroxybutyryl-CoA dehydratase; Ccr, crotonyl-CoA carboxylase/reductase; MclA, malyl-CoA lyase; Bcd, butyryl-CoA dehydrogenase (A). R3HBA concentration in *M. parvus* at pH 10, 11 and 12 in NMS with (black bars) or without (white bars) CH<sub>4</sub> (B). Concentrations of biomass (C) and CH<sub>4</sub> (circles), O<sub>2</sub> (triangles) and CO<sub>2</sub> (square) during the viability assays of *M. parvus* cells previously subjected to a 3 h depolymerization phase at pH 11. Filled and empty symbols correspond to the experiments carried out in NMS and NFMS media, respectively.

PHA at pH 11 with conversions of 76% ( $0.356 \text{ g L}^{-1}$ ) and 21% ( $0.015 \text{ g L}^{-1}$ ) in 6 h, respectively (Ren et al., 2005). Similarly, *P. putida* Bet001 can depolymerize PHAs up to 98% in 0.2 Tris-HCl buffer at pH 9.1 within 48 h (Anis et al., 2018). In Type II methanotrophs, the production of hydroxyacids has only been described in a genetically engineered *Methylosinus trichosporum* OB3b strain able to synthesize R4HBA from  $\text{CH}_4$  via the TCA cycle and the overexpression phosphoenolpyruvate carboxylase (Ppc), isocitrate dehydrogenase (Icd) and 2-oxoglutarate dehydrogenase (SucAB). The highest 4-HB titer obtained was  $10.5 \text{ mg/L}$  after 6 culture days (Nguyen and Lee, 2021).

PHB synthesis and degradation in methanotrophic bacteria seem to be similar to the metabolic processes carried out by most heterotrophic PHB producers (Vecherskaya et al., 2001). However, there is a limited understanding of the mechanisms that bring about the intracellular PHB depolymerization and the formation of its monomer acids such as R3HBA and crotonic acid in Type II methanotrophs. Vecherskaya et al. (2001) demonstrated how products from the anaerobic fermentation of PHB in methanotrophs can be bioconverted in R3HBA, butyrate, acetate, succinate, and other reduced compounds. Fig. 2A shows the pathways of PHB depolymerization and formation of different metabolites in *M. parvus* OBBP based on a genome-scale metabolic model (Bordel et al., 2019) that has been recently reported. This model shows the fluxes of the PHB degradation from crotonyl-CoA to methylmalyl-CoA, which is dissociated into glyoxylate and propionyl-CoA. The glyoxylate originated from methylmalyl-CoA is incorporated into the serine cycle, and the propionyl-CoA is carboxylated into succinyl-CoA by the ethylmalonyl-CoA cycle (EMC) and then incorporated into the TCA cycle (Bordel et al., 2019). Another parallel pathway involves the enzymatic conversion of crotonyl-CoA to butyryl-CoA and finally to butyrate (Vecherskaya et al., 2001).

#### 4. Optimization of pH during PHB depolymerization

The results shown in Fig. 1B indicate that PHB depolymerization at pH 11 in NMS was superior to that at low pHs in NFMS. However, these results do not clarify if pHs closer to 11 could result in higher R3HBA titers, if pH control could improve R3HBA yields or if methane plays a role in the depolymerization of PHB. In this context, *M. parvus* cells containing 18.1% of PHB were resuspended in NMS medium at  $1.32 \pm 0.02 \text{ gTSS L}^{-1}$  and depolymerization was assessed at pHs of 10, 11 and 12 as above described. Unlike previous experiments, the pH of the cultivation broth was periodically monitored and controlled with NaOH during the course of the depolymerization.

*M. parvus* cells rapidly released R3HBA in the pH range of 10–12 following pH adjustment. Thus, the final extracellular monomer concentration reached  $146.6 \pm 3.11 \text{ mg L}^{-1}$  and  $108.2 \pm 0.66 \text{ mg L}^{-1}$  with or without methane at pH 10 (Fig. 2B). On the other hand, the influence of methane was negligible at pH 11 and pH 12, reaching a PHB depolymerization efficiency of  $96.6 \pm 2.22\%$  and  $92.9 \pm 1.5\%$ , respectively, (corresponding to  $204 \pm 7.8 \text{ mg L}^{-1}$  and  $208.44 \pm 11.81 \text{ mg L}^{-1}$  of R3HBA) in the presence of  $\text{CH}_4$ . Similar PHB depolymerization efficiencies of  $98.2 \pm 1.10\%$  and  $93.6 \pm 1.33\%$ , respectively, (corresponding to  $194.3 \pm 6.5 \text{ mg L}^{-1}$  and  $187.4 \pm 8.2 \text{ mg L}^{-1}$  of R3HBA) were recorded in the absence of  $\text{CH}_4$  at the end of the experiment at pH 11 and 12, respectively. These data suggested that methane did not play a significant role on PHB depolymerization and that pHs beyond 11.0 exerted little influence on R3HBA release. Based on these results, pH 11 in NMS and in the absence of  $\text{CH}_4$  was selected for further experiments. Under this condition, a PHB to R3HBA conversion of  $68.0 \pm 3.2\%$  was calculated.

The fine-tuning of pH played a key role in R3HBA release and PHB depolymerization in other bacteria species. For instance, Ren et al. (2005) demonstrated that PHA depolymerization in *Pseudomonas* Gpo1 produced the highest titer of monomers ( $360 \text{ mg L}^{-1}$  of 3-OH-C8) at an initial pH of 11, while a significantly smaller concentration of monomers ( $50 \text{ mg L}^{-1}$ ) was measured at pH 12. Similarly, depolymerization and

R3HBA release in *Azohydromonas lata* peaked at a pH of 4.0 with a PHB to R3HBA conversion of 96% in 30 min, and decreased to 31% at a pH 5.0 (Lee et al., 1999). The production of R3HBA *in vivo* requires a concomitant high PHB depolymerization activity and a low enzymatic activity of Bdh. While intracellular depolymerases have an optimum pH range of 8–10 (Jendrossek and Handrick, 2002), Bdh activity is reported to be pH-dependent, with an activity range of 5–10 and an optimal pH range of 7.5–8.5, decreasing abruptly above pH 10 (Mountassif et al., 2010; Takanashi and Saito, 2006) In this context, this study suggests that the phaZ enzyme, responsible of the depolymerization of PHB towards R3HBA, of *M. parvus* exhibits a high activity at pH 11.

#### 5. Influence of temperature on the kinetic of PHB depolymerization

Since the optimal temperature for both growth and PHB accumulation in *M. parvus* is  $30^\circ\text{C}$  and no growth occurs at temperatures greater than  $40^\circ\text{C}$  (Soni et al., 1998), the kinetics of PHB depolymerization and R3HBA released were investigated at 25 and  $35^\circ\text{C}$ , and pH 11 (manually adjusted to compensate for the release of R3HBA). The R3HBA titers quantified at  $25^\circ\text{C}$  and  $35^\circ\text{C}$  were  $240 \pm 3.81 \text{ mg L}^{-1}$  and  $282 \pm 20.04 \text{ mg L}^{-1}$ , respectively, after 3 h of depolymerization in a cell suspension with an initial PHB concentration of  $1.86 \pm 0.006 \text{ g L}^{-1}$ . The R3HBA production rates per mg of initial PHB were  $48.6 \pm 6.0 \text{ mg R3HBA (mgPHBi)}^{-1}\text{h}^{-1}$  at  $25^\circ\text{C}$  and  $52.7 \pm 2.3 \text{ mg R3HBA (mgPHBi)}^{-1}\text{h}^{-1}$  at  $35^\circ\text{C}$ , while PHB depolymerization reached 16.5% ( $Y_{3HBA} = 64.5\%$ ) and 24.8% ( $Y_{3HBA} = 50.5\%$ ) at 25 and  $35^\circ\text{C}$ , respectively. These results were similar to those obtained by Lee et al. (1999) during the depolymerization of PHB accumulated in *Azohydromonas lata* at 30, 37 and  $45^\circ\text{C}$ . A moderate increase in R3HBA production rate was found when the temperature increased from 30 to  $37^\circ\text{C}$ , while PHB depolymerization suddenly stopped at  $45^\circ\text{C}$  likely due to enzymatic denaturation. Since R3HBA production rate slightly increased with temperature, but R3HBA yields severely decreased, the following experiments were performed at  $30^\circ\text{C}$ .

After 3 h at  $25^\circ\text{C}$  and pH 10.8, cells were harvested and cultured in NMS (to assess cell growth) and NFMS (to assess PHB accumulation) media in the presence of  $\text{CH}_4$  to analyze the viability of the cells post-depolymerization. Cells incubated in NMS medium started to consume methane and oxygen by day 4, being these gases fully depleted after 16 days (Fig. 2C). Biomass concentration increased from  $170 \text{ mg L}^{-1}$  to  $295 \text{ mg L}^{-1}$  (Fig. 2D). However, the specific growth rate ( $\mu$ ) of post-depolymerization cells was lower ( $0.058 \text{ h}^{-1}$ ) than the specific growth rate of  $0.107 \text{ h}^{-1}$  reported for fresh *M. parvus* cultures (Bordel et al., 2019). On the other hand, the culture incubated in NFMS medium experienced cell death during the cell viability experiment due to nitrogen limitation.

#### 6. Influence of the initial R3HBA concentration and aeration rate on PHB depolymerization

To assess the effect of oxygen availability on PHB depolymerization in *M. parvus*, three tests with different liquid to air surface ratios were carried out at a constant pH of 11. Fig. 3A shows the kinetics of R3HBA release for the 72 h experiment and the depolymerization, crotonic acid and R3HBA yields in Fig. 3B. The final R3HBA concentration was similar regardless of the  $\text{O}_2$  supply, while the largest differences were obtained for the R3HBA yield. Indeed, the lowest R3HBA yield ( $73.6 \pm 4.9\%$ ) occurred under the condition restricting  $\text{O}_2$  mass transfer (100 mL of broth in a 100 mL E-flask) while under less restrictive  $\text{O}_2$  supply rates, R3HBA yields reached  $84.3 \pm 1.0\%$  and  $83.7 \pm 2.8\%$  at 50 mL/100 mL and 50 mL/250 mL filling ratios, respectively. In terms of PHB to R3HBA conversion, these values equate to  $77.2 \pm 0.9\%$  and  $75.1 \pm 3.3\%$ . Literature suggests that the oxygen content during the depolymerization process could influence the fate of the monomers produced in rather unpredictable manners. In this regard, the PHB accumulated with

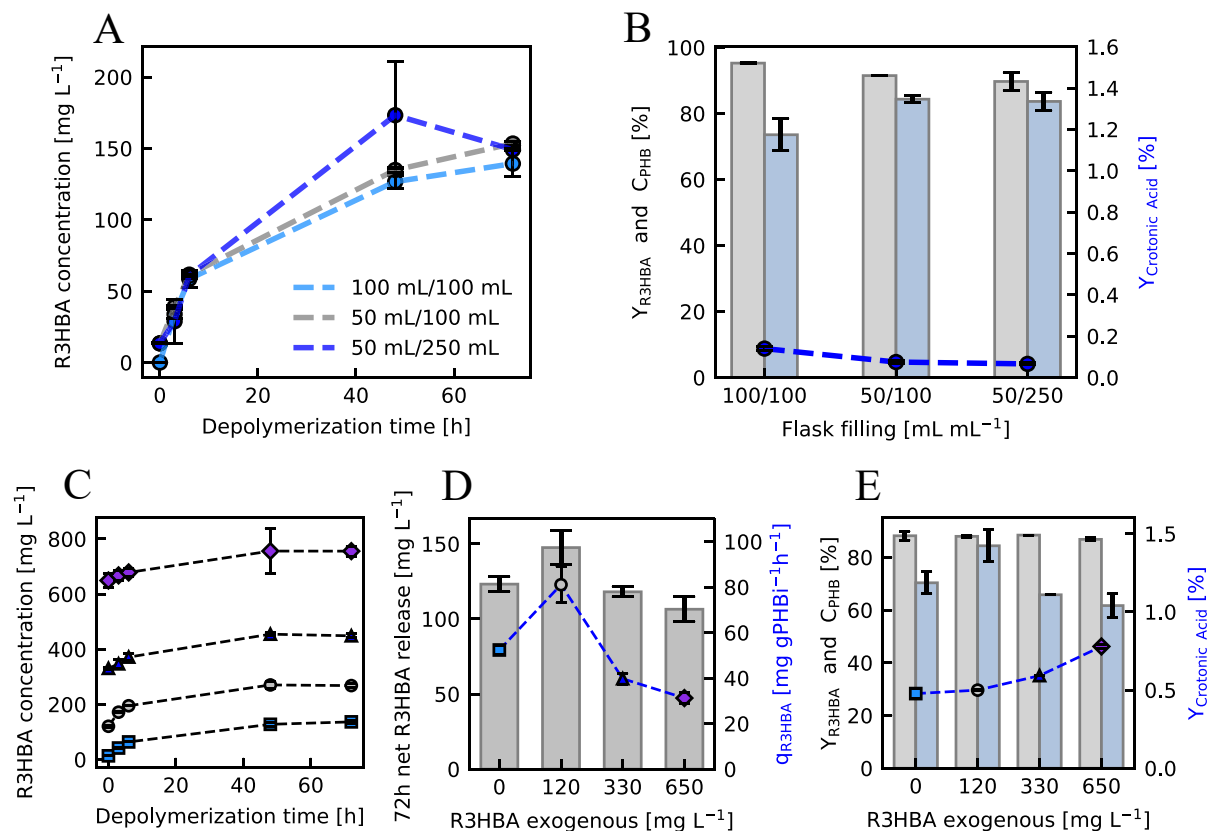


**Fig. 3.** Influence of the oxygen mass transfer rate on the kinetics of R3HBA excretion (A), depolymerization (grey bars) and R3HBA yields (blue bars) (B). Time course of R3HBA concentration at 0 (square), 120 (circle), 330 (triangle) and 650 (diamond)  $\text{mg L}^{-1}$  of initial R3HBA (C), net release (bars) and initial production rate of R3HBA (scatter plot) (D) and R3HBA yield (blue bars), depolymerization yield (gray bars) and crotonic acid yields (scatter plot) (E) at pH 11 and NMS medium in *M. parvus* after 72 h.

glycerol as substrate can be depolymerized to R3HBA in *Halomonas sp.* KM-1 under microaerobic conditions (25 mL of broth in 200 mL E-flasks agitated at 50 rpm) in the presence of a nitrogen source. Indeed,  $15.2 \text{ g L}^{-1}$  of R3HBA were produced in 66 h with a 76.6% PHB to R3HBA conversion under these conditions (Kawata et al., 2012). On the other hand, *Halomonas sp.* OITC1261 behaves differently despite its taxonomic closeness with *Halomonas sp.* KM-1, synthesizing R3HBA concomitantly with PHB under aerobic conditions without extra nitrogen supplementation (Yokaryo et al., 2018).

HPLC analysis of the depolymerization broth at 72 h showed that citric acid (ranging between 1 and  $3 \text{ mg L}^{-1}$  depending on the  $\text{O}_2$  supply rate), malate ( $20\text{--}45 \text{ mg L}^{-1}$ ), succinate ( $5\text{--}20 \text{ mg L}^{-1}$ ) and crotonate (less than  $0.2 \text{ mg L}^{-1}$ ) were present along with R3HBA and two unidentified compounds at 18.5 and 19.5 min in the incubation broth drawn after 72 h of depolymerization assay. In addition, a peak at 14.6 min was resolved, presumably corresponding to R3HBA dimers based on previous reports (Lu et al., 2014).

The oxygen consumption during the PHB depolymerization process at pH 11 (Fig. 1B) and the fact that the yield of R3HBA decreased as the supply of oxygen decreased below a certain threshold, suggests that part of the electrons released from the conversion of the depolymerized PHB towards acetyl-CoA are aerobically oxidized for the provision of maintenance energy. This follows from the subsequent findings: (i) the production of acetoacetate from R3HBA produces a molecule of NADH that could be used for ATP production if  $\text{O}_2$  is available, (ii) a negligible nitrate consumption was measured at pH 11 during the depolymerization experiment, thus growth can be disregarded, (iii) a limited supply of  $\text{O}_2$ , achieved by carrying out the depolymerization process in an almost filled E-flask, decreased the R3HBA yield, suggesting that R3HBA was

routed towards other metabolites to provide energy for maintenance. The latter finding can be considered as a less extreme version of the experiments by Vecherskaya et al. (2001) under anaerobic conditions, where products characteristic of a fermentative metabolism for energy production were obtained.

R3HBA, as the direct product of PHB depolymerization, might act as an inhibitor of the enzymatic depolymerization activity. To test this hypothesis in *M. parvus*, depolymerization assays were carried out adding exogenous R3HBA before the onset of the depolymerization at concentrations ranging from 0 to  $650 \text{ mg L}^{-1}$ . The higher limit was higher than the R3HBA titers achieved in previous experiments, where values slightly above  $200 \text{ mg L}^{-1}$  were found after 48 h of depolymerization at pH 11 with or without methane. Fig. 3C shows the total R3HBA concentration during the 72 h depolymerization experiment, while the net R3HBA released at the end of the experiment (72 h) is shown in Fig. 3D. No significant differences were found between R3HBA concentration released after 72 h with no added R3HBA and any of the experiments with addition of exogenous R3HBA. Fig. 3D also shows the specific initial rate of R3HBA release calculated during the first six hours. This parameter increased from  $52.4 \pm 1.8 \text{ mg of R3HBA per gram of initial PHB (PHBi) per hour}$  in the absence of exogenous R3HBA to  $81.1 \pm 8.0 \text{ mg (g PHBi)}^{-1}\text{h}^{-1}$  in the presence of  $120 \text{ mg R3HBA L}^{-1}$ . This increase could be related to impurities in the *in-house* produced R3HBA, although this was not further investigated. Additional increases in the initial R3HBA concentration led to a decrease in the specific initial rate of R3HBA release. Finally, Fig. 3E shows no differences on the depolymerization yield regardless of the initial R3HBA concentration. Interestingly, the  $Y_{\text{R3HBA}}$  was reduced at 330 and  $650 \text{ mg L}^{-1}$  ( $65.8 \pm 0$  and  $61.7 \pm 4.40\%$ ) compared to non R3HBA addition or to  $120 \text{ mg R3HBA L}^{-1}$

<sup>1</sup> added, while an increment of the crotonic acid yield to  $0.78 \pm 0.014\%$  was evidenced at the highest initial R3HBA concentration.

Surprisingly, literature is scarce regarding the effect of R3HBA on the depolymerization kinetics, although R3HBA is the main reaction product. Scherer et al. (1999) found that an extracellular PHB depolymerase from *Aspergillus fumigatus* was reversibly inhibited by trimers of 3-hydroxybutyrate, but no data was presented concerning inhibition by R3HBA.

To further understand the effects of high R3HBA concentration on the depolymerization kinetics, future work will include depolymerization experiments carried out at high initial PHB concentrations. Indeed, PHB concentrations between 1 and 100 g L<sup>-1</sup> could be attained by biomass concentration to test the possibility of achieving high R3HBA titers without sacrificing yield or increasing the depolymerization time.

## 7. Conclusion

This work showed for the first time the production of the chiral molecule (R)-3-hydroxybutyrate (R3HBA) from methane as a proof of concept to convert this greenhouse gas into a multicarbon value-added product. The process involves the accumulation of PHB in *Methylocystis parvus* OBBP and its in-vivo depolymerization by intracellular enzymes. A PHB to R3HBA conversion of  $77.2 \pm 0.9\%$  was obtained after 72 h of depolymerization at pH 11 in a mineral medium containing nitrate under aerobic conditions. A reduced O<sub>2</sub> supply and increasing concentrations of exogenous R3HBA negatively affected the R3HBA yield and the initial R3HBA release rate.

## CRedit authorship contribution statement

**Luz Yáñez:** Conceptualization, Investigation, Methodology, Writing – original draft. **Yadira Rodríguez:** Conceptualization, Investigation, Methodology, Writing – original draft. **Felipe Scott:** Conceptualization, Formal analysis, Funding acquisition, Supervision, Writing – review & editing. **Alberto Vergara-Fernández:** Funding acquisition, Supervision, Writing – review & editing. **Raúl Muñoz:** Conceptualization, Funding acquisition, Project administration, Supervision, Resources, Writing – review & editing.

## Declaration of Competing Interest

The authors declare that they have no known competing financial interests or personal relationships that could have appeared to influence the work reported in this paper.

## Acknowledgments

This work was supported by the regional government of Castile and Leon and the EU-FEDER program (CLU 2017-09, UIC 315). The present work was also financially supported by the National Agency for Research and Development (ANID Chile), projects ANID/CONICYT Fondecyt Regular 1211434 and ANID/CONICYT Fondecyt Regular 1190521. Support from grant Apoyo a la Formación de Redes Internacionales entre Centros de Investigación REDES190137 (CONICYT-PCI) is also gratefully acknowledged.

## References

Anis, S.N.S., Anuar, M.S.M., Simarani, K., 2018. Microbial biosynthesis and in vivo depolymerization of intracellular medium-chain-length poly-3-hydroxyalkanoates as potential route to platform chemicals. *Biotechnol. Appl. Biochem.* 65, 784–796. <https://doi.org/10.1002/bab.1666>.

Bordel, S., Rojas, A., Muñoz, R., 2019. Reconstruction of a Genome Scale Metabolic Model of the polyhydroxybutyrate producing methanotroph *Methylocystis parvus* OBBP. *Microb. Cell Fact.* 18, 1–11. <https://doi.org/10.1186/s12934-019-1154-5>.

Brigham, C.J., Speth, D.R., Rha, C., Sinskey, A.J., 2012. Whole-Genome Microarray and Gene Deletion Studies Reveal Regulation of the Polyhydroxyalkanoate Production

Cycle by the Stringent Response in *Ralstonia eutropha* H16. *Appl. Environ. Microbiol.* 78, 8033–8044. <https://doi.org/10.1128/AEM.01693-12>.

Cao, Q., Zhang, J., Liu, H., Wu, Q., Chen, J., Chen, G.Q., 2014. The mechanism of anti-osteoporosis effects of 3-hydroxybutyrate and derivatives under simulated microgravity. *Biomaterials* 35, 8273–8283. <https://doi.org/10.1016/j.biomaterials.2014.06.020>.

Donoso, R.A., Pérez-Pantoja, D., González, B., 2011. Strict and direct transcriptional repression of the pobA gene by benzoate avoids 4-hydroxybenzoate degradation in the pollutant degrader bacterium *Cupriavidus necator* JMP134. *Environ. Microbiol.* 13, 1590–1600. <https://doi.org/10.1111/j.1462-2920.2011.02470.x>.

Edenhofer, O., 2014. IPCC 2014 Mitigation of Climate Change. Contribution of Working Group III to the Fifth Assessment Report of the Intergovernmental Panel on Climate. Cambridge University Press, Change, Cambridge.

Etminan, M., Myhre, G., Highwood, E.J., Shine, K.P., 2016. Radiative forcing of carbon dioxide, methane, and nitrous oxide: A significant revision of the methane radiative forcing. *Geophys. Res. Lett.* 43, 12614–12623. <https://doi.org/10.1002/2016GL071930>.

Fruggo. Last accessed: January 28, 2022. <https://www.fruggo.co.uk/contact> 2021.

Irving, S.E., Choudhury, N.R., Corrigan, R.M., 2021. The stringent response and physiological roles of (pp)Gpp in bacteria. *Nat. Rev. Microbiol.* 19, 256–271. <https://doi.org/10.1038/s41579-020-00470-y>.

Jackson, R.B., Saunio, M., Bousquet, P., Canadell, J.G., Poulter, B., Stavert, A.R., Bergamaschi, P., Niwa, Y., Segers, A., Tsuruta, A., 2020. Increasing anthropogenic methane emissions arise equally from agricultural and fossil fuel sources. *Environ. Res. Lett.* 15 (7), 071002.

Jawaharraj, K., Shrestha, N., Chilkoor, G., Dhiman, S.S., Islam, J., Gadhamsetty, V., 2020. Valorization of methane from environmental engineering applications: A critical review. *Water Res* 187, 116400. <https://doi.org/10.1016/j.watres.2020.116400>.

Jendrossek, D., Handrick, R., 2002. Microbial degradation of polyhydroxyalkanoates. *Annu. Rev. Microbiol.* 56 (1), 403–432. <https://doi.org/10.1146/annurev.micro.56.012302.160838>.

Juengert, J.R., Borisova, M., Mayer, C., Wolz, C., Brigham, C.J., Sinskey, A.J., Jendrossek, D., Kivisaar, M., 2017. Absence of ppGpp Leads to Increased Mobilization of Intermediately Accumulated Poly(3-Hydroxybutyrate) in *Ralstonia eutropha* H16. *Appl. Environ. Microbiol.* 83 (13) <https://doi.org/10.1128/AEM.00755-17>.

Kawata, Y., Kawasaki, K., Shigeri, Y., 2012. Efficient secreted production of (R)-3-hydroxybutyric acid from living *Halomonas* sp. KM-1 under successive aerobic and microaerobic conditions. *Appl. Microbiol. Biotechnol.* 96, 913–920. <https://doi.org/10.1007/s00253-012-4218-6>.

Kirschke, S., Bousquet, P., Ciais, P., Saunio, M., Canadell, J.G., Dlugokencky, E.J., Bergamaschi, P., Bergmann, D., Blake, D.R., Bruhwiler, L., Cameron-Smith, P., Castaldi, S., Chevallier, F., Feng, L., Fraser, A., Heimann, M., Hodson, E.L., Houweling, S., Josse, B., Fraser, P.J., Krummel, P.B., Lamarque, J.-F., Langenfelds, R. L., Le Queré, C., Naik, V., O'Doherty, S., Palmer, P.L., Pison, I., Plummer, D., Poulter, B., Prinn, R.G., Rigby, M., Ringeval, B., Santini, M., Schmidt, M., Shindell, D. T., Simpson, J.J., Spahni, R., Steele, L.P., Strode, S.A., Sudo, K., Szopa, S., van der Werf, G.R., Voulgarakis, A., van Weele, M., Weiss, R.F., Williams, J.E., Zeng, G., 2013. Three decades of global methane sources and sinks. *Nat. Geosci.* 6 (10), 813–823.

Latimer, A.A., Kakekhani, A., Kulkarni, A.R., Nørskov, J.K., 2018. Direct Methane to Methanol: The Selectivity-Conversion Limit and Design Strategies. *ACS Catal.* 8, 6894–6907. <https://doi.org/10.1021/acscatal.8b00220>.

Lee, S.Y., Lee, Y., Wang, F., 1999. Chiral compounds from bacterial polyesters: Sugars to plastics to fine chemicals. *Biotechnol. Bioeng.* 65, 363–368. [https://doi.org/10.1002/\(SICI\)1097-0290\(19991105\)65:3<363::AID-BIT15>3.0.CO;2-1](https://doi.org/10.1002/(SICI)1097-0290(19991105)65:3<363::AID-BIT15>3.0.CO;2-1).

Liu, H., Kumar, V., Jia, L., Sarsaiya, S., Kumar, D., Juneja, A., Zhang, Z., Sindhu, R., Binod, P., Bhatia, S.K., Awasthi, M.K., 2021. Biopolymer poly-hydroxyalkanoates (PHA) production from apple industrial waste residues: A review. *Chemosphere* 284, 131427. <https://doi.org/10.1016/j.chemosphere.2021.131427>.

Lu, J., Takahashi, A., Ueda, S., 2014. 3-Hydroxybutyrate Oligomer Hydrolase and 3-Hydroxybutyrate Dehydrogenase Participate in Intracellular Polyhydroxybutyrate and Polyhydroxyvalerate Degradation in *Paracoccus denitrificans*. *Appl. Environ. Microbiol.* 80, 986–993. <https://doi.org/10.1128/AEM.03396-13>.

Matsuyama, A., Yamamoto, H., Kawada, N., Kobayashi, Y., 2001. Industrial production of (R)-1,3-butanediol by new biocatalysts. *J. Mol. Catal. - B Enzym.* 11, 513–521. [https://doi.org/10.1016/S1381-1177\(00\)00032-1](https://doi.org/10.1016/S1381-1177(00)00032-1).

McAdam, B., Fournet, M.B., McDonald, P., Mojicevic, M., 2020. Production of polyhydroxybutyrate (PHB) and factors impacting its chemical and mechanical characteristics. *Polymers (Basel)*. 12, 1–20. <https://doi.org/10.3390/polym12122908>.

Mountassif, D., Andreoletti, P., Cherkaoui-Malki, M., Latruffe, N., Kebbab, M.S.E., 2010. Structural and catalytic properties of the D-3-hydroxybutyrate dehydrogenase from *Pseudomonas aeruginosa*. *Curr. Microbiol.* 61, 7–12. <https://doi.org/10.1007/s00284-009-9568-7>.

Müller-Santos, M., Koskimäki, J.J., Alves, L.P.S., de Souza, E.M., Jendrossek, D., Pirttilä, A.M., 2021. The protective role of PHB and its degradation products against stress situations in bacteria. *FEMS Microbiol. Rev.* 45 (3) <https://doi.org/10.1093/femsre/fuaa058>.

Nguyen, D.T.N., Lee, O.K., Nguyen, T.T., Lee, E.Y., 2021. Type II methanotrophs: A promising microbial cell-factory platform for bioconversion of methane to chemicals. *Biotechnol. Adv.* 47, 107700 <https://doi.org/10.1016/j.biotechadv.2021.107700>.

Nguyen, T.T., Lee, E.Y., 2021. Methane-based biosynthesis of 4-hydroxybutyrate and P (3-hydroxybutyrate-co-4-hydroxybutyrate) using engineered *Methylosinus*

- trichosporium* OB3b. *Bioresour. Technol.* 335, 125263 <https://doi.org/10.1016/j.biortech.2021.125263>.
- Nielsen, R., Møller, N., Gormsen, L.C., Tolbod, L.P., Hansson, N.H., Sorensen, J., Harms, H.J., Frøkiær, J., Eiskjær, H., Jespersen, N.R., Mellemkjær, S., Lassen, T.R., Pryds, K., Botker, H.E., Wiggers, H., 2019. Cardiovascular Effects of Treatment With the Ketone Body 3-Hydroxybutyrate in Chronic Heart Failure Patients. *Circulation* 139 (18), 2129–2141. <https://doi.org/10.1161/CIRCULATIONAHA.118.036459>.
- Pérez-Rivero, C., López-Gómez, J.P., Roy, I., 2019. A sustainable approach for the downstream processing of bacterial polyhydroxyalkanoates: State-of-the-art and latest developments. *Biochem. Eng. J.* 150, 107283 <https://doi.org/10.1016/j.bej.2019.107283>.
- Pieja, A.J., Sundstrom, E.R., Criddle, C.S., 2011. Poly-3-hydroxybutyrate metabolism in the type II Methanotroph *Methylocystis parvus* OBBP. *Appl. Environ. Microbiol.* 77, 6012–6019. <https://doi.org/10.1128/AEM.00509-11>.
- Ravishankara, A.R., Kulenstierna, J., Michalopoulou, E., Höglund-Isaksson, L., et al. 2021. Benefits and Costs of Mitigating Methane Emissions. *Biomacromolecules* 6 (4), 2290–2298. <https://doi.org/10.1021/bm050187s>.
- Ren, Q., Grubelnik, A., Hoerler, M., Ruth, K., Hartmann, R., Felber, H., Zinn, M., 2005. Bacterial Poly(hydroxyalkanoates) as a Source of Chiral Hydroxyalkanoic Acids. *Biomacromolecules* 6 (4), 2290–2298. <https://doi.org/10.1021/bm050187s>.
- Ren, Q., Ruth, K., Thöny-Meyer, L., Zinn, M., 2007. Process engineering for production of chiral hydroxycarboxylic acids from bacterial polyhydroxyalkanoates. *Macromol. Rapid Commun.* 28, 2131–2136. <https://doi.org/10.1002/marc.200700389>.
- Rodríguez, Y., Firmino, P.I.M., Arnáiz, E., Lebrero, R., Muñoz, R., 2020. Elucidating the influence of environmental factors on biogas-based polyhydroxybutyrate production by *Methylocystis hirsuta* CSC1. *Sci. Total Environ.* 706, 135136. <https://doi.org/10.1016/j.scitotenv.2019.135136>.
- Rostkowski, K.H., Pfluger, A.R., Criddle, C.S., 2013. Stoichiometry and kinetics of the PHB-producing Type II methanotrophs *Methylosinus trichosporium* OB3b and *Methylocystis parvus* OBBP. *Bioresour. Technol.* 132, 71–77. <https://doi.org/10.1016/j.biortech.2012.12.129>.
- Ruth, K., Grubelnik, A., Hartmann, R., et al., 2007. Efficient production of (R)-3-hydroxycarboxylic acids by biotechnological conversion of polyhydroxyalkanoates and their purification. *Biomacromolecules* 8, 279–286. <https://doi.org/10.1021/bm060585a>.
- Saunois, M., Bousquet, P., Poulter, B., Peregon, A., et al., 2016. The global methane budget 2000–2012. *Earth Syst. Sci. Data* 8 (2), 697–751.
- Scherer, T.M., Fuller, R.C., Lenz, R.W., Goodwin, S., 1999. Production, purification and activity of an extracellular depolymerase from *Aspergillus fumigatus*. *J. Environ. Polym. Degrad.* 7, 117–125. <https://doi.org/10.1023/A:1022881204565>.
- Scott, F., Yáñez, L., Conejeros, R., Araya, B., Vergara-Fernández, A., 2021. Two internal bottlenecks cause the overflow metabolism leading to poly(3-hydroxybutyrate) production in *Azohydromonas lata* DSM1123. *J. Environ. Chem. Eng.* 9 (4), 105665. <https://doi.org/10.1016/j.jece.2021.105665>.
- Sirohi, R., Prakash Pandey, J., Kumar Gaur, V., Gnansounou, E., Sindhu, R., 2020. Critical overview of biomass feedstocks as sustainable substrates for the production of polyhydroxybutyrate (PHB). *Bioresour. Technol.* 311, 123536. <https://doi.org/10.1016/j.biortech.2020.123536>.
- Soni, B.K., Conrad, J., Kelley, R.L., Srivastava, V.J., 1998. Effect of temperature and pressure on growth and methane utilization by several methanotrophic cultures. *Appl. Biochem. Biotechnol. - Part A Enzym. Eng. Biotechnol.* 70–72, 729–738. <https://doi.org/10.1007/BF02920184>.
- Strong, P.J., Xie, S., Clarke, W.P., 2015. Methane as a resource: Can the methanotrophs add value? *Environ. Sci. Technol.* 49, 4001–4018. <https://doi.org/10.1021/es504242n>.
- Takanashi, M., Saito, T., 2006. Characterization of two 3-hydroxybutyrate dehydrogenases in poly(3-hydroxybutyrate)-degradable bacterium, *Ralstonia pickettii* T1. *J. Biosci. Bioeng.* 101, 501–507. <https://doi.org/10.1263/jbb.101.501>.
- Tieu, K., Perier, C., Caspersen, C., Teismann, P., Wu, D.-C., Yan, S.-D., Naini, A., Vila, M., Jackson-Lewis, V., Ramasamy, R., Przedborski, S., 2003. D-β-Hydroxybutyrate rescues mitochondrial respiration and mitigates features of Parkinson disease. *J. Clin. Invest.* 112 (6), 892–901. <https://doi.org/10.1172/JCI18797>.
- Tokiwa, Y., Ugwu, C.U., 2007. Biotechnological production of (R)-3-hydroxybutyric acid monomer. *J. Biotechnol.* 132, 264–272. <https://doi.org/10.1016/j.jbiotec.2007.03.015>.
- Veckerskaya, M., Dijkema, C., Stams, A.J.M., 2001. Intracellular PHB conversion in a Type II methanotroph studied by 13C NMR. *J. Ind. Microbiol. Biotechnol.* 26, 15–21. <https://doi.org/10.1038/sj.jim.7000086>.
- Wang, F., Lee, S.Y., 1997. Poly(3-Hydroxybutyrate) Production with High Productivity and High Polymer Content by a Fed-Batch Culture of *Alcaligenes latus* under Nitrogen Limitation. *Appl. Environ. Microbiol.* 63 (9), 3703–3706. <https://doi.org/10.1128/aem.63.9.3703-3706.1997>.
- Wendlandt, K.D., Jechorek, M., Helm, J., Stottmeister, U., 2001. Producing poly-3-hydroxybutyrate with a high molecular mass from methane. *J. Biotechnol.* 86, 127–133. [https://doi.org/10.1016/S0168-1656\(00\)00408-9](https://doi.org/10.1016/S0168-1656(00)00408-9).
- Yamanashi, T., Iwata, M., Kamiya, N., Tsunetomi, K., Kajitani, N., Wada, N., Iitsuka, T., Yamauchi, T., Miura, A., Pu, S., Shirayama, Y., Watanabe, K., Duman, R.S., Kaneko, K., 2017. Beta-hydroxybutyrate, an endogenous NLRP3 inflammasome inhibitor, attenuates stress-induced behavioral and inflammatory responses. *Sci. Rep.* 7 (1) <https://doi.org/10.1038/s41598-017-08055-1>.
- Yáñez, L., Conejeros, R., Vergara-Fernández, A., Scott, F., 2020. Beyond Intracellular Accumulation of Polyhydroxyalkanoates: Chiral Hydroxyalkanoic Acids and Polymer Secretion. *Front. Bioeng. Biotechnol.* 8 <https://doi.org/10.3389/fbioe.2020.00248>.
- Yokaryo, H., Teruya, M., Hanashiro, R., Goda, M., Tokiwa, Y., 2018. Direct Production of (R)-3-Hydroxybutyric Acid of High Optical Purity by *Halomonas* sp. OITC1261 Under Aerobic conditions. *Biotechnol. J.* 13, 1–23. <https://doi.org/10.1002/biot.201700343>.
- Zhang, J., Cao, Q., Li, S., Lu, X., Zhao, Y., Guan, J.-S., Chen, J.-C., Wu, Q., Chen, G.-Q., 2013. 3-Hydroxybutyrate methyl ester as a potential drug against Alzheimer's disease via mitochondria protection mechanism. *Biomaterials* 34 (30), 7552–7562. <https://doi.org/10.1016/j.biomaterials.2013.06.043>.